

01 Apr 1995

Interaction buckling of flange, edge stiffener and web of c-sections in bending

Colin A. Rogers

R. M. Schuster

Follow this and additional works at: <https://scholarsmine.mst.edu/ccfss-library>



Part of the [Structural Engineering Commons](#)

Recommended Citation

Rogers, Colin A. and Schuster, R. M., "Interaction buckling of flange, edge stiffener and web of c-sections in bending" (1995). *Center for Cold-Formed Steel Structures Library*. 102.

<https://scholarsmine.mst.edu/ccfss-library/102>

This Technical Report is brought to you for free and open access by Scholars' Mine. It has been accepted for inclusion in Center for Cold-Formed Steel Structures Library by an authorized administrator of Scholars' Mine. This work is protected by U. S. Copyright Law. Unauthorized use including reproduction for redistribution requires the permission of the copyright holder. For more information, please contact scholarsmine@mst.edu.

RESEARCH INTO COLD FORMED STEEL

**FINAL REPORT OF PHASE II
OF CSSBI/IRAP PROJECT**

**INTERACTION BUCKLING OF
FLANGE, EDGE STIFFENER AND WEB
OF C- SECTIONS IN BENDING**

By

**Colin A. Rogers
Research Assistant**

and

**Professor R.M. Schuster
Research Supervisor**

April 1995

**Department of Civil Engineering
University of Waterloo
Waterloo, Ontario**

RESEARCH INTO COLD FORMED STEEL

**FINAL REPORT OF PHASE II
OF CSSBI/IRAP PROJECT**

**INTERACTION BUCKLING OF
FLANGE, EDGE STIFFENER AND WEB
OF C- SECTIONS IN BENDING**

By

**Colin A. Rogers
Research Assistant**

and

**Professor R.M. Schuster
Research Supervisor**

April 1995

**Department of Civil Engineering
University of Waterloo
Waterloo, Ontario**

Abstract

The buckling strength and predictor equations of cold formed steel C and Z-sections in bending were investigated through an analytical and laboratory test program. Recent testing carried out by various researchers indicates that the bending resistance of cold formed steel members which fail by flange/web distortional buckling is unconservatively predicted by current North American Design Standards. However, members in bending which fail by local or distortional buckling of the lip/flange components are adequately modelled by these design Standards.

Data of 174 available test specimens was compiled and supplemented with 59 additional tests carried out at the University of Waterloo, encompassing a full range of section dimensions and material properties. The Waterloo laboratory test program consisted of C-sections with locally stable and unstable webs and systematically varied lip depths and flange widths. Thirty-seven of the 233 tests considered failed in a flange/web distortional mode, where test moments were found to be as low as 64% of the predicted values, according to the current North American Design Standards. Web slenderness ratios exceeding 130 and material yield stresses above 325 MPa were typical for sections which failed by flange/web distortional buckling. Purlin sections commonly used in Canadian and American building industries have dimensions and material properties above these values and are at risk of premature failure due to flange/web distortional buckling.

An overview of the current Canadian Design Standard (S136-94) and the current American Design Specification (AISI 1989 Edition) is presented. Various flange/web analytical models are investigated to determine the method that most accurately predicts the bending strength of test specimens which fail by flange/web distortional buckling. A summary of the suitability of the various distortional buckling analyses is presented and the most appropriate flange/web distortional buckling method is recommended for design.

It is recommended that either model 4 or 5 of the Lau & Hancock method be used as the North American predictor method for the flange/web distortional buckling strength of cold formed steel sections in bending. Further research is required so that the implementation of flange/web distortional buckling for any cross section type can be based on a dimensional parameter limit.

This work also includes an investigation of the flat width ratio limit and effective width calculations for simple lip stiffeners of C-sections in bending. The current S136 Standard specifies that the lip depth ratio limit, d/t , should have a value of 14. C-sections tested at the University of Waterloo were used to compare d/t and d_i/w ratios with test moments to determine whether a d/t limit is required, if the current value of 14 is appropriate, and whether it should remain in the next edition of the S136 Standard. In addition, five methods to determine the effective width of a compressed simple lip stiffener subjected to a stress gradient were evaluated.

It is recommended that a d_i/w warning of 0.4 be introduced for Case III flange sections only. The warning should also indicate that the bending moment resistance will decrease above this characteristic value, yet remain predictable using the S136 Standard. Analysis of the effective width calculation procedures of a simple edge stiffener subjected to a stress gradient revealed that the variation in mean values between the five effective width methods was marginal, therefore, it is recommended that the current effective width procedures remain in the North American Design Standards.

Modifications to the current local buckling procedures, proposed by Dinovitzer and Sooi, were also studied in this work. Dinovitzer proposed a change to the flange buckling coefficient equations to alleviate a discontinuity in the effective width formulation. Sooi developed a method with which the distribution of effective width for a web subjected to a stress gradient could be simplified. These local buckling modifications were compared with the current North American Design Standards and to applicable test data.

Statistical evidence from a combination of Waterloo and available test data showed the Dinovitzer method to be more accurate than the current S136 Standard for the calculation of effective width of an edge-stiffened flange element. It is recommended that the Sooi web method not replace the procedures found in the current North American Design Standards for the distribution of effective width of a web subjected to a stress gradient. The statistical results also indicate that the S136 Standard provides a more accurate prediction of the test bending strength in comparison with the AISI Specification.

Acknowledgements

The authors wish to thank Mr. Steve Fox of the Canadian Sheet Steel Building Institute and Mr. Roger Willoughby of the National Research Council's Industrial Research Assistance Programme for their most valuable help during the course of this phase of the project, as well as, for the financial support given by both the CSSBI and IRAP to have made this research project a reality.

Table of Contents

Abstract.....	iv
Acknowledgements.....	vii
Table of Contents.....	viii
List of Tables	xiii
List of Figures.....	xviii

Chapter 1 - Introduction

1.1 General.....	1
1.2 Objectives of Work.....	5
1.3 Scope of Work	5

Chapter 2 - Literature Review

2.1 Plate Buckling Theory of Uniformly Compressed Plates.....	7
2.1.1 Post-Buckling of Uniformly Compressed Stiffened Elements	9
2.1.2 Plate Buckling Coefficients for Fully and Partially Stiffened Uniformly Compressed Elements.....	11
2.1.3 Unstiffened Uniformly Compressed Elements	12
2.1.4 Buckling Coefficients for Unstiffened Uniformly Compressed Elements.....	14
2.1.5 Buckling Coefficients for Unstiffened Elements Subjected to a Stress Gradient	14
2.1.6 Buckling Coefficients for Stiffened Elements Subjected to a Stress Gradient	15
2.2 Simple Edge Stiffener Definition.....	17
2.3 Flange/Web Interaction.....	19
2.4 Flange/Web Distortional Buckling	20

Chapter 3 - Moment Resistance of Laterally Supported Members

3.1	Gross Moment Resistance.....	22
3.2	Effective Moment Resistance Based on S136-94 [CSA 94].....	23
3.2.1	Effective Width of a Uniformly Compressed Edge-Stiffened Flange Element	23
3.2.2	Effective Width of a Compressed Simple Edge Stiffener (Lip)	26
3.2.3	Effective Width of a Web Element Subjected to a Stress Gradient..	27
3.2.4	Cold Work of Forming.....	29
3.3	Effective Moment Resistance Based on AISI [AISI 89a].....	30
3.3.1	Effective Width of a Uniformly Compressed Edge-Stiffened Flange Element	30
3.3.2	Effective Width of a Compressed Simple Edge Stiffener (Lip)	33
3.3.3	Effective Width of a Web Element Subjected to a Stress Gradient..	34
3.3.4	Cold Work of Forming.....	36

Chapter 4 - Waterloo Test Program

4.1	General.....	37
4.1.1	Designation of Test Specimens.....	38
4.1.2	Flat Width Ratios of Test Specimens.....	39
4.1.3	Fabrication of Test Specimens.....	39
4.1.4	Mechanical Properties of Test Specimens	41
4.1.5	Test Frame Set-Up	41
4.1.6	Test Procedure	43
4.1.7	Description of Failure Modes	44

Chapter 5 - Available Test Data

5.1	General.....	49
5.1.1	Charnvarnichborikarn [Cha 92]	50
5.1.2	Cohen [Coh 87].....	50
5.1.3	Desmond [Des 78a].....	51

5.1.4	LaBoube [LaB 78]	51
5.1.5	Moreyra [Mor 93]	52
5.1.6	Schardt and Schrade [Scha 82]	53
5.1.7	Schuster [Schu 92]	54
5.1.8	Shan [Shan 94]	54
5.1.9	Willis and Wallace [Wil 90a]	55
5.1.10	Winter [Win 47]	56

Chapter 6 - Edge Stiffener Investigation

6.1	Review of Current Flat Width Ratio, d/t , Limit	57
6.1.1	Problems With Current Flat Width Ratio, d/t , Limit	58
6.1.2	Alternate Flat Width Ratio, d_i/w , Limit	58
6.1.3	Bending Moment Resistance Predictability, Using Willis and Wallace Data	60
6.1.4	Bending Moment vs. Lip Dimension Ratio, Using Waterloo Test Data	61
6.1.4.1	Case I Flange Series	61
6.1.4.2	Case II Flange Series	64
6.1.4.3	Case III Flange Series	69
6.2	Plate Buckling Coefficient - Stress Gradient Approach	71
6.2.1	Comparison of Different Stress Gradient Approaches	72
6.2.2	Edge Stiffener Stress Gradient Test Results	74

Chapter 7 - Flange/Web Distortional Buckling Methods of Sections in Bending

7.1	General	78
7.1.1	Lau & Hancock [Lau 87] [Lau 90]	79
7.1.2	Marsh [Mar 90]	82
7.1.3	Moreyra [Mor 93]	87
7.1.4	Charnvarnichborikarn [Cha 92]	92

7.2	Comparison of Flange/Web Distortional Buckling Methods with Waterloo Test Data	95
7.3	Comparison of Flange/Web Distortional Buckling Methods with Available Test Data.....	96
7.4	Comparison of All Test Data and Flange/Web Distortional Buckling Methods.....	99
7.5	Comparison of Additional Lau & Hancock [Lau 87] [Lau 90] Flange/ Web Distortional Buckling Models	101
7.6	Implementation of Flange/Web Distortional Buckling Analysis.....	102

Chapter 8 - Local Buckling Model Improvements

8.1	Edge-Stiffened Flange Method by Dinovitzer [Din 92]	105
8.1.1	Comparison with Waterloo Test Data.....	106
8.1.2	Comparison with Available Test Data.....	107
8.1.2	Comparison with Waterloo and Available Test Data	109
8.2	Web Method by Sooi [Soo 93]	110
8.2.1	Comparison with Waterloo Test Data.....	111
8.2.2	Comparison with Available Test Data.....	112
8.2.3	Comparison with Waterloo and Available Test Data	113

Chapter 9 - Summary, Conclusions and Recommendations

9.1	Summary	115
9.2	Conclusions and Recommendations	117
9.2.1	d/t Limit of Edge Stiffener.....	117
9.2.2	Simple Edge Stiffener Subjected to a Stress Gradient.....	118
9.2.3	Flange/Web Distortional Buckling	118
9.2.4	Local Buckling of Edge-Stiffened Flange Element	121
9.2.5	Local Buckling of Web Element.....	121
9.2.6	Summary of Conclusions and Recommendations	122
9.3	Recommendations for Future Research	123

References	124
Appendix ‘A’ - Waterloo Test Data and Test / Predicted Bending Moment Ratios	130
Appendix ‘B’ - Available Test Data and Test / Predicted Bending Moment Ratios	149
Appendix ‘C’ - Example Calculations	
Example Calculations Test Specimen.....	196
Gross Section Properties	196
S136-94 [CSA 94] Moment Resistance for Laterally Supported Members	198
Dinovitzer [Din 92] Exponent Method with S136-94 [CSA 94] Moment Resistance for Laterally Supported Members.....	203
Sooi [Soo 93] Web Approach with S136-94 [CSA 94] Moment Resistance for Laterally Supported Members.....	205
AISI [AISI 89a]] Moment Resistance for Laterally Supported Members	208
Lau & Hancock [Lau 87] [Lau 90] Flange/Web Distortional Buckling Method 1 with AISI [AISI 89a] Moment Resistance for Laterally Supported Members	211
Lau & Hancock [Lau 87] [Lau 90] Flange/Web Distortional Buckling Method 2 with AISI [AISI 89a] Moment Resistance for Laterally Supported Members	215
Lau & Hancock [Lau 87] [Lau 90] Flange/Web Distortional Buckling Method 3 with AISI [AISI 89a] Moment Resistance for Laterally Supported Members	216
Marsh [Mar 90] Flange/Web Distortional Buckling Method with AISI [AISI 89a] Moment Resistance for Laterally Supported Members	219
Moreyra [Mor 93] Flange/Web Distortional Buckling Method 1 with AISI [AISI 89a] Moment Resistance for Laterally Supported Members	223
Moreyra [Mor 93] Flange/Web Distortional Buckling Method 2 with AISI [AISI 89a] Moment Resistance for Laterally Supported Members	226
Appendix ‘D’ - Additional Lau & Hancock Flange/Web Distortional Buckling Models	227

List of Tables

Table 3.1	Buckling Coefficients for Edge-Stiffened Flange Elements.....	25
Table 4.1	Average Flat Width Ratios.....	39
Table 4.2	Test Specimen Failure Descriptions	48
Table 5.1	List of Researchers and Applicable Available Test Data.....	49
Table 7.1	Comparison of Flange/Web Distortional Bucking Methods with Waterloo Test Data	96
Table 7.2	Comparison of Flange/Web Distortional Bucking Methods with Available Test Data.....	97
Table 7.3	Comparison of Flange/Web Distortional Bucking Methods with Charnvarnichborikarn Test Data [Cha 92].....	98
Table 7.4	Test Data - Test / Predicted Bending Moment Ratios	99
Table 7.5	Geometric Ratios - Flange/Web Distortional Buckling Test Specimens	102
Table 7.6	Geometric Ratios - Industry Standard Floor Joist C-Sections.....	103
Table 8.1	Comparison of Dinovitzer Exponent, n, and k Values with Waterloo Test Data [Din 92]	106
Table 8.2	Comparison of Dinovitzer Exponent, n, and k Values with Available Test Data [Din 92]	108
Table 8.3	Comparison of Test / Predicted Bending Moment Ratios with Waterloo Test Data	111
Table 8.4	Comparison of Test / Predicted Bending Moment Ratios with Available Test Data.....	113
Table 8.5	Comparison of Test / Predicted Bending Moment Ratios with Waterloo and Available Test Data	114
Table A.1a	Test Specimen Dimensions.....	131
Table A.1b	Test Specimen Dimensions.....	132
Table A.2a	Test Specimen Dimension Ratios	133
Table A.2b	Test Specimen Dimension Ratios	134
Table A.2c	Test Specimen Dimension Ratios	135
Table A.3	Material Properties of Test Specimens	136

Table A.4	k Values for Edge Stiffener Stress Gradient Methods	137
Table A.5a	M_T/M_p Ratios - Edge Stiffener Stress Gradient Methods	138
Table A.5b	M_T/M_p Ratios - Edge Stiffener Stress Gradient Methods	139
Table A.5c	M_T/M_p Ratios - Edge Stiffener Stress Gradient Methods	140
Table A.6a	M_T/M_p Ratios - Local Buckling Methods.....	141
Table A.6b	M_T/M_p Ratios - Local Buckling Methods.....	142
Table A.6c	M_T/M_p Ratios - Local Buckling Methods.....	143
Table A.6d	M_T/M_p Ratios - Local Buckling Methods.....	144
Table A.7a	M_T/M_p Ratios - Flange/Web Distortional Buckling Methods	145
Table A.7b	M_T/M_p Ratios - Flange/Web Distortional Buckling Methods	146
Table A.7c	M_T/M_p Ratios - Flange/Web Distortional Buckling Methods	147
Table A.7d	M_T/M_p Ratios - Flange/Web Distortional Buckling Methods	148
Table B.1	Charnvarnichborikarn [Cha 92] Test Specimen Dimensions	150
Table B.2	Charnvarnichborikarn [Cha 92] Test Specimen Dimension Ratios.....	151
Table B.3	Cohen [Coh 87] Test Specimen Dimensions	151
Table B.4	Cohen [Coh 87] Test Specimen Dimension Ratios	152
Table B.5	Desmond [Des 78a] Test Specimen Dimensions.....	153
Table B.6	Desmond [Des 78a] Test Specimen Dimension Ratios	153
Table B.7a	LaBoube [LaB 78] Test Specimen Dimensions.....	154
Table B.7b	LaBoube [LaB 78] Test Specimen Dimensions.....	155
Table B.8a	LaBoube [LaB 78] Test Specimen Dimension Ratios.....	156
Table B.8b	LaBoube [LaB 78] Test Specimen Dimension Ratios.....	157
Table B.8c	LaBoube [LaB 78] Test Specimen Dimension Ratios.....	158
Table B.9	LaBoube [LaB 78] Test Specimen Material Properties.....	159
Table B.10	LaBoube [LaB 78] Test Specimen Material Properties and Bottom Plate Dimensions	159
Table B.11	Moreyra [Mor 93] Test Specimen Information.....	161
Table B.12	Moreyra [Mor 93] Test Specimen Dimension Ratios.....	161
Table B.13	Schardt & Schrade [Scha 82] Test Specimen Information	162
Table B.14	Schardt & Schrade [Scha 82] Test Specimen Dimension Ratios.....	163

Table B.15	Schuster [Schu 92] Test Specimen Dimensions	164
Table B.16	Schuster [Schu 92] Test Specimen Dimension Ratios.....	164
Table B.17	Schuster [Schu 92] Test Specimen Material Properties.....	165
Table B.18	Shan [Shan 94] Test Specimen Dimensions	165
Table B.19a	Shan [Shan 94] Test Specimen Dimension Ratios	166
Table B.19b	Shan [Shan 94] Test Specimen Dimension Ratios	167
Table B.20	Shan [Shan 94] Test Specimen Material Properties.....	168
Table B.21	Willis & Wallace [Wil 90a] Test Specimen Information	168
Table B.22	Willis & Wallace [Wil 90a] Test Specimen Dimension Ratios.....	168
Table B.23	Winter [Win 47] Test Specimen Information	169
Table B.24	Winter [Win 47] Test Specimen Dimension Ratios	170
Table B.25a	k Values for Edge Stiffener Stress Gradient Methods	171
Table B.25b	M_T/M_p Ratios - Edge Stiffener Stress Gradient Methods	171
Table B.25c	M_T/M_p Ratios - Edge Stiffener Stress Gradient Methods	172
Table B.26	Charnvarnichborikarn [Cha 92] M_T/M_p Ratios - Local Buckling Methods.....	173
Table B.27a	Charnvarnichborikarn [Cha 92] M_T/M_p Ratios - Flange/Web Distortional Buckling Methods.....	174
Table B.27b	Charnvarnichborikarn [Cha 92] M_T/M_p Ratios - Flange/Web Distortional Buckling Methods.....	175
Table B.28	Cohen [Coh 87] M_T/M_p Ratios - Local Buckling Methods	175
Table B.29a	Cohen [Coh 87] M_T/M_p Ratios - Flange/Web Distortional Buckling Methods.....	176
Table B.29b	Cohen [Coh 87] M_T/M_p Ratios - Flange/Web Distortional Buckling Methods.....	176
Table B.30	Desmond [Des 78a] M_T/M_p Ratios - Local Buckling Methods.....	177
Table B.31a	Desmond [Des 78a] M_T/M_p Ratios - Flange/Web Distortional Buckling Methods.....	177
Table B.31b	Desmond [Des 78a] M_T/M_p Ratios - Flange/Web Distortional Buckling Methods.....	177
Table B.32a	LaBoube [LaB 78] M_T/M_p Ratios - Local Buckling Methods.....	178
Table B.32b	LaBoube [LaB 78] M_T/M_p Ratios - Local Buckling Methods.....	179

Table B.33a	LaBoube [LaB 78] M_T/M_p Ratios - Flange/Web Distortional Buckling Methods.....	180
Table B.33b	LaBoube [LaB 78] M_T/M_p Ratios - Flange/Web Distortional Buckling Methods.....	181
Table B.33c	LaBoube [LaB 78] M_T/M_p Ratios - Flange/Web Distortional Buckling Methods.....	182
Table B.33d	LaBoube [LaB 78] M_T/M_p Ratios - Flange/Web Distortional Buckling Methods.....	183
Table B.34	Moreyra [Mor 93] M_T/M_p Ratios - Local Buckling Methods.....	184
Table B.35a	Moreyra [Mor 93] M_T/M_p Ratios - Flange/Web Distortional Buckling Methods.....	184
Table B.35b	Moreyra [Mor 93] M_T/M_p Ratios - Flange/Web Distortional Buckling Methods.....	184
Table B.36	Schardt & Schrade [Scha 82] M_T/M_p Ratios - Local Buckling Methods.....	185
Table B.37a	Schardt & Schrade [Scha 82] M_T/M_p Ratios - Flange/Web Distortional Buckling Methods.....	186
Table B.37b	Schardt & Schrade [Scha 82] M_T/M_p Ratios - Flange/Web Distortional Buckling Methods.....	187
Table B.38	Schuster [Schu 92] M_T/M_p Ratios - Local Buckling Methods	188
Table B.39a	Schuster [Schu 92] M_T/M_p Ratios - Flange/Web Distortional Buckling Methods.....	188
Table B.39b	Schuster [Schu 92] M_T/M_p Ratios - Flange/Web Distortional Buckling Methods.....	188
Table B.40	Shan [Shan 94] M_T/M_p Ratios - Local Buckling Methods	189
Table B.41a	Shan [Shan 94] M_T/M_p Ratios - Flange/Web Distortional Buckling Methods.....	190
Table B.41b	Shan [Shan 94] M_T/M_p Ratios - Flange/Web Distortional Buckling Methods.....	191
Table B.42	Willis & Wallace [Wil 90a] M_T/M_p Ratios - Local Buckling Methods.....	192
Table B.43a	Willis & Wallace [Wil 90a] M_T/M_p Ratios - Flange/Web Distortional Buckling Methods.....	192
Table B.43b	Willis & Wallace [Wil 90a] M_T/M_p Ratios - Flange/Web Distortional Buckling Methods.....	192

Table B.44	Winter [Win 47] M_T/M_p Ratios - Local Buckling Methods	193
Table B.45a	Winter [Win 47] M_T/M_p Ratios - Flange/Web Distortional Buckling Methods.....	193
Table B.45b	Winter [Win 47] M_T/M_p Ratios - Flange/Web Distortional Buckling Methods.....	194
Table B.46	Statistical Comparison of Dinovitzer [Din 92] and S136 [CSA 94] Test to Predicted Bending Moment Ratios for Case II Test Specimens	194
Table D.1	Test Data - Test / Predicted Bending Moment Ratios	229
Table D.2	Comparison of Flange/Web Distortional Bucking Methods with Waterloo Test Data	229
Table D.3	Comparison of Flange/Web Distortional Bucking Methods with Available Test Data.....	230
Table D.4	Comparison of Flange/Web Distortional Bucking Methods with Charnvarnichborikarn Test Data [Cha 92].....	231

List of Figures

Figure 1.1	Typical C and Z-Sections.....	2
Figure 1.2	Local and Distortional Buckling Modes	3
Figure 1.3	Channel Section Purlin Buckling Stress versus Half-Wavelength for Major Axis Bending [Han 94b]	4
Figure 2.1	Buckling Coefficients for Flat Rectangular Plates [Yu 91].....	8
Figure 2.2	Elastic to Post-Buckling Stress Distribution of Stiffened Uniformly Compressed Plate [Yu 91]	8
Figure 2.3	Stress Distribution and Effective Width of Stiffened Uniformly Compressed Element	10
Figure 2.4	Stress Distribution and Effective Width of Unstiffened Uniformly Compressed Element	13
Figure 2.5	Unstiffened Element Subjected to a Stress Gradient	15
Figure 2.6	Web Element Subjected to a Stress Gradient.....	16
Figure 2.7	Simple Edge Stiffener Dimension Definition [CSA 94].....	17
Figure 3.1	Edge-Stiffened Flange Element Subjected to Uniform Compressive Stress [CSA 94].....	26
Figure 3.2	Web Element Subjected to a Stress Gradient [CSA 94]	28
Figure 3.3	Edge-Stiffened Flange Element Subjected to Uniform Compressive Stress [AISI 89a].....	32
Figure 3.4	Web Element Subjected to a Stress Gradient [AISI 89a]	34
Figure 4.1	Typical Test Specimen Cross-Section	40
Figure 4.2	Test Frame Elevation	42
Figure 4.3	Test Frame Section	42
Figure 4.4	Test Frame Set-Up	43
Figure 4.5	Test Frame Control System	44
Figure 4.6	Local Flange Buckling of Unstiffened C-Section.....	46
Figure 4.7	Local Flange Buckling of Stiffened C-Section.....	46
Figure 4.8	Lip/Flange Distortional Buckling of Stiffened C-Section	47
Figure 4.9	Flange/Web Distortional Buckling of Stiffened C-Section	47

Figure 6.1	Lip Depth Dimension Comparison	58
Figure 6.2a	Willis & Wallace M_t vs. D_c/t Ratios	59
Figure 6.2b	Willis & Wallace M_t vs. d/t Ratios	59
Figure 6.2c	Willis & Wallace M_t vs. d_i/w Ratios	59
Figure 6.3a	Series C1-1 M_t vs. d/t Ratios	62
Figure 6.3b	Series C1-1 M_t vs. d_i/w Ratios	63
Figure 6.4a	Series C1-2 M_t vs. d/t Ratios	63
Figure 6.4b	Series C1-2 M_t vs. d_i/w Ratios	63
Figure 6.5a	Series C1-3 M_t vs. d/t Ratios	64
Figure 6.5b	Series C1-3 M_t vs. d_i/w Ratios	64
Figure 6.6a	Series C2-2 M_t vs. d/t Ratios	66
Figure 6.6b	Series C2-2 M_t vs. d_i/w Ratios	66
Figure 6.7a	Series C2-3 M_t vs. d/t Ratios	67
Figure 6.7b	Series C2-3 M_t vs. d_i/w Ratios	67
Figure 6.8a	Series C2-4 M_t vs. d/t Ratios	67
Figure 6.8b	Series C2-4 M_t vs. d_i/w Ratios	68
Figure 6.9a	Series C2R-1 M_t vs. d/t Ratios.....	68
Figure 6.9b	Series C2R-1 M_t vs. d_i/w Ratios	68
Figure 6.10a	Series C3-1 M_t vs. d/t Ratios	69
Figure 6.10b	Series C3-1 M_t vs. d_i/w Ratios	70
Figure 6.11a	Series C3-2 M_t vs. d/t Ratios	70
Figure 6.11b	Series C3-2 M_t vs. d_i/w Ratios	70
Figure 6.12	Lip Depth Stress Position Comparison.....	72
Figure 7.1	Lau & Hancock C-Section and Lip/Flange Component [Lau 87]	79
Figure 7.2	Marsh C-Section [Mar 90]	83
Figure 7.3	Moreyra C-Section [Mor 93]	87
Figure 7.4	Flange/Web Rotational Restraint Relationship.....	90
Figure 7.5	Moreyra Lip/Flange Component [Mor 93]	90
Figure 7.6	Charnvarnichborikarn Theoretical Equivalent Column [Cha 92].....	92
Figure 8.1	Sooi Web Element Subjected to a Stress Gradient [Soo 93]	110

Figure A.1	Test Specimen Cross-Sections	136
Figure B.1	Charnvarnichborikarn [Cha 92] Test Specimen Cross-Section	150
Figure B.2	Cohen [Coh 87] Test Specimen Cross-Section.....	152
Figure B.3	Desmond [Des 78a] Test Specimen Cross-Section.....	153
Figure B.4	LaBoube [LaB 78] Test Specimen Cross-Sections.....	160
Figure B.5	Moreyra [Mor 93] Test Specimen Cross-Section	161
Figure B.6	Schardt & Schrade [Scha 82] Test Specimen Cross-Section.....	162
Figure B.7	Schuster [Schu 92] Test Specimen Cross-Section	163
Figure B.8	Shan [Shan 94] Test Specimen Cross-Section.....	167
Figure B.9	Willis & Wallace [Wil 90a] Test Specimen Cross-Section	169
Figure B.10	Winter [Win 47] Test Specimen Cross-Sections	170
Figure C.1	C2-DW65-3-A Test Specimen Dimensions (mm).....	196
Figure C.2	C2-DW20-3-A Test Specimen Dimensions (mm).....	203

Chapter 1

Introduction

1.1 General

Cold formed steel products have been extensively used in the building construction industry for more than fifty years. The popularity of these products has increased due to their wide array of applications, ease of fabrication and high strength to weight ratios. Initially, deck and cladding sections were used in commercial applications to cover and support large open areas such as walls, roofs and floors. The introduction of pre-engineered structures into the marketplace helped in the development of heavier gauge single structural members such as purlins and girts. More recently, lightweight steel C and Z-sections have been used in residential construction in place of typical timber structural elements such as rafters, joists and studs. Cold formed steel sections are used as primary structural framing members in buildings of up to six storeys in height and as secondary structural framing members in buildings of all sizes. Prefabricated building components such as panels or modular units, which can be used to reduce the time and cost involved in building construction, are created by combining structural framing members with cladding and deck sections. Cold formed steel sections can be fabricated in large quantities by roll-forming steel sheet directly from coils, or by press braking flat sheets for individual members. Industry standard C and Z structural sections range from 50mm to 300mm in depth and from 1mm to 5mm in thickness.

The strength of cold formed steel members is largely dependent on the geometric shape of the cross section. A thin flat sheet cannot carry much load, but formed into a geometric shape such as a C or Z-section, its structural performance can be dramatically increased. Typical framing sections will have flanges which incorporate edge stiffeners, commonly known as lips, as shown in Figure 1.1. Edge stiffeners improve the load

carrying capacity of cold formed sections due to the influence of cross section geometry on stress distribution and post-buckling behaviour.

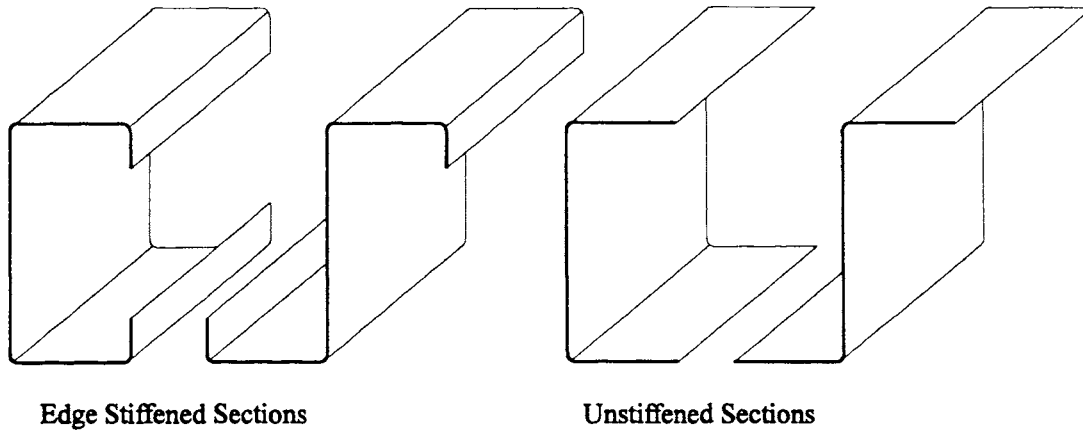


Figure 1.1 - Typical C and Z-Sections

The S136 Standard [CSA 94] defines an unstiffened element as a flat element with one longitudinal free edge and a stiffened element as a flat element with both edges parallel to the direction of stress supported by adequately sized stiffeners. A partially stiffened element is defined as a flat element with one or both longitudinal edges supported by inadequately sized stiffeners. Large flat width ratios, e.g., flange width to thickness, and the ability of thin plates to carry loads beyond the critical elastic buckling level, require the designer to use analysis methods which differ from the standard hot rolled steel procedures.

In North America, the study of cold formed steel structural members began in 1939 at Cornell University under the guidance of Professor G. Winter. These studies resulted in the publication of the first Design Specification for cold formed steel by the American Iron and Steel Institute (AISI) in 1946 [AISI 46]. Subsequent publications of Design Specifications in other countries followed, along with Canada's first cold formed steel Design Standard in 1963 [CSA 63]. Continuing research at various institutions throughout the world has led to the development of the current 1986 AISI Specification

(including the 1989 Addendum) in the United States [AISI 89a] and the S136-94 Standard in Canada [CSA 94] (from herein referred to as the North American Design Standards).

In recent years, the use of cold formed steel members in residential construction has become more popular and has required the introduction of new lightweight geometric variations of typical C and Z-sections. These sections are dimensioned similar to common wood studs and joists, i.e., using 1 5/8" (41mm) lipped flange widths for the full range of section depths from 3 5/8" (92mm) to 12" (305mm), to provide a direct alternative to timber framing. This has led to the use of higher strength steels and the development of sections which have narrow flanges with respect to the depth of the web. C-sections in this range of dimensional ratios have been shown to fail in a unique mode, known as flange/web distortional buckling (see Figure 1.2) [Schu 92] [Shan 94], a failure mode not currently addressed by current North American Design Standards.

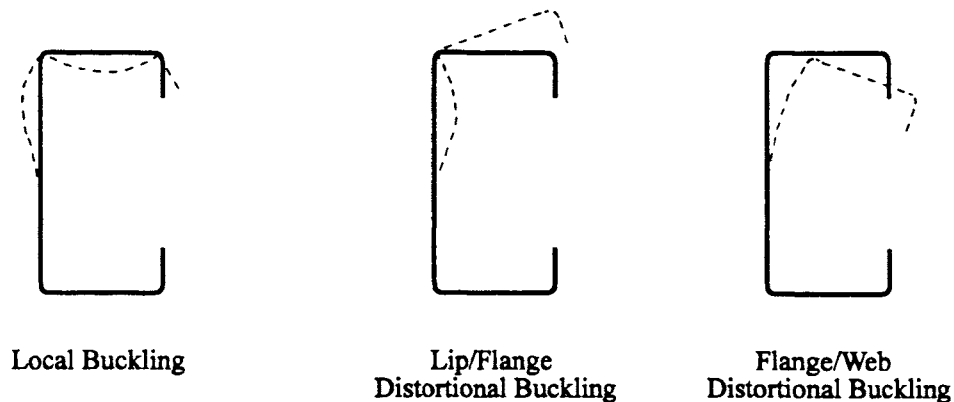


Figure 1.2 - Local and Distortional Buckling Modes

Distinction between the local and distortional buckling modes shown in Figure 1.2 can be made by observing the final position of the lip/flange and flange/web corners. Local buckling occurs when both corners remain in longitudinal alignment, with the adjoining lip, flange and web elements buckling independently. Lip/flange distortional buckling occurs when the lip/flange component rotates about the flange/web corner, which remains

in alignment along the length of the section. Flange/web distortional buckling is evident when both corners move out of alignment, but remain parallel to each other, and an apparent lateral buckling formation of the web appears.

For some cross-sectional geometries distortional buckling will occur at a lower compressive stress and longer half-wavelength than for local buckling. The relationship between compressive stress and half wavelength at buckling for a common C-section subject to local and distortional buckling is shown in Figure 1.3, as detailed by Hancock [Han 94b].

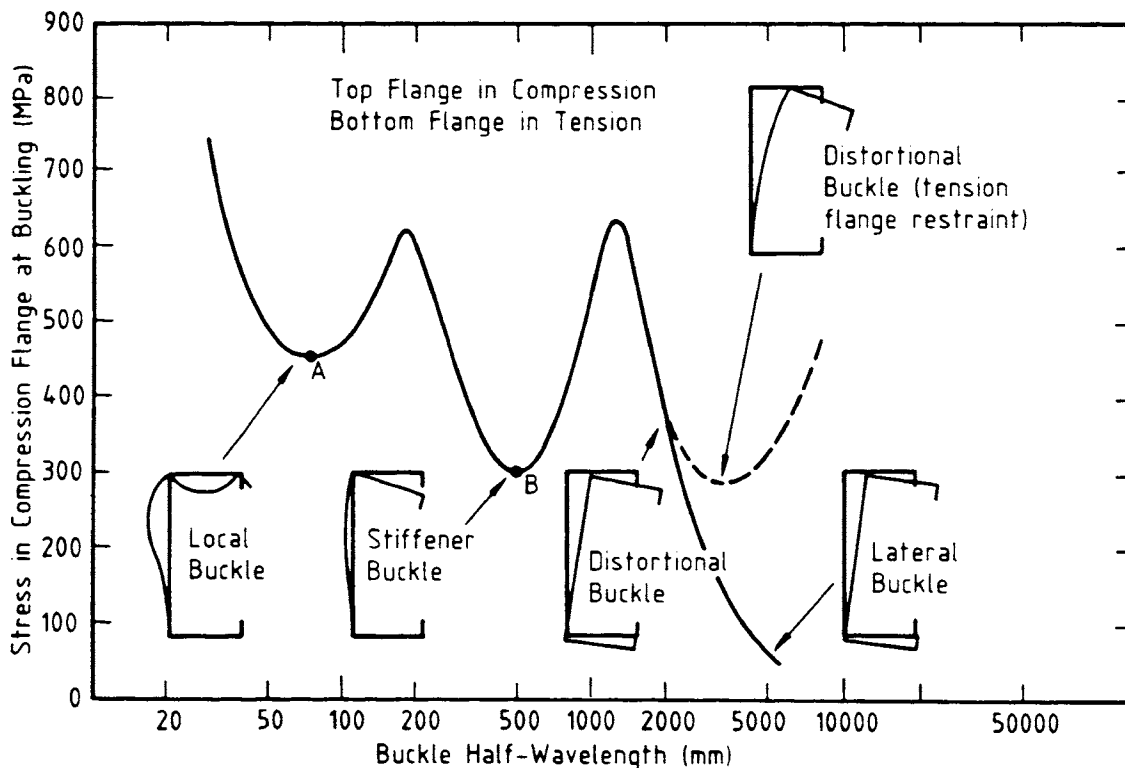


Figure 1.3 - Channel Section Purlin Buckling Stress versus Half-Wavelength for Major Axis Bending [Han 94b]

Currently, the North American Design Standards [AISI 89a] [CSA 94] are based on the effective width concept, which is used to model local buckling and lip/flange distortional buckling of thin plate elements in compression (see Figure 1.2). The latest editions of the North American Design Standards present a unified effective width approach where all

compressive elements are analysed using the basic effective width expression with different plate buckling coefficients incorporated to reflect boundary conditions [Pek 87]. Research of the unified effective width approach consisted of theoretical investigations along with testing of heavier girt and purlin sections, first used in the commercial applications of cold formed steel buildings. These initial test specimens were, in general, not subject to flange/web distortional buckling, hence, the topic is not addressed as a mode of failure by the current North American Design Standards. Structural members which fail by flange/web distortional buckling have shown unconservative test-to-predicted bending moment ratios when compared to current North American Design Standards [Schu 92] [Shan 94]. The introduction of lighter sections into the construction market which exhibit a failure mode not adequately predicted by current design methods has been a factor in initiating this research project.

1.2 Objectives of Work

The main objective of this work is to investigate existing analytical methods and to propose a design formulation for flange/web distortional buckling of cold formed steel sections in bending. Also included are the following secondary objectives; 1) to determine an appropriate size limit for the simple edge stiffeners of cold formed C and Z-sections in bending, 2) to refine the procedures used to calculate the effective width of a simple edge stiffener subjected to a stress gradient, and 3) to compare the existing North American Design Standards with the local buckling modifications developed by Dinovitzer and Sooi.

1.3 Scope of Work

The objectives of this work are accomplished by first carrying out a laboratory program which involved the testing of cold formed steel C-sections in bending. The test

specimens are proportioned so that all the objectives can be studied. In addition to the test program, all applicable available data found in the literature is collected and included in these studies.

The scope of this work also includes an in-depth analysis of existing analytical flange/web distortional buckling methods in comparison with current North American Design Standards. The test-to-predicted bending moment ratios are determined for all predictor methods based on the applicable test results. The current North American Design Standards and flange/web distortional buckling methods are also compared with two variations (Dinovitzer and Sooi) of the existing Canadian Design Standard.

An edge stiffener size limit is investigated by comparing the flat width ratios, d/t and d_i/w , of the applicable test specimens obtained from this study and from available data with test bending moments. Review of the current limit and its origin is also completed.

The existing procedures which are used to calculate the effective width of an edge stiffener subjected to a stress gradient are refined by comparing various plate buckling coefficient methods and magnitudes of the compression stress. The most accurate method is determined by statistically comparing the test-to-predicted bending moment ratios of the applicable test specimens.

Chapter 2

Literature Review

2.1 Plate Buckling Theory of Uniformly Compressed Plates

Prior to the work by Winter [Win 47] [Win 48] related to cold formed steel members commonly used in the building industry, engineers in the aeronautical, nautical and mechanical disciplines had begun to investigate the theory of thin plates and their structural applications. Bryan [Bry 90] found the critical elastic buckling stress for ideal flat rectangular plates, simply supported on all four sides and uniformly compressed as,

$$f_{cr} = \frac{k\pi^2 E}{12(1-\mu^2)(w/t)^2}, \quad (2.1)$$

where k = plate buckling coefficient, E = modulus of elasticity, μ = Poisson's ratio, w = width of the plate and t = thickness of the plate.

The plate buckling coefficient, k , is a function of the aspect ratio, a/w , of the flat plate, the support conditions and the applied load. This results in a plate buckling coefficient of 4 as the number of half sine waves, m , occurring in the deflected shape increases and at integer values of a/w , as shown in Figure 2.1.

Cold formed steel members rarely fail at the critical elastic buckling stress, i.e., considerable post-buckling strength can be achieved with most sections. Post-buckling is the ability of a thin plate to carry load beyond the elastic critical stress. For sections which reach the critical elastic buckling stress prior to material yielding, the post-buckling strength allows for an increase in load capacity by means of a stress redistribution (see Figure 2.2).

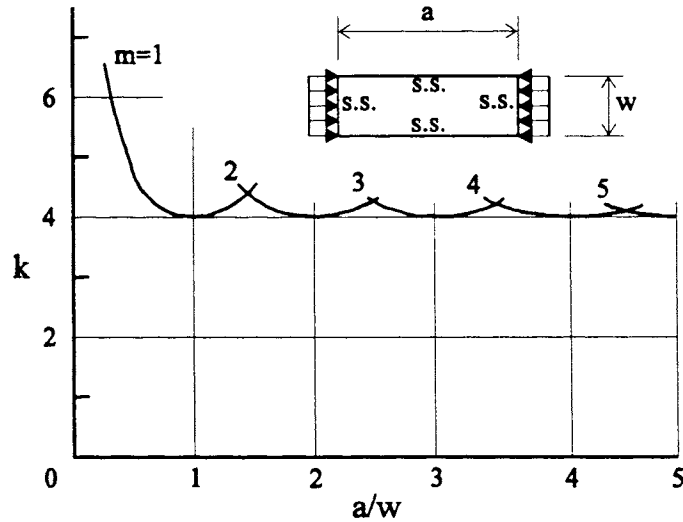


Figure 2.1 - Buckling Coefficients for Flat Rectangular Plates [Yu 91]

The stress distribution of an ideal, fully stiffened, compressed plate is uniform up to the elastic critical buckling level (Figure 2.2(a)). Elastic local buckling occurs when the stress in the centre of the plate reaches its critical value (Eq. 2.1). With increased load the stress redistributes to the outer portions of the plate (Figure 2.2(b)), eventually causing the edges to reach their yield value and ultimate failure to occur (Figure 2.2(c)). In reality, plates have initial imperfections which cause a redistribution of stress and local wave patterns to appear, well before the critical stress level is reached. Out-of-plane

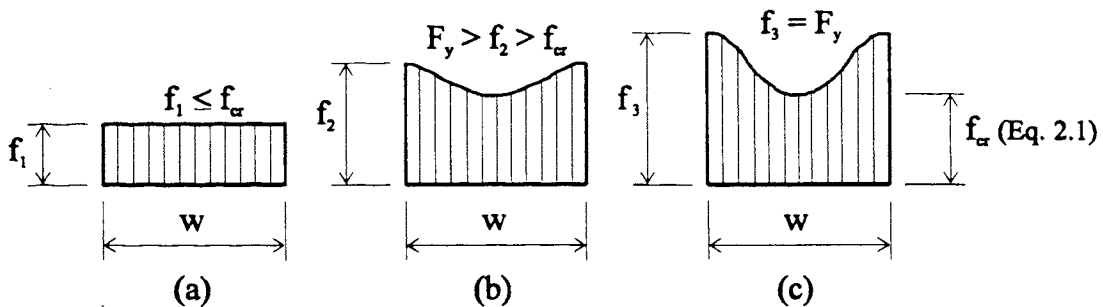


Figure 2.2 - Elastic to Post-Buckling Stress Distribution of Stiffened Uniformly Compressed Plate [Yu 91]

deformations are most pronounced for areas of the plate which have reached the elastic critical stress.

2.1.1 Post-Buckling of Uniformly Compressed Stiffened Elements

The post-buckling behaviour of uniformly compressed simply supported flat plates was first analysed in 1910 by Von Karman [Kar 10], using large deflection theory. The following fourth order partial differential equation was formulated by Von Karman to model this plate characteristic:

$$\frac{\partial^4 \omega}{\partial x^4} + 2 \frac{\partial^4 \omega}{\partial x^2 \partial y^2} + \frac{\partial^4 \omega}{\partial y^4} = \frac{t}{D} \left(\frac{\partial^2 F}{\partial y^2} \frac{\partial^2 \omega}{\partial x^2} - 2 \frac{\partial^2 F}{\partial x \partial y} \frac{\partial^2 \omega}{\partial x \partial y} + \frac{\partial^2 F}{\partial x^2} \frac{\partial^2 \omega}{\partial y^2} \right), \quad (2.2)$$

where F is a stress function and,

$$D = \frac{Et^3}{12(1-\mu^2)}, \quad \tau_{xy} = -\frac{\partial^2 F}{\partial x \partial y}, \quad f_x = \frac{\partial^2 F}{\partial y^2}, \quad f_y = \frac{\partial^2 F}{\partial x^2}.$$

Approximate solutions of Eq. 2.2, using various energy and finite element methods, have been introduced (see Timoshenko and Gere [Tim 61] and Bulson [Bul 69]), however, their application in practical design is not widespread due to their complexities. The current analytical solutions do not reflect actual element behaviour, particularly in the later stages of the post-buckling range where large deflections interact with material non-linearity. Von Karman et al. [Kar 32] developed the first effective width concept to model the post-buckling behaviour of stiffened compressed elements. The actual (solid line) and idealised (dotted line) stress distributions, as well as, the effective width of a uniformly compressed stiffened plate are shown in Figure 2.3.

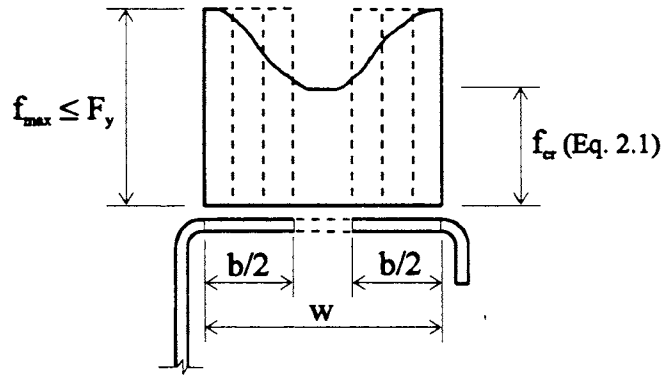


Figure 2.3 - Stress Distribution and Effective Width of Stiffened Uniformly Compressed Element

Von Karman derived an equation for the effective width of a uniformly compressed plate by setting the critical elastic stress (Eq. 2.1) equal to the yield stress, F_y , and solving for, b , as follows,

$$b = \frac{\pi}{\sqrt{3(1-\mu^2)}} t \sqrt{\frac{E}{F_y}} = 1.9t \sqrt{\frac{E}{F_y}} \quad (\text{for } \mu = 0.3). \quad (2.3)$$

Based on extensive testing, Winter [Win 47] [Win 48] modified Von Karman's effective width Eq. 2.3, to include the flat width ratio, w/t , of a uniformly compressed stiffened plate, as follows,

$$b = 1.9t \sqrt{\frac{E}{f_{\max}}} \left[1 - 0.475 \frac{t}{w} \sqrt{\frac{E}{f_{\max}}} \right]. \quad (2.4)$$

The term in the square brackets of Eq. 2.4 is a modification factor to account for the influence of imperfections in the experimental test sections. Winter [Win 56] later reduced the 0.475 coefficient, in Eq. 2.4, to 0.415 on the basis of additional experimental data, resulting in Eq. 2.5.

$$b = 1.9t \sqrt{\frac{E}{f_{\max}}} \left[1 - 0.415 \frac{t}{w} \sqrt{\frac{E}{f_{\max}}} \right] \quad (2.5)$$

Von Karman's Eq. 2.3 and Winter's Eqs. 2.4 and 2.5 were based on studies of simply supported plates without rotational constraint along their edges, hence, a plate buckling coefficient, k , of 4 was used.

2.1.2 Plate Buckling Coefficients for Fully and Partially Stiffened Uniformly Compressed Elements

An adequately sized edge stiffener is an element which enables the compressed flange to reach the same ultimate strength as an identical compressed flange stiffened by webs on both edges. In the post-buckled range the ultimate strength criterion controls the size of the edge stiffener, whereas in the elastic range the linear stability criterion is the basis of the stiffener size [Des 78a]. Chilver [Chi 53a] [Chi 53b] derived the linear stability criterion while Van Der Maas [Maa 54] presented the ultimate strength criterion for edge stiffeners.

Desmond [Des 78a] [Des 78b] [Des 81] investigated the behaviour of longitudinal edge stiffeners, identifying three possible configurations for an edge stiffened compressed element; unstiffened, partially stiffened and adequately stiffened. Desmond developed the following equations, which give the minimum required stiffener rigidity so that a plate can be considered fully stiffened:

$$(I_s / t^4)_{\text{adequate}} = 766 [(w/t) / (w/t)_\alpha - 0.461]^3, \quad (2.6)$$

for $(w/t)_\beta < (w/t) \leq (w/t)_\alpha$,

$$(I_s / t^4)_{\text{adequate}} = 115 (w/t) / (w/t)_\alpha + 5, \quad (2.7)$$

for $(w/t) > (w/t)_\alpha$,

$$\text{where } (w/t)_\alpha = 221/\sqrt{\sigma_y}, \quad (w/t)_\beta = 71.7/\sqrt{\sigma_y}. \quad (2.8)$$

I_s is the moment of inertia of the edge stiffener required to adequately stiffen the flange. The most recent edition of the Canadian Standard [CSA 94] uses Eq. 2.7 and a modified version of Desmond's Eq. 2.6.

Desmond [Des 78a] also developed plate buckling coefficients for a compressed flange, which are a function of the adequacy and depth of the edge stiffener, as well as, the flat width of the flange. The corresponding plate buckling coefficient equations used in both North American Design Standards are given in Chapter 3.

Dinovitzer et al. [Din 92] proposed a modification of the exponent values for the plate buckling coefficient equations derived by Desmond. Dinovitzer's revised exponent method is discussed and compared with the current North American Design Standards in Chapter 8.

2.1.3 Unstiffened Uniformly Compressed Elements

An effective width concept was also derived for a uniformly compressed unstiffened element [Win 47]. The actual (solid line) and idealised (dotted line) stress distributions, as well as, effective width of a uniformly compressed unstiffened plate are shown in Figure 2.4.

Winter [Win 47] developed an equation for the effective width of unstiffened compressed elements, based on the work by Miller [Mil 43], given on the following page (Eq. 2.9).

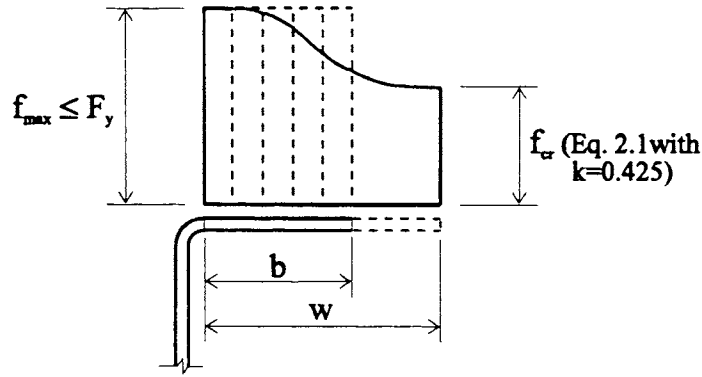


Figure 2.4 - Stress Distribution and Effective Width of Unstiffened Uniformly Compressed Element

$$b = 0.8t \sqrt{\frac{E}{f_{\max}}} \left[1 - 0.202 \frac{t}{w} \sqrt{\frac{E}{f_{\max}}} \right]. \quad (2.9)$$

Equation 2.9 was later modified by Jombock and Clark [Jom 61] to present the effective width as a function of the critical and maximum effective stresses, as follows,

$$\frac{b_e}{w} = 1.19 \sqrt{\frac{f_{cr}}{f_{e \max}}} \left[1 - 0.3 \sqrt{\frac{f_{cr}}{f_{e \max}}} \right]. \quad (2.10)$$

Kalyanaraman [Kal 77] [Kal 78] investigated the theoretical and empirical forms of an equation which could be used to calculate the effective width of a uniformly compressed unstiffened element. The following empirical equation for the effective width was developed:

$$\frac{b_e}{w} = 1.19 \sqrt{\frac{f_{cr}}{f_{e \max}}} \left[1 - 0.298 \sqrt{\frac{f_{cr}}{f_{e \max}}} \right]. \quad (2.11)$$

Kalyanaraman also concluded that Winter's stiffened effective width Eq. 2.5 was adequate, although conservative, for most practical flat width ratios, w/t , of uniformly compressed unstiffened elements. Winter's Eq. 2.5 for stiffened elements is specified in

the most recent North American Design Standards [AISI 89a] [CSA 94] for the calculation of the effective width of a stiffened or unstiffened element.

The Canadian Standard [CSA 94] presents a unified effective width approach which allows for stiffened elements with variable rotational edge conditions, i.e., $0.43 \leq k \leq 4$ and sub-ultimate stress levels, as seen in Eq. 2.12 (see Chapter 3).

$$b = 0.95t \sqrt{\frac{kE}{f}} \left[1 - 0.208 \frac{t}{w} \sqrt{\frac{kE}{f}} \right] \quad (2.12)$$

2.1.4 Buckling Coefficients for Unstiffened Uniformly Compressed Elements

The North American Design Standards [AISI 89a] [CSA 94] specify that the effective width of an unstiffened uniformly compressed element is determined using Eq. 2.12 with a buckling coefficient, k , of 0.43. This procedure has been thoroughly studied by Kalyanaraman [Kal 77] [Kal 78] and appears to be well understood.

2.1.5 Buckling Coefficients for Unstiffened Elements Subjected to a Stress Gradient

In cross sections subjected to bending, where the edge stiffener (lip) is of a simple shape, i.e., without stiffeners of its own, the buckling coefficient is given in the North American Design Standards [AISI 89a] [CSA 94] as 0.43. The applied stress is assumed to be uniform at the maximum compressed position of the lip, i.e., at the top of the flat width (see f_3 in Figure 2.5). Peköz [Pek 87] recommended that this simplified conservative approximation be contained in both the Canadian and the American Standards, since there is a lack of experimental data regarding edge stiffener behaviour under a stress gradient.

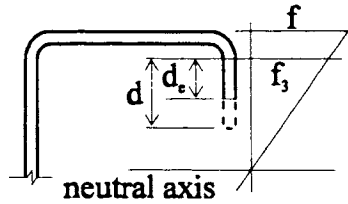


Figure 2.5 - Unstiffened Element Subjected to a Stress Gradient

Equations for the buckling coefficient of an unstiffened element subjected to a stress gradient have been formulated by Kollbrunner and Meister [Kol 58], Thomasson [Tho 78] and Cohen [Coh 87]. These researchers have defined the plate buckling coefficient, k , based on a ratio of compressive stresses at the top and bottom of the flat width. See Chapter 6 for a discussion and comparison of these stress gradient plate buckling coefficient equations with applicable experimental results.

2.1.6 Buckling Coefficients for Stiffened Elements Subjected to a Stress Gradient

LaBoube [LaB 78] studied the behaviour of beam webs subjected to pure bending stress and compared existing web strength formulations with his own effective width and moment reduction techniques. LaBoube developed three methods with which the buckling and post-buckling strength of webs could be evaluated, as follows:

- 1) *Post buckling strength of the web method,*
- 2) *Reduction in moment resistance method,*
- 3) *Simplified reduction in moment resistance method.*

LaBoube concluded that the strength of the web element is a function of the web slenderness ratio, the bending stress ratio, the yield stress and the flat width ratio of the flange. This fourth criterion involves element interaction and is discussed in Section 2.3.

LaBoube's studies led to the web treatment specified in the current North American Design Standards [AISI 89a] [CSA 94]. The Canadian formulation is given in Eqs. 2.13 to 2.15.

$$q = |f_2/f_1| \quad (2.13)$$

$$k_{web} = 4 + 2(1-q)^3 + 2(1-q) \quad \text{for } 0 \leq q \leq 1 \quad (2.14)$$

$$k_{web} = 6(1+q)^2 \quad \text{for } 1 < q \leq 3 \quad (2.15)$$

Where f_1 and f_2 are the stresses at the top and bottom of the flat width of the web, h , respectively (see Figure 2.6). Distribution of the effective width, b_1 and b_2 , as well as the plate buckling coefficient calculation procedure are explained fully in Chapter 3.

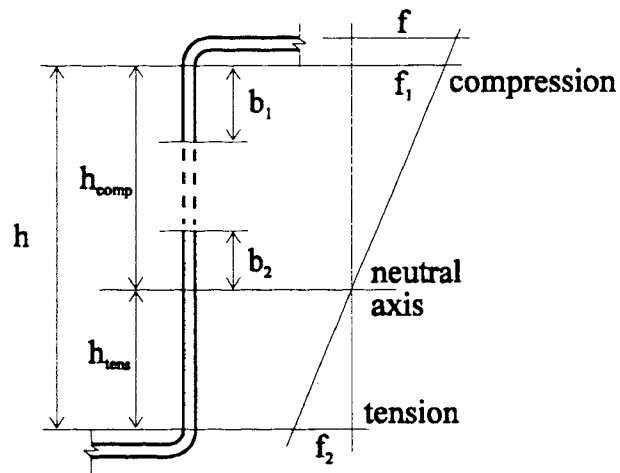


Figure 2.6 - Web Element Subjected to a Stress Gradient

Sooi [Soo 93] proposed a modification of the effective width distribution of the web element subjected to a stress gradient. A discussion of this method and a comparison to the current North American Design Standards are given in Chapter 8.

2.2 Simple Edge Stiffener Definition

The edge stiffener length, d_i , which is found in Desmond's work [Des 78a] has various definitions. In figures it is drawn as the flat width of the lip, d , plus the inside bend radius of the corner, r_i , plus the thickness of the plate, t , and in the notation it is defined as the flat width of the lip plus the inside bend radius of the corner. Cohen [Coh 87] considered three definitions for the lip depth; 1) The sum of the flat width plus the distance along the outside surface of the corner, 2) only the flat width and 3) the sum of the flat width plus the inside bend radius of the corner plus the plate thickness. Cohen concluded that the most appropriate edge stiffener dimension for Desmond's plate buckling coefficient equations was the sum of the flat width, the inside bend radius of the corner and the thickness of the plate. Both North American Design Standards adopted this definition for d_i [AISI 89a] [CSA 94] (see Figure 2.7).

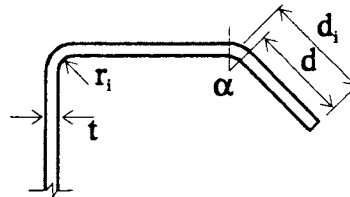


Figure 2.7 - Simple Edge Stiffener Dimension Definition [CSA 94]

The moment of inertia of the edge stiffener, I_s , is consistently defined by the North American Design Standards [AISI 89a] [CSA 94], Cohen [Coh 87] and Desmond [Des 78a] as,

$$I_s = (td^3) (\sin^2 \alpha) / 12, \quad (2.16)$$

where d is the flat width of the edge stiffener and α is its angle with respect to the vertical (see Figure 2.7).

Cohen [Coh 87] experimented with four definitions of the moment of inertia, I_s , varying the definition of d as follows:

- 1) d_{eff} ,
- 2) $d_{eff} + (r_i + t/2) \tan \alpha/2$,
- 3) $d_{eff} + (r_i + t) \tan \alpha/2$,
- 4) *the flat width*,

where d_{eff} is the effective width of the edge stiffener. Cohen [Coh 87] considered the corners to be sharp, where the thickness is approximately equal to the inside bend radius. Therefore, her conclusion that a measurement of the flat width is adequate is understandable, since an increase in stiffener length due to the corner term would be minimal. However, Cohen [Coh 87] did not vary the location of the reference neutral axis, i.e., at the centroid of the edge stiffener or at the centroid of the stiffened element. The later definition involved the transfer formula for moment of inertia, which was investigated by Desmond [Des 78a]. Desmond derived an expression which used the centroid of the stiffened plate as a reference for the moment of inertia of the edge stiffener, as follows,

$$I_{s_{modified}} = I_{s_{centroidal}} + \frac{z_s^2 A_s}{\left(1 + H \frac{A_s}{wt}\right)}, \quad (2.17)$$

where A_s is the flat area of the stiffener, z_s is the distance from the stiffener centroid to the stiffened plate centroid and H is a shear correction term. The shear correction term modelled the relocation of the stiffener neutral axis due to the shear stresses at the stiffener-flange juncture. Desmond graphically compared the modified moment of inertia of the stiffener with various other simplified methods. He concluded that the centroidal moment of inertia was adequate because *the influence of shear stresses at the stiffener-flange juncture is negligible* [Des 78a]. Hence, Desmond proposed that the moment of

inertia of the stiffener be calculated about the centroid of the edge stiffener, as in Eq. 2.16.

2.3 Flange/Web Interaction

Experimental testing recently completed by Schuster [Schu 92] and Shan [Shan 94] has shown that the predicted bending moment resistance for certain types of cold formed C-sections is unconservative. Standard industry C-sections, as tested by Schuster [Schu 92], exhibited a distortional mode of failure of the flange/web elements, which is not addressed in the current North American Design Standards [AISI 89a] [CSA 94].

The local buckling interaction of the web and flange for stiffened and unstiffened singly symmetric sections, i.e., channels, was investigated by Mulligan [Mul 83]. Mulligan created a finite strip analysis computer program which could develop the appropriate plate buckling coefficient, k , and proposed a graphical method to determine the buckling coefficients using the computer results. Mulligan's resulting graphs were based on the ratio of the flat width of the web and flange. This formulation can be used with unstiffened channels but not with stiffened channels since the influence of the lip depth was not included. The scope of his study was limited to sections with stiffeners that had an adequate moment of inertia such that local buckling would originate in the compressed flange.

Cohen [Coh 87] concluded that Mulligan's graphical methods produced acceptable and conservative results but were not required for all dimensional variations. Cohen recommended that for unstiffened channels with $W/H < 0.25$ and $W/H > 0.75$, where W and H are the flat widths of the flange and web, respectively, Mulligan's interaction coefficients can be used. For W/H ratios outside this range the individual plate buckling coefficients can be used. Cohen also stated that for stiffened channels a graphical method cannot be used since the buckling coefficients are dependent on a third criterion, i.e., the

flat width of the edge stiffener. However, when the flange is adequately stiffened, as were Mulligan's tests ($k = 4$), then the interaction coefficients could be used for $W/H < 0.8$ and $W/H > 1.2$. Again, for W/H ratios outside this range the individual element buckling coefficients can be used. Normally the flange of an edge stiffened member is not adequately stiffened and Mulligan's interaction buckling coefficients do not apply. A finite strip method computer program, which accounts for all the variations in the flat width ratios of the web, flange and lip would be required to accurately predict the interaction buckling coefficients of stiffened members.

2.4 Flange/Web Distortional Buckling

Sharp [Sha 66] [Sha 93] developed an analytical model which could be used to predict the flange/web distortional buckling strength of slender aluminum columns. The procedures developed by Sharp were modified by Hancock [Han 85], Lau & Hancock [Lau 87] [Lau 90], Kwon & Hancock [Kwo 91] [Kwo 92] and Charnvarnichborikarn [Cha 92] [Cha 93] to produce flange/web distortional buckling formulae for cold formed steel C and Z-columns. Currently only the Australian steel storage racking Standard [SAA 93] contains guidelines regarding the analysis of the flange/web mode of distortional buckling for columns. The unpublished 3rd Committee Draft of the Australia / New Zealand Cold-formed steel structures Standard [SAA 94] contains methods, developed by Lau & Hancock [Lau 87] [Lau 90], which can be used to calculate the flange/web distortional buckling stress of C and Z-sections in compression and bending.

Initial research into the distortional buckling behaviour of beams was completed by Hancock in 1978 [Han 78]. More recently, a study to develop local interaction buckling coefficients for the web and flange of built-up slender plate girders was completed by Polyzois at the University of Manitoba [Pol 90]. Methods which can be used to determine the bending strength of beams which fail by flange/web distortional buckling have been proposed by Moreyra [Mor 93], Marsh [Mar 90] and Charnvarnichborikarn

[Cha 92]. These beam methods have yet to be adequately compared using all relevant test data currently available. The existing flange/web distortional buckling methods for members in bending are thoroughly discussed in Chapter 7.

Chapter 3

Moment Resistance of Laterally Supported Members

3.1 Gross Moment Resistance

The linear method of computation is commonly used to calculate the pertinent gross cross section properties of cold formed steel sections. The S136 Standard [CSA 94] and the AISI Specification [AISI 89a] follow the guidelines given in Part III, Supplementary Information, of the AISI Cold-Formed Steel Design Manual [AISI 86a]. Members are divided into line elements of consistent shape and thickness, usually the flat width, e.g., flange flat width, and corner components. The length, L , moment of inertia, I' , and distance from the extreme compressive fibre, Y , are calculated for each element and summed to determine gross properties. The moment of inertia for elements parallel to the neutral axis is negligible and assumed to be zero. The centre of gravity of the gross cross-section, Y_{CG} , is given as,

$$Y_{CG} = \frac{\sum(L \cdot Y)}{\sum L}. \quad (3.1)$$

The gross moment of inertia, I_{XG} , about the centre of gravity of the gross cross-section is calculated from the following equation,

$$I_{XG} = t(\sum I' + \sum(L \cdot Y^2) - \sum L \cdot Y_{CG}^2). \quad (3.2)$$

The gross section moduli, S_{XGT} tensile and S_{XGC} compressive, are calculated and the lesser is used to determine the nominal gross bending moment resistance, M_{RG} , as shown on the following page:

$$S_{XGC} = \frac{I_{XG}}{Y_{CG}}, \quad (3.3)$$

$$S_{XGT} = \frac{I_{XG}}{\text{depth} - Y_{CG}}, \quad (3.4)$$

$$M_{RG} = \phi S_{XG} F_y, \quad (3.5)$$

where $\phi = 1$ when the actual yield strength is known. If the section does not need to be reduced in size, arising from the effective width calculations (see Sections 3.2 and 3.3), then the gross bending moment resistance is used in comparison with test moments. Detailed numerical examples for the S136 Design Standard [CSA 94] and the AISI Design Specification [AISI 89a] can be found in Appendix 'C'.

3.2 Effective Moment Resistance Based on S136-94 [CSA 94]

The following is a list of the procedures outlined in the S136-94 Design Standard [CSA 94] for the effective moment resistance of laterally supported cold formed steel members in bending. The origins of the procedures shown in this Chapter were previously discussed in Chapter 2. Detailed numerical examples of these procedures can be found in Appendix 'C'.

The effective widths of the compressed edge stiffener, flange and the web elements are calculated with an iterative procedure using the gross centre of gravity as an initial point of zero stress. If multiple iterations are required, the most current centre of gravity is used for all stress level calculations.

3.2.1 Effective Width of a Uniformly Compressed Edge-Stiffened Flange Element

The flat width of the flange, w , is calculated as the overall width minus the thickness, t ,

and inside bend radius, r_i , for each corner. The flat width ratio, w/t , has a limit of 60 as given in Clause 5.4 of S136-94 [CSA 94].

The "Case" of the flange is determined depending on the following flat width ratio limits,

$$W_{lim1} = 0.644\sqrt{kE/f} \quad \text{with } k = 0.43,$$

$$W_{lim2} = 0.644\sqrt{kE/f} \quad \text{with } k = 4,$$

where $f = F_y$ or F_y' when cold work of forming is used. The "Case" of the flange is determined as follows,

$$\text{Case I flange} \quad w/t \leq W_{lim1},$$

$$\text{Case II flange} \quad W_{lim1} < w/t \leq W_{lim2},$$

$$\text{Case III flange} \quad w/t > W_{lim2}$$

The influence of the edge stiffener (lip) is determined by means of the adequate moment of inertia, I_a , equations, as follows,

$$\text{Case I flange} \quad I_a = 0 \text{ (no edge stiffener required),}$$

$$\text{Case II flange} \quad I_a = 399t^4 (W / W_{lim2} - 0.327)^3,$$

$$\text{Case III flange} \quad I_a = t^4 [115 (W / W_{lim2}) + 5],$$

where $W = w/t$.

The flat width ratio of the lip, d/t , is limited to 14 and the ratio of the out-to-out depth of the lip to the flat width of the flange, d_i/w , is limited to 0.8, given in Clause 5.6.2.3 of S136-94 [CSA 94]. The moment of inertia of the simple edge stiffener is calculated about its own centroid, as previously defined in Eq. 2.16.

$$I_s = t d^3 \sin^2(\alpha) / 12$$

The ratio of actual to adequate moment of inertia ($I_r = I_s / I_a$) is calculated and used with the following equations to determine the plate buckling coefficient for the compressed flange element.

Table 3.1 - Buckling Coefficients for Edge-Stiffened Flange Elements

		$d_i/w \leq 0.25$	$0.25 < d_i/w \leq 0.8$
Case II	$I_r \geq 1$	$k = 4$	$k = 5.25 - 5(d_i/w)$
	$I_r < 1$	$k = 3.57 (I_r)^{1/2} + 0.43$	$k = [4.82 - 5(d_i/w)] (I_r)^{1/2} + 0.43$
Case III	$I_r \geq 1$	$k = 4$	$k = 5.25 - 5(d_i/w)$
	$I_r < 1$	$k = 3.57 (I_r)^{1/3} + 0.43$	$k = [4.82 - 5(d_i/w)] (I_r)^{1/3} + 0.43$

Note: $d/t \leq 14$

If the flange is not supported by an edge stiffener, the plate buckling coefficient, k , is equal to 0.43. The flat width ratio limit, W_{lim} , is calculated and compared to the flat width ratio of the flange, w/t .

$$W_{lim} = 0.644 \sqrt{kE / f} \quad \text{with } f = F_y \quad \text{or } f = F_y'$$

If $w/t > W_{lim}$ then the flange must be reduced in width according to the following equation,

$$B = 0.95 \sqrt{\frac{kE}{f}} \left[1 - \frac{0.208}{W} \sqrt{\frac{kE}{f}} \right],$$

where $W = w/t$ and $b = Bt$ is the effective width of the flange, which is separated into components using the equations on the following page:

$$b_1 = I_r Bt/2 \leq Bt/2,$$

$$b_2 = Bt - b_1.$$

Figure 3.1 shows the gross dimensions, effective widths and stress distribution of a typical edge-stiffened flange element subjected to a uniform compressive stress.

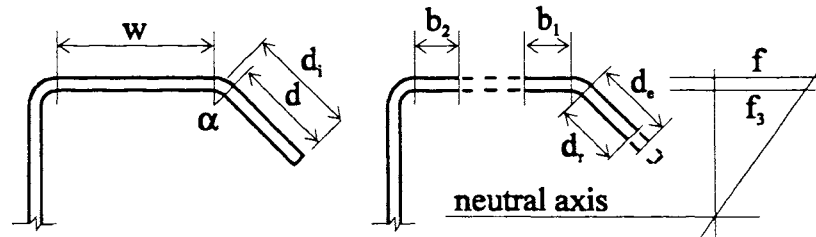


Figure 3.1 - Edge-Stiffened Flange Element Subjected to Uniform Compressive Stress [CSA 94]

The compressive stress in the flange, f , is not dependent on the position of the neutral axis unless failure of the tensile flange initially occurs. If the cross-section of the member is such that the tensile flange reaches the maximum allowable stress, F_y or F_y' , prior to failure of the compressive flange, then the stress values used in the effective width formulation will depend on the position of the neutral axis.

3.2.2 Effective Width of a Compressed Simple Edge Stiffener (Lip)

The flat width of the simple edge stiffener, d , is calculated as the out-to-out width of the lip, d_1 , minus the thickness and the inside bend radius. The flat width ratio, d/t , has a limit of 14 as given in Clause 5.6.2.3 of S136-94 [CSA 94]. The plate buckling coefficient, k , equals 0.43 and the lip is assumed to be subjected to a uniform compressive stress, f_3 , which is located at the top of the flat width (see Figure 3.1).

The flat width ratio limit, W_{lim} , is calculated and compared to the flat width ratio of the lip, d/t .

$$W_{lim} = 0.644\sqrt{kE/f} \quad \text{with } f = f_3 \text{ and } k = 0.43$$

If $d/t > W_{lim}$ then the lip must be reduced in width according to the basic effective width equation, as follows,

$$d_e = 0.95t\sqrt{\frac{kE}{f}} \left[1 - 0.208\frac{t}{d}\sqrt{\frac{kE}{f}} \right],$$

where d_e is the effective width of the lip which may be further reduced if the lip does not have an adequate moment of inertia to support the flange. Inadequately stiffened elements typically fail in the lip/flange distortional mode with both the flange element and the stiffener buckling out-of-plane together. If $I_r < 1$, then the effective width of the lip is represented by d_r where $d_r = d_e \cdot I_r$.

3.2.3 Effective Width of a Web Element Subjected to a Stress Gradient

The flat width of a web element, h , is calculated as the out-to-out depth minus the thickness and the inside bend radius at the top and bottom of the section. The flat width ratio, h/t , for sections with unreinforced webs is limited to 200 as given in Clause 5.5.1 of S136-94 [CSA 94].

The plate buckling coefficient for the web is dependent on the ratio of the compressive and tensile stresses at the top and bottom of the flat width, respectively, and is expressed as on the following page:

$$k = 4 + 2(1 + q)^3 + 2(1 + q) \quad 0 \leq q \leq 1$$

$$k = 6(1 + q)^2 \quad 1 < q \leq 3$$

Where $q = |f_2 / f_1|$.

Figure 3.2 shows the gross dimension and effective widths of a typical web element subjected to a stress gradient.

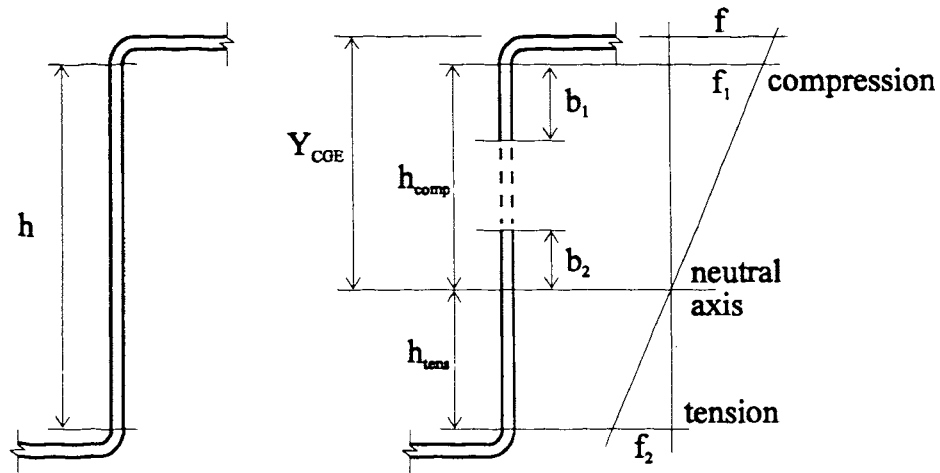


Figure 3.2 - Web Element Subjected to a Stress Gradient [CSA 94]

The flat width ratio limit, W_{lim} , is calculated and compared to the flat width ratio of the web, h/t .

$$W_{lim} = 0.644\sqrt{kE/f} \quad \text{with } f = f_1$$

If $h/t > W_{lim}$, then the web must be reduced in width according to the basic effective width equation, as follows,

$$h_e = 0.95t\sqrt{\frac{kE}{f}} \left[1 - 0.208\frac{t}{h}\sqrt{\frac{kE}{f}} \right],$$

where h_e is the effective width of the web which is separated into components, as follows,

$$b_1 = h_e / (3 + q),$$

$$b_2 = h_e / (1 + q) - b_1.$$

If $b_1 + b_2 > h_{comp}$ then $b_2 = h_{comp} - b_1$.

The length, moment of inertia and the distance from the extreme compressive fibre are updated for the elements of the partially effective lip, flange and web. The effective centre of gravity, Y_{CGE} , is calculated as in Eq. 3.1 and compared to the previous centre of gravity. If the effective centre of gravity is not approximately equal to the previous centre of gravity then further iterations are required, with Y_{CGE} used to determine the stress values for each of the elements. When the position of the centre of gravity converges, the effective moment of inertia, I_{XE} , effective section modulus, S_{XE} , and nominal effective moment resistance, M_{RE} , can be calculated according to Eqs. 3.1 - 3.5, substituting gross element dimensions with calculated effective widths.

3.2.4 Cold Work of Forming

Cold formed steel sections are unique in that they experience an increase in the material yield stress depending on the amount of cold work that occurs during the forming process. The increase in yield stress, F_y , is due to strain hardening of the material as it is bent at the corners and is calculated using the following equation,

$$F_y' = F_y + 5D_A (F_u - F_y) / W^*,$$

where F_y' is the average yield strength of the section incorporating cold work of forming, D_A is the number of 90° corners in the compressed flange, F_u is the ultimate tensile strength and W^* is the ratio of the centreline length of the flange cross section to the thickness. Cold work of forming is only applicable if the compressed flange and edge

stiffener are fully effective, i.e., $w/t < W_{lim}$, $d/t < W_{lim}$, and the lip has an adequate moment of inertia, i.e., $I_r > 1$.

3.3 Effective Moment Resistance Based on AISI [AISI 89a]

The following is a list of the procedures outlined in the AISI Design Specification [AISI 89a] for the effective moment resistance of laterally supported cold formed steel members in bending. The AISI and S136 [CSA 94] design criteria differ primarily in the syntax used, distribution of the effective web elements, b_1 and b_2 , and in the treatment of cold work of forming. The basic theory of the Canadian and American Standards was derived from the same research and theoretical approaches. The origins of the procedures shown in this Chapter were previously discussed in Chapter 2. Detailed numerical examples of these procedures can be found in Appendix 'C'.

The effective widths of the compressed edge stiffener, flange and the web elements are calculated with an iterative procedure using the gross centre of gravity as an initial point of zero stress. If multiple iterations are required, the most current centre of gravity is used for all stress level calculations. This is identical to the procedure outlined in Section 3.2 for the S136-94 Standard [CSA 94].

3.3.1 Effective Width of a Uniformly Compressed Edge-Stiffened Flange Element

The flat width of the flange, w , is calculated as the overall width minus the thickness, t , and inside bend radius, R , for each corner. The flat width ratio, w/t , has a limit of 60 as given in Sec. B1.1 of the AISI Specification [AISI 89a].

The "Case" of the flange is determined depending on the following flat width ratio limit,

$$S = 1.28\sqrt{E/f},$$

where $f = F_y$ or F_{ya} when cold work of forming is used and the "Case" of the flange is determined as follows,

Case I flange	$w/t \leq S/3,$
Case II flange	$S/3 < w/t \leq S,$
Case III flange	$S < w/t.$

The influence of the edge stiffener (lip) is determined by means of the applicable adequate moment of inertia, I_a , equation. The flat width ratio of the lip, d/t , is limited to 60 and the ratio of the out-to-out depth of the lip to the flat width of the flange, D/w , is limited to 0.8 given in Sec. B1.1 and Sec. B4.2, respectively, of the AISI Specification [AISI 89a].

Case I flange	$I_a = 0$ (no edge stiffener required)
Case II flange	$I_a = 399t^4((w/t)/S - 0.33)^3$
Case III flange	$I_a = t^4[115((w/t)/S) + 5]$

The moment of inertia of the simple edge stiffener is calculated about its own centroid, as previously defined in Eq. 2.16.

$$I_s = t d^3 \sin^2(\theta) / 12$$

The equations found below and on the following page are used to determine the plate buckling coefficient for a compressed flange.

Case I	$k = 4$
--------	---------

$$\begin{aligned} \text{Case II} & \quad k = [4.82 - 5(D/w)] (I_s/I_a)^n + 0.43 \leq 5.25 - 5(D/w) \\ & \quad \text{for } 0.8 \geq D/w > 0.25 \\ & \quad \& \\ \text{Case III} & \quad k = 3.57 (I_s/I_a)^n + 0.43 \leq 4 \\ & \quad \text{for } D/w \leq 0.25 \end{aligned}$$

For Case II $n = 1/2$ and for Case III $n = 1/3$.

If the flange is not supported by an edge stiffener, the plate buckling coefficient, k , is equal to 0.43. The flat width slenderness factor limit of 0.673 is compared to the actual slenderness factor of the flange, λ .

$$\lambda = \frac{1.052}{\sqrt{k}} \left(\frac{w}{t} \right) \sqrt{\frac{f}{E}} \quad \text{with } f = F_y \quad \text{or } f = F_{ya}$$

If $\lambda > 0.673$, then the flange must be reduced in width according to the following equations,

$$b = \rho w,$$

$$\rho = (1 - 0.22/\lambda)/\lambda,$$

where b is the effective width of the flange which is separated into components with the following equations,

$$C_2 = I_s/I_a \leq 1,$$

$$C_1 = 2 - C_2.$$

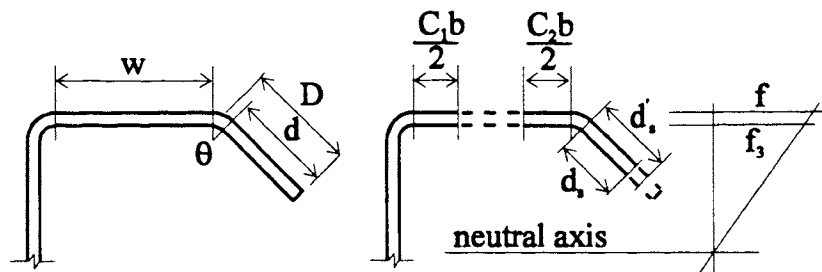


Figure 3.3 - Edge-Stiffened Flange Element Subjected to Uniform Compressive Stress [AISI 89a]

Figure 3.3 shows the gross dimensions, effective widths and stress distribution of a typical edge-stiffened flange element subjected to uniform compressive stress.

The compressive stress in the flange, f , is not dependent on the position of the neutral axis unless failure of the tensile flange initially occurs. If the cross-section of the member is such that the tensile flange reaches the maximum allowable stress, F_y or F_{ya} , prior to failure of the compressive flange, then the stress values used in the effective width formulation will depend on the position of the neutral axis.

3.3.2 Effective Width of a Compressed Simple Edge Stiffener (Lip)

The flat width of the simple edge stiffener, d , is calculated as the out-to-out width of the lip, D , minus the thickness and the inside bend radius. The flat width ratio, d/t , has a limit of 60 as given in Sec. B1.1 of the AISI Specification [AISI 89a]. The plate buckling coefficient, k , equals 0.43 and the lip is assumed to be subjected to a uniform compressive stress, f_3 , which is located at the top of the flat width (see Figure 3.3).

The flat width slenderness factor limit of 0.673 is compared to the actual slenderness factor of the lip, λ .

$$\lambda = \frac{1.052}{\sqrt{k}} \left(\frac{d}{t} \right) \sqrt{\frac{f}{E}} \quad \text{with } f = f_3 \text{ and } k = 0.43$$

If $\lambda > 0.673$, then the lip must be reduced in width according to the following equations,

$$d'_s = \rho w,$$

$$\rho = (1 - 0.22/\lambda)/\lambda,$$

where d'_s is the effective width of the lip which may be further reduced if the lip does not have an adequate moment of inertia. If $I_s/I_a < 1$, then the effective width of the lip is represented by d_s where $d_s = d'_s \cdot I_s/I_a$.

3.3.3 Effective Width of a Web Element Subjected to a Stress Gradient

The flat width of the web element, h , is calculated as the out-to-out depth minus the thickness and the inside bend radius at the top and bottom of the section. The flat width ratio, h/t for sections with unreinforced webs is limited to 200 as given by the AISI Specification [AISI 89a].

The plate buckling coefficient for the web is dependent on the ratio of the compressive and tensile stresses at the top and bottom of the flat width, respectively, and is given as follows.

$$k = 4 + 2(1 - \psi)^3 + 2(1 + \psi),$$

where $\psi = f_2 / f_1$.

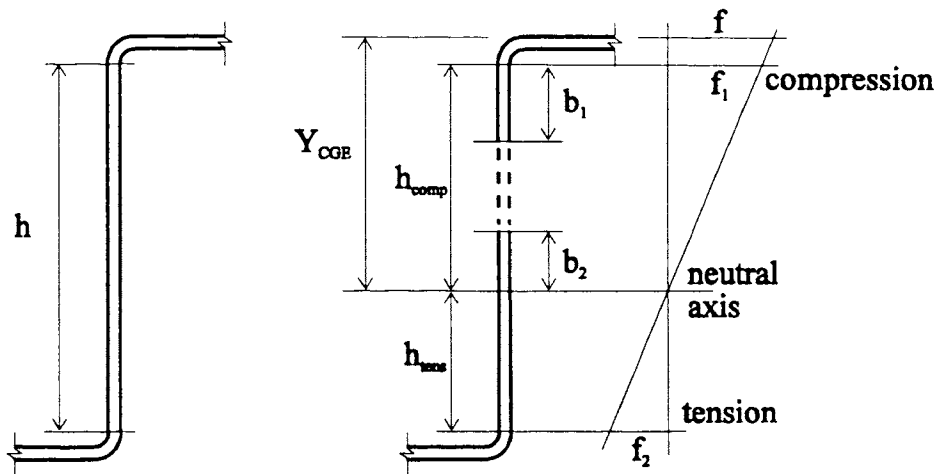


Figure 3.4 - Web Element Subjected to a Stress Gradient [AISI 89a]

Figure 3.4 shows the gross dimensions, effective widths of a typical web element subjected to a stress gradient.

The flat width slenderness factor limit of 0.673 is compared to the actual slenderness factor of the web, λ .

$$\lambda = \frac{1.052}{\sqrt{k}} \left(\frac{h}{t} \right) \sqrt{\frac{f}{E}} \quad \text{with } f = f_1$$

If $\lambda > 0.673$, then the web must be reduced in width according to the following equations,

$$b_e = \rho w,$$

$$\rho = (1 - 0.22/\lambda)/\lambda,$$

where b_e is the effective width of the web which is separated into components, as follows,

$$b_1 = b_e/(3 - \psi),$$

$$\text{for } \psi \leq -0.236 \quad b_2 = b_e/2,$$

$$\text{for } \psi > -0.236 \quad b_2 = b_e - b_1.$$

If $b_1 + b_2 > h_{\text{comp}}$ then $b_2 = h_{\text{comp}} - b_1$.

The length, moment of inertia and the distance from the extreme compressive fibre are updated for the partially effective lip, flange and web. The effective centre of gravity, Y_{CGE} , is calculated as in Eq. 3.1 and compared to the previous centre of gravity. If the effective centre of gravity is not approximately equal to the previous centre of gravity then further iterations are required with Y_{CGE} used to determine the stress values for each of the elements. When the position of the centre of gravity converges, the effective moment of inertia, I_{XE} , effective section modulus, S_{XE} , and nominal effective bending

moment resistance, M_{RE} , are calculated according to Eqs. 3.1 - 3.5, substituting gross element dimensions with calculated effected widths.

3.3.4 Cold Work of Forming

The AISI Design Specification [AISI 89a] also allows for an increase in yield stress, F_y , depending on the amount of cold work that occurs during the forming process. The influence of cold work of forming is determined from the following equations:

$$F_{ya} = C F_{yc} + (1 - C) F_y,$$

$$F_{yc} = B_c F_y / (R/t)^m,$$

$$B_c = 3.69 (F_u / F_y) - 0.819 (F_u / F_y)^2 - 1.79,$$

$$m = 0.192 (F_u / F_y) - 0.068,$$

where F_{ya} is the average yield strength of the section incorporating cold work of forming, C is the ratio of the total corner cross sectional area of the controlling flange to the full cross sectional area of the controlling flange and F_u is the ultimate tensile strength of the steel. Cold work of forming is only applicable if the flange and edge stiffener are fully effective, i.e., $\lambda \leq 0.673$.

Chapter 4

Waterloo Test Program

4.1 General

Fifty-nine beam specimens were tested in the structures laboratory at the University of Waterloo in order to accomplish the stated objectives of this work. The main objective of the experimental testing phase was to complete a series of tests consisting of sections with locally stable webs, i.e., fully effective according to S136 [CSA 94], constant flange widths and systematically varied edge stiffener (lip) depths. This series was then repeated with sections that had increased web depths, resulting in locally unstable or partially effective webs according to S136, with all other dimensions as per the previous series. For example, the C1-1 series consisted of sections with locally stable webs, whereas the C1-2 series consisted of sections with the same flange and edge stiffener dimensions, but locally unstable webs. This sizing philosophy was used to isolate the interaction behaviour of the lip/flange component and to allow the flange/web interaction problem to be studied independently.

Edge stiffener depths were varied so that investigations of the d/t limit and the stress gradient approach for effective width calculations could be completed, as well as, to determine the effect of edge stiffener size on the flange/web interaction problem. The depth of the tensile lip was held constant so that a direct comparison of compressed edge stiffener depth and moment resistance could be made (except for series C2-1). Test specimens were also proportioned to cover the full range of dimensions allowed by the North American Design Standards [AISI 89a] [CSA 94], e.g., $h/t \leq 200$. A summary of the out-to-out dimensions for all test specimens can be found in Tables A.1a and A.1b of Appendix 'A', with corresponding cross sections given in Figure A.1 of Appendix 'A'.

Based on the North American Design Standards [AISI 89a] [CSA 94], effective width analysis requires that a "Case" (I, II or III) be determined from the flat width ratio of the compressed flange. Various equations for adequate moment of inertia of the supporting edge stiffener and the flange plate buckling coefficient are dependent on this "Case" classification (see Chapter 3). Sections with Case I, II and III flanges were included, all of which had flat width ratios, w/t , within the specified limit of 60.

4.1.1 Designation of Test Specimens

Each test specimen was identified by an alpha-numeric title, e.g., C2-DW35-3-A,B, which gives certain basic information regarding the properties of the C-sections used. The prefix of the specimen identification number indicates the particular "Case" of the flange used in sizing the members, e.g., C2 = Case II. However, the limits which were used to determine the flange "Case" were dependent on the tensile yield strength of the steel, F_y . Yield strength ranges were estimated for each series based on preliminary tensile coupon tests. In some instances the actual yield strength was above the assumed range, thus changing the "Case" of the flange. Specimen identification numbers were not altered for these occurrences. For example, the C2R-1 series was added because test specimens in the C2-1 series fluctuated between Case II and III due to higher than predicted yield strengths. Also affected by elevated yield strengths were test specimens in the C1-3 series which had flange flat width ratios, w/t , slightly above the W_{lim1} limit, resulting in Case II C-sections.

The second segment of the specimen identification number gives an approximate value for the d_l/w ratio (lip out-to-out width / flange flat width) so that lip dimensions can be compared, e.g., DW35 : $d_l/w = 0.35$. Due to limitations in the accuracy of the press-brake and die equipment, the identification values varied from the actual lip to flange measurements. The original identification numbers were not altered to reflect the true dimensions of the test specimen C-sections.

The third portion of the identification number consists of a numeral which identifies the number of series within each flange "Case", i.e., multiple series exist within each "Case". The suffix of the identification number denotes the individual C-section, A or B, for each test specimen. When data for a complete test specimen is given, then the suffix 'A,B' is printed.

4.1.2 Flat Width Ratios of Test Specimens

The average flat width ratios of the flange, web, and a range of flat width ratios of the simple edge stiffener for each of the test series are summarised in Table 4.1.

Table 4.1 - Average Flat Width Ratios

Series	Web (h/t)	Flange (w/t)	Lip (d/t)
C1-1	46.9	9.19	0 → 4.34
C1-2	158	9.48	0 → 4.58
C1-3	213	10.0	0 → 7.66
C2-1	82.4	30.1	0 → 17.2
C2-2	47.7	15.7	0 → 9.87
C2-3	192	25.4	0 → 19.4
C2-4	154	15.4	0 → 9.66
C2R-1	78.5	26.1	0 → 15.7
C3-1	77.8	48.9	0 → 18.4
C3-2	220	55.3	0 → 31.3

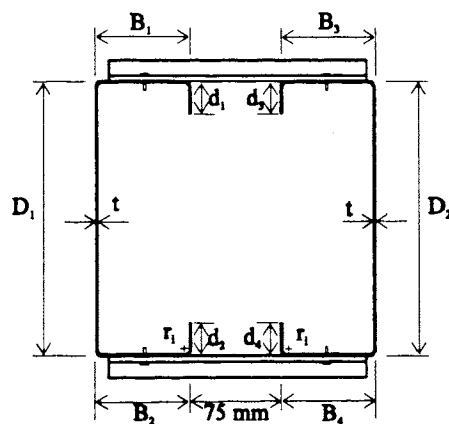
Detailed summaries of all specimen flat widths and flat width ratios are given in Tables A.2a, A.2b and A.2c of Appendix 'A'.

4.1.3 Fabrication of Test Specimens

All test specimens were constructed of two equally sized C-sections 1525mm in length,

except for sections in the C1-3 series, which were 2134mm long. All of the C-sections had solid webs and edge stiffeners (lips) at right angles to the flanges. Sections were brake formed by the following cold formed steel fabricators; Bailey Metal Products, Canadian Metal Rolling Mills, Canadian Steel Manufacturing Inc. (CSM), and Crona Steel Products Inc.. The following C-sections were supplied with oversized compressive lips which were then accurately proportioned on a milling machine at the University of Waterloo machine shop; C1-DW30-1, C1-DW40-1, C1-DW60-1, C2-DW20-1 and C2R-DW20-1. This was necessary because of limitations in the available dies and press brakes used by the material suppliers.

The C-sections were placed facing each other in a box-beam arrangement with a 75mm space separating the edge stiffener components (see Figure 4.1). This configuration was used to create a symmetric section so that the shear centre eccentricity problem associated with C-sections could be avoided. In construction, cold formed sections are typically braced on one or both flanges by sheathing, e.g., plywood, as well as, blocking or strapping between members to minimise the effect of shear eccentricity. Aluminum bracing angles (42x42x4mm) were secured to the flanges of the specimens with #12 self-drilling screws. Two bracing angles were located on the tensile and compressive flanges in the shear span of each test specimen. The compressive flange angles were spaced at



Note: All section dimensions are given in Appendix 'A'.

Figure 4.1 - Typical Test Specimen Cross Section

350mm and the tensile flange angles at 300mm to allow for a clearance of the support reaction beam and subsequent specimen deflection under load. Bracing angles were not placed in the constant moment region to allow for the unrestrained movement of the C-sections under loading.

4.1.4 Mechanical Properties of Test Specimens

Tensile coupon tests were carried out in the Mechanical Engineering materials laboratory at the University of Waterloo. Coupons were cut from the web of each specimen and machined to size according to ASTM A370-92 [ASTM 370]. Galvanised coatings were removed prior to testing using an hydrochloric acid bath. Thickness, yield, ultimate strength and percent elongation, based on a 50mm gauge length, were determined from an average of four coupons per test series. All coupon tests exhibited sharp yielding steel with yield strengths ranging from 302 MPa to 418 MPa. A summary of the material properties is given in Table A.3 of Appendix 'A'.

4.1.5 Test Frame Set-Up

The test specimens were simply supported (roller and pin) and subjected to a two point load as shown in Figures 4.2 and 4.4. A point load was applied to the spreader beam and then transferred by a roller and pin support system to the box-beam. All loads and reactions were carried by 75×14mm plates bolted to the webs of each specimen through pre-drilled holes, as shown in Figures 4.2 and 4.3. The plates were installed to avoid localised crippling of the web at points of concentrated load.

The shear spans of each test specimen were set at 500mm and the constant moment region at 420mm except for the C3-1 series which had shear spans 800mm long and a constant moment region 445mm long. An increased beam length was used for the C3-1

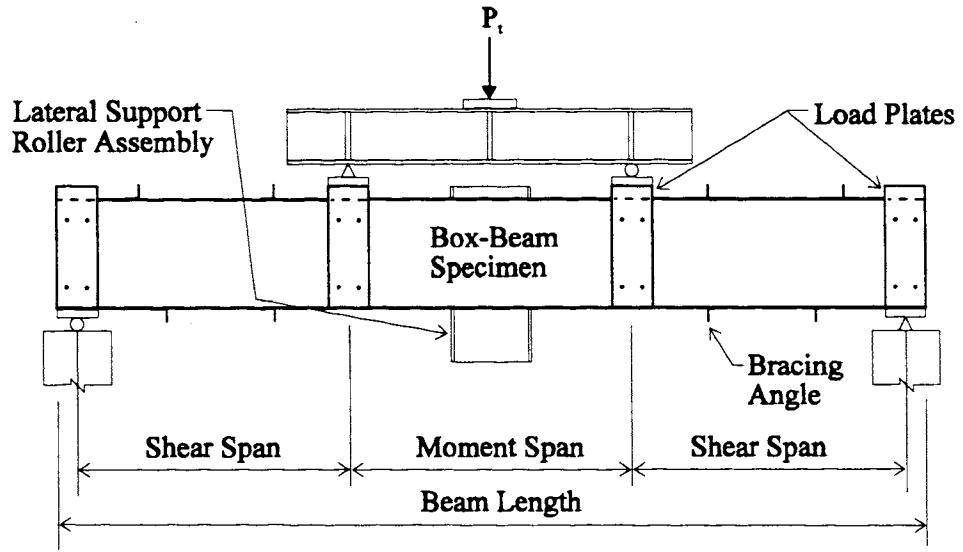


Figure 4.2 - Test Frame Elevation

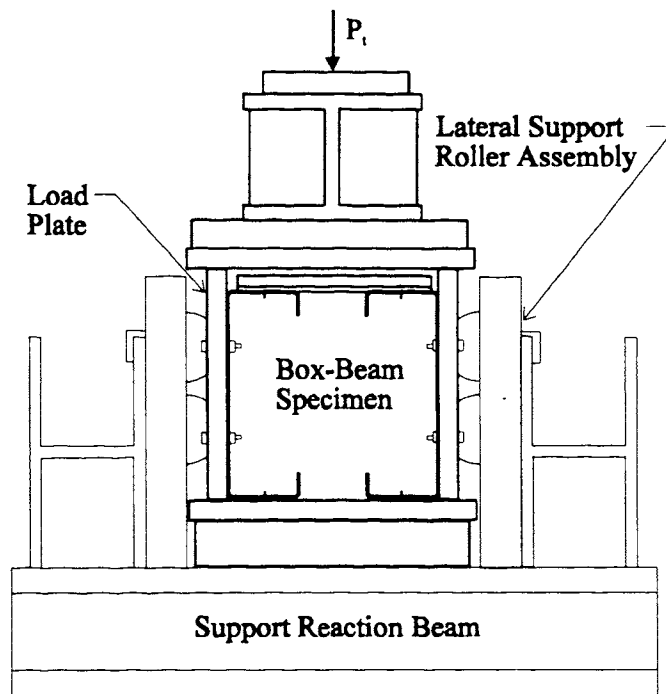


Figure 4.3 - Test Frame Section

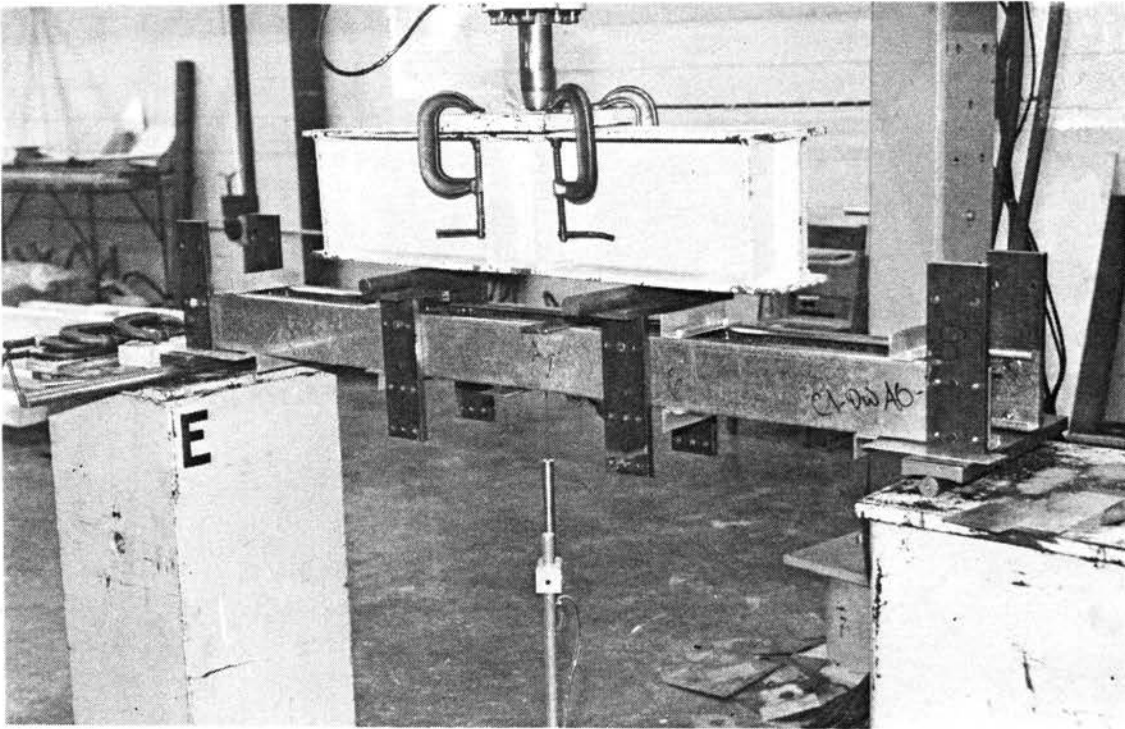


Figure 4.4 - Test Frame Set-Up

series to allow for unrestricted displacement of the elements in each C-section.

Lateral support was provided at the midpoint of the specimens with a roller assembly placed on either side of the box-beam. Light-duty 152mm diameter gravity conveyor rollers were secured to a 500mm long C180 channel with corresponding attachment holes. Each assembly was supported by a wide flange hot rolled beam which was attached to the support reaction beams at either end of the test frame (see Figure 4.3).

4.1.6 Test Procedure

The box-beam specimens were placed in the test frame and carefully positioned and aligned. The reaction and test beams were shimmed level to allow for an even distribution of load through each C-section. A displacement transducer was placed at the centre position of the box-beam to record the maximum deflection and the lateral support

roller assemblies were secured to the supporting W-flange beams. Loading was applied at a constant rate under stroke control until failure occurred.

The test loads were applied with an MTS 446 Electro-Hydraulic Servo Control System, having a 156kN capacity load cell (see Figure 4.5). A load-deflection history was recorded for each test using a Hewlett-Packard 7046A X-Y plotter connected to a DC displacement transducer located at the centre of the moment span. Loads were displayed in volts with the maximum failure reading recorded with a voltmeter.

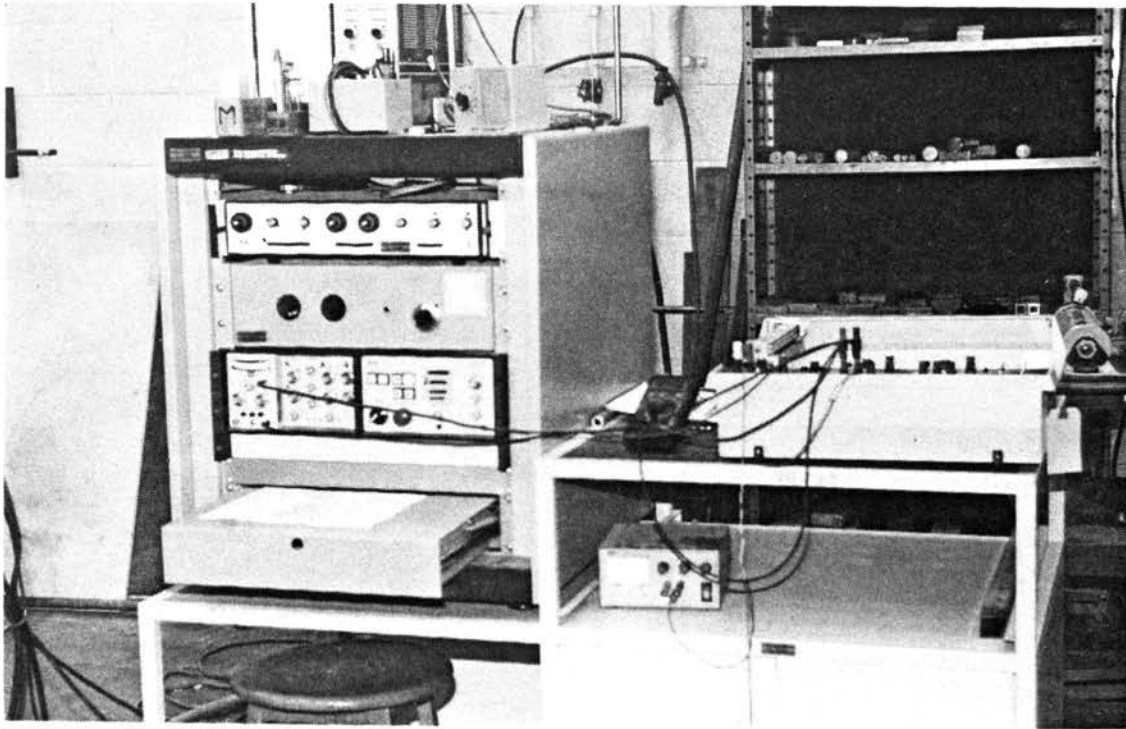


Figure 4.5 - Test Frame Control System

4.1.7 Description of Failure Modes

The predominant mode of failure for each of the experimental specimens was recorded at the time of testing. The position of the failed C-sections was categorised into one of three

possible buckling patterns (local, lip/flange distortional, or flange/web distortional) as previously shown in Figure 1.2. Typical local and distortional buckling patterns of Waterloo test specimens are shown in Figures 4.6 to 4.9.

A distinction between buckling patterns was made by observing the final position of the lip/flange and flange/web corners. If local buckling was the dominant mode of failure then both corners remained in place with plate buckling independently occurring in the adjoining elements. Lip/flange distortional buckling occurred when the lip/flange component rotated about the flange/web corner, which remained in alignment along the length of the section. Flange/web distortional buckling was deemed to be the cause of failure when both corners moved out of original alignment, but remained parallel to each other, with an apparent lateral buckling formation of the web.

The significant difference between flange/web distortional buckling and lateral buckling lies in the rotated position and lateral movement of the failed section. A C-section which undergoes lateral buckling will rotate about the tensile flange/web corner and will move laterally at the same time, i.e., the entire section will move in the horizontal plane. Flange/web distortional buckling has neither of these characteristics. The tensile portion of the section remains in plane without rotational or lateral movement. A rotation of the lip/flange component and a portion of the compressed web about a point located in the compressed section of the web occurs.

The applied load was assumed to be shared equally by the C-sections in each test specimen. Similar failure patterns were normally evident in both C-sections, however, when one section failed prior to the other the test specimen was categorised according to the initial failure mode.

Figure 4.6 shows an elevation view of an unstiffened C-section with a local flange buckle.

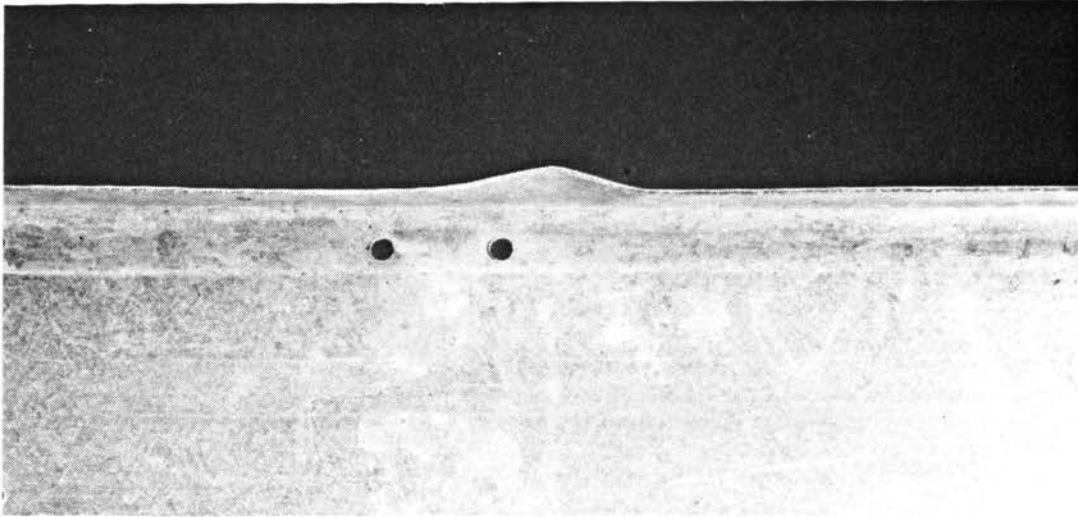


Figure 4.6 - Local Flange Buckling of Unstiffened C-Section.

Figure 4.7 shows a top view of a stiffened C-section with a local flange buckle.

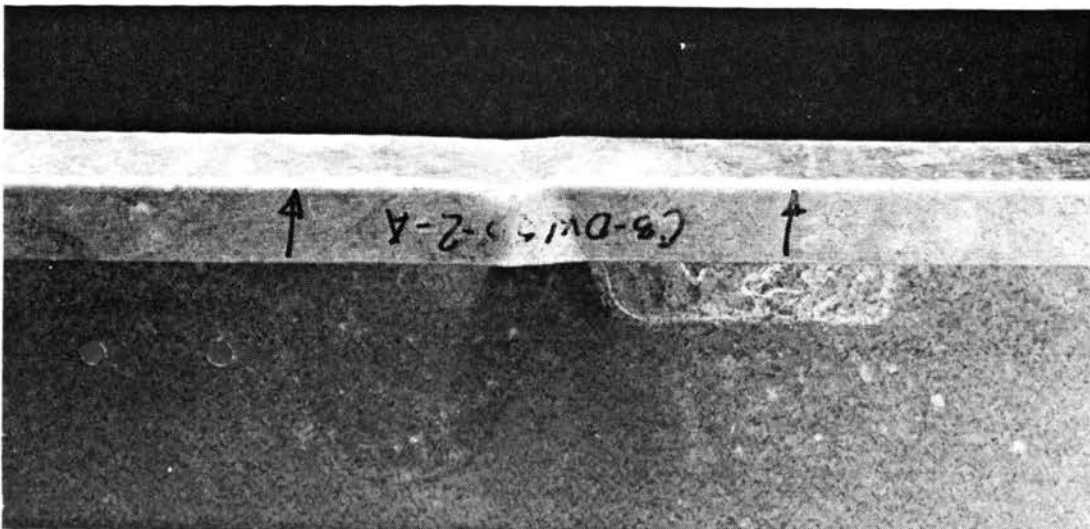


Figure 4.7 - Local Flange Buckling of Stiffened C-Section.

Figure 4.8 shows an elevation view of a stiffened C-section with a lip/flange distortional buckle.

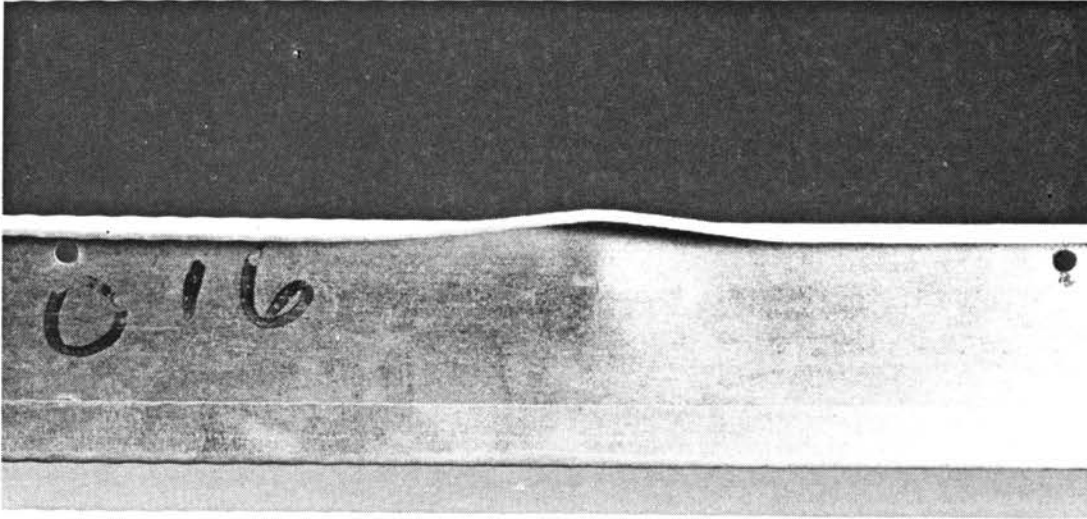


Figure 4.8 - Lip/Flange Distortional Buckling of Stiffened C-Section.

Figure 4.9 shows a top view of a stiffened C-section with a flange/web distortional buckle.

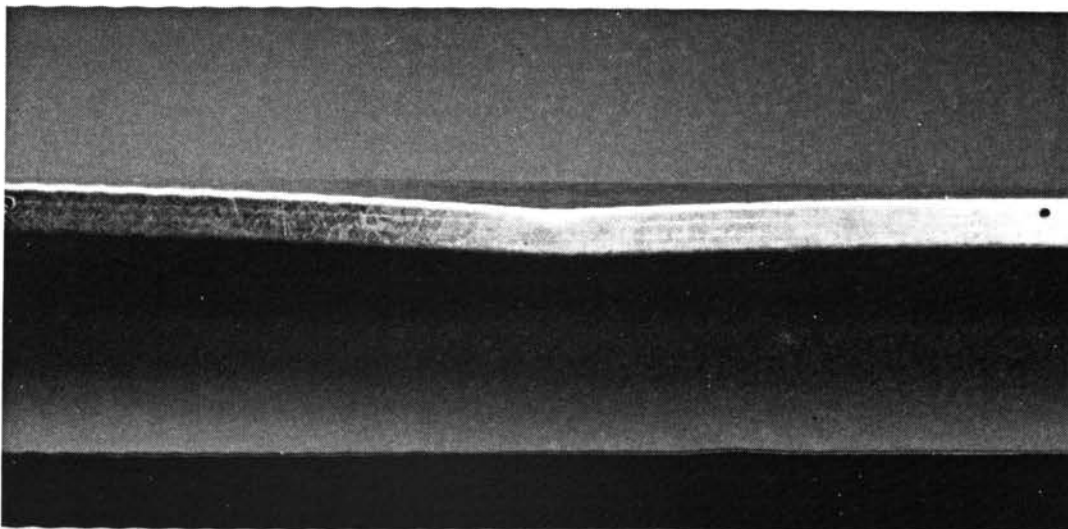


Figure 4.9 - Flange/Web Distortional Buckling of Stiffened C-Section.

Table 4.2 lists the basic modes of failure for each of the specimens observed during testing.

Table 4.2 - Test Specimen Failure Descriptions

Specimen	Failure Mode	Specimen	Failure Mode
C1-DW0-1-A,B	Local/F	C2-DW35-3-A,B	Local/F
C1-DW30-1-A,B	L/F Dist.	C2-DW45-3-A,B	Local/F
C1-DW40-1-A,B	L/F Dist.	C2-DW55-3-A,B	Local/L
C1-DW60-1-A,B	L/F Dist.	C2-DW65-3-A,B	Local/L
C1-DW80-1-A,B	L/F Dist.	C2-DW80-3-A,B	Local/L
C1-DW0-2-A,B	Local/F	C2-DW0-4-A,B	Local/F
C1-DW30-2-A,B	F/W Dist.	C2-DW25-4-A,B	Local/F
C1-DW40-2-A,B	F/W Dist.	C2-DW40-4-A,B	Local/F
C1-DW60-2-A,B	F/W Dist.	C2-DW50-4-A,B	Local/F
C1-DW80-2-A,B	F/W Dist.	C2-DW60-4-A,B	Local/F
C1-DW0-3-A,B	Local/W	C2-DW70-4-A,B	Local/F
C1-DW30-3-A,B	Local/W	C2-DW80-4-A,B	Local/F
C1-DW40-3-A,B	Local/W	C2R-DW0-1-A,B	Local/F
C1-DW60-3-A,B	L/F Dist.	C2R-DW20-1-A,B	Local/F
C2-DW0-1-A,B	Local/F	C2R-DW35-1-A,B	Local/F
C2-DW20-1-A,B	Local/F	C2R-DW45-1-A,B	Local/F
C2-DW35-1-A,B	Local/F	C2R-DW55-1-A,B	Local/L
C2-DW45-1-A,B	Local/F	C2R-DW65-1-A,B	Local/L
C2-DW55-1-A,B	Local/F	C3-DW0-1-A,B	Local/F
C2-DW65-1-A,B	Local/F	C3-DW20-1-A,B	Local/F
C2-DW0-2-A,B	Local/F	C3-DW30-1-A,B	Local/F
C2-DW25-2-A,B	L/F Dist.	C3-DW35-1-A,B	Local/F
C2-DW40-2-A,B	L/F Dist.	C3-DW45-1-A,B	Local/F
C2-DW50-2-A,B	L/F Dist.	C3-DW0-2-A,B	Local/F
C2-DW60-2-A,B	Local/F	C3-DW20-2-A,B	Local/F
C2-DW70-2-A,B	Local/L	C3-DW30-2-A,B	Local/F
C2-DW80-2-A,B	Local/L	C3-DW35-2-A,B	Local/F
C2-DW0-3-A,B	Local/F	C3-DW45-2-A,B	Local/F
C2-DW20-3-A,B	L/F Dist.	C3-DW50-2-A,B	Local/F/L
		C3-DW60-2-A,B	Local/F/L

Note:

- L/F Dist. = Lip/Flange distortional buckling.
- F/W Dist. = Flange/Web distortional buckling
- Local/L = Local lip buckling.
- Local/F = Local flange buckling.
- Local/W = Local web buckling.
- Local/F/L = Local flange and lip buckling.

Chapter 5

Available Test Data

5.1 General

Numerous reports regarding the flexural behaviour of C and Z-sections were reviewed and summarised. Data for a total of 174 relevant test beams was compiled and included in this work. The available test specimens were required to meet the following criteria; 1) the cross section was either a Z or a C-shape, 2) adequate lateral support was provided during testing, 3) perforations were not present, and 4) all edge stiffeners were simple lips at right angles to the flange. Table 5.1 lists all the researchers who have provided applicable data, the year, the research institution and the number and type of specimens tested.

Table 5.1 - List of Researchers and Applicable Available Test Data

Charnvarnichborikarn (1992 - Manitoba) [Cha 92]	20 Z-sections
Cohen (1987 - Cornell) [Coh 87]	14 C-sections
Desmond (1977 - Cornell) [Des 78a]	4 C-sections
LaBoube (1978 - Missouri-Rolla) [LaB 78]	52 C-sections
Moreyra (1993 - Cornell) [Mor 93]	6 C-sections
Schardt & Schrade (1982 - Darmstadt) [Scha 82]	25 Z-sections
Schuster (1992 - Waterloo) [Schu 92]	5 C-sections
Shan (1994 - Missouri-Rolla) [Shan 94]	29 C-sections
Willis & Wallace (1990 - Oklahoma) [Wil 90a]	4 C-sections
Winter (1947 - Cornell) [Win 47]	15 C-sections

The procedures for testing used by each researcher, a general description of the test set-up and specimen dimensions are given in the following sections. Detailed summaries of all applicable available test sections, section dimensions, material properties, test moments and specimen cross sections can be found in Appendix 'B'.

5.1.1 Charnvarnichborikarn [Cha 92]

The main topic of Charnvarnichborikarn's [Cha 92] Ph.D. thesis was the analysis of the distortional buckling mode of failure for cold formed steel Z-sections in compression, bending and combined compression and bending. In the second phase of his work twenty Z-sections were tested in bending. The beams, 1372mm in length, were simply supported and subjected to a two point load scheme with a constant moment region of 610mm. Lateral bracing was provided at the load points and at the centre of the test beam, however, the specimens were loosely fastened to the support columns at each end.

All of the Z-sections had consistent web ($129 < h/t < 132$) and flange ($42.9 < w/t < 48.1$) dimensions and material properties ($F_y \approx 324$ MPa). The flat width ratio of the edge stiffener, d/t , was systematically varied from 0 to 33.7. Section dimensions, material properties and dimension ratios are summarised in Tables B.1 and B.2 of Appendix 'B', respectively, and a cross section is given in Figure B.1 of Appendix 'B'.

5.1.2 Cohen [Coh 87]

Cohen's [Coh 87] test specimens were designed to verify the then current effective web depth equations and the effective width equations for edge stiffened compressive flanges. Fourteen of Cohen's simply supported beams were used as data for this work. Each beam specimen was subjected to a two point load, with a cold formed test specimen in the constant moment region (1219mm or 1930mm) and built-up hot-rolled steel sections in the shear spans (610mm). Lateral bracing was provided at the load points and at third points in the constant moment span. The cold formed section of each test specimen was made up of two C-sections secured back-to-back. A plate was also attached to the tensile flanges of the C-sections to ensure compressive failure of the beam (see Figure B.2 of Appendix 'B'). Two typical sections with constant material properties ($F_y \approx 375$ MPa or 418 MPa), web depths ($h/t \approx 73.4$ or 124) and flange widths ($w/t \approx 28.4$ or 50.7) were

used with various edge stiffener sizes ($7.18 < d/t < 13.7$). Section dimensions, material properties and dimension ratios can be found in Tables B.3 and B.4 of Appendix 'B'.

5.1.3 Desmond [Des 78a]

Desmond's [Des 78a] research involved the experimental study of the influence of stiffener rigidity on the performance of flat plates in compression. Part of his research consisted of the laboratory testing of four I-beam specimens fabricated from C-sections placed back-to-back. These tests were meant to isolate the behaviour of edge stiffener / flange interaction. Hence, a thin steel diaphragm was tack-welded to the web and flanges to prevent local buckling of the web (see Figure B.3 of Appendix 'B'). All beams were simply supported, with a span length of 2845mm, and subjected to a two point load with a constant moment region of 950mm. The test beams had similar material properties ($379 \text{ MPa} < F_y < 399 \text{ MPa}$) and dimensions ($65.5 < h/t < 67.1$ and $45.6 < w/t < 46.3$), except for the size of the edge stiffeners ($6.76 < d/t < 20.0$). Section dimensions, material properties and dimension ratios can be found in Tables B.5 and B.6 of Appendix 'B'.

5.1.4 LaBoube [LaB 78]

A research project completed by LaBoube [LaB 78] dealt with the investigation of beam webs subjected to bending. This project consisted of an experimental phase where a total of fifty-two specimens were tested. All test specimens were simply supported, with span lengths ranging from 1911mm to 3454mm, and subjected to a two point load applied at the third points. Each test specimen consisted of two similar sized C-sections attached with aluminum angles and self-drilling screws in the form of a box-beam, as shown in Figure B.4 of Appendix 'B'. Short C-sections were attached to the webs of the test beams at load points to prevent web crippling. Lateral support was provided with vertical

rollers at the end of each test beam and with steel braces, attached to the top flange of the C-sections over the interior of the span.

The experimental phase of the project consisted of two series; 'B' which included 32 beams fabricated from two C-sections and 'MB' which included 20 beams fabricated from two C-sections with an additional plate attached to the tensile flanges to ensure compressive failure (see Figure B.4 of Appendix 'B'). The test beams ranged in web depth ($72.8 < h/t < 266$), flange width ($24.4 < w/t < 71.2$), lip depth ($8.83 < d/t < 12.7$) and in material properties ($231 \text{ MPa} < F_y < 371 \text{ MPa}$). Section dimensions and material properties of the specimens tested by LaBoube are summarised in Tables B.7a, B.7b, B.8a, B.8b, B.8c, B.9 and B.10 of Appendix 'B'.

5.1.5 Moreyra [Mor 93]

Moreyra's [Mor 93] work consisted of research concerning the effect of a varying lip size on the bending resistance of standard C-sections. Nine beams, fabricated from two C-sections (see Figure B.5 of Appendix 'B') 914mm apart, 5486mm in length, simply supported and connected with three bracing arrangements, were tested with a uniformly distributed load applied in a vacuum chamber. Plywood strips and steel panels were used as decking above the test sections and a polyethylene plastic sheet acted as a vacuum seal.

Three experimental series (A, B and C), each with three bracing variations, were tested. Specimens with a suffix 'W' were braced every 610mm at the webs. The web braces were made from the same C-sections as the test beams and plywood strips were used as decking. A second type of test, denoted with a suffix 'T', was braced at the top flange with a steel panel attached with self drilling screws. The final type of bracing, type 'TB', consisted of steel panels attached to the top and bottom flanges except for the middle third of the bottom flange where small steel channels were used.

Section dimensions were held near constant ($113 < h/t < 117$ and $26.4 < w/t < 28.1$) except for the depth of the simple edge stiffener which was systematically varied ($8.31 < d/t < 12.3$). Material properties, F_y , were determined for each beam and varied from 392 MPa to 438 MPa. The edge stiffener dimension of C-sections in test series 'C' was reduced with a portable electric shear. Section dimensions, material properties and dimension ratios for all test specimens are summarised in Tables B.11 and B.12 of Appendix 'B'. However, only six of the beams, W and TB braced were used in this investigation. All of the beams which were braced at the top flange only, series T, failed by lateral buckling, hence, they did not meet the lateral bracing requirement of this work.

5.1.6 Schardt and Schrade [Scha 82]

Schardt and Schrade [Scha 82] tested thirty-eight Z-sections, of which twenty-five met the requirements necessary for this work. Test beams were simply supported and laterally braced at the top and bottom flanges. Loading was provided in a reverse manner to that usually found in experimental testing. Point loads were applied upwards at the outside end of the shear spans with the reactions occurring adjacent to the constant moment region. The complete test beam consisted of one Z-section which extended over the constant moment region (see Figure B.6 of Appendix 'B') and two end extensions (IPB 140 beams) for the shear spans (1000mm). The cold formed steel Z-sections were bolted to the end extensions with a plate and angle system.

Four test series were completed by Schardt and Schrade with varying beam lengths, section dimensions and material properties. For series 1-3, the constant moment region was 1750mm long with a Z-section length of 2000mm. Series 4 consisted of a 2750mm constant moment region and a Z-section length of 3000mm. All section dimensions varied slightly with web depth ratios, h/t , ranging from 170 to 181, flange width ratios, w/t , from 41.1 to 66.6 and lip depth ratios, d/t , from 7.52 to 13.4. Material properties, F_y , were determined for each Z-section and ranged from 339 MPa to 411 MPa. Tables B.13

and B.14 of Appendix 'B' contain summaries of the test specimen dimensions, material properties and dimension ratios.

5.1.7 Schuster [Schu 92]

Schuster [Schu 92] investigated the effect of perforation size on the bending capacity of standard industry type C-sections commonly used as light weight steel framing members. Solid web sections were also included in the investigation to act as a basis for comparison with S136-M89 [CSA 89]. Simply supported sections, 4267mm in length, were tested under a two point loading scheme with a constant moment region of 1829mm. Each test specimen consisted of two identical C-sections attached with aluminum angles and self-drilling screws to form a box-beam similar to that used by LaBoube [LaB 78] (see Figure B.7 of Appendix 'B'). Short C-sections were attached to the webs of the test purlins at load points to prevent web crippling. Lateral bracing was provided by wood blocks spaced at 500mm, which were supported by two wide flange sections fastened to the load pedestals at either end of the test frame.

The five unperforated beams tested by Schuster were included as data in this work. These beams consisted of two series (CS and BS) with near uniform dimensions ($160 < h/t < 162$, $26.8 < w/t < 27.9$ and $6.92 < d/t < 7.66$) and varying material properties ($F_y \approx 271$ MPa or 331 MPa). Section dimensions, dimension ratios and material properties can be found in Tables B.15, B.16 and B.17 of Appendix 'B', respectively.

5.1.8 Shan [Shan 94]

Shan's [Shan 94] work comprised of an investigation into the behaviour of industry standard perforated C-section beams subjected to bending, shear and combined bending and shear forces. Of these tests, twenty-nine bending specimens with solid web elements

were used as data. All beams were simply supported, with span lengths of 3810mm or 4877mm, and subjected to a two point load with a constant moment region of 1829mm. Each test specimen consisted of two similar C-sections attached with aluminum angles and self-drilling screws in the form of a box beam, as shown in Figure B.8 of Appendix 'B'. The beam set-up is similar to that used by LaBoube [LaB 78] and Schuster [Schu 92] in their investigations. Short C-sections were attached to the webs of the test purlins at load points to prevent web crippling. Lateral support was provided by vertical rollers at the end of each test beam and by steel braces attached to the top flange of the C-sections over the interior of the span.

The test beams covered a wide array of dimensions with web depth ratios, h/t , from 38.2 to 249, flange width ratios, w/t , from 14.2 to 51.5 and lip depth ratios, d/t , from 3.20 to 16.0. The material property values, F_y , also varied greatly, ranging from 205 MPa to 448 MPa. Section dimensions and material properties of the C-sections tested by Shan are summarised in Tables B.18, B.19a, B.19b, and B.20 of Appendix 'B'.

5.1.9 Willis and Wallace [Wil 90a]

Willis and Wallace [Wil 90a] [Wil 90b] presented two papers on the bending capacity of cold formed C and Z-purlins. The main objectives of the study were to determine the effect of lip size and fastener position (with respect to the web) on the bending capacity of cold formed sections. The experimental tests consisted of full size steel roof systems with two support purlins spaced 1520mm apart. The roof systems consisted of standard deck sections, 2130mm in length, fastened with self-drilling screws. Tests with one and three spans, 6100mm in length, subjected to a uniformly distributed gravity load using concrete blocks were completed. Lateral bracing was provided at the top flange of the purlins by the steel deck.

Four single span tests from the Willis and Wallace study were included in the data base for this work. Of these tests, three (1C2, 1C3 and 1C4) had consistent material properties ($F_y \approx 372$) and section dimensions ($h/t \approx 125.1$ and $w/t \approx 31.9$), except for the size of the edge stiffener, which was varied using a portable electric shear ($10.8 < d/t < 14.4$). The fourth test (1C5) was fabricated using the same chord length, a smaller web ($h/t \approx 120$), a wider flange ($w/t \approx 33.7$) and a smaller edge stiffener ($d/t \approx 10.9$) in order to optimise bending capacity. Section dimensions, material properties and dimension ratios can be found in Tables B.21 and B.22 of Appendix 'B' and a typical purlin cross section is found in Figure B.9 of Appendix 'B'.

5.1.10 Winter [Win 47]

Winter [Win 47] completed a variety of beam tests to determine the strength and behaviour of thin, wide flange sections in compression. Fifteen test sections from Winter's experiments were included as data for this work. All beams were simply supported, with span lengths of 2032mm, and subjected to a two point load. Two sets of tests were used; 'B' consisted of ten beams which had constant moment regions of 1016mm, and 'C' consisted of five beams which had constant moment regions of 677mm. Test specimens were fabricated from two identical C-sections, spot-welded together, to form a built-up I-section. Series 'B' consisted of two vertical channels placed back-to-back (see Figure B.10 of Appendix 'B'). Series 'C' consisted of two vertical channels and an additional horizontal channel used to increase the tensile area of the beam to ensure compressive failure of the flange (see Figure B.10 of Appendix 'B').

Web height ratios, h/t , ranged from 32.8 to 168, flange width ratios, w/t , from 19.2 to 86.6, lip depth ratios, d/t , from 3.03 to 13.7 and material properties, F_y , from 208 MPa to 261 MPa. All section dimensions and material properties used by Winter are summarised in Tables B.23 and B.24 of Appendix 'B'.

Chapter 6

Edge Stiffener Investigation

6.1 Review of Current Flat Width Ratio, d/t , Limit

The most recent edition of the Canadian Design Standard [CSA 94] contains a limiting flat width ratio for simple lip stiffeners of $d/t \leq 14$. The maximum value of 14 was recommended by Willis and Wallace [Wil 90a] [Wil 90b] based on the results of only three C-section purlins, placed into a conventional single span test apparatus and subjected to a uniformly distributed gravity load (see Section 5.1.9). Purlins which had an edge stiffener flat width ratio exceeding 14 experienced a decrease in their load carrying capacity. All of the test C-sections had locally unstable webs, Case III flanges and constant section dimensions except for the systematically varied compressive lip depths (see Tables B.21 and B.22 and Figure B.9 of Appendix 'B'). The S136-94 Technical Committee included the d/t limit of 14 in Clause 5.6.2.3 (Table 6) of the S136 Standard [CSA 94], with the understanding that further testing would be completed to substantiate the findings of Willis and Wallace.

The existing d/t limit is based on a restricted number of beam tests which do not represent the entire range of possible web, flange and lip size combinations. The edge stiffener flat width ratio limit investigation reported on in this Chapter consists of the analysis of 53 C-section beams with Case I, II and III flanges, locally stable and unstable webs and systematically varied lip depths (see Chapter 4, Waterloo Test Program). The d/t and d_i/w ratios of the experimental C-sections were compared with the applied test moments for nine of the test series. The recommendations and data presented by Willis and Wallace [Wil 90a] [Wil 90b] were also reviewed and compared with the findings of this research.

6.1.1 Problems With Current Flat Width Ratio, d/t , Limit

Willis and Wallace [Wil 90a] [Wil 90b] defined the parameters of their edge stiffener limit as D_c , the out-to-out depth and t , the thickness of the lip. A reduction in test bending moment occurred at D_c/t approximately equal to 14, as seen in Figure 6.2a. The S136 Standard [CSA 94] defines the limit as $d/t \leq 14$, where d is the flat width of the lip and t is the thickness. Since the Willis and Wallace and the S136 limits are based on different definitions of the lip size (see Figure 6.1), an adjustment must be made to the Canadian Standard. Had Willis and Wallace used d/t values instead of D_c/t , the result would probably have been a limit of 12, as seen in Figure 6.2b.

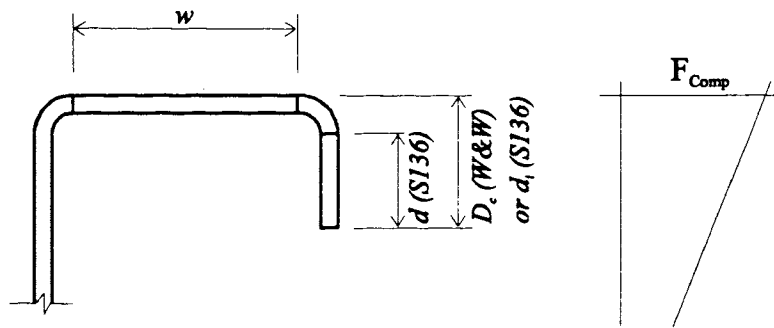


Figure 6.1 - Lip Depth Dimension Comparison

6.1.2 Alternate Flat Width Ratio, d_i/w , Limit

It is also possible to define a limit based on the ratio of d_i/w (out-to-out lip depth / flange flat width). Willis and Wallace [Wil 90a] [Wil 90b] suggested that a limiting value for D_c/w of 0.4 or 0.45 be used in place of the edge stiffener flat width ratio limit. Desmond stated that *for D_c/w ratios larger than about .4, critical buckling is initiated solely by local plate buckling ... local instability of the edge stiffener interacts with the to-be-stiffened flange and initiates a premature local buckling of that element* [Des 81] (where

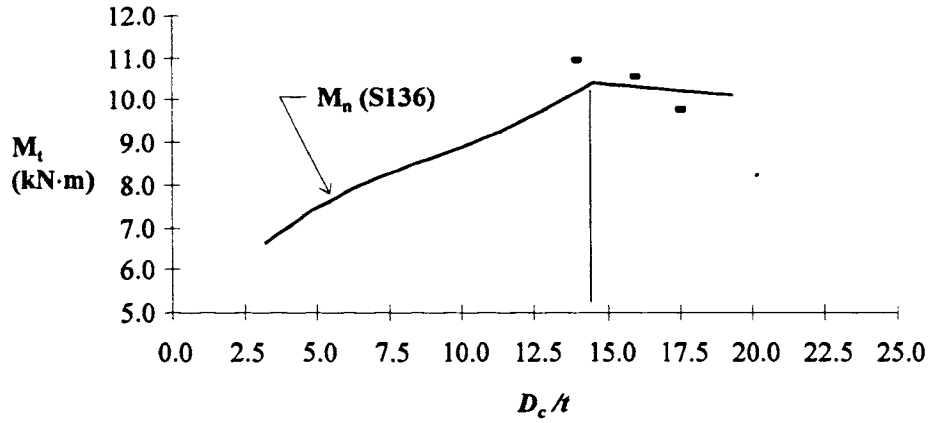


Figure 6.2a - Willis & Wallace M_t vs. D_c/t Ratios

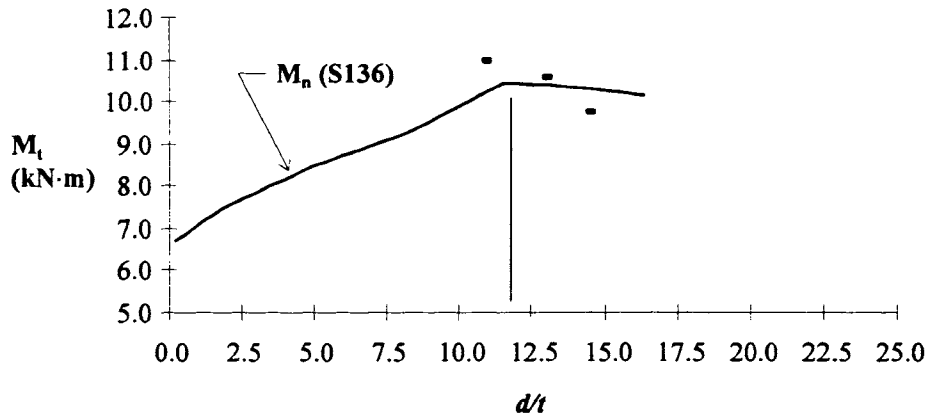


Figure 6.2b - Willis & Wallace M_t vs. d/t Ratios

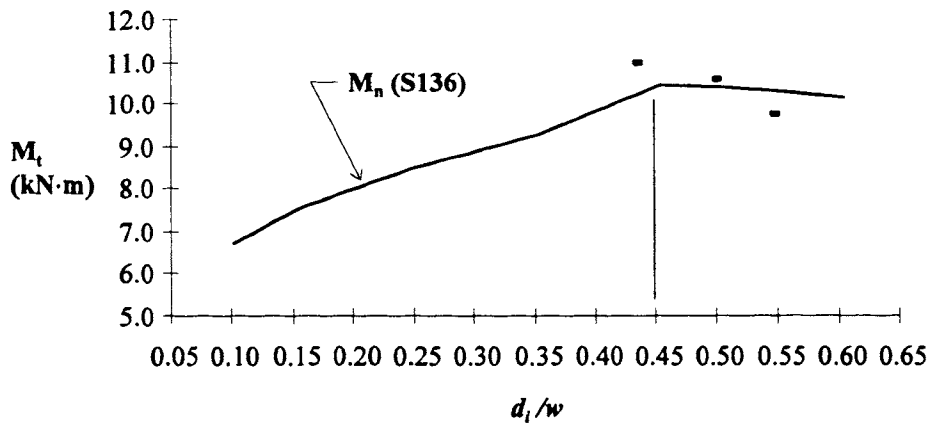


Figure 6.2c - Willis & Wallace M_t vs. d_i/w Ratios

D_s is the out-to-out depth of the simple edge stiffener). Regarding the conclusions of both Desmond and Willis and Wallace, a lip depth limited to d_i/w less than 0.4 would apply (see Figure 6.2c).

6.1.3 Bending Moment Resistance Predictability, Using Willis and Wallace Data

Willis and Wallace [Wil 90a] [Wil 90b] also concluded that the then governing 1986 AISI Specification [AISI 86b] over-predicted the bending capacity of purlins with large simple edge stiffeners. A comparison of the Willis and Wallace test data with the current North American design methods showed that the S136 Standard [CSA 94] adequately predicted the bending resistance of the four purlin sections. The test-to-predicted moment ratios ranged from 0.95 to 1.12 with a mean of 1.04, a standard deviation of 0.073 and a coefficient of variation of 0.121. Analysis using the current AISI Specification [AISI 89a] resulted in unconservative predicted bending moments with test-to-predicted ratios ranging from 0.86 to 1.01 with a mean of 0.942, a standard deviation of 0.065 and a coefficient of variation of 0.120 (see Table B.42 of Appendix 'B' for individual test results).

Since the bending moment resistance of the Willis and Wallace [Wil 90a] [Wil 90b] test purlins decreased with increasing lip depths and can adequately be predicted by the S136 Standard [CSA 94], the existing d/t limit needs to be changed. If a conclusion is based solely on the Willis and Wallace test data, then it is recommended that either a $d/t \leq 12$ or a $d_i/w \leq 0.4$ *warning* be included in the S136 Standard. In addition to this warning, a statement is needed which indicates that the bending moment resistance will remain predictable, although decrease, above these characteristic values.

6.1.4 Bending Moment vs. Lip Dimension Ratio, Using Waterloo Test Data

A comparison study, similar to that completed by Willis and Wallace [Wil 90a] [Wil 90b], was completed to determine the relationship between the tested bending moment capacity, M_t , (Tables A.6a and A.6b of Appendix 'A') and two lip dimension ratios, d/t and d_i/w (Tables A.2a, A.2b and A.2c of Appendix 'A'). Since Willis and Wallace tested only C-purlin sections with locally unstable webs and Case III flanges, the Waterloo test specimens were proportioned to consist of C-sections which covered the entire range of possible lip, flange and web dimensions. Specimens with Case I, II and III flanges, locally stable and unstable webs and systematically varied compressive lip depths were analysed. Nine of the ten series tested as part of this work were separately examined by charting the M_t vs. d/t and M_t vs. d_i/w parameters. A direct comparison between these variables can be made because all section dimensions were held near constant within each test series, except for the compressive lip depth (see Tables A.1a and A.1b of Appendix 'A'). Series C2-1 was not included in this study due to a variation of the tensile lip depth between C-sections.

Graphs showing the bending moment to lip depth ratio relationship for the nine series are found in Figures 6.3a to 6.11b. Included with each graph is a curve which represents the nominal moment resistance, M_n , as predicted for a typical section by the current S136 Standard [CSA 94]. A typical section was determined from the average dimensions of the C-sections within each series. The graphs give only an approximate value for the predicted bending moment resistance of the test beams, due to variations between the typical and actual C-sections. Accurate test-to-predicted bending moment ratios for each individual beam can be found in Tables A.6a and A.6b of Appendix 'A'.

6.1.4.1 Case I Flange Series

Test series C1-1 gave no indication of a loss in bending moment capacity as the lip depth

was increased from 0mm to 14mm (Figures 6.3a and 6.3b). The revised d/t limit of 12 was not exceeded, however four of the five sections had d_i/w values near or above the proposed 0.4 limit. The bending moment capacity was adequately predicted for the sections in this series using cold work of forming. Without this allowable increase in yield strength, the nominal moment resistance is overly conservative (see Table A.6a of Appendix 'A'). Test series C1-2, consisted of locally unstable webs and also gave no indication of a loss in bending moment capacity as the lip depth was increased (0mm to 14mm) (Figures 6.4a and 6.4b). As in the previous series, the revised d/t limit was not exceeded and four of the five sections had d_i/w values near or above the proposed 0.4 limit. The bending moment capacity was unconservatively predicted by the S136 Standard [CSA 94] due to the flange/web distortional buckling mode of failure (see Table 4.2 for failure descriptions). Similarly, the final series, C1-3, with Case I flanges, did not exhibit a decrease in the bending moment capacity as the lip depth was increased (0mm - 19.5mm) (Figures 6.5a and 6.5b). The revised d/t limit was not exceeded and three of the four sections had d_i/w values above the proposed 0.4 limit. Local web buckling caused the predicted nominal moment values to be above the actual test results except for specimen C1-DW60-3-A,B. This section was restricted from buckling in the local web pattern by placing additional wooden blocks within the box-beam and as lateral support.

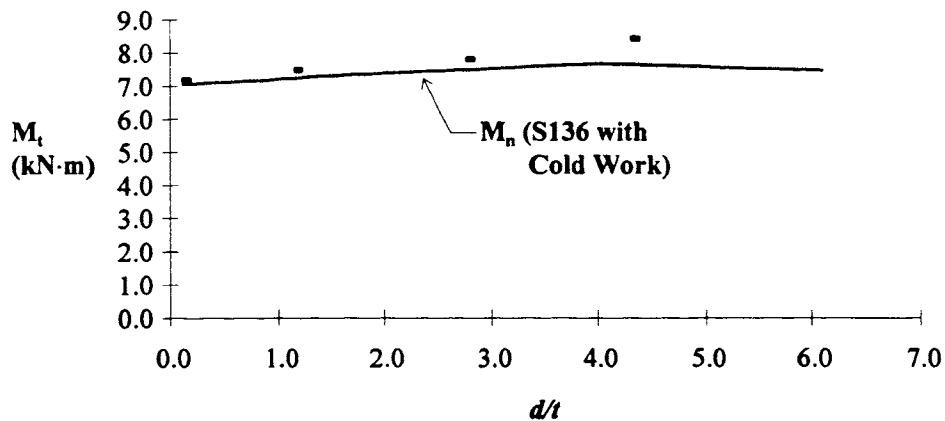


Figure 6.3a - Series C1-1 M_t vs. d/t Ratios

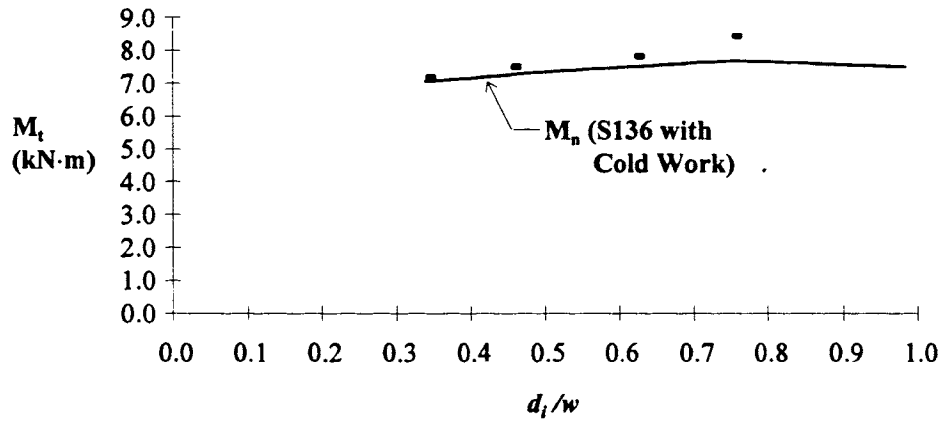


Figure 6.3b - Series C1-1 M_t vs. d_i/w Ratios

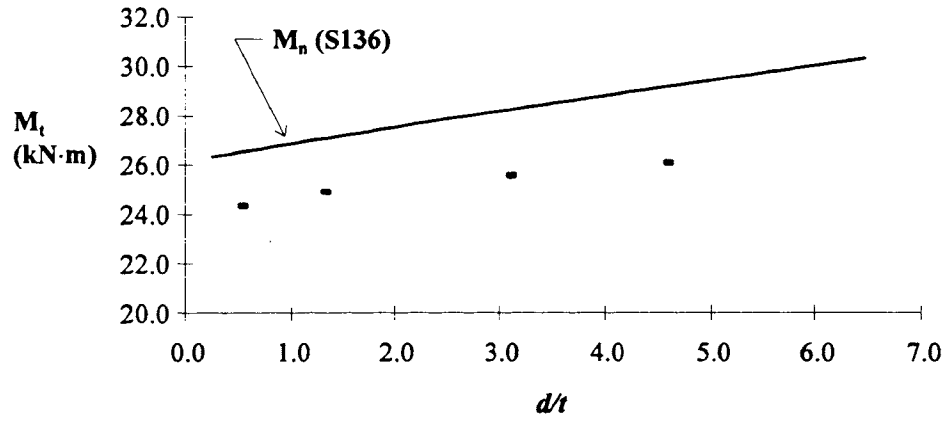


Figure 6.4a - Series C1-2 M_t vs. d/t Ratios

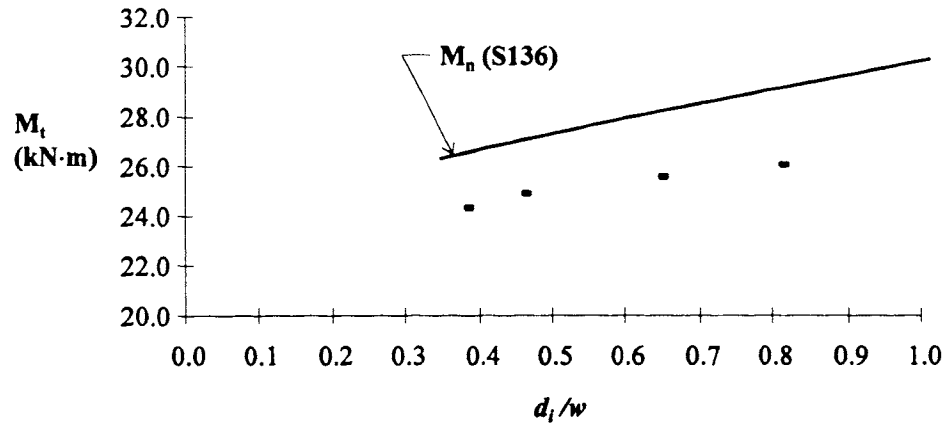


Figure 6.4b - Series C1-2 M_t vs. d_i/w Ratios

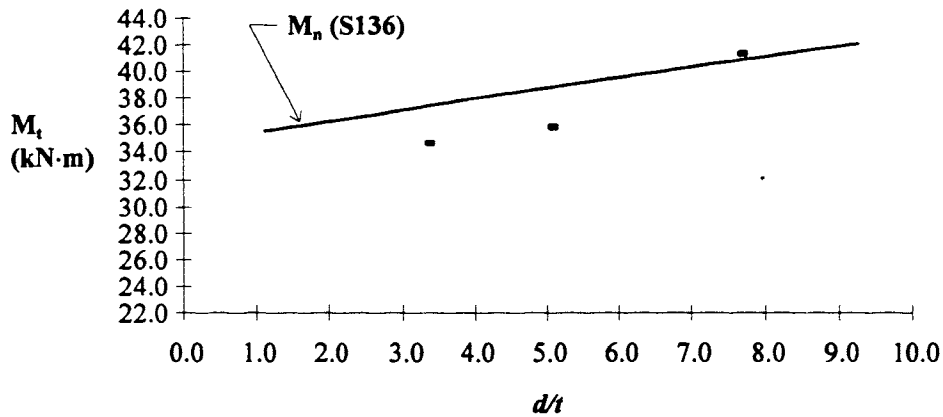


Figure 6.5a - Series C1-3 M_t vs. d/t Ratios

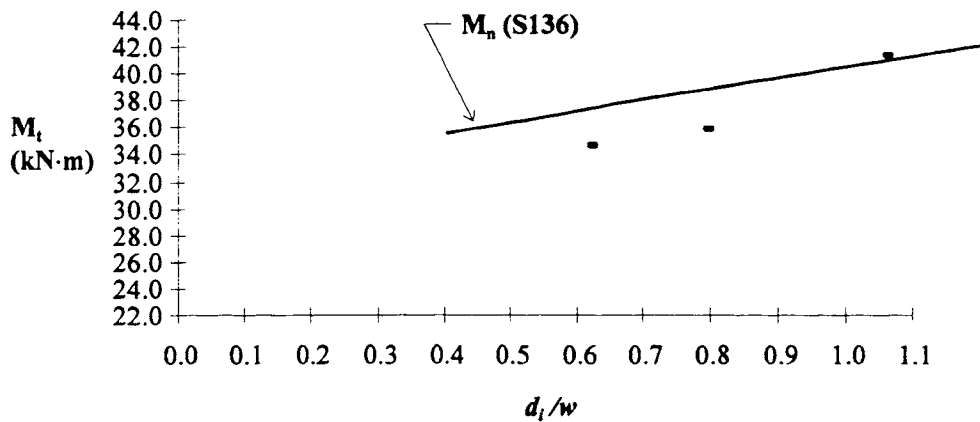


Figure 6.5b - Series C1-3 M_t vs. d_i/w Ratios

All of the C-sections with Case I flanges exhibited an increase in bending moment capacity as the compressive lip depth was increased. The test sections did not violate the revised d/t limit of 12, although the proposed d_i/w limit of 0.4 was exceeded by nine of the specimens in these three series.

6.1.4.2 Case II Flange Series

The C-sections contained in the C2-2 and C2-4 series were sized to have flange flat width ratios slightly above the W_{lim1} limit. Hence, their bending moment capacity relative to lip

depth ratio was predicted to be similar to the Case I flange sections. Series C2-2 consisted of C-sections with locally stable webs and lip depths which varied from 0mm to 24mm. The bending moment capacity did not decrease as the lip depths were gradually increased (see Figures 6.6a and 6.6b). All of the sections had d/t ratios below the revised limit of 12 and five of the seven sections had d_i/w values above the proposed 0.4 limit. The predicted nominal bending moment capacity was below the actual test results for all of the sections in the series. Cold work of forming could have been used to more accurately calculate the bending resistance for four of the C-sections (see Table A.6a of Appendix 'A'). Series C2-4 consisted of beams with locally unstable webs and lip depths which ranged from 0mm to 24mm. The test results showed an increasing trend in bending moment capacity as the lip depth was increased (see Figures 6.8a and 6.8b). The specimen with a test moment greater than the predicted nominal value (C2-DW60-4-A,B) seems to reveal a decrease in the bending moment capacity. However, the general trend of this series is an increasing bending moment and the extreme moment value of this specimen can be attributed to scatter of results, as normally experienced with laboratory testing. As in the previous Case II series, all of the sections had d/t ratios below the revised limit of 12 and five of the seven sections had d_i/w values above the proposed 0.4 limit. Bending moment resistance was adequately predicted with the S136 Standard [CSA 94] without cold work of forming. Whereas, for five of the sections where cold work of forming was applicable, the test-to-predicted bending moment ratios were unconservative (see Table A.6b of Appendix 'A').

Series C2-3 and C2R-1 were sized to have flange flat width ratios near the W_{lim2} limit. Hence, the results of this analysis were predicted to be similar to that found for the Case III sections tested by Willis and Wallace [Wil 90a] [Wil 90b]. Yet series C2R-1, which consisted of sections with locally stable webs and lip depths that ranged from 0mm to 22.5mm, did not show the characteristic drop in bending moment (see Figures 6.9a and 6.9b). The revised d/t limit of 12 was surpassed by two of six sections and the d_i/w limit of 0.4 was exceeded by four of six sections. The nominal bending moment curve accurately traced the behaviour of the test sections as the lip depth was increased. Series

C2-3, which was made up of sections with locally unstable webs and lip depths that ranged from 0mm to approximately 27mm, exhibited an increasing trend in bending moment capacity, except for the final beam in the series (C2-DW80-3-A,B) (see Figures 6.7a and 6.7b). The maximum bending moment resistance occurred at approximately $d/t = 15$ or $d_i/w = 0.7$ with two of seven sections above the revised d/t limit of 12 and five of seven sections above the proposed d_i/w limit of 0.4. The test bending moment capacity was adequately predicted with the S136 Standard [CSA 94].

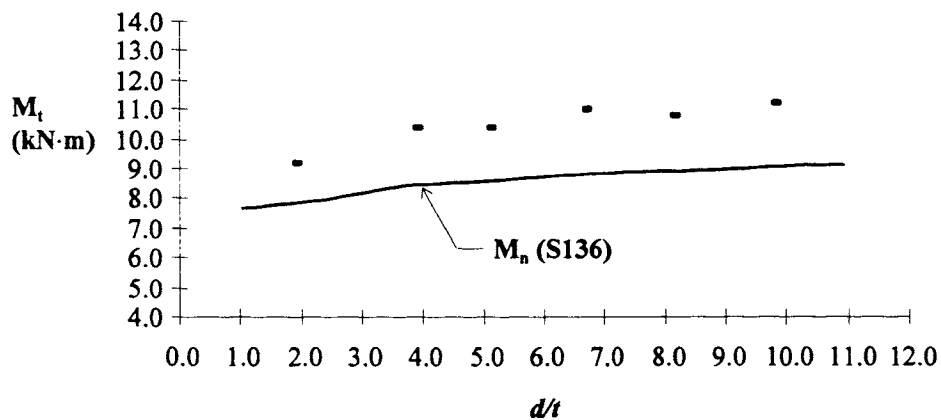


Figure 6.6a - Series C2-2 M_t vs. d/t Ratios

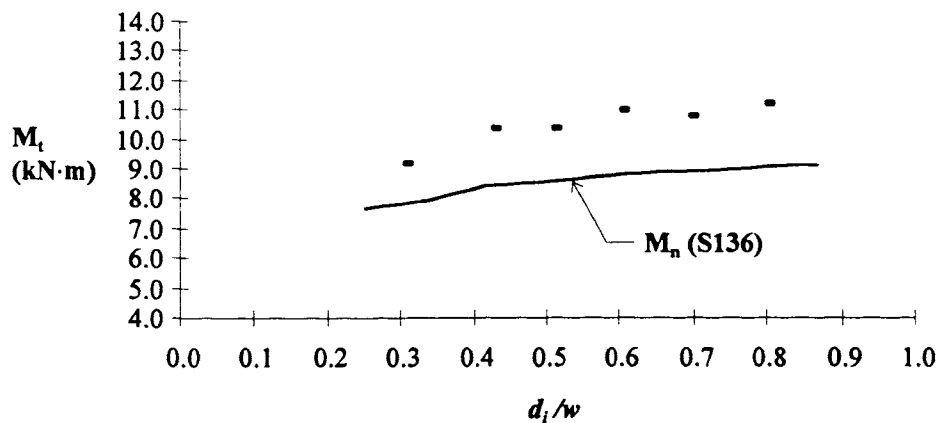


Figure 6.6b - Series C2-2 M_t vs. d_i/w Ratios

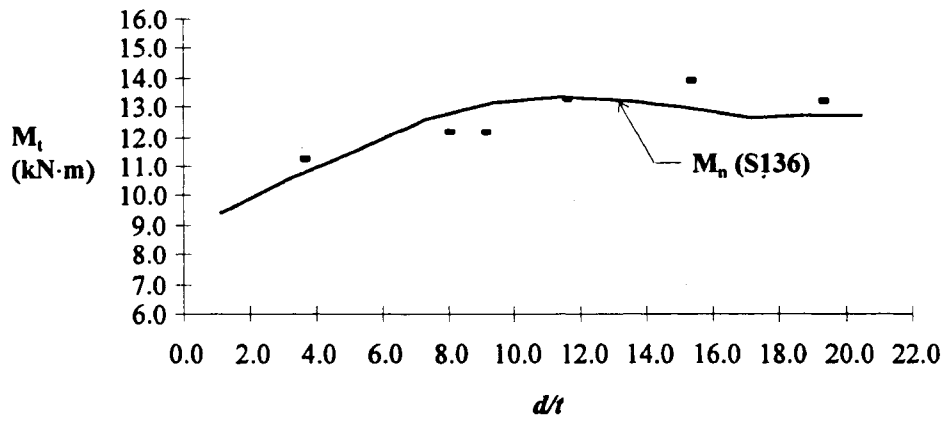


Figure 6.7a - Series C2-3 M_t vs. d/t Ratios

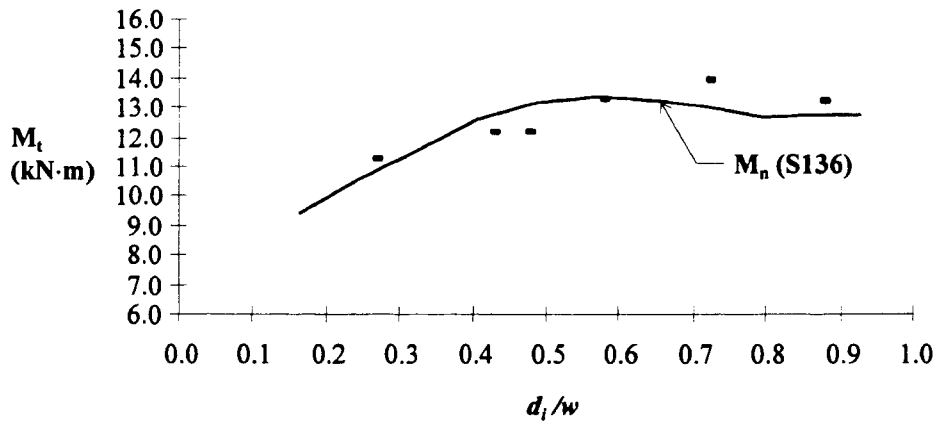


Figure 6.7b - Series C2-3 M_t vs. d_i/w Ratios

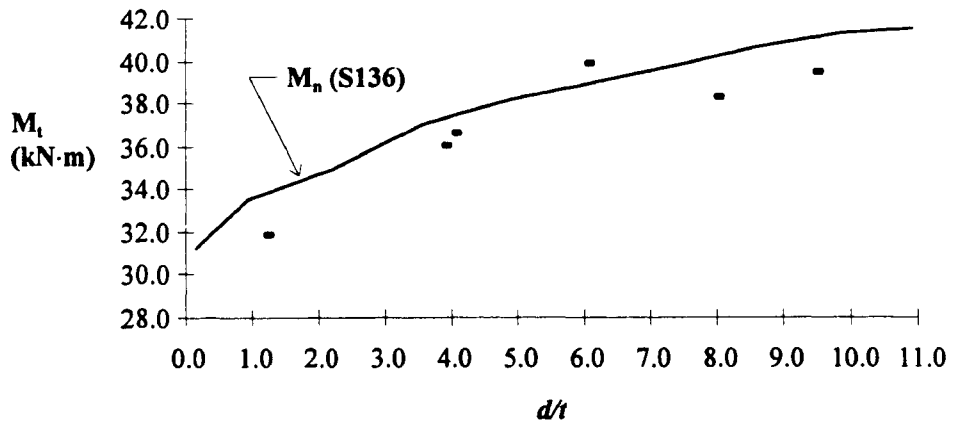


Figure 6.8a - Series C2-4 M_t vs. d/t Ratios

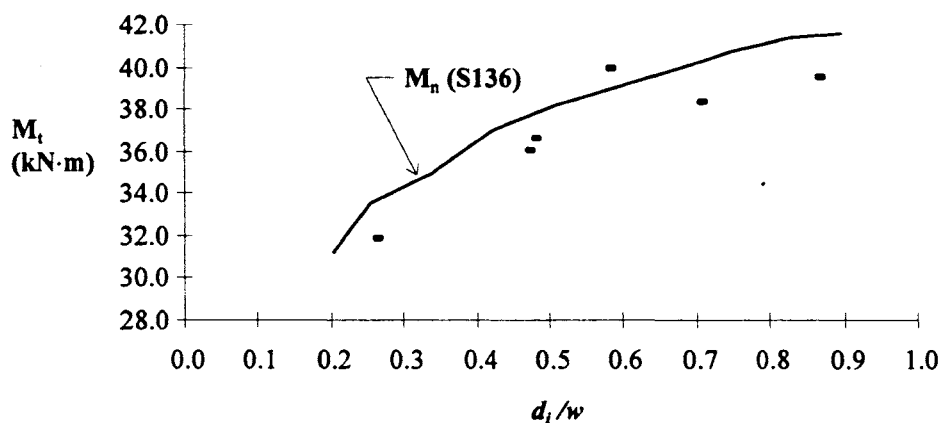


Figure 6.8b - Series C2-4 M_t vs. d_i/w Ratios

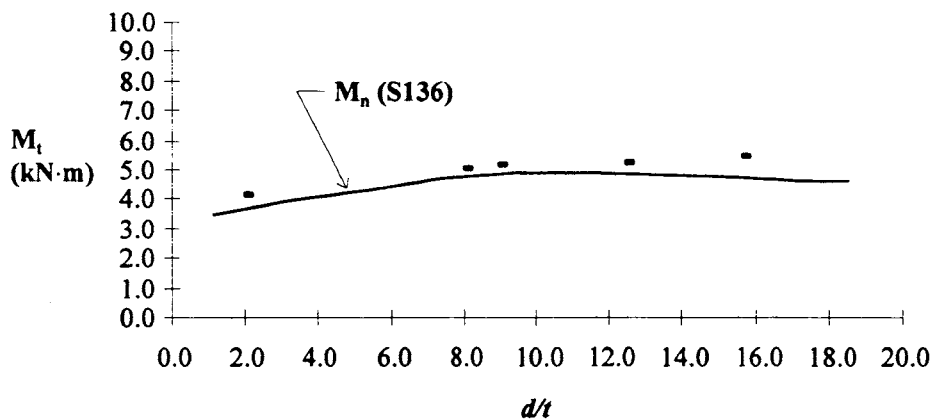


Figure 6.9a - Series C2R-1 M_t vs. d/t Ratios

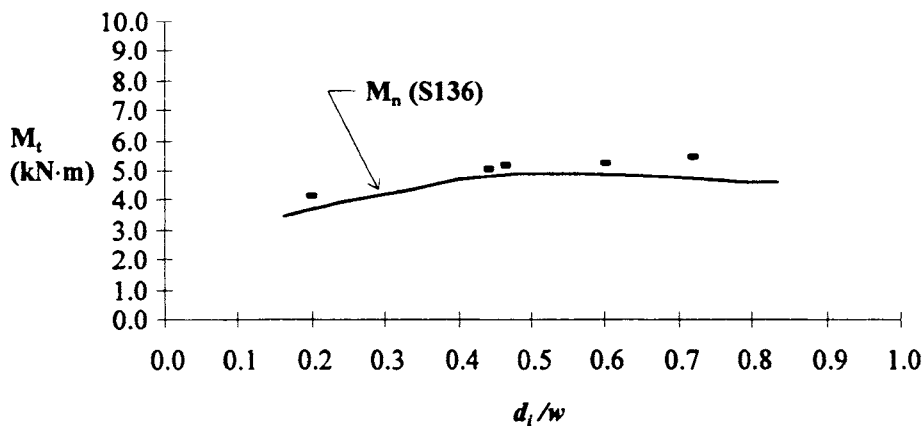


Figure 6.9b - Series C2R-1 M_t vs. d_i/w Ratios

All of the C-sections with Case II flanges, except for specimen C2-DW80-3-A,B exhibited an increase in bending moment capacity as the compressive lip depth was increased. Four of the test sections had d/t values greater than the revised limit of 12 and nineteen of the sections had d_i/w values greater than the proposed 0.4 limit.

6.1.4.3 Case III Flange Series

Two series were tested with Case III flanges, so that additional specimens similar to those used by Willis and Wallace [Wil 90a] [Wil 90b] could be analysed. Series C3-1 consisted of C-sections with locally stable webs and lip depths that ranged from 0mm to 26mm. Series C3-2 consisted of C-sections with locally unstable webs and lip depths that ranged from 0mm to approximately 36.8mm. The bending moment resistance of both series flattened out as the depth of the compression lip was increased rather than decreasing sharply as occurred with the Willis and Wallace data (see Figures 6.10a, 6.10b, 6.11a and 6.11b). For the C3-1 series, the bending moment capacity levelled off at approximately $d/t = 16$ or $d_i/w = 0.4$ and for the C3-2 series the levelling trend occurred at approximately $d/t = 20$ or $d_i/w = 0.4$. The S136 Standard [CSA 94] adequately predicted the bending moment resistance for all sections in the Case III flange range.

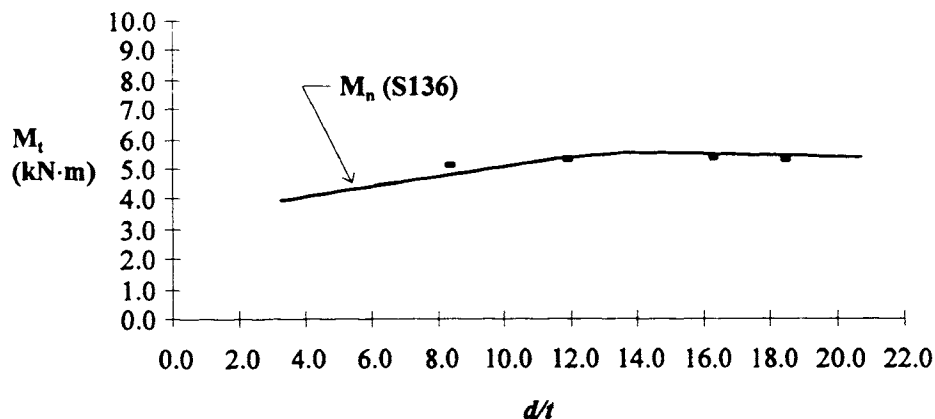


Figure 6.10a - Series C3-1 M_t vs. d/t Ratios

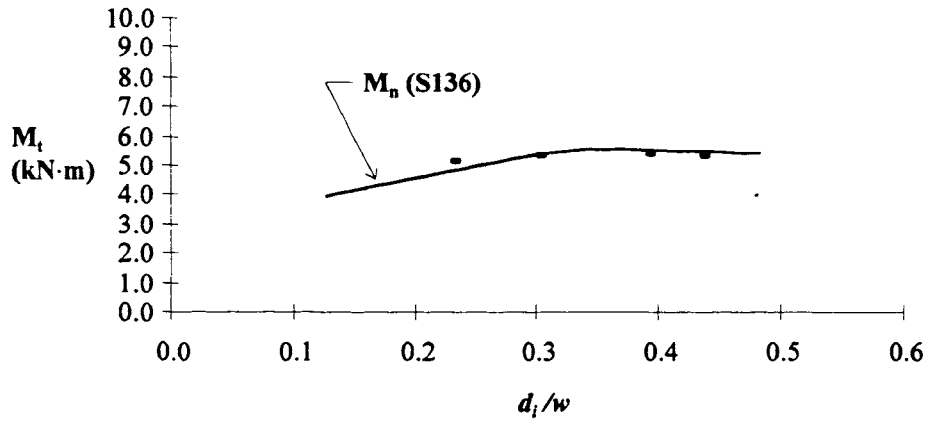


Figure 6.10b - Series C3-1 M_t vs. d_i/w Ratios

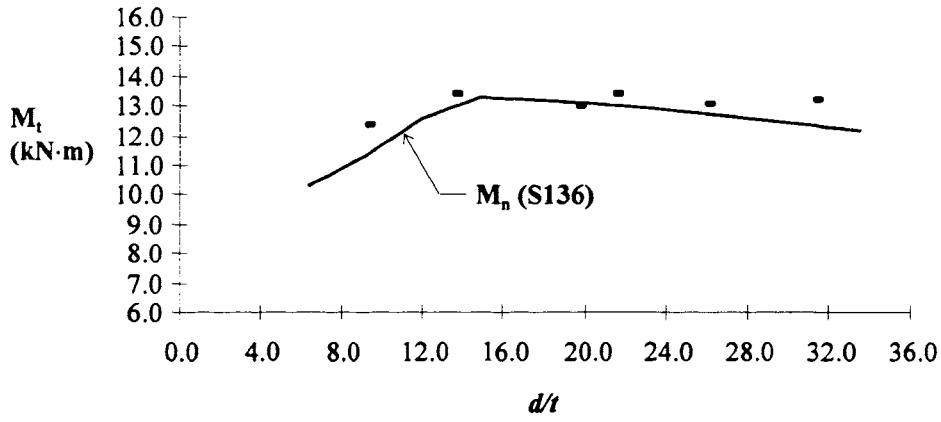


Figure 6.11a - Series C3-2 M_t vs. d/t Ratios

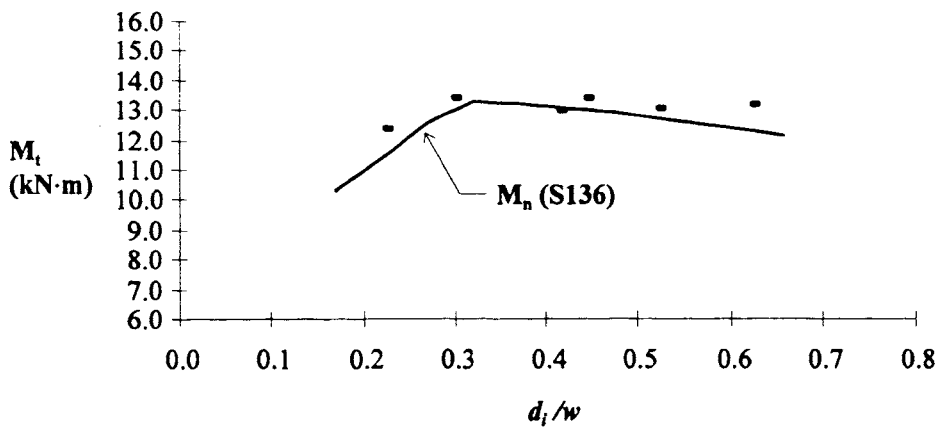


Figure 6.11b - Series C3-2 M_t vs. d_i/w Ratios

The Case III sections tested as part of this work indicated that a levelling of the bending moment capacity appeared at approximately $d_i/w = 0.4$. This result is in agreement with the previous conclusions given by Willis and Wallace [Wil 90a] [Wil 90b], where the bending moment capacity decreased at approximately the same point. However, a conclusion can not be reached regarding a value for a flat width limit, d/t , of the simple edge stiffener.

Based on the Waterloo test data and the Willis and Wallace study [Wil 90a] [Wil 90b], it is recommended that a $d_i/w \leq 0.4$ *warning* for Case III sections be included in the S136 Standard [CSA 94], with a similar explanation as given in Section 6.1.3.

6.2 Plate Buckling Coefficient - Stress Gradient Approach

Although the simple edge stiffener of a section in bending is under a stress gradient, the North American Design Standards [AISI 89a] [CSA 94] specify that the edge stiffener be treated as a uniformly compressed element subjected to the maximum stress. The present method used to determine the effective width of this type of element is outlined by Peköz [Pek 87] and the S136 [CSA 91] and AISI [AISI 89b] Commentaries. Reviews of the current simple edge stiffener effective width calculation procedures for the North American Design Standards are given in Chapter 3.

Due to the lack of relevant data available in the literature, Peköz recommended that further testing be completed regarding this topic [Pek 87]. C-sections tested as part of this work were used to compare various modifications of the existing effective width approach for the simple edge stiffener. Three uniform stress methods were analysed where the magnitude of the compressive stress was defined at different points over the depth of the edge stiffener. Two stress gradient approaches were also examined where the plate buckling coefficient, used in the characteristic stress function, was varied. All other components of the analysis were based on the effective moment resistance method

specified in the S136 Standard [CSA 94]. The stress gradient approaches used can be found in Cohen's Ph.D. work [Coh 87], the ISO Standard [ISO 91] and the Eurocode 3 Standard [Eur 89].

A comparison of the effective width modifications was completed by analysing the resulting test-to-predicted bending moment ratios of the applicable test sections. An attempt to isolate the contribution of the simple edge stiffener to the bending moment resistance was made by using test beams which had locally stable webs, i.e., fully effective, according to the S136 Standard [CSA 94]. Cold formed sections tested by other researchers were used only when the web element was found to be fully effective. However, C-sections tested as part of this work were deemed applicable when the web element ranged between 90% to 100% effective.

6.2.1 Comparison of Different Stress Gradient Approaches

Five methods were used to determine the nominal moment resistance of the applicable test sections. The first three methods altered the magnitude of the compressive stress (see Figure 6.12) and held the plate buckling coefficient constant ($k = 0.43$). The f_3 position refers to the maximum compressive stress in the element, which is specified in the current S136 Standard [CSA 94]. The f_5 position refers to the third point compressive stress and the f_6 position refers to the mid-point compressive stress. The final two methods

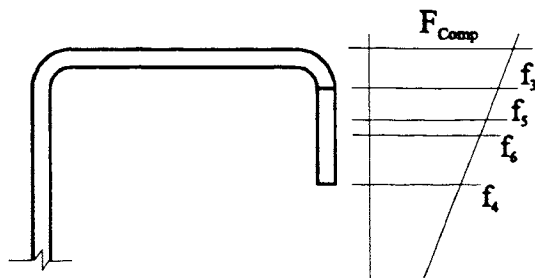


Figure 6.12 - Lip Depth Stress Position Comparison

involved the calculation of a plate buckling coefficient, k , which was dependent on the ratio of stresses f_3 and f_4 . For these two procedures the compressive stress, f_3 , was held constant in the characteristic stress function.

The initial stress gradient method, recommended by Cohen [Coh 87], is formulated as follows,

$$\psi = \frac{f_3}{f_4},$$

$$k = \frac{1.70}{1 + 3/\psi},$$

where $0.43 \leq k \leq 1.70$.

Another version of the previous stress gradient approach is contained in the Eurocode 3 Standard [Eur 89], under Clause A3.3 - Singly Supported Elements Case IIa., where the plate buckling coefficient is calculated as follows,

$$\psi = \frac{f_4}{f_3},$$

$$k = \frac{0.578}{\psi + 0.34}.$$

The Eurocode [Eur 89] stress gradient method uses the inverse ratio of the applied stresses but otherwise yields the same results as Cohen's [Coh 87] equations and is considered equivalent for this study. These plate buckling equations are valid only if the edge stiffener remains in compression over its entire length, i.e., $0 \leq \psi \leq 1$, and $0.43 \leq k \leq 1.70$.

The ISO Standard [ISO 91] lists the stress gradient approach for simple edge stiffeners under Clause 3.2.2 case IIa., where the plate buckling coefficient is determined as follows,

$$Q = \frac{f_4}{f_3},$$

$$k = \frac{1.967}{1 + 3Q},$$

where both f_3 and f_4 are compressive stresses ($f_4 \leq f_3$) and the plate buckling coefficient is in the following range; $0.43 \leq k \leq 1.70$.

6.2.2 Edge Stiffener Stress Gradient Test Results

The plate buckling coefficients and bending moment ratios for all applicable test results are listed in Tables A.4 to A.5c of Appendix 'A' and B.25a to B.25c of Appendix 'B'.

The subscripts used in these listings correspond to the following gradient methods:

- 1) *S136 uniform compressive stress at the top of the flat width (Current).*
- 2) *S136 uniform compressive stress at the mid-point of the flat width.*
- 3) *S136 uniform compressive stress at the third point of the flat width.*
- 4) *Cohen/Eurocode stress gradient.*
- 5) *ISO stress gradient.*

The Waterloo Case I flange specimens, C1-1, were found to be fully effective at their yield stress, hence, cold work of forming was applied for the moment resistance calculations. The existing unified effective width formulation accurately predicted the moment resistance of the C-sections as did all other stress gradient methods (see Tables A.5a to A.5c of Appendix 'A'). The plate buckling coefficients ranged from 0.430 to 0.570 using the ISO [ISO 91] and Cohen/Eurocode [Coh 87] [Eur 89] stress gradient expressions (see Table A.4 of Appendix 'A').

Test series C2-1 was included in the gradient method investigation, because the "Case" of the flange did not influence the final conclusions. The C2-1 specimens were subject to local buckling of the flange and / or edge stiffener, hence, cold work of forming was not applied. The ISO [ISO 91] and Cohen/Eurocode [Coh 87] [Eur 89] stress gradient methods closely predicted the moment resistance of the sections (see Tables A.5b and A.5c of Appendix 'A') as did the existing S136 [CSA 94] method (see Table A.5a of Appendix 'A'). Since the variation in test-to-predicted ratios between methods was minimal, it can be recommended that the less complex S136 method be used. The plate buckling coefficients ranged from 0.430 to 0.699 (see Table A.4 of Appendix 'A').

The results of test series C2R are summarised in Tables A.5a to A.5c of Appendix 'A'. Again, the five stress gradient methods resulted in similar test-to-predicted bending moment ratios. The plate buckling coefficients ranged from 0.430 to 0.693 (see Table A.4 of Appendix 'A').

Test series C2-2 also contained sections which were found to be fully effective. Specimen DW25 did not utilise cold work of forming properties as either the edge stiffener or flange was found to be partially effective at the yield stress. The five gradient methods yielded the same test-to-predicted ratios for all of the specimens in this series (see Tables A.5a to A.5c of Appendix 'A'). The plate buckling coefficients ranged from 0.430 to 0.711 (see Table A.4 of Appendix 'A').

Test series four, C3, was accurately predicted by the five gradient methods (see Tables A.5a to A.5c of Appendix 'A'). The existing S136 [CSA 94] method, as well as, the Cohen/Eurocode [Coh 87] [Eur 89] and the ISO [ISO 91] methods resulted in near similar test-to-predicted bending moment ratios. The plate buckling coefficients ranged from 0.430 to 0.738 (see Table A.4 of Appendix 'A').

Overall, the Waterloo test specimens were accurately predicted by all five of the stress gradient methods. Mean, standard deviation and coefficient of variation values for the test methods indicated no advantage to revising the current S136 [CSA 94] procedure to calculate the effective width of a simple edge stiffener subject to a stress gradient (see Tables A.5a - A.5c of Appendix 'A').

A limited number of available test specimens were found to have fully effective web elements and were included in the simple edge stiffener stress gradient study. These consisted of all four of Desmond's [Des 78a] C-sections, test B-10-1 by LaBoube [LaB 78], tests 2G,16,1&2 (N) and 2G,16,3&4 (N) by Shan [Shan 94] and specimens B2 and B4 to B10 by Winter [Win 47]. The resulting plate buckling coefficients and test-to-predicted bending moment ratios are summarised in Tables B.25a, B.25b and B.25c of Appendix 'B', respectively.

The test-to-predicted bending moment ratios for Desmond's [Des 78a] test section E-45.6B-4 ranged from 1.10 for the existing S136 [CSA 94] method to 1.07 for the ISO [ISO 91] method (see Tables B.25b and B.25c of Appendix 'B'). All other sections exhibited a smaller range in test-to-predicted bending moment ratios between the various stress gradient methods. Plate buckling coefficients ranged from 0.489 to 0.726 for the Cohen/Eurocode [Coh 87] [Eur 89] method and from 0.566 to 0.842 for the ISO method (see Table B.25a of Appendix 'B').

LaBoube's [LaB 78] single applicable section had a consistent test-to-predicted bending moment ratio of 1.06 for all five simple edge stiffener effective width methods (see Tables B.25b and B.25c of Appendix 'B'). The plate buckling coefficients were approximately 0.518 for the Cohen/Eurocode [Coh 87] [Eur 89] method and 0.600 for the ISO [ISO 91] method (see Table B.25a of Appendix 'B').

Shan's [Shan 94] two test sections also showed constant test-to-predicted bending moment ratios for each of the stress gradient methods. The plate buckling coefficients ranged from 0.529 to 0.561 for the Cohen/Eurocode [Coh 87] [Eur 89] method and from 0.612 to 0.649 for the ISO [ISO 91] method (see Table B.25a of Appendix 'B').

Winter's [Win 47] eight applicable C-sections produced test-to-predicted bending moment ratios which ranged from 1.00 to 1.14 (see Tables B.25b and B.25c of Appendix 'B'). This range of values remained constant for each of the stress gradient methods. The plate buckling coefficients ranged from 0.466 to 0.564 for the Cohen/Eurocode [Coh 87] [Eur 89] method and from 0.540 to 0.652 for the ISO [ISO 91] method (see Table B.25a of Appendix 'B').

As found with the Waterloo test data, the available test specimens were accurately predicted by all of the stress gradient methods. Mean, standard deviation and coefficient of variation values for the test methods indicated no advantage to revising the current S136 [CSA 94] procedure to calculate the effective width of a simple edge stiffener subject to a stress gradient (see Tables B.25b and B.25c of Appendix 'B'). Since the variation in statistical results between the five effective width methods was slight, for all the Waterloo and available test data, it can be recommended that current procedures for the calculation of the effective width of a simple edge stiffener subject to a stress gradient remain in the North American Design Standards [AISI 89a] [CSA 94].

Chapter 7

Flange/Web Distortional Buckling Methods of Sections in Bending

7.1 General

Analytical models which can be used to predict the bending strength of cold formed steel sections subjected to flange/web distortional buckling have been developed by various researchers. The basic premise upon which these methods were developed was first established for aluminum structures under uniform compression by Sharp [Sha 66] [Sha 93]. Sharp's distortional buckling formulae considered the geometric properties of an effective column, i.e., one half wave length of the lip/flange component, restrained about the flange/web junction. A reduced distortional buckling stress is first calculated, which is then used with the traditional effective width approach to determine the effective section properties. Presently, there is no flange/web distortional buckling criterion contained in the North American Design Standards [AISI 89a] [CSA 94].

The following researchers from Australia, the United States and Canada have developed similar analytical methods for flange/web distortional buckling of cold formed steel sections in bending:

- 1) Lau & Hancock (Sydney) [Lau 87] [Lau 90]
- 2) Marsh (Concordia) [Mar 90]
- 3) Moreyra (Cornell) [Mor 93]
- 4) Charnvarnichborikarn (Manitoba) [Cha 92]

In each case, Sharp's approach was used as the basis for the analytical method. The procedures recommended by each of the above researchers are presented in the following Sections.

7.1.1 Lau & Hancock [Lau 87] [Lau 90]

The flange/web distortional buckling method detailed below is a modification of the flange/web distortional buckling equations for uniform compression members presented by Lau & Hancock [Lau 87] [Lau 90]. The modification was made in collaboration with Professor G. Hancock. The basic Lau & Hancock method is divided into three models which differ only in the formulation of the strength expressions used to determine the nominal buckling stress. Figure 7.1 shows a schematic diagram of a typical C-section and its lip/flange component, with all the applicable dimensional variables required for analysis.

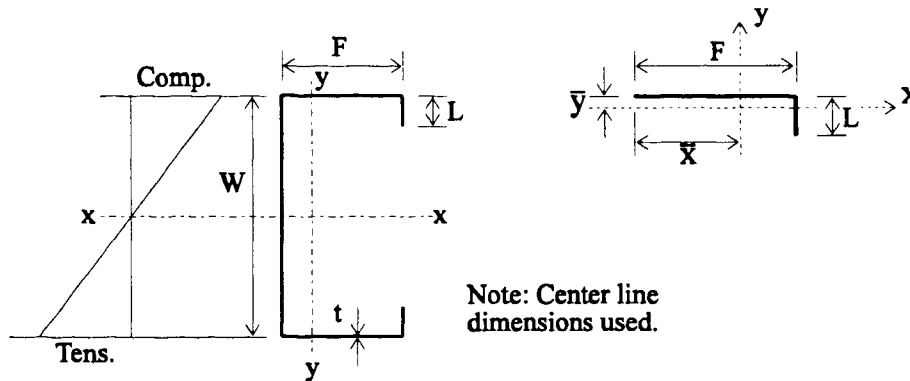


Figure 7.1 - Lau & Hancock C-Section and Lip/Flange Component [Lau 87]

Geometric properties of lip/flange components.

$$A = t(F + L) \quad (7.1)$$

$$\bar{y} = \frac{L^2 / 2}{F + L} \quad (7.2)$$

$$\bar{x} = \frac{F^2 / 2 + L F}{F + L} \quad (7.3)$$

$$J = \frac{t^3}{3}(F + L) \quad (7.4)$$

$$I_x = \frac{F t^3}{12} + \frac{t L^3}{12} + F t \bar{y}^2 + L t (L/2 - \bar{y})^2 \quad (7.5)$$

$$I_y = \frac{t F^3}{12} + \frac{L t^3}{12} + F t (\bar{x} - F/2)^2 + L t (F - \bar{x})^2 \quad (7.6)$$

$$I_{xy} = F t (F/2 - \bar{x})(-\bar{y}) + L t (L/2 - \bar{y}) (F - \bar{x}) \quad (7.7)$$

$$\beta_1 = \bar{x}^2 + \frac{I_x + I_y}{A} \quad (7.8)$$

Buckling half wavelength, λ .

The buckling half wavelength which corresponds to the minimum load for flange/web distortional buckling is expressed as follows.

$$\lambda = 4.80 \left(\frac{I_x F^2 W}{2 t^3} \right)^{0.25} \quad (7.9)$$

Rotational restraint about the flange/web juncture, k_ϕ .

Equation 7.10 was derived from the work by Bleich [Ble 53] regarding the rotational restraint between adjacent plate elements for local buckling. Reduction factors have been included to ensure that k_ϕ becomes zero when the web and flange elements buckle at similar stresses. A further modification, i.e., 0.06λ , has been determined from the results of a number of parametric studies [Lau 87].

$$k_\phi = \frac{2 E t^3}{5.46 (W + 0.06 \lambda)} \quad (7.10)$$

Distortional buckling stress, F_{DB} .

$$\eta = \left(\frac{\pi}{\lambda} \right)^2 \quad (7.11)$$

$$\alpha_1 = \frac{\eta}{\beta_1} (I_x F^2 + 0.039 J \lambda^2) + \frac{k_\phi}{\beta_1 \eta E} \quad (7.12)$$

$$\alpha_2 = \eta \left(I_y + \frac{2}{\beta_1} \bar{y} F I_{xy} \right) \quad (7.13)$$

$$\alpha_3 = \eta \left(\alpha_1 I_y - \frac{\eta}{\beta_1} I_{xy}^2 F^2 \right) \quad (7.14)$$

$$F_{DB} = \frac{P_{CR}}{A} = \frac{E}{2A} \left[(\alpha_1 + \alpha_2) \pm \sqrt{(\alpha_1 + \alpha_2)^2 - 4\alpha_3} \right] \quad (7.15)$$

(use smaller positive value)

Nominal buckling stress, F_N .

Model 1

Based on the column strength expressions specified in the current S136-94 Standard [CSA 94], the nominal buckling stress is computed as follows.

$$\text{If } F_{DB} > F_y/2 \quad \text{then} \quad F_N = F_y (1 - F_y / (4 F_{DB})). \quad (7.16)$$

$$\text{If } F_{DB} \leq F_y/2 \quad \text{then} \quad F_N = F_{DB}. \quad (7.17)$$

Model 2

Based on the column strength expressions developed by Hancock et al. [Han 94a] for post-buckling and sections formed from high yield strength steel, the nominal buckling stress is computed as follows.

$$\text{If } F_{DB} > F_y/2 \quad \text{then} \quad F_N = F_y (1 - F_y / (4 F_{DB})). \quad (7.18)$$

$$\text{If } F_{DB} \leq F_y/2 \quad \text{then} \quad F_N = F_y \left(0.055 \left(\sqrt{\frac{F_y}{F_{DB}}} - 3.6 \right)^2 + 0.237 \right). \quad (7.19)$$

Model 3

Based on the column strength expressions provided in Appendix 'A' of the Eurocode 3 Standard [Eur 89], the nominal buckling stress is computed as follows.

$$\lambda_c = \sqrt{\frac{F_y}{F_{DB}}} \quad (7.20)$$

$$\text{If } \lambda_c \leq 1.5 \quad \text{then} \quad F_N = (0.658^{\lambda_c^2}) F_y. \quad (7.21)$$

$$\text{If } \lambda_c > 1.5 \quad \text{then} \quad F_N = \left(\frac{0.877}{\lambda_c^2} \right) F_y. \quad (7.22)$$

Effective widths of lip, flange and web elements using either the AISI Specification or the S136 Standard at stress F_N .

$$k_L = 0.43 \quad k_F = 4.0 \quad k_W = \text{varies according to the Sooi [Soo 93] web method}$$

Effective section properties.

I_{XE} and S_{XE} are based on the linear method of computation as described in Chapter 3.

Moment resistance.

$$M_{RE} = \phi S_{XE} F_N \quad (7.23)$$

Where ϕ is taken as 1.0 for test data where the yield strength of the steel is known.

A detailed numerical example can be found in Appendix 'C'.

7.1.2 Marsh [Mar 90]

The method developed by Marsh [Mar 90] is being considered by the International Standards Organisation [ISO 93] for the analysis of the flange/web distortional buckling mode of failure of cold formed aluminum sections in bending. Modifications, which were necessary to ensure the method was applicable to non-symmetric sections in bending, were made in collaboration with Professor C. Marsh. The Marsh method is unique with respect to the existing North American Design Standards [AISI 89a] [CSA 94] and the other flange/web distortional buckling methods discussed in this Chapter. The difference is in the calculation of effective section properties, where a reduced

thickness is used for compressed elements instead of the reduced width concept. However, the basic theory upon which the method is based still originates from Sharp's [Sha 66] [Sha 93] work with aluminum structures.

The distortional buckling stress is a function of the geometric properties of the compressed lip/flange components and is calculated in accordance with the strength expressions specified in the current S136 Standard [CSA 94]. An overall normalised section slenderness is calculated and compared with the normalised slenderness of the lip, flange and web elements. Elements which have a normalised slenderness greater than that of the overall section are reduced in thickness. Figure 7.2 shows a schematic diagram of a typical C-section with all the applicable dimensional variables required for the analysis.

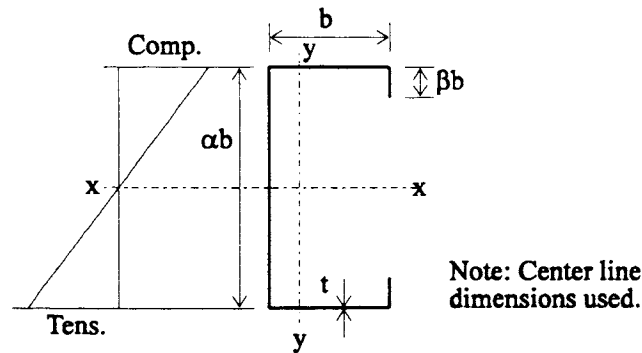


Figure 7.2 - Marsh C-Section [Mar 90]

Geometric properties of lip/flange components.

$$J = (1 + \beta)bt^3 / 3 \quad (7.24)$$

$$k = \frac{3}{16} Et^3 / (\alpha + 0.6)b \quad (7.25)$$

$$C_w = \frac{b^3 t^3}{3} (\beta^3 (b/t)^2 + 0.1) \quad (7.26)$$

$$I_p = (1 + \beta(\beta^2 + 3))b^3 t / 3 \quad (7.27)$$

Where I_p is the polar moment of inertia about the flange/web juncture and α and β represent ratios of the web to flange and lip to flange widths, respectively.

Section slenderness.

$$\lambda = \pi \left(\frac{EI_p}{GJ + 2(EC_w k)^{1/2}} \right)^{1/2} \quad (7.28)$$

Normalised section slenderness, $\bar{\lambda}$.

$$\bar{\lambda} = \frac{\lambda}{\pi} \sqrt{\frac{F}{E}} \quad (7.29)$$

Where F is the maximum compressive stress in the section, e.g., F_y .

Normalised distortional buckling stress, F_c .

$$\text{If } \bar{\lambda} \leq \sqrt{2} \quad \text{then} \quad F_c = F(1 - \bar{\lambda}^2/4). \quad (7.30)$$

$$\text{If } \bar{\lambda} > \sqrt{2} \quad \text{then} \quad F_c = F/\bar{\lambda}^2. \quad (7.31)$$

Where $F_c \leq F_y$.

Web element slenderness, λ_w .

$$\lambda_w = m\alpha b/t, \quad (7.32)$$

where,

$$\text{if } |f_2/f_1| \leq 1 \quad \text{then} \quad m = 1.1 + f_2/2f_1, \quad (7.33)$$

$$\text{if } |f_2/f_1| > 1 \quad \text{then} \quad m = 1.2/(1 - f_2/f_1), \quad (7.34)$$

f_1 = stress in extreme compressive fibre (-),

f_2 = stress in extreme tensile fibre (+).

Normalised web element slenderness, $\bar{\lambda}_w$.

$$\bar{\lambda}_w = \frac{\lambda_w}{\pi} \sqrt{\frac{F}{E}} \quad (7.35)$$

If $\bar{\lambda}_w > \bar{\lambda}$, then the compressed web thickness is reduced, as follows.

$$t'_w = t \sqrt{\bar{F}_w}, \quad (7.36)$$

$$\text{if } \bar{\lambda}_w \leq \sqrt{2} \quad \text{then} \quad \bar{F}_w = (1 - \bar{\lambda}_w^2/4), \quad (7.37)$$

$$\text{if } \bar{\lambda}_w > \sqrt{2} \quad \text{then} \quad \bar{F}_w = 1/\bar{\lambda}_w^2. \quad (7.38)$$

Flange element slenderness, λ_F .

$$\lambda_F = mb/t, \quad (7.39)$$

where $m = 1.6$ for flanges supported by an edge stiffener and the following for unsupported flanges:

$$\text{If } \alpha \leq 3 \quad \text{then} \quad m = 3 + 0.7\alpha \quad (m \leq 5), \quad (7.40)$$

$$\text{If } \alpha > 3 \quad \text{then} \quad m = 5, \quad (7.41)$$

$$\text{and if } \alpha > 3, \text{ then web slenderness is calculated for } \lambda_w = 1.6\alpha b/t. \quad (7.42)$$

Normalised flange element slenderness, $\bar{\lambda}_F$.

$$\bar{\lambda}_F = \frac{\lambda_F}{\pi} \sqrt{\frac{F}{E}} \quad (7.43)$$

If $\bar{\lambda}_F > \bar{\lambda}$ then the compressed flange thickness is reduced, as follows.

$$t'_F = t \sqrt{\bar{F}_F}, \quad (7.44)$$

$$\text{if } \bar{\lambda}_F \leq \sqrt{2} \quad \text{then} \quad \bar{F}_F = (1 - \bar{\lambda}_F^2/4), \quad (7.45)$$

$$\text{if } \bar{\lambda}_F > \sqrt{2} \quad \text{then} \quad \bar{F}_F = 1/\bar{\lambda}_F^2. \quad (7.46)$$

Edge stiffener element slenderness, λ_L .

$$\lambda_L = m\beta b/t, \quad (7.47)$$

where,

$$m = (3 + 0.6 \cdot \beta) \quad (7.48)$$

Normalised edge stiffener element slenderness, $\bar{\lambda}_L$.

$$\bar{\lambda}_L = \frac{\lambda_L}{\pi} \sqrt{\frac{F}{E}} \quad (7.49)$$

If $\bar{\lambda}_L > \bar{\lambda}$, then the compressed edge stiffener thickness is reduced, as follows.

$$t'_L = t \sqrt{\bar{F}_L}, \quad (7.50)$$

$$\text{if } \bar{\lambda}_L \leq \sqrt{2} \quad \text{then} \quad \bar{F}_L = (1 - \bar{\lambda}_L^2/4), \quad (7.51)$$

$$\text{if } \bar{\lambda}_L > \sqrt{2} \quad \text{then} \quad \bar{F}_L = 1/\bar{\lambda}_L^2. \quad (7.52)$$

Effective section properties using reduced element thickness.

I_{XE} and S_{XE} are based on the linear method of computation as described in Chapter 3.

Moment resistance.

$$M_{RE} = \phi S_{XE} F_c \quad (7.53)$$

Where ϕ is taken as 1.0 for test data where the yield strength of the steel is known.

If $\bar{\lambda}_L \leq \bar{\lambda}$, $\bar{\lambda}_F \leq \bar{\lambda}$ and $\bar{\lambda}_w \leq \bar{\lambda}$, then the section is unreduced and gross section properties are used. A detailed numerical example can be found in Appendix 'C'.

7.1.3 Moreyra [Mor 93]

Moreyra [Mor 93] presented a new method to model flange/web distortional buckling of cold formed steel sections in bending. This method consists of a one step nominal edge stress equation, developed from a finite element parametric study. Cold formed steel C-sections with systematically varied dimensions and loaded with member-end bending moments were analysed. The ABAQUS computer software [ABA 89] was used for the finite element analysis, with test A-TB specified as a control to check the accuracy of the computer results. Based on this study, Moreyra concluded that only the web and flange elements influence the distortional buckling stress of a cold formed section subjected to bending. Hence, the lack of an edge stiffener term in the nominal edge stress equation.

Once the initial nominal edge stress is calculated, Sharp's [Sha 66] approach is used to determine the effective width of the flange element. The current AISI Specification [AISI 89a] and the Sooi [Soo 93] web approach are used to determine the effective widths of the simple edge stiffener and web elements, respectively.

Three modifications of Moreyra's method, detailed on the following pages, were included in the procedures used in this work. Two models were used in the comparison study with the web/flange rotational restraint term, K_ϕ , as the only variation. Figure 7.3 shows a

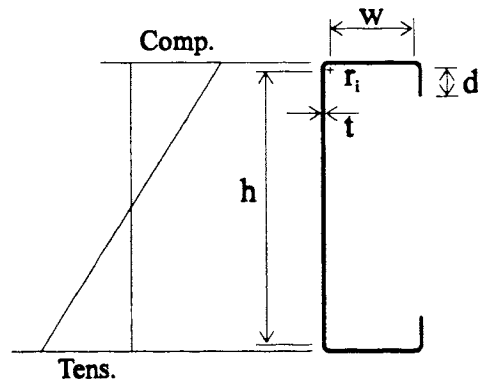


Figure 7.3 - Moreyra C-Section [Mor 93]

schematic diagram of a typical C-section with all of the applicable dimensional variables required for this analysis.

Nominal edge stress, F_n .

$$F_n = \frac{F_y}{\left(\frac{h}{t}\right)^{2/3} \left(0.186 + 0.114 \frac{w}{h}\right)^2} \leq F_y \quad (7.54)$$

Compressed edge stiffener buckling slenderness ratio, λ .

$$\lambda = \frac{1.052}{\sqrt{k}} \left(\frac{d}{t}\right) \sqrt{\frac{F_n}{E}} \quad (7.55)$$

Where $k = 0.43$.

Compressed edge stiffener effective width, d_e .

$$d_e = \rho d \quad (7.56)$$

$$\rho = 1 \quad \text{if } \lambda \leq 0.673. \quad (7.57)$$

$$\rho = \frac{1}{\lambda} \left(1 - \frac{0.22}{\lambda}\right) \quad \text{if } \lambda > 0.673. \quad (7.58)$$

Compressed flange buckling slenderness ratio, λ .

$$\lambda = \frac{\lambda_e}{\pi} \sqrt{\frac{F_n}{E}}, \quad (7.59)$$

where,

$$\lambda_e = \pi \sqrt{\frac{I_p}{\frac{GJ}{E} + 2\sqrt{\frac{K_w C_w}{E}}}} \geq 1.65 \frac{w}{t} \quad (7.60)$$

The ratio of shear modulus to elastic modulus, G/E , used in Eq. 7.60 was simplified to a constant of 0.375 by Sharp [Sha 66] and also by Moreyra [Mor 93]. Since the values of

the shear and elastic moduli are different for aluminum and steel, the base variables were used in this work.

Lip/flange component warping coefficient, C_w .

$$C_w = w^2 \left(I_{yc} - \frac{wt^3}{12} \right) \geq 0 \quad (7.61)$$

Moreyra [Mor 93] included a d/t limit with the above expression, to eliminate the problem of negative values for the warping coefficient, C_w , of the lip/flange component. The d/t limit resulted in the warping coefficient to be equal to zero for sections with small edge stiffeners, although positive C_w values are calculated for these sections. Therefore, the d/t limit was removed from Moreyra's method and replaced with a $C_w \geq 0$ constraint.

Rotational restraint at the flange/web juncture, K_ϕ .

$$K_\phi = \frac{2D_w}{h} \left(\frac{1}{1 + \frac{2w}{3h}} \right) \quad \text{model 1,} \quad (7.62)$$

or

$$K_\phi = \frac{4D_w}{h} \left(\frac{1}{1 + \frac{2w}{3h}} \right) \quad \text{model 2.} \quad (7.63)$$

Sharp's [Sha 66] approach was based on a uniformly compressed member subject to flange/web distortional buckling (see Figure 7.4(a)). Moreyra's [Mor 93] method was developed to model the flange/web distortional buckling of a cold formed steel section in bending. The web element of a section in bending is under a stress gradient (see Figure 7.4(b)) and must only resist the rotational forces of one compressed flange, therefore, the rotational restraint term, K_ϕ , was increased by a factor of two.

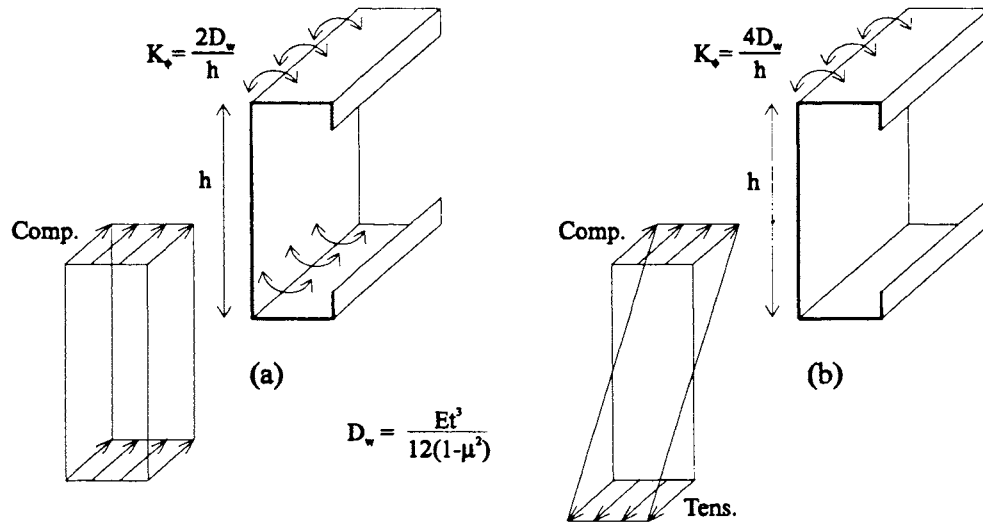


Figure 7.4 - Flange/Web Rotational Restraint Relationship

Lip/flange component section properties.

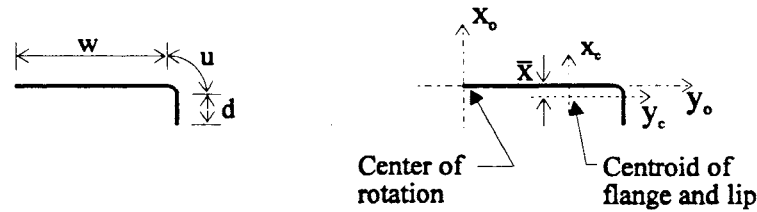


Figure 7.5 - Moreyra Lip/Flange Component [Mor 93]

Figure 7.5 shows the element flat widths and the orientation of axes for the lip/flange component of the Moreyra [Mor 93] flange/web distortional buckling method.

$$u = 1.57r, \quad (7.64)$$

$$c = 0.637r, \quad (7.65)$$

where u and c are the length and centroid of the corner element, respectively.

$$I_{x_o} = t[u(r - c)^2 + d(r + d/2)^2 + d^3/12] \quad (7.66)$$

$$I_{y_o} = t[w^3/3 + u(w + c)^2 + d(w + r)^2] \quad (7.67)$$

$$I_p = I_{x_o} + I_{y_o} \quad (7.68)$$

$$J = \frac{t^3}{3}[w + u + d] \quad (7.69)$$

$$\bar{x} = \frac{u(r-c) + d(d/2 + r)}{w + u + d} \quad (7.70)$$

$$I_{yc} = t[w\bar{x}^2 + u(\bar{x} - r + c)^2 + d(d/2 + r - \bar{x})^2 + d^3/12] \quad (7.71)$$

$$D_w = \frac{Et^3}{12(1 - \mu^2)} \quad (7.72)$$

Compressed flange effective width, w_e .

$$w_e = \rho w \quad (7.73)$$

Where ρ is defined as shown previously.

Web buckling slenderness ratio, λ .

$$\lambda = \frac{1.052}{\sqrt{k}} \left(\frac{h}{t} \right) \sqrt{\frac{f_1}{E}}, \quad (7.74)$$

where,

$$k = 4 + 2(1 - \psi)^3 + 2(1 - \psi) \quad \text{for } -1 < \psi \leq 1, \quad (7.75)$$

$$k = 6(1 - \psi)^2 \quad \text{for } -3 \leq \psi \leq -1, \quad (7.76)$$

$$\psi = \frac{f_2}{f_1}, \quad (7.77)$$

f_1 = stress at the extreme flat width compressive fibre (-),

f_2 = stress at the extreme flat width tensile fibre (+).

Web effective width, h_e .

$$h_e = \rho h \quad (7.78)$$

Where the Sooi [Soo 93] web approach is used to distribute the effective width of the compressed portion of the web element (see Chapter 8).

$$h_1 = h_e - h_t. \quad (7.79)$$

Effective section properties.

I_{XE} and S_{XE} are based on the linear method of computation as described in Chapter 3.

Nominal bending moment resistance.

$$M_n = F_n S_{XE}. \quad (7.80)$$

For purposes of testing, the nominal bending moment capacity is used since the yield strength of the steel is known.

A detailed numerical example can be found in Appendix 'C'.

7.1.4 Charnvarnichborikarn [Cha 92]

Charnvarnichborikarn [Cha 92] modelled the flange/web distortional buckling capacity of a cold formed steel beam with an approach similar to the method first proposed by Sharp [Sha 66]. The flange/web distortional buckling stress of the cross section is determined by using the critical buckling stress of the equivalent lip/flange/web column (see solid line of Figure 7.6) and the column strength expressions specified in the current S136Standard [CSA 94

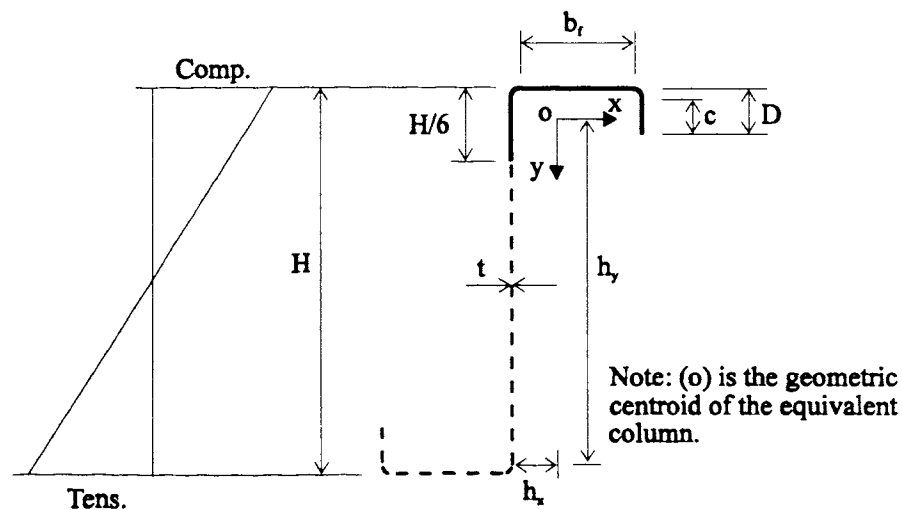


Figure 7.6 - Charnvarnichborikarn Theoretical Equivalent Column [Cha 92]

The following equations give the simplified beam model developed by Charnvarnichborikarn:

Equivalent column section properties.

A_c - gross cross sectional area.

I_{cx} - x-axis moment of inertia.

I_{cy} - y-axis moment of inertia.

I_{cxy} - product moment of inertia.

J_c - St. Venant torsion constant.

C_w - warping constant.

x_{co} - x-co-ordinate of the shear centre.

y_{co} - y-co-ordinate of the shear centre.

$$\chi_1 = h_x^2 + \frac{I_{cx} + I_{cy}}{A_c} \quad (7.81)$$

$$\chi_2 = C_w + I_{cx}(x_{co} - h_x)^2 \quad (7.82)$$

$$\chi_3 = I_{cxy}(x_{co} - h_x) \quad (7.83)$$

$$\chi_4 = \chi_2 + (y_{co} - h_y)(I_{cy}(y_{co} - h_y) - 2\chi_3) \quad (7.84)$$

$$k_\phi = \frac{Et^3}{4w} \quad (7.85)$$

Where w is the flat width of the web element.

$$\lambda = \pi \left(\frac{E\chi_4}{k_\phi} \right)^{1/4} \quad (7.86)$$

$$\eta = \left(\frac{\pi}{\lambda} \right)^2 \quad (7.87)$$

Distortional buckling stress of equivalent lip/flange/web column, σ_c .

$$\alpha_1 = \frac{\eta}{\chi_1} \left(\chi_2 + \frac{GJ_c}{E\eta} \right) + \frac{k_\phi}{\chi_1 E \eta} \quad (7.88)$$

$$\alpha_2 = \eta \left(I_{cy} - \frac{2y_{co}\chi_3}{\chi_1} + \frac{I_{cy}y_{co}^2}{\chi_1} \right) \quad (7.89)$$

$$\alpha_3 = \eta \left(\alpha_1 I_{cy} - \frac{\eta \chi_3^2}{\chi_1} \right) \quad (7.90)$$

$$\sigma_c = \frac{E}{2A_c} \left[(\alpha_1 + \alpha_2) - \sqrt{(\alpha_1 + \alpha_2)^2 - 4\alpha_3} \right] \quad (7.91)$$

Elastic critical stress at outer compressive fibre of cross section, σ_{dcr} .

$$\sigma_{dcr} = \frac{\sigma_c d_c}{d} \quad (7.92)$$

Where,

d_c - distance from the neutral axis of the cross section to the extreme compressive fibre,

d - distance from the neutral axis of the cross section to the centroid of the equivalent column.

Critical flange/web distortional buckling stress of cross section, σ_{cr} .

$$\text{If } \sigma_{dcr} > F_y/2 \quad \text{then} \quad \sigma_{cr} = F_y (1 - F_y / (4 \sigma_{dcr})) \quad (7.93)$$

$$\text{If } \sigma_{dcr} \leq F_y/2 \quad \text{then} \quad \sigma_{cr} = \sigma_{dcr} \quad (7.94)$$

Gross cross section properties.

I_X and S_X are based on the linear method of computation as described in Chapter 3.

Bending moment resistance.

$$M_{cr} = S_X \sigma_{cr} \quad (7.95)$$

The beam model developed by Charnvarnichborikarn [Cha 92] was not used in the comparison of the flange/web distortional buckling methods (see Sections 7.2 to 7.4). Test-to-predicted bending moment ratios, which ranged from 1.29 to 1.41 for specimens tested by Charnvarnichborikarn, indicate that the above model yields significantly conservative results (see Table 6.6 of Charnvarnichborikarn's Ph.D. thesis) [Cha 92]. Furthermore, equations for the geometric properties of the equivalent column were not presented in Charnvarnichborikarn's work, e.g., C_w . If this model is to be considered for placement in the North American Design Standards [AISI 89a] [CSA 94] it is required that all equivalent column properties and equations be presented.

7.2 Comparison of Flange/Web Distortional Buckling Methods with Waterloo Test Data

Four of the specimens tested as part of this work were included in the flange/web distortional buckling method investigation (see Table 4.2 for test specimen failure modes). Test-to-predicted bending moment ratios, M_T/M_p , for local buckling analyses of all individual tests are found in Tables A.6a to A.6d of Appendix 'A' and for flange/web distortional buckling analyses in Tables A.7a to A.7d of Appendix 'A'. Table 7.1 contains a list of the local and flange/web distortional buckling test-to-predicted bending moment ratios as well as the pertinent statistical results.

The statistical comparisons of the flange/web distortional buckling results of Table 7.1 reveal that the method proposed by Marsh [Mar 90] gives the best results, considering the mean test-to-predicted moment ratios. The Lau & Hancock [Lau 87] [Lau 90], as well as the Moreyra [Mor 93] methods are conservative, hence, better predictor methods in comparison to the unconservative North American Design Standards [AISI 89a] [CSA 94].

Table 7.1 - Comparison of Flange/Web Distortional Buckling Methods with Waterloo Test Data

Test Specimen	S136	AISI	L&H 1	L&H 2	L&H 3	Mar	Mor 1	Mor 2	
	M_T (kN·m)	M_T/M_P							
C1-DW30-2-A,B	24.3	0.91	0.83	1.14	1.14	1.18	1.02	1.11	1.11
C1-DW40-2-A,B	24.9	0.93	0.84	1.14	1.14	1.19	1.02	1.11	1.11
C1-DW60-2-A,B	25.6	0.90	0.81	1.12	1.12	1.16	0.96	1.10	1.10
C1-DW80-2-A,B	26.1	0.89	0.80	1.11	1.11	1.15	0.93	1.09	1.09
Mean		0.909	0.817	1.13	1.13	1.17	0.982	1.10	1.10
Std. Dev.		0.017	0.016	0.015	0.015	0.017	0.043	0.012	0.012
Coeff. of Var.		0.032	0.035	0.024	0.024	0.025	0.075	0.019	0.018

Note: L&H, Mar and Mor refer to the Lau & Hancock [Lau 87] [Lau 90], Marsh [Mar 90] and Moreyra [Mor 93] flange/web distortional buckling methods, respectively.

7.3 Comparison of Flange/Web Distortional Buckling Methods with Available Test Data

Seventeen of the C-section tests completed in the research programs outlined in Chapter 5 were included in this section of the flange/web distortional buckling method investigation. The applicable sections were chosen based on the failure descriptions provided by the respective researchers and the extent to which the tests were unconservatively predicted by the S136 Design Standard [CSA 94]. Test specimens with unconservative test-to-predicted bending moment ratios according to the AISI Specification [AISI 89a] and adequate test-to-predicted bending moment ratios according to the S136 Standard were not considered applicable to this investigation. For this reason, all specimens tested by Willis & Wallace [Wil 90a] and five specimens tested by Shan [Shan 94] (8B,14,5&6(N), 8B,14,7&8(N), 8B,20,1&2(N), 8B,20,3&4(N), and 8B,20,5&6(N)) were not included in the flange/web distortional buckling investigation. Since the bending moment resistance of these test specimens was adequately predicted by the S136 Standard, their analysis using a flange/web distortional buckling method is not required. Test-to-predicted bending moment ratios for each of the applicable test

specimens are given in Tables B.34, B.35a and B.35b (Moreyra [Mor 93]), B.38, B.39a and B.39b (Schuster [Schu 92]) and B.40, B.41a and B.41b (Shan [Shan 94]) of Appendix 'B'. Test-to-predicted bending moment ratios, as well as statistical information for the applicable C-section test specimens are given in Table 7.2.

Similar to that observed from the statistical information in Table 7.1, the Marsh [Mar 90] flange/web distortional buckling method produces the best results for the available applicable C-section test specimens. However, the Lau & Hancock 1 and 2 [Lau 87] [Lau

Table 7.2 - Comparison of Flange/Web Distortional Buckling Methods with Available Test Data

Test Specimen	S136	AISI	L&H 1	L&H 2	L&H 3	Mar	Mor 1	Mor 2	
	M_T (kN·m)	M_T/M_P							
<u>Moreyra [Mor 93]</u>									
A-W	14.0	0.93	0.86	1.06	1.06	1.17	1.02	0.96	0.92
A-TB	14.4	0.87	0.80	1.01	1.01	1.12	0.96	0.91	0.88
B-W	13.2	0.87	0.81	1.01	1.01	1.12	1.00	0.92	0.89
B-TB	14.0	0.91	0.82	1.01	1.01	1.13	1.01	0.92	0.89
C-W	15.6	1.12	1.02	1.24	1.24	1.38	1.24	1.14	1.09
C-TB	15.0	1.00	0.90	1.10	1.10	1.23	1.10	1.00	0.96
<u>Schuster [Schu 92]</u>									
BS1	8.46	0.93	0.82	1.08	1.08	1.17	1.05	1.13	1.10
BS2	8.61	0.95	0.84	1.10	1.10	1.19	1.07	1.15	1.12
CS1	9.05	0.83	0.76	1.01	1.01	1.09	0.96	1.05	1.01
CS2	9.05	0.83	0.76	1.01	1.01	1.09	0.96	1.05	1.01
CS3	9.29	0.86	0.78	1.03	1.03	1.12	0.98	1.07	1.04
<u>Shan [Shan 94]</u>									
8A,14,7&8(N)	15.3	0.88	0.80	0.98	0.98	1.05	0.99	0.89	0.87
8A,14,9&10(N)	15.7	0.90	0.82	1.01	1.01	1.08	1.01	0.91	0.89
8A,20,1&2(N)	4.07	0.89	0.86	1.29	1.29	1.39	1.08	1.49	1.44
8A,20,3&4(N)	4.12	0.89	0.85	1.30	1.30	1.40	1.08	1.50	1.45
12B,16,1&2(N)	22.5	0.78	0.74	1.14	1.14	1.21	0.94	1.19	1.16
12B,16,3&4(N)	23.4	0.82	0.78	1.19	1.19	1.27	1.00	1.25	1.21
Mean		0.899	0.825	1.09	1.09	1.19	1.03	1.09	1.06
Std. Dev.		0.078	0.065	0.105	0.105	0.111	0.072	0.188	0.182
Coeff. of Var.		0.093	0.085	0.103	0.103	0.100	0.075	0.185	0.184

90], as well as the Moreyra 1 and 2 [Mor 93] methods also provided adequate predictions of the flange/web distortional buckling strength of the test specimens.

The Z-section specimens tested by Charnvarnichborikarn [Cha 92] which were subject to flange/web distortional buckling were included in this investigation. Test-to-predicted bending moment ratios for each of the test specimens are found in Tables B.26, B.27a and B.27b of Appendix 'B'. Test-to-predicted bending moment ratios, as well as statistical information for the applicable test specimens are given in Table 7.3. The tests completed by Charnvarnichborikarn were separated from the available test data, listed in Table 7.2, due to a difference in cross section type.

Table 7.3 - Comparison of Flange/Web Distortional Buckling Methods with Charnvarnichborikarn Test Data [Cha 92]

Test Specimen	S136	AISI	L&H 1	L&H 2	L&H 3	Mar	Mor 1	Mor 2	
	M_T (kN·m)	M_T/M_P							
2.7-0.15-1	6.11	0.944	0.865	1.46	1.26	1.67	1.87	1.03	0.987
2.7-0.15-2	6.00	0.906	0.826	1.37	1.21	1.56	1.75	0.980	0.942
2.7-0.25-1	6.11	0.861	0.788	1.11	1.11	1.28	1.35	0.942	0.900
2.7-0.25-2	6.51	0.919	0.839	1.25	1.21	1.43	1.55	0.997	0.953
2.7-0.50-1	6.58	0.797	0.724	0.878	0.878	1.01	0.927	0.877	0.835
2.7-0.50-2	6.64	0.790	0.718	0.867	0.867	0.998	0.903	0.873	0.832
2.7-0.75-1	7.02	0.731	0.669	0.819	0.819	0.928	0.807	0.850	0.819
2.7-0.75-2	6.62	0.697	0.637	0.778	0.778	0.882	0.768	0.809	0.778
2.7-1.00-1	7.13	0.735	0.671	0.797	0.797	0.890	0.821	0.836	0.829
2.7-1.00-2	6.82	0.726	0.662	0.789	0.789	0.882	0.817	0.832	0.826
2.7-1.25-1	6.94	0.729	0.667	0.764	0.764	0.851	0.763	0.797	0.797
2.7-1.25-2	7.29	0.787	0.723	0.826	0.826	0.921	0.825	0.867	0.867
2.7-1.50-1	7.05	0.780	0.721	0.797	0.797	0.891	0.770	0.837	0.837
2.7-1.50-2	7.21	0.783	0.722	0.797	0.797	0.889	0.767	0.835	0.835
2.7-2.00-1	6.90	0.839	0.785	0.828	0.828	0.939	0.743	0.824	0.824
2.7-2.00-2	7.13	0.849	0.792	0.834	0.834	0.945	0.748	0.827	0.827
Mean		0.805	0.738	0.935	0.910	1.06	1.01	0.876	0.855
Std. Dev.		0.075	0.070	0.228	0.176	0.266	0.386	0.071	0.059
Coeff. of Var.		0.100	0.102	0.262	0.208	0.270	0.410	0.087	0.074

The statistical data given in Table 7.3 indicates that the flange/web distortional bending moment strength of the Z-sections tested by Charnvarnichborikarn [Cha 92] is not predicted as accurately in comparison to the previous applicable test data listed in Tables 7.1 and 7.2. The Marsh [Mar 90] method remains the best predictor method, however, the test results were not as consistent, shown by the increased standard deviation and coefficient of variation values. The Lau & Hancock 1 and 2 [Lau 87] [Lau 90], as well as Moreyra [Mor 93] models resulted in more accurate strength predictions compared to the current North American Design Standards [AISI 89a] [CSA 94], although, the mean values remained unconservative.

7.4 Comparison of All Test Data and Flange/Web Distortional Buckling Methods

The applicable Waterloo and available test data were combined and analysed, with the results presented in Table 7.4. Similar to the previous comparison sections, the Marsh [Mar 90] method provided the best prediction of the flange/web distortional buckling strength of the test specimens based on the statistical evidence. Methods proposed by Lau & Hancock [Lau 87] [Lau 90], as well as Moreyra [Mor 93] also provided adequate predictions of the bending strength of the test specimens.

Table 7.4 - Test Data - Test / Predicted Bending Moment Ratios

Test Specimen	S136 M_T/M_P	AISI M_T/M_P	L&H 1 M_T/M_P	L&H 2 M_T/M_P	L&H 3 M_T/M_P	Mar M_T/M_P	Mor 1 M_T/M_P	Mor 2 M_T/M_P
<u>Excluding Charn...</u>								
<u>Data (21 Tests)</u>								
Mean	0.900	0.823	1.10	1.10	1.19	1.02	1.09	1.06
Std. Dev.	0.070	0.059	0.095	0.095	0.100	0.069	0.168	0.164
Coeff. of Var.	0.082	0.075	0.091	0.091	0.089	0.071	0.163	0.162
<u>Including Charn...</u>								
<u>Data (37 Tests)</u>								
Mean	0.859	0.786	1.03	1.02	1.13	1.02	0.998	0.974
Std. Dev.	0.086	0.076	0.183	0.164	0.197	0.254	0.172	0.165
Coeff. of Var.	0.103	0.100	0.183	0.166	0.180	0.258	0.177	0.175

The North American Design Standards [AISI 89a] [CSA 94] are based on the unified effective width approach, where the flat width of an element is reduced according to the effective width equation. Although the distortional buckling model proposed by Marsh [Mar 90] yields the most accurate test-to-predicted bending moment ratios, it does not follow the unified effective width approach. Element thickness, instead of width, is reduced according to the slenderness of the cross section (see Section 7.1.2). Since the Marsh method requires a change in design philosophy from the North American Design Standards, it is not recommended as a predictor method for the flange/web distortional buckling mode of failure of sections in bending.

The Lau & Hancock [Lau 87] [Lau 90] and Moreyra [Mor 93] flange/web distortional buckling methods were developed in accordance with the unified effective width approach (see Sections 7.1.1 and 7.1.3). Based on the statistical results of the test-to-predicted bending moment ratios, excluding the Charnvornichborikarn [Cha 92] data (see Table 7.4), the Lau & Hancock 1 and 2 methods yield the most accurate strength predictions. The Moreyra methods have less conservative mean values, however, the standard deviations and coefficient of variations indicate a lack of precision in the predicted bending moment strength. In addition, the procedures specified by Moreyra involve a nominal buckling stress equation, F_n , which was derived from the results of a parametric study using the ABAQUS [ABA 89] finite element computer software. The parametric study involved simple edge stiffened C-sections in bending, hence, the nominal buckling stress equation is not valid for other cross section configurations. The nominal buckling stress equation does not have a theoretical origin and is not dependent on the dimension of the simple edge stiffener. Furthermore, the Moreyra method first requires a reduced nominal buckling stress, then further reduces this stress in the calculation of the effective compressed flange width according to the Sharp approach [Sha 66]. Sharp's approach is itself a method with which the distortional buckling stress of the equivalent column can be determined. Therefore, the initial nominal buckling

stress calculation is a doubling of the distortional buckling stress reduction procedure and is unnecessary.

The three Lau & Hancock [Lau 87] [Lau 90] models follow the procedures recommended by Sharp [Sha 66] for the calculation of the equivalent column distortional buckling stress (see Section 7.1.1). The Sharp approach is based on the geometric properties of the lip/flange component, which allows for various edge stiffener configurations in addition to the simple lip. The Lau & Hancock methods vary only in the required column strength expression used to find the stress at which bending failure occurs. The Lau & Hancock 1 and 2 models yield the same results for the test specimens included in this investigation. Model 1 specifies the column strength expressions found in the current North American Design Standards. Model 2 consists of an adaptation of these column strength expressions to account for post-buckling and the use of high strength steels commonly found in the Australian construction industry. Models 1 and 2 have also been included in the most recent edition of the Australian Standard [SAA 94] for the analysis of flange/web and lip/flange distortional buckling, respectively. Since model 2 of the Lau & Hancock method accounts for post-buckling and high strength steels and has been adopted by the Standards Association of Australia, it is recommended that it be used as the North American predictor method for the flange/web distortional buckling strength of cold formed steel sections in bending.

7.5 Comparison of Additional Lau & Hancock [Lau 87] [Lau 90] Flange/Web Distortional Buckling Models

Two additional Lau & Hancock [Lau 87] [Lau 90] models were included in the comparison of flange/web distortional buckling methods. These models are presented in Appendix 'D' because the main body of this work had been printed prior to completion of their analysis. Test-to-predicted bending moment ratios for each of the test specimens subject to flange/web distortional buckling are given in Tables D.2 to D.4 of Appendix 'D'.

Models 4 and 5 of the Lau & Hancock method [Lau 87] [Lau 90] result in accurate predictions of bending moment values for the Waterloo and available test data subject to flange/web distortional buckling (see Table D.1 of Appendix 'D'). Statistical results indicate that test-to-predicted mean values for all applicable test specimens, excluding Charnvarnichborikarn's data [Cha 92], are better predicted using models 4 and 5 in comparison to model 2 of the Lau & Hancock method. The resulting standard deviations and coefficient of variations indicate only a marginal increase in scatter of results. Hence, it is recommended that either model 4 or 5 of the Lau & Hancock method be used as the North American predictor method for the flange/web distortional buckling strength of cold formed steel sections in bending.

7.6 Implementation of Flange/Web Distortional Buckling Analysis

The Australian steel storage racking [SAA 93] and Cold-formed steel structures [SAA 94] design standards have adopted the procedures recommended by Lau & Hancock [Lau 87] [Lau 90] to predict the bending moment resistance of a section subject to flange/web distortional buckling. However, a limiting equation or ratio of dimensional parameters which could be used to denote when distortional buckling analysis need be applied has not been specified by these standards. Since only certain sections included in this work failed by flange/web distortional buckling, a limit must be defined to indicate when this additional buckling analysis is required.

An attempt to determine a characteristic limiting ratio of dimensional parameters from the test specimens identified as being subject to flange/web distortional buckling was completed. Section dimension ratios of the applicable test specimens used in this investigation are contained in Table 7.5. Comparisons of the following dimensional parameters; h/t , w/t , d/t , d_i/w and h/w with yield stress, the S136 [CSA 94] test-to-predicted bending moment ratios and with one another were inconclusive. This result led to the conclusion that the use of a distortional buckling analysis is at the discretion of the

design engineer. The above mentioned Australian steel standards [SAA 93] [SAA 94] also rely upon the knowledge of the design engineer, as well as, refer to the publications of Hancock [Han 85] and Lau & Hancock [Lau 87] for background information.

Table 7.5 - Geometric Ratios - Flange/Web Distortional Buckling Test Specimens

Test Specimen	F_y (MPa)	t (mm)	h/t	w/t	d/t	d _f /w	w/h
C1-DW30-2-A,B	396	1.85	159	9.26	0.520	0.380	0.058
C1-DW40-2-A,B	396	1.85	157	9.34	1.30	0.461	0.060
C1-DW60-2-A,B	396	1.85	159	9.38	3.08	0.646	0.059
C1-DW80-2-A,B	396	1.85	159	9.36	4.57	0.810	0.059
<u>Moreyra [Mor 93]</u>							
A-W	397	1.80	113	26.7	12.2	0.591	0.236
A-TB	438	1.80	114	27.4	12.3	0.581	0.240
B-W	396	1.80	113	27.5	10.2	0.502	0.244
B-TB	425	1.80	114	27.8	9.74	0.482	0.243
C-W	413	1.75	117	28.1	9.02	0.454	0.241
C-TB	432	1.80	114	27.5	8.73	0.449	0.241
<u>Schuster [Schu 92]</u>							
BS1	271	1.21	162	27.9	6.92	0.356	0.172
BS2	271	1.21	162	27.9	6.92	0.356	0.172
CS1	331	1.22	160	26.8	7.66	0.398	0.167
CS2	331	1.22	161	26.8	7.66	0.398	0.166
CS3	331	1.22	161	27.6	7.66	0.392	0.169
<u>Shan [Shan 94]</u>							
8A,14,7&8(N)	384	1.68	117	16.3	4.63	0.733	0.140
8A,14,9&10(N)	384	1.68	117	16.3	4.55	0.428	0.139
8A,20,1&2(N)	274	0.79	248	36.5	9.69	0.376	0.147
8A,20,3&4(N)	274	0.79	248	36.3	10.2	0.392	0.147
12B,16,1&2(N)	425	1.57	188	21.3	6.04	0.402	0.113
12B,16,3&4(N)	425	1.57	188	21.4	5.64	0.382	0.114
<u>Charn... [Cha 92]</u>							
2.7-0.15-1	324	1.47	132	43.8	1.53	0.114	0.332
2.7-0.15-2	324	1.50	129	42.9	1.70	0.115	0.331
2.7-0.25-1	324	1.47	132	44.5	3.46	0.155	0.337
2.7-0.25-2	324	1.50	129	44.5	3.00	0.141	0.346
2.7-0.50-1	324	1.50	129	43.9	7.14	0.239	0.340
2.7-0.50-2	324	1.50	129	43.8	7.68	0.252	0.338
2.7-0.75-1	324	1.50	129	43.6	11.6	0.346	0.338
2.7-0.75-2	324	1.50	129	43.9	11.4	0.336	0.340
2.7-1.00-1	324	1.50	129	43.8	16.2	0.441	0.338
2.7-1.00-2	324	1.47	131	44.5	16.1	0.434	0.340
2.7-1.25-1	324	1.50	129	43.6	20.2	0.541	0.337
2.7-1.25-2	324	1.47	132	44.2	20.4	0.538	0.336
2.7-1.50-1	324	1.47	132	45.0	24.5	0.620	0.342
2.7-1.50-2	324	1.50	130	44.6	24.4	0.616	0.343
2.7-2.00-1	324	1.47	132	45.2	33.7	0.816	0.344
2.7-2.00-2	324	1.50	129	44.6	33.2	0.813	0.344

Cold formed steel sections fabricated for the North American construction industry, as beams or beam columns, are typically limited in number and similarly dimensioned by the various steel fabricators. A list of the most common floor joists was included in Table 7.6, so that a comparison of standard C-sections to the test sections which failed by flange/web distortional buckling could be made.

Table 7.6 - Geometric Ratios - Industry Standard Floor Joist C-Sections

Test Specimen	F_y (MPa)	t (mm)	h/t	w/t	d/t	d_f/w	w/h
152 x .838	230	0.838	147	36.2	10.2	0.350	0.246
152 x .914	230	0.914	147	35.8	9.96	0.355	0.244
152 x 1.12	230	1.12	146	34.6	9.35	0.367	0.237
152 x 1.22	230	1.22	145	34.0	9.04	0.374	0.234
152 x 1.52	345	1.52	143	32.1	8.13	0.395	0.224
152 x 1.91	345	1.91	141	29.8	6.99	0.426	0.212
203 x 1.22	230	1.22	196	34.0	9.04	0.374	0.173
203 x 1.52	345	1.52	194	32.1	8.13	0.395	0.166
203 x 1.91	345	1.91	192	29.8	6.99	0.426	0.156

The dimensions of common floor joist C-sections consistently fall within the range set by the test specimens which failed by flange/web distortional buckling (see Table 7.5). To determine a mode of failure based solely on this range of dimensions would be false, therefore, it is recommended that a study to determine which industry standard sections undergo flange/web distortional buckling be completed. The recommended study would be limited in size due to the small number of variations in cross section dimensions currently provided by sheet steel fabricators. Completion of this recommendation would only be a temporary measure to address concerns regarding cold formed steel sections currently used in construction. Further investigation of an actual theoretical or empirical limit used to identify the need for flange/web distortional buckling analysis for any type of cross section is also required.

Chapter 8

Local Buckling Model Improvements

8.1 Edge-Stiffened Flange Method by Dinovitzer [Din 92]

Dinovitzer et al. [Din 92] completed an investigation of compressed flanges where a discontinuity in the effective width equation for sections with partially stiffened flanges and simple edge stiffeners (lips) was discovered. A partially stiffened flange is an element that is supported by a web on one side and an edge stiffener of inadequate rigidity ($I_r < 1$) on the other. The S136-M89 Design Standard [CSA 89] was examined to find the source of this discontinuity in the flange effective width formulation. Dinovitzer determined that the plate buckling coefficient, k , equations were identical for Case II and Case III flanges except for an exponent change from $1/2$ to $1/3$. The objective of the investigation was to then develop an equation which would allow the exponent to vary from $1/2$ to $1/3$. Dinovitzer concluded that *The stepwise transition from design Case II to Case III should be replaced with the linear formulation of the plate buckling exponent transition* [Din 92]. For Case II and Case III sections with an edge stiffener of inadequate rigidity ($I_r < 1$), the following plate buckling coefficient equations and linear formulation of the exponent, n , are recommended:

$$d_i/w \leq 0.25 \quad k = 3.57 (I_r)^n + 0.43,$$

$$0.25 < d_i/w \leq 0.8 \quad k = [4.82 - 5(d_i/w)] (I_r)^n + 0.43,$$

$$n = \frac{25}{43} - \frac{37W}{192} \sqrt{\frac{f}{E}} \quad (1/3 \leq n \leq 1/2).$$

Where $W = w/t$. This new formulation only affects the plate buckling coefficient of sections with Case II flanges, since $n = 1/3$ for $w/t > W_{lim2}$. Dinovitzer's flange method

also simplifies the procedures required for the analysis of compressed flanges, by eliminating the need to differentiate between Case II and Case III elements.

8.1.1 Comparison with Waterloo Test Data

Five of the series tested as part of this work contained test specimens with inadequately stiffened ($I_r < 1$) Case II flanges. In total, seven test specimens from these series were applicable to the Dinovitzer [Din 92] flange method investigation. The specimen identification numbers and the resulting Dinovitzer exponents, n , plate buckling coefficients and the S136 [CSA 94] plate buckling coefficients are summarised in Table 8.1. Test-to-predicted bending moment ratios for the current S136 Design procedure can be found in Tables A.6a and A.6b of Appendix 'A' and for the proposed Dinovitzer method in Tables A.6c and A.6d of Appendix 'A'. Considering the test specimens listed in Table 8.1, the Dinovitzer method resulted in more accurate predictions of the bending moment resistance, without cold work of forming. A mean of 1.04, a standard deviation

Table 8.1 - Comparison of Dinovitzer Exponent, n , and k Values with Waterloo Test Data [Din 92]

Specimen	n	k (Din)	k (S136)
C2-DW20-1-A	0.338	1.43	0.972
C2-DW20-1-B	0.342	1.29	0.877
C2-DW45-1-A	0.349	2.92	2.90
C2-DW45-1-B	0.345	2.85	2.76
C2-DW25-2-A	0.446	1.83	1.69
C2-DW25-2-B	0.447	1.76	1.63
C2-DW20-3-A	0.388	1.90	1.57
C2-DW20-3-B	0.388	1.92	1.60
C2-DW35-3-A	0.383	3.11	3.11
C2-DW35-3-B*	0.500	3.11	3.11
C2-DW25-4-A	0.438	1.07	0.934
C2-DW25-4-B	0.437	1.24	1.09
C2R-DW20-1-A	0.384	1.15	0.874
C2R-DW20-1-B	0.384	1.15	0.874

Note: * $I_r > 1$ for test specimen C2-DW35-3-B.

of 0.090 and a coefficient of variation of 0.106 were calculated for the Dinovitzer method as compared to a mean of 1.06, a standard deviation of 0.097 and a coefficient of variation of 0.111 for the current S136 Design procedure (see Table B.46 of Appendix 'B').

8.1.2 Comparison with Available Test Data

Twenty available test specimens consisting of sections with inadequately supported ($I_r < 1$) Case II flanges were included in this study. Table 8.2 lists the applicable sections tested by Cohen [Coh 87], Moreyra [Mor 93], Schuster [Schu 92], Shan [Shan 94] and Winter [Win 47] and the corresponding Dinovitzer [Din 92] exponents, n , plate buckling coefficients and the S136 [CSA 94] plate buckling coefficients. Test-to-predicted bending moment ratios for both the Dinovitzer exponent method and the current S136 procedure are found in Tables B.28 (Cohen), B.34 (Moreyra), B.38 (Schuster), B.40 (Shan) and B.44 (Winter) of Appendix 'B'. Similar to the Waterloo test result comparison, the Dinovitzer method more accurately predicted the bending moment resistance of the available test data. Dinovitzer's flange method resulted in a mean of 1.00, a standard deviation of 0.147 and a coefficient of variation of 0.090 for the available test data. In comparison, the current S136 procedure yielded a mean of 1.01, a standard deviation of 0.158 and a coefficient of variation of 0.166 (see Table B.46 of Appendix 'B').

However, it must be noted that eleven of the applicable test specimens were subject to the flange/web mode of distortional buckling at failure. The test-to-predicted bending moment ratios of these sections were significantly unconservative (< 1). Specimens tested by Moreyra [Mor 93], Schuster [Schu 92] and Shan (12B,16,...) [Shan 94] were removed from the comparison so that local buckling concerns could be isolated. The Dinovitzer [Din 92] method remained more accurate for the available test data with a mean of 1.13, a standard deviation of 0.087 and a coefficient of variation of 0.090, as

Table 8.2 - Comparison of Dinovitzer Exponent, n, and k Values with Available Test Data[Din 92]

Specimen	n	k (Din)	k (S136)
<u>Cohen [Coh 87]</u>			
It2-rmin-d90-1L1	0.333	2.44	2.03
It2-rmin-d90-2L1	0.333	2.44	2.03
IIt2-rmin-d90-1L1	0.333	2.44	2.03
<u>Moreyra [Mor 93]</u>			
B-W*	0.347	2.69	2.67
B-TB*	0.337	2.54	2.41
C-W*	0.337	2.51	2.31
C-TB*	0.337	2.45	2.22
<u>Schuster [Schu 92]</u>			
BS1-A*	0.385	3.08	2.97
BS1-B*	0.385	3.08	2.97
BS2-A*	0.385	3.08	2.97
BS2-B*	0.385	3.08	2.97
CS1-A*	0.373	2.91	2.80
CS1-B*	0.373	2.91	2.80
CS2-A*	0.373	2.91	2.80
CS2-B*	0.373	2.91	2.80
CS3-A*	0.367	2.83	2.67
CS3-B*	0.373	2.91	2.80
<u>Shan [Shan 94]</u>			
2B,16,1&2(N)_A	0.384	2.37	2.11
2B,16,1&2(N)_B	0.382	2.36	2.09
2B,16,3&4(N)_A	0.385	2.67	2.51
2B,16,3&4(N)_B	0.382	2.41	2.15
12B,16,1&2(N)_A*	0.394	2.63	2.47
12B,16,1&2(N)_B*	0.394	2.79	2.70
12B,16,3&4(N)_A*	0.393	2.37	2.13
12B,16,3&4(N)_B*	0.394	2.79	2.70
<u>Winter [Win 47]</u>			
B4	0.433	2.55	2.39
B6	0.365	2.32	1.92
B7	0.345	3.57	3.54
C5	0.350	3.08	2.84

Note: * Subject to flange/web distortional buckling mode of failure.

compared to a mean of 1.15, a standard deviation of 0.100 and a coefficient of variation of 0.101 for the S136 [CSA 94] method (see Table B.46 of Appendix 'B').

8.1.3 Comparison with Waterloo and Available Test Data

The Dinovitzer [Din 92] flange method was again more accurate in comparison with the current S136 [CSA 94] procedure when the applicable Waterloo and available test data were analysed together. Analysis of the test-to-predicted bending moment ratios for the twenty-seven test specimens resulted in a mean of 1.01, a standard deviation of 0.134 and a coefficient of variation of 0.138 for Dinovitzer's method and a mean of 1.02, a standard deviation of 0.145 and a coefficient of variation of 0.147 for the current S136 procedure (see Table B.46 of Appendix 'B').

The Dinovitzer [Din 92] method remained more accurate in comparison with the current S136 [CSA 94] procedure when the Waterloo and available test data were combined, excluding the sections which failed by flange/web distortional buckling. This comparison of test-to-predicted bending moment ratios produced a mean of 1.09, a standard deviation of 0.096 and a coefficient of variation of 0.095 for the Dinovitzer method and a mean of 1.11, a standard deviation of 0.104 and a coefficient of variation of 0.101 for the S136 procedure (see Table B.46 of Appendix 'B').

The Dinovitzer [Din 92] exponent method used to calculate the plate buckling coefficient of an inadequately supported compressed flange was more accurate than the current S136 [CSA 94] procedure for all applicable Waterloo and available test data. Since the Dinovitzer flange method is more accurate than the current S136 procedure and it simplifies the current plate buckling coefficient equations, it can be recommended that the Dinovitzer flange method be included in the North American Design Standards [AISI 89a] [CSA 94].

8.2 Web Method by Sooi [Soo 93]

Sooi [Soo 93] developed a method with which the distribution of effective width for a web subjected to a stress gradient could be improved and simplified. The effective width of the web, h_e , is calculated as outlined in the current S136 Standard [CSA 94], discussed previously in Section 3.2.3, and is then distributed to the tensile portion of the web and to the extreme compressive portion of the web as shown in Figure 8.1.

The following equation is used to determine the effective width of the compressed portion, b_1 , of the web,

$$b_1 = h_e - b_{\text{tens}},$$

where b_{tens} is the tension portion of the web as shown in Figure 8.1.

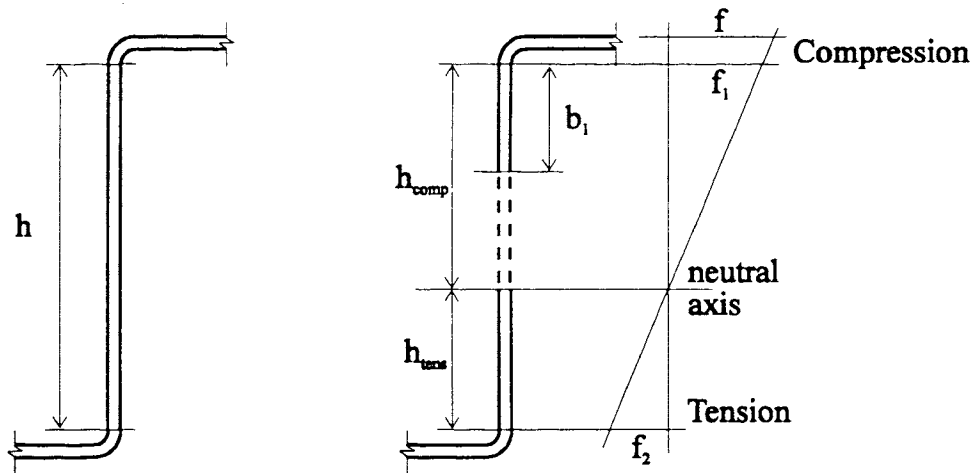


Figure 8.1 - Sooi Web Element Subjected to a Stress Gradient [Soo 93]

Sooi's [Soo 93] effective width method has been included as a modification of the existing local buckling procedures since it is used in the Lau & Hancock [Lau 87] [Lau 90], as well as, Moreyra [Mor 93] flange/web distortional buckling analysis methods (see Chapter 7). With its inclusion, a direct comparison of the existing S136 Standard [CSA

94] and AISI Specification [AISI 89a] with the Sooi modified S136 Standard can be completed. As well, a comparison of the Sooi modified S136 Standard with the flange/web distortional buckling analysis methods (see Chapter 7) can readily be made.

8.2.1 Comparison with Waterloo Test Data

All of the specimens tested as part of this work, 59 in total, were included in the Sooi [Soo 93] web method investigation. Test-to-predicted bending moment ratios for each of the individual tests can be found in Tables A.6a to A.6d of Appendix 'A'. Statistical results of the test-to-predicted bending moment ratios were calculated for each test series, for all of the Waterloo test data and for all of the Waterloo test data excluding sections which failed by flange/web distortional buckling (see Table 8.3 and Table 4.2 for failure

Table 8.3 - Comparison of Test / Predicted Bending Moment Ratios with Waterloo Test Data

Test Data	S136			Sooi Web Method			AISI		
	Mean	S.D.	C.o.V	Mean	S.D.	C.o.V	Mean	S.D.	C.o.V
C1-1*	1.04	0.016	0.022	1.04	0.016	0.022	1.02	0.016	0.022
C1-2*	0.846	0.028	0.047	1.01	0.012	0.016	0.763	0.029	0.053
C1-3*	0.858	0.069	0.140	0.858	0.069	0.140	0.809	0.059	0.127
C2-1	1.04	0.076	0.094	1.02	0.078	0.099	1.02	0.079	0.100
C2-2*	1.14	0.041	0.044	1.14	0.041	0.044	1.11	0.043	0.048
C2-3	1.01	0.052	0.064	1.19	0.061	0.063	0.954	0.052	0.067
C2-4	0.980	0.038	0.048	1.08	0.041	0.047	0.903	0.040	0.054
C2R-1	1.07	0.064	0.078	1.07	0.062	0.075	1.07	0.063	0.076
C3-1	1.07	0.116	0.154	1.05	0.090	0.122	1.05	0.087	0.117
C3-2	1.05	0.047	0.055	1.28	0.044	0.042	1.02	0.051	0.061
Σ Lab. Test Data	1.02	0.099	0.100	1.12	0.121	0.110	0.979	0.114	.0118
Σ Lab. Test Data w/o F/W Dist. Bckl.	1.04	0.084	0.083	1.13	0.115	0.104	1.00	0.094	0.095

Note: * Cold work of forming used when applicable.

modes). Test specimens which failed by flange/web distortional buckling, series C1-2, are fully investigated in Chapter 7.

The results of the Sooi [Soo 93] web method investigation reveal that for certain individual series the modified web method is more accurate than the existing Design Standards, e.g., C2-1. However, both the current S136 Standard [CSA 94] and AISI Specification [AISI 89a] more accurately predict the bending moment resistance of the specimens when all tests are included in the analysis (see Table 8.3). Based on the Waterloo test results, the current method of distribution for the effective width of a web subjected to a stress gradient results in better predictability than the Sooi web method.

8.2.2 Comparison with Available Test Data

All of the test data found in the literature, as outlined in Chapter 5, was included in this section of the Sooi [Soo 93] web method investigation. Test-to-predicted bending moment ratios for each of the individual test specimens are given in Tables B.26 (Charnvarnichborikarn [Cha 92]), B.28 (Cohen [Coh 87]), B.30 (Desmond [Des 78a]), B.32a and B.32b (LaBoube [LaB 78]), B.34 (Moreyra [Mor 93]), B.36 (Schardt & Schrade [Scha 82]), B.38 (Schuster [Schu 92]), B.40 (Shan [Shan 94]), B.42 (Willis & Wallace [Wil 90a]) and B.44 (Winter [Win 47]) in Appendix 'B'. Statistical information for the tests completed by each researcher and for all available data is given in Table 8.4. Results were also calculated excluding specimens which failed by flange/web distortional buckling and excluding specimens tested by Charnvarnichborikarn. Analysis of the available test data was completed without these specimens since they exhibited an extreme unconservative nature in the test-to-predicted bending moment ratios. Specimens which failed by flange/web distortional buckling were tested by Moreyra, Schuster and Shan and are fully examined in Chapter 7.

Table 8.4 - Comparison of Test / Predicted Bending Moment Ratios with Available Test Data

Test Data	S136			Sooi Web Method			AISI		
	Mean	S.D.	C.o.V	Mean	S.D.	C.o.V	Mean	S.D.	C.o.V
Charn...	0.820	0.083	0.108	0.802	0.074	0.099	0.752	0.077	0.109
Cohen	1.20	0.073	0.066	1.15	0.070	0.066	1.15	0.064	0.060
Desmond	1.15	0.081	0.123	1.14	0.077	0.117	1.14	0.077	0.117
LaBoube	1.08	0.079	0.075	1.10	0.100	0.093	1.03	0.078	0.077
Moreyra (W, TB)	0.951	0.097	0.131	0.940	0.096	0.132	0.869	0.081	0.121
Schardt & Schrade	1.09	0.127	0.122	1.18	0.091	0.080	1.03	0.112	0.113
Schuster	0.881	0.055	0.089	0.935	0.037	0.056	0.792	0.038	0.067
Shan	1.03	0.120	0.119	1.10	0.127	0.118	0.983	0.134	0.138
Willis & Wallace	1.04	0.073	0.121	1.04	0.073	0.122	0.942	0.065	0.120
Winter	1.10	0.064	0.063	1.08	0.061	0.062	1.07	0.061	0.062
Σ Exist. Test Data	1.05	0.134	0.128	1.07	0.141	0.132	0.994	0.140	0.141
Σ Exist. Test Data w/o F/W Dist. Bckl.	1.06	0.129	0.122	1.08	0.140	0.130	1.01	0.133	0.132
Σ Exist. Test Data w/o F/W Dist. Bckl. w/o Charn... Data	1.09	0.096	0.089	1.12	0.101	0.091	1.05	0.097	0.094

As determined with the Waterloo test data, the Sooi [Soo 93] modified web method is more accurate for certain individual researchers such as Schuster [Schu 92] and Moreyra [Mor 93]. However, based on all of the test results, the current S136 Standard [CSA 94] and AISI Specification [AISI 89a] more accurately predicted the bending moment resistance of the available test data (see Table 8.4). Based on the analysis of the available test data, the current method of distribution for the effective width of a web subjected to a stress gradient results in better predictability than the Sooi web method.

8.2.3 Comparison with Waterloo and Available Test Data

The Waterloo and available test data was combined and analysed, with the results presented in Table 8.5. Similar to the previous Sections 8.2.1 and 8.2.2, statistical information was provided for the following data sets; 1) all test data, 2) all test data

excluding sections which failed by flange/web distortional buckling and 3) all test data excluding both sections which failed by flange/web distortional buckling and specimens tested by Charnvarnichborikarn [Cha 92].

Table 8.5 - Comparison of Test / Predicted Bending Moment Ratios with Waterloo and Available Test Data

Test Data	S136			Sooi Web Method			AISI		
	Mean	S.D.	C.o.V	Mean	S.D.	C.o.V	Mean	S.D.	C.o.V
Σ Test Data	1.04	0.126	0.122	1.08	0.137	0.128	0.991	0.134	0.135
Σ Test Data w/o F/W Dist. Bckl	1.06	0.119	0.113	1.09	0.136	0.125	1.01	0.124	0.124
Σ Test Data w/o F/W Dist. Bckl w/o Charn... Data	1.08	0.096	0.089	1.12	0.105	0.094	1.03	0.098	0.095

Based on the results determined by analysing all of the test data, it can be recommended that the Sooi [Soo 93] web method not replace the current methods defined in the S136 Standard [CSA 94] and AISI Specification [AISI 89a], for the distribution of the effective width of a web subjected to a stress gradient. The statistical results summarised in Table 8.5, specifically standard deviation and coefficient of variation, also indicate that the S136 Standard provides a more accurate prediction of the test bending strength in comparison with the AISI Specification.

Chapter 9

Summary, Conclusions and Recommendations

9.1 Summary

The investigation of local and distortional buckling of cold formed steel C and Z-sections in bending involved four distinct segments; 1) the determination of a size limit for simple edge stiffeners of C and Z-sections, 2) the comparison of various procedures to calculate the effective width of a simple edge stiffener subjected to a stress gradient, 3) the investigation of existing analytical methods to model the flange/web distortional buckling mode of failure, and 4) the comparison of existing North American Design Standards with local buckling modifications for edge-stiffened flange elements and webs developed by Dinovitzer and Sooi, respectively.

The general topic of cold formed steel is introduced in Chapter 1, identifying its use in construction, the initial development of design Standards, as well as, the modes of buckling commonly experienced in bending failure. The objectives and scope of this work are also included in Chapter 1.

Chapter 2 consists of a literature review in which the original plate buckling theory is detailed. Various types of compressed elements are discussed along with the theory upon which the current design Standards are based. Clarifications of simple edge stiffener definitions and an introduction of flange/web interaction, as well as, flange/web distortional buckling are included.

Contained in Chapter 3 are the current linear computation procedures used to determine the gross moment resistance of cold formed steel sections in bending. Procedures specified by the S136 Standard and AISI Specification for the calculation of effective moment resistance are also discussed. In addition to Chapter 3, detailed example

calculations for the gross and effective moment resistance procedures are provided in Appendix 'C'.

Chapter 4 presents the Waterloo test program, detailing the philosophy used in sizing the test specimens along with a discussion of the specimen designations. Fabrication and testing procedures, mechanical properties and failure modes of the C-sections are included. Pertinent material properties and dimensions, as well as, results of the local and flange/web distortional buckling analyses for the Waterloo test specimens are given in Appendix 'A'.

Briefly discussed in Chapter 5 are the experimental test procedures, general descriptions of the test set-ups and specimen dimensions used by other researchers in testing cold formed steel sections in bending. Test specimens from the following researchers are included; Charnvarnichborikarn, Cohen, Desmond, LaBoube, Moreyra, Schardt & Schrade, Schuster, Shan, Willis & Wallace and Winter. Pertinent material properties and dimensions, as well as, results of the local and flange/web distortional buckling analyses for the available test specimens are given in Appendix 'B'.

Chapter 6 contains the results of the edge stiffener investigation, more specifically, a comparison to determine a d/t or d_i/w limiting ratio for the simple edge stiffener using the Willis & Wallace and Waterloo test data. Various modifications of the current effective width method for a simple edge stiffener subjected to a stress gradient are also reviewed.

Chapter 7 involves a presentation of the existing flange/web distortional buckling methods for cold formed steel sections in bending, developed by Lau & Hancock, Marsh, Moreyra and Charnvarnichborikarn. All of the methods are discussed in detail with a comparison of test-to-predicted bending moment ratios completed using applicable test data.

Chapter 8 briefly outlines modifications to the current local buckling methods, regarding the edge-stiffened flange and web elements, developed by Dinovitzer and Sooi, respectively. A comparison of test-to-predicted bending moment ratios using the S136 Standard and AISI Specification is also included.

Individual test specimen results for the comparisons completed in Chapters 6, 7 and 8 for all Waterloo test data can be found in Appendix 'A' and for all available test data in Appendix 'B'. In addition, detailed example calculations for all design methods used in Chapters 6, 7 and 8 are provided in Appendix 'C'.

9.2 Conclusions and Recommendations

9.2.1 d/t Limit of Edge Stiffener

Based on the findings of the edge stiffener study, the d/t limit of 14 currently specified in Table 6 of the S136 Standard [CSA 94] was inadequately defined. The Willis and Wallace study on which the limit was based used the overall depth of the simple edge stiffener, whereas, the S136 Standard specifies the flat width (see Figures 6.1 and 6.2a). If an adjustment had been made for this change in definition of the simple edge stiffener depth the d/t limit would be 12 (see Figure 6.2b). An alternate limit based on the ratio of d_i/w approximately equal to 0.4 or 0.45 could also be used according to the recommendations of Willis and Wallace (see Figure 6.2c), as well as, Desmond.

Use of the Waterloo test data allowed for the comparison of sections within all three flange "Cases", as per the North American Design Standards. This was an improvement to the Willis and Wallace data, which relied on three sections in the Case III flange range only. Results from the Case I and Case II Waterloo tests indicated that the characteristic drop in bending moment resistance did not occur, as did with the Willis and Wallace tests (see Figures 6.3a -6.9b). Analysis of the Waterloo Case III flange series did not reveal a

sharp drop in moment resistance, rather a levelling off at approximately $d/t = 16$ or $d_i/w = 0.4$ (see Figures 6.10a - 6.11b). Since agreement between the revised d/t limit, 12, and results obtained from the Waterloo test data was not reached, it is recommended that a **d_i/w limit of 0.4** be introduced for **Case III flange sections only**. In addition, the d_i/w limit need only be stated as a **warning** which indicates that the bending moment resistance will decrease above this characteristic value, yet remain predictable using the S136 Standard.

9.2.2 Simple Edge Stiffener Subjected to a Stress Gradient

The S136 Standard and AISI Specification require that a simple edge stiffener subjected to a stress gradient be treated as a uniformly compressed element subjected to a maximum stress and $k=0.43$. Modifications to the current effective width procedure involving three methods where the magnitude of the compressive stress was altered (see Figure 6.12) were compared. Two stress gradient approaches (Cohen/Eurocode and ISO) where the plate buckling coefficient is based on the ratio of compressive stresses at the top and bottom of the flat width were also studied. Analysis of results indicated that the variation in mean values between the five effective width methods was marginal, therefore, it is recommended that the current effective width procedures remain in the North American Design Standards.

9.2.3 Flange/Web Distortional Buckling

Recent testing by Schuster and Shan has revealed that standard cold formed steel sections, commonly used in the lightweight framing industry, can fail in a unique mode known as flange/web distortional buckling (see Figure 1.2). Sharp originally developed a method to model this type of failure for aluminum sections subjected to uniform compressive stress. Flange/web distortional buckling methods for cold formed steel

sections in bending have recently been developed by Lau & Hancock, Marsh, Moreyra and Charnvarnichborikarn.

The method proposed by Charnvarnichborikarn was not included in the comparison of flange/web distortional buckling methods because test-to-predicted bending moment ratios indicate that the formulae yield overly conservative results (see Table 6.6 of Charnvarnichborikarn's Ph.D. thesis). Furthermore, equations for the geometric properties of the equivalent column were not adequately defined in Charnvarnichborikarn's work.

Based on the statistical evidence of test-to-predicted bending moment ratios for all applicable test data, excluding Charnvarnichborikarn's data (see Table 7.4), the Marsh method is the most accurate. However, the method which Marsh has developed does not follow the unified effective width approach currently contained in the North American Design Standards. Element thickness, instead of width, is reduced according to the slenderness of the cross section (see Section 7.1.2). Since the Marsh method requires a change in design philosophy from the North American Design Standards, it is not recommended as a predictor method for the flange/web distortional buckling mode of failure of sections in bending.

The Lau & Hancock and Moreyra methods were developed in accordance with the unified effective width approach (see Sections 7.1.1 and 7.1.3). Based on the statistical results of the test-to-predicted bending moment ratios, excluding the Charnvarnichborikarn data (see Table D.1 of Appendix 'D'), models 4 and 5 of the Lau & Hancock method yield the most accurate strength predictions. The Moreyra methods have less conservative mean values and the standard deviations and coefficient of variations indicate a lack of precision in the predicted bending moment strength. In addition, the procedures specified by Moreyra involve a nominal buckling stress equation, F_n , which was derived from the results of a parametric study of edge stiffened

C-sections using the ABAQUS finite element computer software. The nominal buckling stress equation does not have a theoretical origin and also is not dependent on the dimension of the simple edge stiffener. Furthermore, the Moreyra method first requires a reduced nominal buckling stress, then further reduces this stress in the calculation of the effective compressed flange width according to the Sharp approach. Sharp's approach is itself a method with which the distortional buckling stress of the equivalent column can be determined directly. Therefore, the initial nominal buckling stress calculation is a doubling of the distortional buckling stress reduction procedure and is unnecessary.

Similar to the Sharp approach, the Lau & Hancock models allow for various edge stiffener configurations in addition to the simple lip. The only variation between the models is in the required column strength expressions used to find the stress at which bending failure occurs. Models 4 and 5 of the Lau & Hancock method yield the same results for the test specimens included in this investigation. Models 4 and 5 consist of an adaptation of the column strength expressions to account for post-buckling and the use of high strength steels. They are also similar to models 1 and 2 which have been included in the most recent edition of the Australian standard for the analysis of flange/web and lip/flange distortional buckling, respectively. Since models 4 and 5 of the Lau & Hancock method account for post-buckling, as well as, high strength steels, and similar models have been adopted by the Standards Association of Australia, it is recommended that either be used as the North American predictor model for the flange/web distortional buckling strength of cold formed steel sections in bending.

It is recommended that implementation of models 4 and 5 of the Lau & Hancock flange/web distortional buckling method be at the discretion of the design engineer at this time. An attempt to determine a characteristic limiting ratio of dimensional parameters from the applicable test specimens was inconclusive, based on the scope of this work. Further research is required so that the implementation of flange/web distortional buckling for any cross section type can be based on a dimensional parameter limit.

9.2.4 Local Buckling of Edge-Stiffened Flange Element

Dinovitzer developed an equation to eliminate the discontinuity in the flange effective width formulation. The exponents used for the plate buckling coefficient equations of a compressed flange supported by a web on one side and an edge stiffener of inadequate rigidity ($I_r < 1$) on the other side were modified (see Section 8.1). Comparison of applicable Waterloo Case II flange sections revealed that the Dinovitzer method was marginally more accurate than the S136 Standard, which was also found to be true for the applicable available Case II flange data (see Table B.46 of Appendix 'B'). Statistical evidence from a combination of Waterloo and available test data again showed the Dinovitzer method to be more accurate than the current S136 Standard (see Table B.46 of Appendix 'B').

9.2.5 Local Buckling of Web Element

Sooi's method was studied to compare his simplified approach in distributing the effective width of a web subjected to a stress gradient (see Section 8.2) with the current North American Design Standards. Statistical results which were based on the Waterloo and available test data, excluding sections which failed by flange/web distortional buckling and Charnvarnichborikarn's data, revealed that the Sooi web method yielded more conservative results than both the S136 Standard and AISI Specification (see Table 8.5). However, these statistical results also indicate that the S136 Standard provides a more accurate prediction of the test bending strength compared to the AISI Specification. Therefore, it is recommended that the Sooi web method not replace the procedures found in the current North American Design Standards for the distribution of effective width of a web subjected to a stress gradient.

9.2.6 Summary of Conclusions and Recommendations

- 1) It is recommended that a d_i/w limit of 0.4 be introduced for **Case III flange sections only**. The d_i/w limit need only be stated as a **warning** which indicates that the bending moment resistance will decrease above this characteristic value, yet remain predictable using the S136 Standard.
- 2) Analysis of the effective width calculation procedures of a simple edge stiffener subjected to a stress gradient revealed that the variation in mean values between the five effective width methods was marginal, therefore, it is recommended that the current effective width procedures remain in the North American Design Standards.
- 3) It is recommended that either model 4 or 5 of the Lau & Hancock method be used as the North American predictor method for the flange/web distortional buckling strength of cold formed steel sections in bending. It is also recommended that implementation of model 4 or 5 of the Lau & Hancock method be at the discretion of the design engineer at this time. An attempt to determine a characteristic limiting ratio of dimensional parameters from the applicable test specimens was inconclusive, based on the scope of this work. Further research is required so that the implementation of flange/web distortional buckling for any cross section type can be based on a dimensional parameter limit.
- 4) Statistical evidence from a combination of Waterloo and available test data showed the Dinovitzer method to be more accurate than the current S136 Standard for the calculation of effective width of an edge-stiffened flange element.
- 5) It is recommended that the Sooi web method not replace the procedures found in the current North American Design Standards for the distribution of effective width of a web subjected to a stress gradient. The statistical results also indicate that the S136 Standard provides a more accurate prediction of the test bending strength in comparison with the AISI Specification.

9.3 Recommendations for Future Research

The recommendations for future research involve implementation of either model 4 or 5 of the Lau & Hancock flange/web distortional buckling method. Since the attempt to determine a characteristic limiting ratio of dimensional parameters from the applicable test specimens was inconclusive, further study in this area is required. It is recommended that a study to determine which industry standard sections undergo flange/web distortional buckling be completed. The recommended study would be limited in size due to the small number of variations in cross section dimensions currently provided by sheet steel fabricators. Completion of this recommendation would only be a temporary measure to address concerns regarding cold formed steel sections currently used in construction.

In order to establish a characteristic limiting ratio of dimensional parameters for any cross section type, further analysis of the various flange/web distortional buckling methods and applicable test specimens is required. It is also suggested that further laboratory testing of cold formed steel specimens which are subject to flange/web distortional buckling be carried out. An increased amount of test data would aid in the study of a precise definition of a characteristic limiting ratio for the implementation of flange/web distortional buckling.

It may also be possible to determine a limiting ratio of dimensional parameters by carrying out a sensitivity study involving variables used in the various flange/web distortional buckling methods. This study would be independent of any results obtained by laboratory testing, hence, it could be used as a comparison tool to assist in the development of a precise limiting ratio of dimensional parameters.

References

- [ABA 89] Hibbit, Karlson and Sorensen Inc., "ABAQUS Users Manual Version 4.8".
- [AISI 46] American Iron and Steel Institute, "Specification for the Design of Light Gage Steel Structural Members", New York, N.Y., April, 1946.
- [AISI 86a] American Iron and Steel Institute, "Cold-Formed Steel Design Manual", Washington D.C., 1986.
- [AISI 86b] American Iron and Steel Institute, "Specification for the Design of Cold-Formed Steel Structural Members", August 19, 1986 Edition, Washington D.C., USA, 1986.
- [AISI 89a] American Iron and Steel Institute, "Specification for the Design of Cold-Formed Steel Structural Members", August 19, 1986 Edition with December 11, 1989 Addendum, Washington D.C., USA, 1989.
- [AISI 89b] American Iron and Steel Institute, "Commentary on the Specification for the Design of Cold-Formed Steel Structural Members", August 19, 1986 Edition with December 11, 1989 Addendum, Washington D.C., USA, 1989.
- [ASTM 370] American Standard of Testing and Materials A370-92, "Standard Methods and Definitions for Mechanical Testing of Steel Products".
- [Ble 53] Bleich, F., "Buckling strength of metal structures", McGraw-Hill Book Co. Inc., New York, N.Y., 1953.
- [Bry 90] Bryan, G.H., "On the Stability of a Plane Plate under Thrusts in its Own Plane, with Applications to the Buckling of the Sides of a Ship", Proceedings, London Mathematical Society, Vol. 22, Dec., 1890, pp. 54-67.
- [Bul 69] Bulson, P.S., "The Stability of Flat Plates", American Elsevier, New York, 1969.
- [Cha 92] Charnvarnichborikarn, P. "Distortional Buckling of Cold Formed Steel Z-Sections", Thesis in partial fulfilment of the requirements for the Degree Doctor of Philosophy in the Department of Civil Engineering, The University of Manitoba, Winnipeg, Manitoba, April, 1992.

- [Cha 93] Charnvarnichborikarn, P., Polyzois, D., "Web-Flange Interaction in Cold-Formed Steel Z-Section Columns", *Journal of Structural Engineering*, ASCE, Vol. 119, No. 9, September 1993, pp. 2607-2628.
- [Chi 53a] Chilver, A.H., "A Generalised Approach to the Local Instability of Certain Thin Walled Struts", *The Aeronautical Quarterly*, Volume IV, August 1953.
- [Chi 53b] Chilver, A.H., "The Stability and Strength of Thin-Walled Steel Struts", *The Engineer*, Vol. 196, August 1953, pp. 180-183.
- [Coh 87] Cohen, J.M., "Local Buckling Behaviour of Plate Elements", A thesis presented to the Faculty of the Graduate School of Cornell University in partial fulfilment for the Degree of Doctor of Philosophy, Department of Structural Engineering., Cornell University, Ithaca N.Y., August 1987.
- [CSA 63] CSA S136 Standard-1963, "Cold Formed Steel Structural Members", Canadian Standards Association, Rexdale (Toronto), Ontario, Canada, 1963.
- [CSA 89] CAN/CSA-S136-M89, "Cold Formed Steel Structural Members", Canadian Standards Association, Rexdale (Toronto), Ontario, Canada, 1989.
- [CSA 91] CAN/CSA-S136.1-M1991, "Commentary on CSA Standard CAN/CSA-S136-M89, Cold Formed Steel Structural Members", Canadian Standards Association, Rexdale (Toronto), Ontario, Canada, 1991.
- [CSA 94] S136-M94, "Cold Formed Steel Structural Members", Canadian Standards Association, Rexdale (Toronto), Ontario, Canada, 1994.
- [Des 78a] Desmond, T.P., "The Behaviour and Strength of Thin-Walled Compression Elements with Longitudinal Stiffeners", A thesis presented to the Faculty of the Graduate School of Cornell University in partial fulfilment for the Degree of Doctor of Philosophy, Department of Structural Engineering, Cornell University, Ithaca, New York, February 1978.
- [Des 78b] Desmond, T.P., Peköz, T., Winter, G., "Edge Stiffeners for Cold-Formed Steel Members", *Fourth International Specialty Conference on Cold-Formed Steel Structures*, University of Missouri-Rolla, June 1978, pp. 119-156.

- [Des 81] Desmond, T.P., Peköz, T., Winter, G., "Edge Stiffeners for Thin Walled Members", *Journal of the Structural Division, ASCE*, Vol. 107, No. ST2, February 1981, pp 329-353.
- [Din 92] Dinovitzer, A.S., Sohrabpour, M., Schuster, R.M., "Observations and Comments Pertaining to CAN/CSA-S136-M89", *Proceedings of the Eleventh International Specialty Conference on Cold-Formed Steel Structures*, University of Missouri-Rolla, Rolla, Missouri, 1992, pp. 551-569.
- [Eur 89] Appendix 'A' Eurocode 3, "Cold Formed Steel Sheeting and Members", Revised version according to the Karlsruhe meeting, March 1989.
- [Han 78] Hancock, G.J., "Local, Distortional and Lateral Buckling of I Beams", *Journal of the Structural Division, ASCE*, Vol. 104, No. ST11, November 1978, pp 1787-1798.
- [Han 85] Hancock, G.J., "Distortional Buckling of Steel Storage Rack Columns", *Journal of the Structural Division, ASCE*, Vol. 111, No. 12, December 1985, pp. 2770-2783.
- [Han 94a] Hancock, G.J., Kwon, Y.B., Bernard, E.S., "Strength Design Curves for Thin-Walled Sections Undergoing Distortional Buckling", *Journal of Construction Steel Research*, Vol. 31, 1994, pp. 169-186.
- [Han 94b] Hancock, G.J., "Design of Cold-Formed Steel Structures (To Australian Standard AS 1538-1988) 2nd Edition", Australian Institute of Steel Construction, Sydney, Australia, 1994.
- [ISO 91] ISO TC167 WG2, "Steel Structures Part Two : Design of Cold Formed Steel Members and Sheeting", Working Draft #3, 1991
- [ISO 93] ISO/TC 167/SC3, "Aluminium Structures Material and Design Part I: Ultimate Limit State - Static Loading", Technical Report, June 1993.
- [Jom 61] Jombock, J.R., Clark, J.W., "Postbuckling Behaviour of Flat Plates", *Journal of the Structural Division, ASCE*, Vol. 87, No. ST5, June 1961, pp. 17-33.
- [Kal 77] Kalyanaraman, V., Peköz, T., Winter, G., "Unstiffened Compression Elements", *Journal of the Structural Division, ASCE*, No. ST9, September 1977, pp. 1833-1849.

- [Kal 78] Kalyanaraman, V., Peköz, T., "Analytical Study of Unstiffened Elements", Journal of the Structural Division, ASCE, Vol. 104, No. ST9, September 1977, pp. 1833-1849.
- [Kar 10] Von Karman, T., "Festigkeits Probleme im Mashinenbau", Encyc. der Math. Wiss., 4, 1910.
- [Kar 32] Von Karman, T., Sechler, E.E., Donnel, L.H., "The Strength of Thin Plates in Compression", Transactions, ASME., Vol. 54, No. 2, Jan. 1932, pp. 53-57.
- [Kol 58] Kollbrunner, C.F., Meister, M., "Ausbeulen - Theorie und Berechnung von Blechen", Springer-Verlag, Berlin, West Germany, 1958.
- [Kwo 91] Kwon, Y.B., Hancock, G.J., "Strength Tests of Cold-Formed Channel Sections Undergoing Local and Distortional Buckling", Research Report No. R640, School of Civil and Mining Engineering, The University of Sydney, Sydney, Australia, June 1991.
- [Kwo 92] Kwon, Y.B., Hancock, G.J., "Tests of Cold-Formed Channels with Local and Distortional Buckling", Journal of the Structural Division, ASCE, Vol. 117, No. 7, July 1992, pp. 1786-1803.
- [LaB 78] LaBoube, R.A., Yu, W.W., "Webs for Cold-Formed Steel Flexural Members - Structural Behaviour of Beam Webs Subjected to Bending Stress", Final Report, Civil Engineering Study 78-1, Structural Series, University of Missouri-Rolla, Rolla, Missouri, June 1978.
- [Lau 87] Lau, S.C.W., Hancock, G.J., "Distortional Buckling Formulas for Channel Columns", Journal of the Structural Division, ASCE, Vol. 113, No. 5, May 1987, pp. 1063-1078.
- [Lau 90] Lau, S.C.W., Hancock, G.J., "Inelastic Buckling of Channel Columns in the Distortional Mode", Thin Walled Structures, Vol. 10, 1990, pp. 59-84.
- [Maa 54] Van Der Maas, C.J., "Charts for the Calculation of the Critical Compressive Stress for Local Instability of Columns with Hat Sections", Journal of the Aeronautical Sciences, Vol. 21, No. 6, June 1954, pp. 399-403.
- [Mar 90] Marsh, C., "Influence of Lips on Local and Overall Stability of Beams and Columns", Proceedings Structural Stability Research Council, Annual Technical Session, 1990, pp. 145-153.

- [Mil 43] Miller, E.A., "A Study of the Strength of Short, Thin Walled Steel Studs", M.S. Thesis, Cornell University, Ithaca, New York, 1943.
- [Mor 93] Moreyra, M.E., Peköz, T., "Behavior of Cold-Formed Steel Lipped Channels Under Bending and Design of Edge Stiffened Elements", Research Report 93-4, School of Civil and Environmental Engineering, Cornell University, Ithaca N.Y., June 1993.
- [Mul 83] Mulligan, G.P., Peköz, T., "The Influence of Local Buckling on the Structural Behaviour of Singly Symmetric Cold-Formed Steel Columns", Department of Structural Engineering Report No. 83-1, School of Civil and Environmental Engineering, Cornell University, Ithaca N.Y., March 1983.
- [Pek 87] Peköz, T., "Development of a Unified Approach to the Design of Cold-Formed Steel Members", Report to the Advisory Group on the Specification for the Design of Cold-Formed Steel Structural Members, AISI, Report CF 87-1, March 1987.
- [Pol 90] Polyzois, D. "Web-Flange Interaction in Slender Plate Girders" Proceedings- Structural Stability Research Council, Annual Technical Session, 1990, pp. 291-303.
- [SAA 93] Standards Association of Australia, "Steel storage racking -AS4084-1993", Sydney, Australia.
- [SAA 94] Standards Association of Australia, "Cold-formed steel structures - AS1538-1994", Draft Revision of AS 1538 - 1988, Sydney, Australia.
- [Scha 82] Scharadt, R., Schrade, W., "Kaltprofil - Pfetten", Institut Für Statik, Technische Hochschule Darmstadt, Bericht Nr. 1, Darmstadt, 1982.
- [Schu 92] Schuster, R.M., "Testing of Perforated C-Stud Sections in Bending", Report for the Canadian Sheet Steel Building Institute, University of Waterloo, Waterloo Ontario, March 1992.
- [Shan 94] Shan, M.Y., LaBoube, R.A., Yu, W.W., "Behaviour of Web Elements with Openings Subjected to Bending, Shear and the Combination of Bending and Shear", Final Report, Civil Engineering Study 94-2 Structural Series, University of Missouri-Rolla, Rolla, Missouri, May 1994.
- [Sha 66] Sharp, M.L., "Longitudinal Stiffeners for Compression Members", Journal of the Structural Division, ASCE, ST5, October 1966, pp. 187-211.

- [Sha 93] Sharp, M.L., "Behaviour and Design of Aluminum Structures", McGraw-Hill Inc., New York, N.Y., 1993, pp. 135-138.
- [Soo 93] Sooi, T.K., "The Behaviour of Component Elements of Aluminum Members", A thesis presented to the Faculty of the Graduate School of Cornell University, Department of Structural Engineering., Cornell University, Ithaca N.Y., 1993
- [Tho 78] Thomasson, P.O., "Thin-walled C-shaped panels in axial compression", Document D1;1978, Swedish Council for Building Research, Stockholm, Sweden, 1978.
- [Tim 61] Timoshenko, S.P., Gere, J.M., "Theory of Elastic Stability", McGraw-Hill Book Co., New York, 1961.
- [Wil 90a] Willis, C.T., Wallace, B.J., "Wide Lips - A Problem with the 1986 AISI Code", Proceedings of the Tenth International Specialty Conference on Cold-Formed Steel Structures, University of Missouri-Rolla, Rolla, Missouri, 1990, pp. 441-450.
- [Wil 90b] Willis, C.T., Wallace, B.J., "Behaviour of Cold-Formed Steel Purlins Under Gravity Loading", Journal of the Structural Division, ASCE, Vol. 116, No. 8, August 1990, pp. 2061-2069.
- [Win 47] Winter, G., "Strength of Thin Steel Compression Flanges", Transactions, ASCE, Vol. 112, 1947, pp. 527-6576.
- [Win 48] Winter, G., "Performance of Thin Steel Compression Flanges", The International Association for Bridge and Structural Engineering, Preliminary Publication, 3rd Congress, Liege, 1948, pp. 137-148.
- [Win 56] Winter, G., "Design of Light Weight Steel Structures", International Association for Bridge and Structural Engineering, Fifth Congress Final Report, 1956, pp. 481-485.
- [Yu 91] Yu, W.W., "Cold-Formed Steel Design - Second Edition", John Wiley & Sons. Inc., New York, 1991.

Appendix 'A'

Waterloo Test Data and Test / Predicted Bending Moment Ratios

Table A.1a - Test Specimen Dimensions

Specimen	d ₁ (mm)	B ₁ (mm)	D ₁ (mm)	B ₂ (mm)	d ₂ (mm)	d ₃ (mm)	B ₃ (mm)	D ₂ (mm)	B ₄ (mm)	d ₄ (mm)	t (mm)	r _i (mm)
C1-DW0-1-A,B	-	23.0	101	33.0	-	-	23.0	101	33.0	-	1.92	3.84
C1-DW30-1-A,B	6.00	29.0	102	29.0	13.0	6.00	29.0	101	29.0	13.0	1.92	3.84
C1-DW40-1-A,B	8.00	29.0	102	29.0	13.0	8.00	29.0	102	29.0	13.0	1.92	3.84
C1-DW60-1-A,B	11.0	29.0	101	29.0	13.0	11.0	29.0	102	29.0	13.0	1.92	3.84
C1-DW80-1-A,B	14.0	30.0	102	30.0	14.0	14.0	30.0	102	30.0	14.0	1.92	3.84
C1-DW0-2-A,B	-	24.0	302	29.5	14.7	-	24.0	305	26.7	14.5	1.85	3.70
C1-DW30-2-A,B	6.60	28.2	305	28.3	14.3	6.40	28.2	305	28.1	14.3	1.85	3.70
C1-DW40-2-A,B	7.90	28.3	298	28.4	14.2	8.00	28.4	305	28.4	14.3	1.85	3.70
C1-DW60-2-A,B	11.3	28.4	306	28.3	14.2	11.1	28.4	305	28.4	15.0	1.85	3.70
C1-DW80-2-A,B	14.0	28.4	305	28.3	14.3	14.0	28.4	305	28.2	14.3	1.85	3.70
C1-DW0-3-A,B	-	23.1	401	29.5	14.2	-	23.4	401	29.7	14.6	1.83	3.66
C1-DW30-3-A,B	11.7	29.5	401	29.0	14.4	11.4	29.8	401	29.6	14.6	1.83	3.66
C1-DW40-3-A,B	14.5	29.4	401	29.8	14.5	14.9	29.6	401	29.7	14.0	1.83	3.66
C1-DW60-3-A,B	19.4	29.3	402	30.0	14.1	19.5	29.4	401	29.3	14.7	1.83	3.66
C2-DW0-1-A,B	-	38.0	101	38.0	-	-	38.0	101	38.0	-	1.14	2.29
C2-DW20-1-A,B	7.00	41.0	102	41.0	13.0	6.50	40.5	103	40.0	13.0	1.14	2.29
C2-DW35-1-A,B	13.0	42.5	102	42.5	13.0	13.0	42.5	102	42.5	13.0	1.14	2.29
C2-DW45-1-A,B	15.0	39.5	100	39.5	15.0	14.5	40.0	99.0	40.0	15.0	1.14	2.29
C2-DW55-1-A,B	18.0	38.5	101	38.5	18.0	18.0	38.5	101	38.5	18.0	1.14	2.29
C2-DW65-1-A,B	23.0	44.0	101	44.0	23.5	23.0	44.0	101	43.0	23.5	1.14	2.29
C2-DW0-2-A,B	-	32.4	102	42.7	26.0	-	31.6	102	42.9	26.5	1.87	3.73
C2-DW25-2-A,B	9.20	41.2	99.0	40.9	26.4	9.00	41.0	99.0	41.3	26.6	1.87	3.73
C2-DW40-2-A,B	12.8	41.2	100	41.3	26.4	12.8	41.1	100	41.2	26.7	1.87	3.73
C2-DW50-2-A,B	15.2	40.8	99.3	41.1	26.3	15.0	41.0	99.8	41.1	26.5	1.87	3.73
C2-DW60-2-A,B	18.0	41.0	100	41.2	26.5	18.0	41.1	101	41.2	26.6	1.87	3.73
C2-DW70-2-A,B	20.7	40.9	100	41.0	26.7	20.7	41.0	99.9	41.0	26.8	1.87	3.73
C2-DW80-2-A,B	23.7	41.2	102	41.4	26.4	24.0	40.8	100	41.0	26.5	1.87	3.73

Table A.1b - Test Specimen Dimensions

Specimen	d ₁ (mm)	B ₁ (mm)	D ₁ (mm)	B ₂ (mm)	d ₂ (mm)	d ₃ (mm)	B ₃ (mm)	D ₂ (mm)	B ₄ (mm)	d ₄ (mm)	t (mm)	r _i (mm)
C2-DW0-3-A,B	-	35.2	240	38.6	26.0	-	35.0	240	38.4	26.0	1.21	2.43
C2-DW20-3-A,B	8.00	37.6	241	38.0	27.1	8.10	37.7	242	37.9	25.7	1.21	2.43
C2-DW35-3-A,B	13.2	38.4	240	38.6	25.9	13.3	38.3	240	38.5	25.8	1.21	2.43
C2-DW45-3-A,B	14.8	38.0	241	37.9	25.7	14.4	38.0	241	38.1	26.1	1.21	2.43
C2-DW55-3-A,B	17.6	37.9	241	38.0	26.0	17.6	37.9	241	38.4	25.7	1.21	2.43
C2-DW65-3-A,B	22.1	37.8	242	37.8	25.8	22.0	37.8	241	37.8	25.8	1.21	2.43
C2-DW80-3-A,B	26.8	38.2	239	38.1	26.0	27.2	38.0	239	38.0	25.8	1.21	2.43
C2-DW0-4-A,B	-	35.3	304	41.3	25.9	-	35.3	303	41.3	25.6	1.90	3.81
C2-DW25-4-A,B	7.90	42.7	301	42.3	26.2	8.40	42.9	300	42.2	25.6	1.90	3.81
C2-DW40-4-A,B	13.4	40.0	307	38.8	25.3	13.1	39.6	307	40.0	26.0	1.90	3.81
C2-DW50-4-A,B	13.6	39.9	305	40.0	25.8	13.7	40.8	305	40.0	26.0	1.90	3.81
C2-DW60-4-A,B	17.3	41.4	303	42.0	26.0	17.5	42.0	303	41.4	25.8	1.90	3.81
C2-DW70-4-A,B	21.1	41.5	305	41.3	25.0	21.1	41.7	305	41.5	24.5	1.90	3.81
C2-DW80-4-A,B	24.1	38.7	308	40.0	25.0	23.8	40.0	308	40.2	24.6	1.90	3.81
C2R-DW0-1-A,B	-	37.2	102	38.3	26.7	-	37.4	102	38.5	26.6	1.21	2.42
C2R-DW20-1-A,B	6.00	38.0	101	38.3	25.8	6.00	38.0	102	38.2	26.1	1.21	2.42
C2R-DW35-1-A,B	13.2	37.7	102	38.3	26.3	13.4	37.7	102	38.6	26.0	1.21	2.42
C2R-DW45-1-A,B	14.2	38.4	103	38.7	25.8	14.7	38.8	103	38.5	25.4	1.21	2.42
C2R-DW55-1-A,B	18.5	38.3	102	38.5	25.5	18.8	38.8	102	38.6	25.3	1.21	2.42
C2R-DW65-1-A,B	22.6	38.7	103	38.8	26.7	22.5	38.8	102	38.5	26.5	1.21	2.42
C3-DW0-1-A,B	-	61.5	103	65.6	25.8	-	61.9	103	65.6	25.9	1.20	2.40
C3-DW20-1-A,B	13.5	65.6	98.0	66.4	25.8	13.5	65.7	99.0	66.0	25.9	1.20	2.40
C3-DW30-1-A,B	17.6	65.9	99.8	66.1	25.8	17.9	65.9	100	66.0	25.9	1.20	2.40
C3-DW35-1-A,B	23.0	66.0	102	66.2	25.8	23.1	66.2	102	66.1	25.7	1.20	2.40
C3-DW45-1-A,B	25.7	66.2	99.0	66.0	26.0	25.6	66.2	99.0	66.0	25.8	1.20	2.40
C3-DW0-2-A,B	-	62.6	241	65.3	26.6	-	62.8	240	65.4	26.8	1.07	2.13
C3-DW20-2-A,B	13.1	65.6	244	65.4	26.0	13.2	65.4	244	65.4	25.8	1.07	2.13
C3-DW30-2-A,B	17.5	65.5	243	65.5	26.6	17.8	65.4	243	65.5	25.5	1.07	2.13
C3-DW35-2-A,B	24.5	65.4	240	64.2	25.8	24.3	65.6	240	64.2	25.4	1.08	2.16
C3-DW45-2-A,B	26.2	65.7	242	65.6	26.2	26.1	65.5	242	65.8	26.2	1.07	2.13
C3-DW50-2-A,B	31.0	65.7	240	65.5	25.7	30.8	65.7	240	65.5	25.9	1.07	2.13
C3-DW60-2-A,B	36.6	65.4	240	65.2	25.3	36.8	65.3	240	65.1	25.1	1.07	2.13

Table A.2a - Test Specimen Dimension Ratios

Specimen	h (mm)	h/t	w (mm)	w/t	d (mm)	d/t	d _i /w	w/h
C1-DW0-1-A	89.5	46.6	17.2	8.97	0.00	0.00	0.000	0.193
C1-DW0-1-B	89.5	46.6	17.2	8.97	0.00	0.00	0.000	0.193
C1-DW30-1-A	90.5	47.1	17.5	9.10	0.24	0.12	0.343	0.193
C1-DW30-1-B	89.5	46.6	17.5	9.10	0.24	0.12	0.343	0.195
C1-DW40-1-A	90.5	47.1	17.5	9.10	2.24	1.16	0.458	0.193
C1-DW40-1-B	90.5	47.1	17.5	9.10	2.24	1.16	0.458	0.193
C1-DW60-1-A	89.5	46.6	17.5	9.12	5.29	2.75	0.628	0.196
C1-DW60-1-B	90.5	47.1	17.6	9.17	5.39	2.80	0.624	0.195
C1-DW80-1-A	90.5	47.1	18.5	9.64	8.29	4.31	0.756	0.205
C1-DW80-1-B	90.5	47.1	18.6	9.67	8.34	4.34	0.754	0.205
C1-DW0-2-A	291	157	18.5	10.0	0.00	0.00	0.000	0.063
C1-DW0-2-B	293	159	18.5	10.0	0.00	0.00	0.000	0.063
C1-DW30-2-A	294	159	17.1	9.26	1.06	0.57	0.386	0.058
C1-DW30-2-B	294	159	17.1	9.26	0.86	0.46	0.374	0.058
C1-DW40-2-A	287	155	17.2	9.31	2.36	1.27	0.459	0.060
C1-DW40-2-B	294	159	17.3	9.37	2.46	1.33	0.462	0.059
C1-DW60-2-A	294	159	17.4	9.39	5.80	3.14	0.651	0.059
C1-DW60-2-B	293	159	17.3	9.37	5.56	3.01	0.641	0.059
C1-DW80-2-A	294	159	17.3	9.37	8.46	4.58	0.809	0.059
C1-DW80-2-B	294	159	17.3	9.34	8.41	4.55	0.811	0.059
C1-DW0-3-A	390	213	17.6	9.62	0.00	0.00	0.000	0.045
C1-DW0-3-B	390	213	17.9	9.79	0.00	0.00	0.000	0.046
C1-DW30-3-A	390	213	18.5	10.1	6.21	3.39	0.632	0.047
C1-DW30-3-B	390	213	18.8	10.3	5.91	3.23	0.606	0.048
C1-DW40-3-A	390	213	18.4	10.1	9.01	4.92	0.787	0.047
C1-DW40-3-B	390	213	18.6	10.2	9.41	5.14	0.800	0.048
C1-DW60-3-A	391	214	18.3	10.0	13.9	7.60	1.059	0.047
C1-DW60-3-B	390	213	18.4	10.1	14.0	7.66	1.059	0.047
C2-DW0-1-A	94.1	82.4	34.6	30.2	0.00	0.00	0.000	0.367
C2-DW0-1-B	94.1	82.4	34.6	30.2	0.00	0.00	0.000	0.367
C2-DW20-1-A	95.1	83.2	34.2	29.9	3.60	3.15	0.205	0.359
C2-DW20-1-B	96.1	84.1	33.7	29.5	3.16	2.76	0.193	0.351
C2-DW35-1-A	95.1	83.2	35.7	31.3	9.66	8.45	0.364	0.376
C2-DW35-1-B	95.1	83.2	35.7	31.3	9.66	8.45	0.364	0.376
C2-DW45-1-A	93.1	81.5	32.7	28.6	11.7	10.2	0.458	0.351
C2-DW45-1-B	92.1	80.6	33.2	29.1	11.2	9.76	0.436	0.361
C2-DW55-1-A	93.6	81.9	31.7	27.8	14.7	12.8	0.567	0.339
C2-DW55-1-B	93.6	81.9	31.8	27.8	14.7	12.9	0.567	0.339
C2-DW65-1-A	94.1	82.4	37.2	32.6	19.7	17.2	0.618	0.395
C2-DW65-1-B	94.1	82.4	37.2	32.6	19.7	17.2	0.618	0.395

Table A.2b - Test Specimen Dimension Ratios

Specimen	h (mm)	h/t	w (mm)	w/t	d (mm)	d/t	d ₁ /w	w/h
C2-DW0-2-A	90.7	48.6	26.8	14.4	0.00	0.00	0.000	0.296
C2-DW0-2-B	90.4	48.5	26.0	13.9	0.00	0.00	0.000	0.288
C2-DW25-2-A	87.8	47.1	30.0	16.1	3.60	1.93	0.307	0.342
C2-DW25-2-B	87.8	47.1	29.8	16.0	3.40	1.83	0.302	0.339
C2-DW40-2-A	88.8	47.6	30.0	16.1	7.20	3.86	0.427	0.338
C2-DW40-2-B	89.0	47.7	29.9	16.0	7.20	3.86	0.428	0.336
C2-DW50-2-A	88.1	47.2	29.6	15.9	9.60	5.15	0.513	0.336
C2-DW50-2-B	88.6	47.5	29.8	16.0	9.40	5.04	0.503	0.336
C2-DW60-2-A	89.1	47.8	29.8	16.0	12.4	6.65	0.604	0.335
C2-DW60-2-B	89.3	47.9	29.9	16.0	12.4	6.65	0.602	0.335
C2-DW70-2-A	88.8	47.6	29.7	15.9	15.1	8.10	0.697	0.335
C2-DW70-2-B	88.7	47.6	29.8	16.0	15.1	8.10	0.694	0.336
C2-DW80-2-A	90.3	48.4	30.0	16.1	18.1	9.71	0.790	0.332
C2-DW80-2-B	89.0	47.7	29.6	15.9	18.4	9.87	0.811	0.333
C2-DW0-3-A	232	191	31.6	26.0	0.00	0.00	0.000	0.136
C2-DW0-3-B	232	191	31.4	25.9	0.00	0.00	0.000	0.135
C2-DW20-3-A	233	192	30.2	24.9	4.26	3.52	0.265	0.130
C2-DW20-3-B	234	193	30.4	25.0	4.40	3.62	0.267	0.130
C2-DW35-3-A	233	192	31.1	25.7	9.56	7.88	0.424	0.134
C2-DW35-3-B	233	192	31.1	25.6	9.72	8.02	0.428	0.134
C2-DW45-3-A	233	192	30.8	25.4	11.2	9.23	0.481	0.132
C2-DW45-3-B	234	193	30.8	25.4	10.8	8.92	0.468	0.132
C2-DW55-3-A	234	193	30.6	25.2	14.0	11.5	0.575	0.131
C2-DW55-3-B	234	193	30.6	25.2	14.0	11.5	0.575	0.131
C2-DW65-3-A	234	193	30.6	25.2	18.5	15.3	0.723	0.131
C2-DW65-3-B	234	193	30.6	25.2	18.4	15.2	0.719	0.131
C2-DW80-3-A	231	191	31.0	25.5	23.2	19.1	0.865	0.134
C2-DW80-3-B	231	191	30.8	25.4	23.6	19.4	0.884	0.133
C2-DW0-4-A	293	154	29.6	15.5	0.00	0.00	0.000	0.101
C2-DW0-4-B	292	153	29.6	15.5	0.00	0.00	0.000	0.101
C2-DW25-4-A	290	152	31.1	16.3	1.99	1.04	0.254	0.107
C2-DW25-4-B	289	152	31.4	16.5	2.59	1.36	0.268	0.109
C2-DW40-4-A	296	155	28.3	14.9	7.38	3.88	0.474	0.096
C2-DW40-4-B	296	155	28.2	14.8	7.39	3.88	0.465	0.095
C2-DW50-4-A	294	154	28.4	14.9	7.79	4.09	0.479	0.097
C2-DW50-4-B	294	154	29.0	15.2	7.58	3.98	0.473	0.099
C2-DW60-4-A	292	153	29.8	15.7	11.4	6.01	0.580	0.102
C2-DW60-4-B	292	153	30.3	15.9	11.5	6.06	0.577	0.104
C2-DW70-4-A	294	154	30.0	15.8	15.3	8.03	0.704	0.102
C2-DW70-4-B	294	154	30.0	15.8	15.1	7.93	0.704	0.102

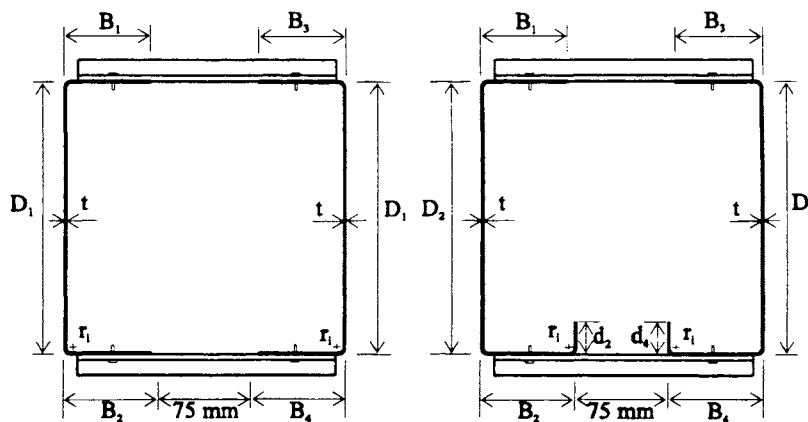
Table A.2c - Test Specimen Dimension Ratios

Specimen	h (mm)	h/t	w (mm)	w/t	d (mm)	d/t	d _c /w	w/h
C2-DW80-4-A	296	156	27.3	14.3	18.4	9.66	0.883	0.092
C2-DW80-4-B	296	156	28.2	14.8	17.7	9.29	0.845	0.095
C2R-DW0-1-A	94.9	78.5	33.6	27.8	0.00	0.00	0.000	0.354
C2R-DW0-1-B	95.3	78.9	33.8	28.0	0.00	0.00	0.000	0.355
C2R-DW20-1-A	93.9	77.7	30.8	25.5	2.38	1.97	0.195	0.328
C2R-DW20-1-B	94.3	78.0	30.8	25.5	2.38	1.97	0.195	0.326
C2R-DW35-1-A	94.6	78.3	30.5	25.2	9.58	7.93	0.433	0.322
C2R-DW35-1-B	94.3	78.0	30.5	25.2	9.78	8.09	0.440	0.323
C2R-DW45-1-A	95.8	79.3	31.2	25.8	10.6	8.75	0.456	0.325
C2R-DW45-1-B	95.8	79.3	31.6	26.1	11.1	9.17	0.466	0.330
C2R-DW55-1-A	94.7	78.4	31.1	25.7	14.9	12.3	0.596	0.328
C2R-DW55-1-B	94.6	78.3	31.6	26.1	15.2	12.6	0.596	0.334
C2R-DW65-1-A	95.4	78.9	31.5	26.0	19.0	15.7	0.719	0.330
C2R-DW65-1-B	94.6	78.3	31.6	26.1	18.9	15.6	0.713	0.334
C3-DW0-1-A	96.2	80.2	57.9	48.3	0.00	0.00	0.000	0.602
C3-DW0-1-B	96.2	80.2	58.3	48.6	0.00	0.00	0.000	0.606
C3-DW20-1-A	90.8	75.7	58.4	48.7	9.90	8.25	0.231	0.643
C3-DW20-1-B	91.8	76.5	58.5	48.7	9.90	8.25	0.231	0.637
C3-DW30-1-A	92.6	77.2	58.7	48.9	14.0	11.7	0.300	0.634
C3-DW30-1-B	93.1	77.6	58.7	48.9	14.3	11.9	0.305	0.631
C3-DW35-1-A	94.6	78.8	58.8	49.0	19.4	16.2	0.391	0.622
C3-DW35-1-B	94.6	78.8	59.0	49.2	19.5	16.2	0.392	0.624
C3-DW45-1-A	91.8	76.5	59.0	49.2	22.1	18.4	0.436	0.643
C3-DW45-1-B	91.8	76.5	59.0	49.2	22.0	18.3	0.434	0.643
C3-DW0-2-A	234	220	59.4	55.7	0.00	0.00	0.000	0.254
C3-DW0-2-B	234	219	59.6	55.9	0.00	0.00	0.000	0.255
C3-DW20-2-A	238	223	59.0	55.4	9.73	9.13	0.222	0.248
C3-DW20-2-B	238	223	59.0	55.4	10.0	9.38	0.224	0.248
C3-DW30-2-A	237	222	59.0	55.4	14.2	13.4	0.296	0.250
C3-DW30-2-B	237	222	58.9	55.2	14.5	13.6	0.302	0.249
C3-DW35-2-A	234	216	58.9	54.5	21.2	19.7	0.416	0.252
C3-DW35-2-B	234	216	59.1	54.8	21.1	19.5	0.411	0.253
C3-DW45-2-A	236	221	59.3	55.6	23.0	21.6	0.442	0.252
C3-DW45-2-B	235	221	59.0	55.3	22.8	21.4	0.442	0.251
C3-DW50-2-A	234	219	59.2	55.5	27.7	26.0	0.524	0.253
C3-DW50-2-B	234	219	59.3	55.6	27.6	25.9	0.520	0.254
C3-DW60-2-A	233	219	58.9	55.2	33.3	31.2	0.621	0.253
C3-DW60-2-B	234	219	58.7	55.1	33.4	31.3	0.627	0.251

Table A.3 - Material Properties of Test Specimens

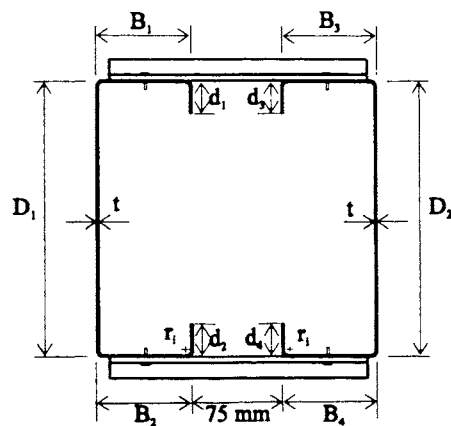
Series	t (mm)	F _y (MPa)	F _u (MPa)	% Elong.
C1-1	1.92	359	457	31.5
C1-2	1.85	396	470	29.2
C1-3	1.83	379	444	32.8
C2-1	1.14	362	439	28.3
C2-2	1.87	386	492	30.6
C2-3	1.21	326	369	38.8
C2-4	1.90	418	515	27.2
C2R-1	1.21	329	381	34.4
C3-1	1.20	302	372	39.6
C3-2	1.07	341	381	37.1
C3-DW35-2	1.08	332	372	36.8

Note: Material properties are based on an average of four coupon tests per series. Percent elongation is based on a 50mm gauge length.



Unlippped Sections
C1-1, C2-1

Unlippped Sections
C1-1, C2-1



Lipped Sections

Figure A.1 Test Specimen Cross Sections

Table A.4 - k Values for Edge Stiffener Stress Gradient Methods

Specimen	$k_{1,2,3}$	k_4	k_5	Specimen	$k_{1,2,3}$	k_4	k_5
C1-DW30-1-A	0.430	0.430	0.494	C2R-DW55-1-A	0.430	0.552	0.638
C1-DW30-1-B	0.430	0.430	0.494	C2R-DW55-1-B	0.430	0.555	0.643
C1-DW40-1-A	0.430	0.441	0.510	C2R-DW65-1-A	0.430	0.597	0.691
C1-DW40-1-B	0.430	0.441	0.510	C2R-DW65-1-B	0.430	0.598	0.693
C1-DW60-1-A	0.430	0.465	0.539				
C1-DW60-1-B	0.430	0.465	0.538	C2-DW25-2-A	0.430	0.451	0.522
C1-DW80-1-A	0.430	0.492	0.570	C2-DW25-2-B	0.430	0.449	0.520
C1-DW80-1-B	0.430	0.492	0.570	C2-DW40-2-A	0.430	0.481	0.557
				C2-DW40-2-B	0.430	0.481	0.556
C2-DW20-1-A	0.430	0.447	0.517	C2-DW50-2-A	0.430	0.505	0.584
C2-DW20-1-B	0.430	0.444	0.513	C2-DW50-2-B	0.430	0.502	0.581
C2-DW35-1-A	0.430	0.495	0.573	C2-DW60-2-A	0.430	0.534	0.617
C2-DW35-1-B	0.430	0.495	0.573	C2-DW60-2-B	0.430	0.533	0.617
C2-DW45-1-A	0.430	0.521	0.602	C2-DW70-2-A	0.430	0.567	0.656
C2-DW45-1-B	0.430	0.515	0.596	C2-DW70-2-B	0.430	0.568	0.657
C2-DW55-1-A	0.430	0.551	0.638	C2-DW80-2-A	0.430	0.606	0.701
C2-DW55-1-B	0.430	0.551	0.638	C2-DW80-2-B	0.430	0.614	0.711
C2-DW65-1-A	0.430	0.602	0.698				
C2-DW65-1-B	0.430	0.604	0.699	C3-DW20-1-A	0.430	0.495	0.573
				C3-DW20-1-B	0.430	0.495	0.572
C2R-DW20-1-A	0.430	0.440	0.509	C3-DW30-1-A	0.430	0.536	0.620
C2R-DW20-1-B	0.430	0.439	0.508	C3-DW30-1-B	0.430	0.539	0.623
C2R-DW35-1-A	0.430	0.497	0.575	C3-DW35-1-A	0.430	0.595	0.689
C2R-DW35-1-B	0.430	0.499	0.578	C3-DW35-1-B	0.430	0.596	0.690
C2R-DW45-1-A	0.430	0.506	0.585	C3-DW45-1-A	0.430	0.639	0.740
C2R-DW45-1-B	0.430	0.511	0.591	C3-DW45-1-B	0.430	0.637	0.738

- Note:
- 1) S136 uniform compressive stress at the top of the flat width (Current).
 - 2) S136 uniform compressive stress at the mid-point of the flat width.
 - 3) S136 uniform compressive stress at the third point of the flat width.
 - 4) Cohen/Eurocode stress gradient.
 - 5) ISO stress gradient.

Table A.5a - M_T/M_P Ratios - Edge Stiffener Stress Gradient Methods

Specimen	S136 ₁		S136 ₁ *		S136 ₂		S136 ₂ *		
	M_T (kN·m)	M_P (kN·m)	M_T/M_P	M_P (kN·m)	M_T/M_P	M_P (kN·m)	M_T/M_P	M_P (kN·m)	M_T/M_P
C1-DW30-1-A,B	7.17	6.03	1.19	7.00	1.03	6.03	1.19	7.00	1.03
C1-DW40-1-A,B	7.48	6.25	1.20	7.25	1.03	6.25	1.20	7.25	1.03
C1-DW60-1-A,B	7.83	6.44	1.22	7.47	1.05	6.44	1.22	7.47	1.05
C1-DW80-1-A,B	8.43	6.84	1.23	7.90	1.07	6.84	1.23	7.90	1.07
C2-DW20-1-A,B	4.19	3.73	1.12	3.73	1.12	3.73	1.12	3.73	1.12
C2-DW35-1-A,B	4.43	4.71	0.94	4.71	0.94	4.71	0.94	4.71	0.94
C2-DW45-1-A,B	5.16	4.84	1.07	4.84	1.07	4.84	1.07	4.84	1.07
C2-DW55-1-A,B	5.09	4.87	1.04	4.87	1.04	4.90	1.04	4.90	1.04
C2-DW65-1-A,B	5.57	5.01	1.11	5.01	1.11	5.06	1.10	5.06	1.10
C2R-DW20-1-A,B	4.16	3.64	1.14	3.64	1.14	3.64	1.14	3.64	1.14
C2R-DW35-1-A,B	5.05	4.77	1.06	4.93	1.02	4.77	1.06	4.93	1.02
C2R-DW45-1-A,B	5.22	4.97	1.05	5.18	1.01	4.97	1.05	5.18	1.01
C2R-DW55-1-A,B	5.26	4.93	1.07	4.93	1.07	4.95	1.06	4.95	1.06
C2R-DW65-1-A,B	5.49	4.81	1.14	4.81	1.14	4.85	1.13	4.85	1.13
C2-DW25-2-A,B	9.21	7.75	1.19	7.75	1.19	7.75	1.19	7.75	1.19
C2-DW40-2-A,B	10.4	8.45	1.23	8.85	1.18	8.45	1.23	8.85	1.18
C2-DW50-2-A,B	10.4	8.51	1.22	9.50	1.10	8.51	1.22	9.50	1.10
C2-DW60-2-A,B	11.0	8.81	1.24	9.83	1.12	8.81	1.24	9.83	1.12
C2-DW70-2-A,B	10.8	8.89	1.22	9.91	1.09	8.89	1.22	9.91	1.09
C2-DW80-2-A,B	11.2	9.16	1.23	9.96	1.13	9.16	1.23	9.96	1.13
C3-DW20-1-A,B	5.14	4.67	1.10	4.67	1.10	4.67	1.10	4.67	1.10
C3-DW30-1-A,B	5.37	5.38	1.00	5.38	1.00	5.39	1.00	5.39	1.00
C3-DW35-1-A,B	5.43	5.60	0.97	5.60	0.97	5.64	0.96	5.64	0.96
C3-DW45-1-A,B	5.37	5.36	1.00	5.36	1.00	5.40	0.99	5.40	0.99
Mean			1.12		1.07		1.12		1.07
Std. Dev.			0.094		0.065		0.095		0.065
Coeff. of Var.			0.087		0.063		0.089		0.064

Note: * - Cold work of forming used.

Note: 1) S136 uniform compressive stress at the top of the flat width (Current).
2) S136 uniform compressive stress at the mid-point of the flat width.

Table A.5b - M_T/M_P Ratios - Edge Stiffener Stress Gradient Methods

Specimen	S136 ₃			S136 ₃ *		S136 ₄		S136 ₄ *	
	M_T (kN·m)	M_P (kN·m)	M_T/M_P	M_P (kN·m)	M_T/M_P	M_P (kN·m)	M_T/M_P	M_P (kN·m)	M_T/M_P
C1-DW30-1-A,B	7.17	6.03	1.19	7.00	1.03	6.03	1.19	7.00	1.03
C1-DW40-1-A,B	7.48	6.25	1.20	7.25	1.03	6.25	1.20	7.25	1.03
C1-DW60-1-A,B	7.83	6.44	1.22	7.47	1.05	6.44	1.22	7.47	1.05
C1-DW80-1-A,B	8.43	6.84	1.23	7.90	1.07	6.84	1.23	7.90	1.07
C2-DW20-1-A,B	4.19	3.73	1.12	3.73	1.12	3.73	1.12	3.73	1.12
C2-DW35-1-A,B	4.43	4.71	0.94	4.71	0.94	4.71	0.94	4.71	0.94
C2-DW45-1-A,B	5.16	4.84	1.07	4.84	1.07	4.84	1.07	4.84	1.07
C2-DW55-1-A,B	5.09	4.89	1.04	4.89	1.04	4.91	1.04	4.91	1.04
C2-DW65-1-A,B	5.57	5.04	1.11	5.04	1.11	5.08	1.10	5.08	1.10
C2R-DW20-1-A,B	4.16	3.64	1.14	3.64	1.14	3.64	1.14	3.64	1.14
C2R-DW35-1-A,B	5.05	4.77	1.06	4.93	1.02	4.77	1.06	4.93	1.02
C2R-DW45-1-A,B	5.22	4.97	1.05	5.18	1.01	4.97	1.05	5.18	1.01
C2R-DW55-1-A,B	5.26	4.94	1.06	4.94	1.06	4.96	1.06	4.96	1.06
C2R-DW65-1-A,B	5.49	4.83	1.14	4.83	1.14	4.87	1.13	4.87	1.13
C2-DW25-2-A,B	9.21	7.75	1.19	7.75	1.19	7.75	1.19	7.75	1.19
C2-DW40-2-A,B	10.4	8.45	1.23	8.85	1.18	8.45	1.23	8.85	1.18
C2-DW50-2-A,B	10.4	8.51	1.22	9.50	1.10	8.51	1.22	9.50	1.10
C2-DW60-2-A,B	11.0	8.81	1.24	9.83	1.12	8.81	1.24	9.83	1.12
C2-DW70-2-A,B	10.8	8.89	1.22	9.91	1.09	8.89	1.22	9.91	1.09
C2-DW80-2-A,B	11.2	9.16	1.23	9.96	1.13	9.16	1.23	9.96	1.13
C3-DW20-1-A,B	5.14	4.67	1.10	4.67	1.10	4.67	1.10	4.67	1.10
C3-DW30-1-A,B	5.37	5.38	1.00	5.38	1.00	5.39	1.00	5.39	1.00
C3-DW35-1-A,B	5.43	5.63	0.96	5.63	0.96	5.66	0.96	5.66	0.96
C3-DW45-1-A,B	5.37	5.39	1.00	5.39	1.00	5.42	0.99	5.42	0.99
Mean			1.12		1.07		1.12		1.07
Std. Dev.			0.095		0.065		0.096		0.065
Coeff. of Var.			0.088		0.063		0.090		0.064

Note: * - Cold work of forming used.

Note: 3) S136 uniform compressive stress at the third point of the flat width.
4) Cohen/Eurocode stress gradient.

Table A.5c - M_T/M_P Ratios - Edge Stiffener Stress Gradient Methods

Specimen	S136 ₅			S136 ₅ *	
	M_T (kN·m)	M_P (kN·m)	M_T/M_P	M_P (kN·m)	M_T/M_P
C1-DW30-1-A,B	7.17	6.03	1.19	7.00	1.03
C1-DW40-1-A,B	7.48	6.25	1.20	7.25	1.03
C1-DW60-1-A,B	7.83	6.44	1.22	7.47	1.05
C1-DW80-1-A,B	8.43	6.84	1.23	7.90	1.07
C2-DW20-1-A,B	4.19	3.73	1.12	3.73	1.12
C2-DW35-1-A,B	4.43	4.71	0.94	4.71	0.94
C2-DW45-1-A,B	5.16	4.84	1.07	4.84	1.07
C2-DW55-1-A,B	5.09	4.93	1.03	4.93	1.03
C2-DW65-1-A,B	5.57	5.11	1.09	5.11	1.09
C2R-DW20-1-A,B	4.16	3.64	1.14	3.64	1.14
C2R-DW35-1-A,B	5.05	4.77	1.06	4.93	1.02
C2R-DW45-1-A,B	5.22	4.97	1.05	5.18	1.01
C2R-DW55-1-A,B	5.26	4.96	1.06	4.96	1.06
C2R-DW65-1-A,B	5.49	4.89	1.12	4.89	1.12
C2-DW25-2-A,B	9.21	7.75	1.19	7.75	1.19
C2-DW40-2-A,B	10.4	8.45	1.23	8.85	1.18
C2-DW50-2-A,B	10.4	8.51	1.22	9.50	1.10
C2-DW60-2-A,B	11.0	8.81	1.24	9.83	1.12
C2-DW70-2-A,B	10.8	8.89	1.22	9.91	1.09
C2-DW80-2-A,B	11.2	9.16	1.23	9.96	1.13
C3-DW20-1-A,B	5.14	4.67	1.10	4.67	1.10
C3-DW30-1-A,B	5.37	5.39	1.00	5.39	1.00
C3-DW35-1-A,B	5.43	5.68	0.95	5.68	0.95
C3-DW45-1-A,B	5.37	5.45	0.98	5.45	0.98
Mean			1.12		1.07
Std. Dev.			0.097		0.066
Coeff. of Var.			0.090		0.064

Note: * - Cold work of forming used.

Note: 5) ISO stress gradient.

Table A.6a - M_T/M_P Ratios - Local Buckling Methods

Specimen	S136			S136*		AISI		AISI*	
	M_T (kN·m)	M_P (kN·m)	M_T/M_P	M_P (kN·m)	M_T/M_P	M_P (kN·m)	M_T/M_P	M_P (kN·m)	M_T/M_P
C1-DW0-1-A,B	5.95	5.17	1.15	5.72	1.04	5.17	1.15	5.80	1.03
C1-DW30-1-A,B	7.17	6.03	1.19	7.00	1.03	6.03	1.19	7.14	1.00
C1-DW40-1-A,B	7.48	6.25	1.20	7.25	1.03	6.25	1.20	7.40	1.01
C1-DW60-1-A,B	7.83	6.44	1.22	7.47	1.05	6.44	1.22	7.62	1.03
C1-DW80-1-A,B	8.43	6.84	1.23	7.90	1.07	6.84	1.23	8.06	1.05
C1-DW0-2-A,B	21.0	23.6	0.89	23.6	0.89	26.0	0.81	26.0	0.81
C1-DW30-2-A,B	24.3	26.6	0.91	28.9	0.84	29.4	0.83	32.0	0.76
C1-DW40-2-A,B	24.9	26.8	0.93	29.2	0.85	29.8	0.84	32.4	0.77
C1-DW60-2-A,B	25.6	28.4	0.90	30.9	0.83	31.5	0.81	34.3	0.75
C1-DW80-2-A,B	26.1	29.3	0.89	31.9	0.82	32.7	0.80	35.6	0.73
C1-DW0-3-A,B	23.9	30.7	0.78	31.0	0.77	32.2	0.74	32.4	0.74
C1-DW30-3-A,B	34.7	37.5	0.93	40.3	0.86	39.6	0.88	42.8	0.81
C1-DW40-3-A,B	35.9	38.8	0.93	41.8	0.86	41.0	0.88	44.5	0.81
C1-DW60-3-A,B	41.4	40.8	1.01	44.0	0.94	43.3	0.96	47.0	0.88
C2-DW0-1-A,B	2.78	2.89	0.96	2.89	0.96	3.03	0.92	3.03	0.92
C2-DW20-1-A,B	4.19	3.73	1.12	3.73	1.12	3.88	1.08	3.88	1.08
C2-DW35-1-A,B	4.43	4.71	0.94	4.71	0.94	4.79	0.92	4.79	0.92
C2-DW45-1-A,B	5.16	4.84	1.07	4.84	1.07	4.86	1.06	4.86	1.06
C2-DW55-1-A,B	5.09	4.87	1.04	4.87	1.04	4.91	1.04	4.91	1.04
C2-DW65-1-A,B	5.57	5.01	1.11	5.01	1.11	5.09	1.10	5.09	1.10
C2-DW0-2-A,B	7.29	6.18	1.18	6.18	1.18	6.18	1.18	6.18	1.18
C2-DW25-2-A,B	9.21	7.75	1.19	7.75	1.19	7.75	1.19	8.75	1.05
C2-DW40-2-A,B	10.4	8.45	1.23	8.85	1.18	8.45	1.23	9.41	1.11
C2-DW50-2-A,B	10.4	8.51	1.22	9.50	1.10	8.51	1.22	9.64	1.08
C2-DW60-2-A,B	11.0	8.81	1.24	9.83	1.12	8.81	1.24	9.97	1.10
C2-DW70-2-A,B	10.8	8.89	1.22	9.91	1.09	8.89	1.22	10.1	1.08
C2-DW80-2-A,B	11.2	9.16	1.23	9.96	1.13	9.16	1.23	9.85	1.14

Note: * - Cold work of forming used.

Table A.6b - M_T/M_P Ratios - Local Buckling Methods

Specimen	S136			S136*		AISI		AISI*	
	M_T (kN·m)	M_P (kN·m)	M_T/M_P	M_P (kN·m)	M_T/M_P	M_P (kN·m)	M_T/M_P	M_P (kN·m)	M_T/M_P
C2-DW0-3-A,B	8.36	8.09	1.03	8.09	1.03	8.41	0.99	8.41	0.99
C2-DW20-3-A,B	11.3	10.8	1.04	10.8	1.04	11.4	0.99	11.4	0.99
C2-DW35-3-A,B	12.2	12.9	0.94	13.0	0.94	13.7	0.89	14.1	0.87
C2-DW45-3-A,B	12.2	13.1	0.93	13.6	0.90	13.9	0.88	14.4	0.85
C2-DW55-3-A,B	13.3	13.4	0.99	13.4	0.99	14.2	0.94	14.2	0.94
C2-DW65-3-A,B	13.9	13.1	1.06	13.1	1.06	13.8	1.00	13.8	1.00
C2-DW80-3-A,B	13.2	12.6	1.05	12.6	1.05	13.4	0.99	13.4	0.99
C2-DW0-4-A,B	28.8	27.6	1.04	27.6	1.04	29.5	0.98	29.5	0.98
C2-DW25-4-A,B	31.9	33.9	0.94	33.9	0.94	36.6	0.87	36.6	0.87
C2-DW40-4-A,B	36.1	37.3	0.97	40.6	0.89	40.6	0.89	44.1	0.82
C2-DW50-4-A,B	36.7	37.5	0.98	40.7	0.90	40.8	0.90	44.3	0.83
C2-DW60-4-A,B	40.0	39.2	1.02	42.5	0.94	42.8	0.94	46.4	0.86
C2-DW70-4-A,B	38.4	40.8	0.94	44.2	0.87	44.5	0.86	48.3	0.80
C2-DW80-4-A,B	39.6	41.0	0.97	41.0	0.97	44.9	0.88	44.9	0.88
C2R-DW0-1-A,B	3.01	3.00	1.00	3.00	1.00	3.13	0.96	3.13	0.96
C2R-DW20-1-A,B	4.16	3.64	1.14	3.64	1.14	3.71	1.12	3.71	1.12
C2R-DW35-1-A,B	5.05	4.77	1.06	4.93	1.02	4.78	1.06	5.03	1.00
C2R-DW45-1-A,B	5.22	4.97	1.05	5.18	1.01	4.97	1.05	5.25	0.99
C2R-DW55-1-A,B	5.26	4.93	1.07	4.93	1.07	4.92	1.07	4.92	1.07
C2R-DW65-1-A,B	5.49	4.81	1.14	4.81	1.14	4.82	1.14	4.82	1.14
C3-DW0-1-A,B	3.76	3.01	1.25	3.01	1.25	3.19	1.18	3.19	1.18
C3-DW20-1-A,B	5.14	4.67	1.10	4.67	1.10	4.69	1.10	4.69	1.10
C3-DW30-1-A,B	5.37	5.38	1.00	5.38	1.00	5.37	1.00	5.37	1.00
C3-DW35-1-A,B	5.43	5.60	0.97	5.60	0.97	5.61	0.97	5.61	0.97
C3-DW45-1-A,B	5.37	5.36	1.00	5.36	1.00	5.36	1.00	5.36	1.00
C3-DW0-2-A,B	7.64	6.82	1.12	6.82	1.12	6.91	1.11	6.91	1.11
C3-DW20-2-A,B	12.4	11.5	1.08	11.5	1.08	11.8	1.05	11.8	1.05
C3-DW30-2-A,B	13.4	13.4	1.00	13.4	1.00	13.8	0.97	13.8	0.97
C3-DW35-2-A,B	13.0	13.1	0.99	13.1	0.99	13.5	0.96	13.5	0.96
C3-DW45-2-A,B	13.4	13.1	1.02	13.1	1.02	13.4	1.00	13.4	1.00
C3-DW50-2-A,B	13.1	12.7	1.03	12.7	1.03	13.0	1.00	13.0	1.00
C3-DW60-2-A,B	13.2	12.3	1.07	12.3	1.07	12.6	1.05	12.6	1.05

Note: * - Cold work of forming used.

Table A.6c - M_T/M_p Ratios - Local Buckling Methods

Specimen	Dinovitzer			Sooi*	
	M_T (kN·m)	M_p (kN·m)	M_T/M_p	M_p (kN·m)	M_T/M_p
C1-DW0-1-A,B	5.95	5.17	1.15	5.17	1.15
C1-DW30-1-A,B	7.17	6.03	1.19	6.03	1.19
C1-DW40-1-A,B	7.48	6.25	1.20	6.25	1.20
C1-DW60-1-A,B	7.83	6.44	1.22	6.44	1.22
C1-DW80-1-A,B	8.43	6.84	1.23	6.84	1.23
C1-DW0-2-A,B	21.0	23.6	0.89	20.6	1.02
C1-DW30-2-A,B	24.3	26.6	0.91	22.8	1.06
C1-DW40-2-A,B	24.9	26.8	0.93	23.2	1.07
C1-DW60-2-A,B	25.6	28.4	0.90	24.3	1.05
C1-DW80-2-A,B	26.1	29.3	0.89	25.0	1.04
C1-DW0-3-A,B	23.9	30.7	0.78	31.0	0.77
C1-DW30-3-A,B	34.7	37.5	0.93	40.3	0.86
C1-DW40-3-A,B	35.9	38.8	0.93	41.8	0.86
C1-DW60-3-A,B	41.4	40.8	1.01	44.0	0.94
C2-DW0-1-A,B	2.78	2.89	0.96	3.01	0.92
C2-DW20-1-A,B	4.19	3.98	1.05	3.85	1.09
C2-DW35-1-A,B	4.43	4.71	0.94	4.78	0.93
C2-DW45-1-A,B	5.16	4.85	1.06	4.87	1.06
C2-DW55-1-A,B	5.09	4.87	1.04	4.91	1.04
C2-DW65-1-A,B	5.57	5.01	1.11	5.08	1.10
C2-DW0-2-A,B	7.29	6.18	1.18	6.18	1.18
C2-DW25-2-A,B	9.21	7.75	1.19	7.75	1.19
C2-DW40-2-A,B	10.4	8.45	1.23	8.45	1.23
C2-DW50-2-A,B	10.4	8.51	1.22	8.51	1.22
C2-DW60-2-A,B	11.0	8.81	1.24	8.81	1.24
C2-DW70-2-A,B	10.8	8.89	1.22	8.89	1.22
C2-DW80-2-A,B	11.2	9.16	1.23	9.16	1.23

Note: * - Cold work of forming used.

Table A.6d - M_T/M_P Ratios - Local Buckling Methods

Specimen	Dinovitzer			Sooi*	
	M_T (kN-m)	M_P (kN-m)	M_T/M_P	M_P (kN-m)	M_T/M_P
C2-DW0-3-A,B	8.36	8.09	1.03	7.23	1.15
C2-DW20-3-A,B	11.3	11.1	1.01	9.22	1.22
C2-DW35-3-A,B	12.2	12.9	0.94	10.9	1.12
C2-DW45-3-A,B	12.2	13.1	0.93	11.0	1.11
C2-DW55-3-A,B	13.3	13.4	0.99	11.2	1.19
C2-DW65-3-A,B	13.9	13.1	1.06	10.9	1.27
C2-DW80-3-A,B	13.2	12.6	1.05	10.6	1.24
C2-DW0-4-A,B	28.8	27.6	1.04	25.3	1.14
C2-DW25-4-A,B	31.9	34.4	0.93	30.4	1.05
C2-DW40-4-A,B	36.1	37.3	0.97	32.7	1.10
C2-DW50-4-A,B	36.7	37.5	0.98	33.0	1.11
C2-DW60-4-A,B	40.0	39.2	1.02	34.7	1.15
C2-DW70-4-A,B	38.4	40.8	0.94	35.7	1.08
C2-DW80-4-A,B	39.6	41.0	0.97	35.7	1.11
C2R-DW0-1-A,B	3.01	3.00	1.00	3.11	0.97
C2R-DW20-1-A,B	4.16	3.80	1.09	3.70	1.12
C2R-DW35-1-A,B	5.05	4.77	1.06	4.78	1.06
C2R-DW45-1-A,B	5.22	4.97	1.05	4.97	1.05
C2R-DW55-1-A,B	5.26	4.93	1.07	4.93	1.07
C2R-DW65-1-A,B	5.49	4.81	1.14	4.82	1.14
C3-DW0-1-A,B	3.76	3.01	1.25	3.17	1.19
C3-DW20-1-A,B	5.14	4.67	1.10	4.69	1.10
C3-DW30-1-A,B	5.37	5.38	1.00	5.38	1.00
C3-DW35-1-A,B	5.43	5.60	0.97	5.61	0.97
C3-DW45-1-A,B	5.37	5.36	1.00	5.36	1.00
C3-DW0-2-A,B	7.64	6.82	1.12	6.19	1.24
C3-DW20-2-A,B	12.4	11.5	1.08	9.30	1.34
C3-DW30-2-A,B	13.4	13.4	1.00	10.7	1.26
C3-DW35-2-A,B	13.0	13.1	0.99	10.6	1.23
C3-DW45-2-A,B	13.4	13.1	1.02	10.4	1.28
C3-DW50-2-A,B	13.1	12.7	1.03	10.2	1.28
C3-DW60-2-A,B	13.2	12.3	1.07	9.87	1.33

Note: * - Cold work of forming used.

Table A.7a - M_T/M_P Ratios - Flange/Web Distortional Buckling Methods

Specimen	Lau & Hancock 1			Lau & Hancock 2		Lau & Hancock 3		Marsh	
	M_T (kN·m)	M_P (kN·m)	M_T/M_P	M_P (kN·m)	M_T/M_P	M_P (kN·m)	M_T/M_P	M_P (kN·m)	M_T/M_P
C1-DW0-1-A,B	5.95	-	-	-	-	-	-	-	-
C1-DW30-1-A,B	7.17	5.49	1.31	5.49	1.31	5.20	1.38	5.39	1.33
C1-DW40-1-A,B	7.48	5.76	1.30	5.76	1.30	5.48	1.36	5.71	1.31
C1-DW60-1-A,B	7.83	5.99	1.31	5.99	1.31	5.73	1.37	6.01	1.30
C1-DW80-1-A,B	8.43	6.34	1.33	6.34	1.33	6.06	1.39	6.43	1.31
C1-DW0-2-A,B	21.0	-	-	-	-	-	-	-	-
C1-DW30-2-A,B	24.3	21.4	1.14	21.4	1.14	20.6	1.18	23.8	1.02
C1-DW40-2-A,B	24.9	21.8	1.14	21.8	1.14	21.0	1.19	24.5	1.02
C1-DW60-2-A,B	25.6	22.9	1.12	22.9	1.12	22.1	1.16	26.7	0.96
C1-DW80-2-A,B	26.1	23.5	1.11	23.5	1.11	22.6	1.15	28.0	0.93
C1-DW0-3-A,B	23.9	-	-	-	-	-	-	-	-
C1-DW30-3-A,B	34.7	23.7	1.47	23.7	1.47	23.0	1.51	33.8	1.03
C1-DW40-3-A,B	35.9	24.3	1.48	24.3	1.48	23.6	1.52	35.6	1.01
C1-DW60-3-A,B	41.4	25.0	1.65	25.0	1.65	24.1	1.72	38.1	1.09
C2-DW0-1-A,B	2.78	-	-	-	-	-	-	-	-
C2-DW20-1-A,B	4.19	3.53	1.18	3.53	1.18	3.06	1.37	3.24	1.29
C2-DW35-1-A,B	4.43	4.34	1.02	4.34	1.02	3.89	1.14	4.31	1.03
C2-DW45-1-A,B	5.16	4.21	1.22	4.21	1.22	3.82	1.35	4.26	1.21
C2-DW55-1-A,B	5.09	4.30	1.18	4.30	1.18	3.92	1.30	4.49	1.13
C2-DW65-1-A,B	5.57	4.62	1.21	4.62	1.21	4.18	1.33	4.69	1.19
C2-DW0-2-A,B	7.29	-	-	-	-	-	-	-	-
C2-DW25-2-A,B	9.21	6.94	1.33	6.94	1.33	6.40	1.44	6.76	1.36
C2-DW40-2-A,B	10.4	7.51	1.39	7.51	1.39	7.01	1.49	7.46	1.40
C2-DW50-2-A,B	10.4	7.63	1.36	7.63	1.36	7.16	1.45	7.66	1.36
C2-DW60-2-A,B	11.0	7.92	1.39	7.92	1.39	7.44	1.48	8.04	1.37
C2-DW70-2-A,B	10.8	7.97	1.36	7.97	1.36	7.48	1.45	8.19	1.32
C2-DW80-2-A,B	11.2	8.15	1.38	8.15	1.38	7.62	1.47	8.45	1.33

Table A.7b - M_T/M_P Ratios - Flange/Web Distortional Buckling Methods

Specimen	Lau & Hancock		Lau & Hancock		Lau & Hancock		Marsh		
	M_T (kN·m)	M_P (kN·m)	M_T/M_P	M_P (kN·m)	M_T/M_P	M_P (kN·m)	M_T/M_P	M_P (kN·m)	M_T/M_P
C2-DW0-3-A,B	8.36	-	-	-	-	-	-	-	-
C2-DW20-3-A,B	11.3	8.59	1.31	8.59	1.31	7.93	1.42	8.88	1.27
C2-DW35-3-A,B	12.2	9.56	1.27	9.56	1.27	8.95	1.36	10.8	1.13
C2-DW45-3-A,B	12.2	9.71	1.26	9.71	1.26	9.11	1.34	11.1	1.10
C2-DW55-3-A,B	13.3	10.0	1.33	10.0	1.33	9.40	1.42	11.8	1.13
C2-DW65-3-A,B	13.9	10.1	1.38	10.1	1.38	9.44	1.47	12.5	1.11
C2-DW80-3-A,B	13.2	9.89	1.34	9.89	1.34	9.20	1.44	12.9	1.02
C2-DW0-4-A,B	28.8	-	-	-	-	-	-	-	-
C2-DW25-4-A,B	31.9	27.4	1.16	27.4	1.16	25.3	1.26	27.1	1.17
C2-DW40-4-A,B	36.1	29.5	1.22	29.5	1.22	27.9	1.29	32.3	1.12
C2-DW50-4-A,B	36.7	29.7	1.24	29.7	1.24	28.0	1.31	32.5	1.13
C2-DW60-4-A,B	40.0	31.2	1.28	31.2	1.28	29.4	1.36	34.8	1.15
C2-DW70-4-A,B	38.4	32.0	1.20	32.0	1.20	30.2	1.27	37.0	1.04
C2-DW80-4-A,B	39.6	31.8	1.24	31.8	1.24	29.8	1.33	38.1	1.04
C2R-DW0-1-A,B	3.01	-	-	-	-	-	-	-	-
C2R-DW20-1-A,B	4.16	3.37	1.23	3.37	1.23	2.97	1.40	3.14	1.32
C2R-DW35-1-A,B	5.05	4.10	1.23	4.10	1.23	3.77	1.34	4.12	1.23
C2R-DW45-1-A,B	5.22	4.27	1.22	4.27	1.22	3.92	1.33	4.31	1.21
C2R-DW55-1-A,B	5.26	4.32	1.22	4.32	1.22	3.99	1.32	4.47	1.18
C2R-DW65-1-A,B	5.49	4.34	1.27	4.34	1.27	3.99	1.38	4.49	1.22
C3-DW0-1-A,B	3.76	-	-	-	-	-	-	-	-
C3-DW20-1-A,B	5.14	4.43	1.16	4.43	1.16	3.86	1.33	4.16	1.23
C3-DW30-1-A,B	5.37	4.93	1.09	4.93	1.09	4.36	1.23	4.43	1.21
C3-DW35-1-A,B	5.43	5.28	1.03	5.28	1.03	4.74	1.15	4.96	1.09
C3-DW45-1-A,B	5.37	5.17	1.04	5.17	1.04	4.65	1.15	4.94	1.09
C3-DW0-2-A,B	7.64	-	-	-	-	-	-	-	-
C3-DW20-2-A,B	12.4	8.04	1.55	8.15	1.52	7.29	1.70	7.17	1.73
C3-DW30-2-A,B	13.4	9.40	1.43	9.40	1.43	8.45	1.59	9.74	1.38
C3-DW35-2-A,B	13.0	10.3	1.26	10.3	1.26	9.36	1.39	10.8	1.20
C3-DW45-2-A,B	13.4	10.3	1.30	10.3	1.30	9.31	1.43	11.1	1.20
C3-DW50-2-A,B	13.1	10.3	1.27	10.3	1.27	9.39	1.39	11.4	1.14
C3-DW60-2-A,B	13.2	10.2	1.29	10.2	1.29	9.25	1.42	11.8	1.11

Table A.7c - M_T/M_P Ratios - Flange/Web Distortional Buckling Methods

Specimen	Moreyra 1			Moreyra 2	
	M_T (kN·m)	M_P (kN·m)	M_T/M_P	M_P (kN·m)	M_T/M_P
C1-DW0-1-A,B	5.95	-	-	-	-
C1-DW30-1-A,B	7.17	6.03	1.19	6.03	1.19
C1-DW40-1-A,B	7.48	6.25	1.20	6.25	1.20
C1-DW60-1-A,B	7.83	6.44	1.22	6.44	1.22
C1-DW80-1-A,B	8.43	6.84	1.23	6.84	1.23
C1-DW0-2-A,B	21.0	-	-	-	-
C1-DW30-2-A,B	24.3	21.9	1.11	22.0	1.11
C1-DW40-2-A,B	24.9	22.4	1.11	22.4	1.11
C1-DW60-2-A,B	25.6	23.3	1.10	23.3	1.10
C1-DW80-2-A,B	26.1	24.0	1.09	24.0	1.09
C1-DW0-3-A,B	23.9	-	-	-	-
C1-DW30-3-A,B	34.7	22.6	1.53	22.6	1.53
C1-DW40-3-A,B	35.9	23.3	1.54	23.3	1.54
C1-DW60-3-A,B	41.4	24.4	1.70	24.4	1.70
C2-DW0-1-A,B	2.78	-	-	-	-
C2-DW20-1-A,B	4.19	4.26	0.98	4.44	0.94
C2-DW35-1-A,B	4.43	5.00	0.89	5.22	0.85
C2-DW45-1-A,B	5.16	4.85	1.06	5.04	1.02
C2-DW55-1-A,B	5.09	4.98	1.02	5.08	1.00
C2-DW65-1-A,B	5.57	5.39	1.03	5.46	1.02
C2-DW0-2-A,B	7.29	-	-	-	-
C2-DW25-2-A,B	9.21	7.81	1.18	8.02	1.15
C2-DW40-2-A,B	10.4	8.45	1.23	8.45	1.23
C2-DW50-2-A,B	10.4	8.51	1.22	8.51	1.22
C2-DW60-2-A,B	11.0	8.81	1.24	8.81	1.24
C2-DW70-2-A,B	10.8	8.89	1.22	8.89	1.22
C2-DW80-2-A,B	11.2	9.15	1.23	9.15	1.23

Table A.7d - M_T/M_P Ratios - Flange/Web Distortional Buckling Methods

Specimen	Moreyra 1			Moreyra 2	
	M_T (kN·m)	M_P (kN·m)	M_T/M_P	M_P (kN·m)	M_T/M_P
C2-DW0-3-A,B	8.36	-	-	-	-
C2-DW20-3-A,B	11.3	8.08	1.40	8.32	1.36
C2-DW35-3-A,B	12.2	8.93	1.36	9.16	1.33
C2-DW45-3-A,B	12.2	9.09	1.34	9.25	1.32
C2-DW55-3-A,B	13.3	9.45	1.41	9.52	1.40
C2-DW65-3-A,B	13.9	9.69	1.43	9.69	1.43
C2-DW80-3-A,B	13.2	9.81	1.35	9.81	1.35
C2-DW0-4-A,B	28.8	-	-	-	-
C2-DW25-4-A,B	31.9	28.2	1.13	28.8	1.11
C2-DW40-4-A,B	36.1	30.1	1.20	30.7	1.17
C2-DW50-4-A,B	36.7	30.4	1.21	31.0	1.18
C2-DW60-4-A,B	40.0	32.1	1.25	32.5	1.23
C2-DW70-4-A,B	38.4	33.3	1.15	33.5	1.15
C2-DW80-4-A,B	39.6	33.6	1.18	33.6	1.18
C2R-DW0-1-A,B	3.01	-	-	-	-
C2R-DW20-1-A,B	4.16	3.93	1.06	4.08	1.02
C2R-DW35-1-A,B	5.05	4.67	1.08	4.78	1.06
C2R-DW45-1-A,B	5.22	4.87	1.07	4.97	1.05
C2R-DW55-1-A,B	5.26	4.99	1.06	4.99	1.05
C2R-DW65-1-A,B	5.49	5.07	1.08	5.07	1.08
C3-DW0-1-A,B	3.76	-	-	-	-
C3-DW20-1-A,B	5.14	4.39	1.17	4.61	1.12
C3-DW30-1-A,B	5.37	4.80	1.12	4.81	1.12
C3-DW35-1-A,B	5.43	4.96	1.09	4.96	1.09
C3-DW45-1-A,B	5.37	4.80	1.12	4.80	1.12
C3-DW0-2-A,B	7.64	-	-	-	-
C3-DW20-2-A,B	12.4	7.69	1.62	8.10	1.53
C3-DW30-2-A,B	13.4	8.32	1.61	8.64	1.55
C3-DW35-2-A,B	13.0	8.90	1.46	8.90	1.46
C3-DW45-2-A,B	13.4	8.79	1.52	8.79	1.52
C3-DW50-2-A,B	13.1	8.81	1.48	8.81	1.48
C3-DW60-2-A,B	13.2	8.84	1.49	8.84	1.49

Appendix 'B'

Available Test Data and Test / Predicted Bending Moment Ratios

Table B.1 - Charnvarnichborikarn [Cha 92] Test Specimen Dimensions

Specimen	d_1 (mm)	B_1 (mm)	D_1 (mm)	B_2 (mm)	d_2 (mm)	t (mm)	r_i (mm)	F_y (MPa)
2.7-0.00-1a	0.00	75.9	205	75.9	0.00	1.47	3.58	324
2.7-0.00-2a	0.00	75.9	204	75.9	0.00	1.50	3.31	324
2.7-0.00-1b	6.90	76.2	204	76.2	6.90	1.50	3.57	324
2.7-0.00-2b	7.60	76.1	205	76.1	7.60	1.47	3.84	324
2.7-0.15-1	7.40	74.6	204	74.6	7.40	1.47	3.58	324
2.7-0.15-2	7.40	73.9	204	73.9	7.40	1.50	3.31	324
2.7-0.25-1	10.2	75.6	205	75.6	10.2	1.47	3.58	324
2.7-0.25-2	9.40	76.7	203	76.7	9.4	1.50	3.57	324
2.7-0.50-1	15.7	75.9	204	75.9	15.7	1.50	3.57	324
2.7-0.50-2	16.5	75.7	204	75.7	16.5	1.50	3.57	324
2.7-0.75-1	22.6	75.9	204	75.9	22.6	1.50	3.82	324
2.7-0.75-2	22.1	75.9	204	75.9	22.1	1.50	3.57	324
2.7-1.00-1	29.0	75.2	204	75.2	29.0	1.50	3.31	324
2.7-1.00-2	28.4	75.1	203	75.1	28.4	1.47	3.33	324
2.7-1.25-1	35.3	75.4	204	75.4	35.3	1.50	3.57	324
2.7-1.25-2	35.1	75.1	204	75.1	35.1	1.47	3.58	324
2.7-1.50-1	41.1	76.4	204	76.4	41.1	1.47	3.58	324
2.7-1.50-2	41.1	75.9	204	75.9	41.1	1.50	3.06	324
2.7-2.00-1	54.4	76.1	203	76.1	54.4	1.47	3.33	324
2.7-2.00-2	54.4	75.9	203	75.9	54.4	1.50	3.06	324

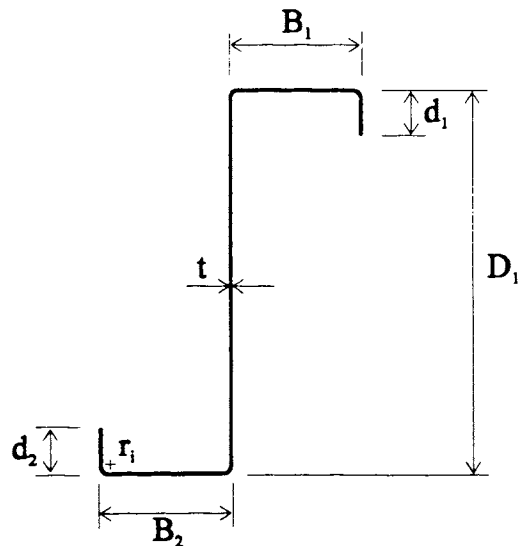
**Figure B.1 - Charnvarnichborikarn [Cha 92] Test Specimen Cross Section**

Table B.2 - Charnvarnichborikarn [Cha 92] Test Specimen Dimension Ratios

Specimen	h (mm)	h/t	w (mm)	w/t	d (mm)	d/t	d _i /w	w/h
2.7-0.00-1a	195	132	70.9	48.1	0.00	0.00	0.000	0.364
2.7-0.00-2a	194	130	71.1	47.5	0.00	0.00	0.000	0.366
2.7-0.00-1b	194	129	66.0	44.1	1.79	1.19	0.104	0.341
2.7-0.00-2b	194	132	65.5	44.5	2.31	1.57	0.116	0.338
2.7-0.15-1	194	132	64.5	43.8	2.25	1.53	0.114	0.332
2.7-0.15-2	194	129	64.3	42.9	2.54	1.70	0.115	0.331
2.7-0.25-1	195	132	65.5	44.5	5.10	3.46	0.155	0.337
2.7-0.25-2	193	129	66.7	44.5	4.50	3.00	0.141	0.346
2.7-0.50-1	194	129	65.8	43.9	10.7	7.14	0.239	0.340
2.7-0.50-2	194	129	65.6	43.8	11.5	7.68	0.252	0.338
2.7-0.75-1	193	129	65.4	43.6	17.4	11.6	0.346	0.338
2.7-0.75-2	194	129	65.9	43.9	17.1	11.4	0.336	0.340
2.7-1.00-1	194	129	65.6	43.8	24.2	16.2	0.441	0.338
2.7-1.00-2	193	131	65.6	44.5	23.7	16.1	0.434	0.340
2.7-1.25-1	194	129	65.3	43.6	30.3	20.2	0.541	0.337
2.7-1.25-2	194	132	65.1	44.2	30.1	20.4	0.538	0.336
2.7-1.50-1	194	132	66.3	45.0	36.1	24.5	0.620	0.342
2.7-1.50-2	195	130	66.8	44.6	36.6	24.4	0.616	0.343
2.7-2.00-1	194	132	66.6	45.2	49.6	33.7	0.816	0.344
2.7-2.00-2	194	129	66.8	44.6	49.8	33.2	0.813	0.344

Table B.3 - Cohen [Coh 87] Test Specimen Dimensions

Specimen	d ₁ (mm)	B ₁ (mm)	D ₁ (mm)	B ₂ (mm)	bpl (mm)	t (mm)	r _i (mm)	F _y (MPa)
It1-rmin-d90-1L1	17.5	88.9	208	88.9	88.9	1.63	1.60	375
It1-rmin-3/2d90-1L1	25.4	88.9	208	88.9	88.9	1.63	1.60	375
It1-rmin-3/2d90-2L1	25.4	88.9	208	88.9	88.9	1.63	1.60	375
It1-rmin-3/2d90-3L1	25.4	88.9	208	88.9	88.9	1.63	1.60	375
It2-rmin-d90-1L1	25.4	88.9	211	88.9	88.9	2.72	3.18	418
It2-rmin-d90-2L1	25.4	88.9	211	88.9	88.9	2.72	3.18	418
It2-rmin-3/2d90-1L1	38.1	88.9	211	88.9	88.9	2.72	3.18	418
It2-rmin-3/2d90-2L1	38.1	88.9	211	88.9	88.9	2.72	3.18	418
IIt1-rmin-d90-1L0	17.5	88.9	208	88.9	88.9	1.63	1.60	375
IIt1-rmin-d90-1L1	17.5	88.9	208	88.9	88.9	1.63	1.60	375
IIt1-rmin-d90-2L1	17.5	88.9	208	88.9	88.9	1.63	1.60	375
IIt1-rmin-3/2d90-1L1	25.4	88.9	208	88.9	88.9	1.63	1.60	375
IIt2-rmin-d90-1L1	25.4	88.9	211	88.9	88.9	2.72	3.18	418
IIt2-rmin-3/2d90-1L1	38.1	88.9	211	88.9	88.9	2.72	3.18	418

Table B.4 - Cohen [Coh 87] Test Specimen Dimension Ratios

Specimen	h (mm)	h/t	w (mm)	w/t	d (mm)	d/t	d ₁ /w	w/h
It1-rmin-d90-1L1	202	124	82.4	50.7	14.2	8.77	0.212	0.409
It1-rmin-3/2d90-1L1	202	124	82.4	50.7	22.2	13.6	0.308	0.409
It1-rmin-3/2d90-2L1	202	124	82.5	50.7	22.2	13.7	0.308	0.409
It1-rmin-3/2d90-3L1	202	124	82.5	50.7	22.2	13.6	0.308	0.409
It2-rmin-d90-1L1	199	73.4	77.2	28.4	19.6	7.20	0.329	0.387
It2-rmin-d90-2L1	199	73.4	77.1	28.4	19.5	7.18	0.329	0.387
It2-rmin-3/2d90-1L1	199	73.4	77.1	28.4	32.2	11.8	0.494	0.387
It2-rmin-3/2d90-2L1	199	73.4	77.1	28.4	32.2	11.9	0.494	0.387
IIt1-rmin-d90-1L0	202	124	82.4	50.7	14.2	8.76	0.212	0.409
IIt1-rmin-d90-1L1	202	124	82.5	50.7	14.3	8.77	0.212	0.409
IIt1-rmin-d90-2L1	202	124	82.5	50.7	14.3	8.77	0.212	0.409
IIt1-rmin-3/2d90-1L1	202	124	82.5	50.7	22.2	13.6	0.308	0.409
IIt2-rmin-d90-1L1	199	73.4	77.2	28.4	19.6	7.20	0.329	0.387
IIt2-rmin-3/2d90-1L1	199	73.4	77.1	28.4	32.2	11.8	0.494	0.387

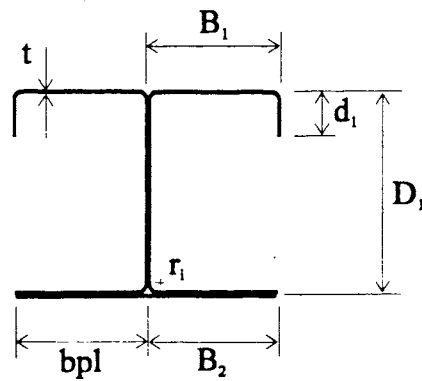
**Figure B.2 - Cohen [Coh 87] Test Specimen Cross Section**

Table B.5 - Desmond [Des 78a] Test Specimen Dimensions

Specimen	d_1 (mm)	B_1 (mm)	D_1 (mm)	B_2 (mm)	d_2 (mm)	t (mm)	r_i (mm)	F_y (MPa)
E-45.6B-1	17.4	95.8	135	95.8	17.4	1.88	2.82	399
E-45.6B-2	21.2	95.7	135	95.7	21.2	1.87	2.82	399
E-45.6B-3	33.2	95.8	133	95.8	33.2	1.89	2.82	383
E-45.6B-4	42.3	95.8	133	95.8	42.3	1.88	2.82	379

Table B.6 - Desmond [Des 78a] Test Specimen Dimension Ratios

Specimen	h (mm)	h/t	w (mm)	w/t	d (mm)	d/t	d/w	w/h
E-45.6B-1	125	66.6	86.4	45.9	12.7	6.76	0.201	0.690
E-45.6B-2	125	67.1	86.4	46.3	16.5	8.84	0.245	0.690
E-45.6B-3	124	65.5	86.4	45.6	28.4	15.0	0.384	0.697
E-45.6B-4	124	65.9	86.4	45.9	37.6	20.0	0.490	0.697

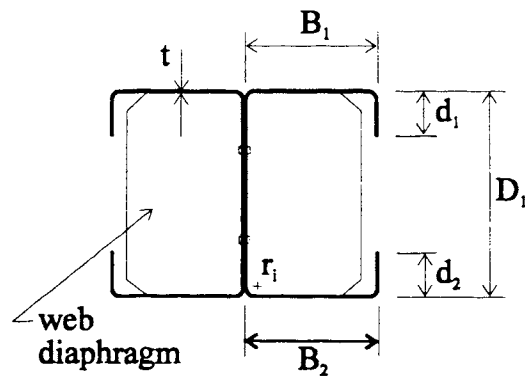
**Figure B.3 - Desmond [Des 78a] Test Specimen Cross Section**

Table B.7a - LaBoube [LaB 78] Test Specimen Dimensions

Specimen	d ₁ (mm)	B ₁ (mm)	D ₁ (mm)	B ₂ (mm)	d ₂ (mm)	d ₃ (mm)	B ₃ (mm)	D ₂ (mm)	B ₄ (mm)	d ₄ (mm)	t (mm)	r _i (mm)
B-1-1	15.4	51.3	125	50.9	15.4	15.4	50.8	124	51.4	15.4	1.27	1.27
B-1-2	15.4	51.1	126	50.8	15.4	15.4	50.9	125	51.1	15.4	1.26	1.26
B-2-1	15.4	50.5	157	50.2	15.4	15.4	50.2	157	50.5	15.4	1.27	1.27
B-2-2	15.2	50.1	158	49.9	15.8	15.2	50.4	158	50.2	15.8	1.26	1.26
B-3-1	15.5	50.0	186	51.0	15.4	15.5	50.9	186	50.9	15.4	1.26	1.26
B-3-2	15.6	51.3	186	50.9	15.5	15.6	50.9	187	51.2	15.5	1.24	1.24
B-10-1	14.2	37.7	103	37.8	15.3	14.2	37.5	102	37.8	15.3	1.29	1.29
B-10-2	15.1	37.6	102	37.5	15.1	15.1	38.2	102	38.0	15.1	1.23	1.23
B-11-1	15.4	37.6	151	38.1	15.0	15.4	38.2	151	37.7	15.0	1.27	1.27
B-11-2	15.4	38.0	151	38.2	15.3	15.4	38.4	150	38.2	15.3	1.28	1.28
B-12-1	15.4	37.8	187	37.9	15.3	15.4	38.2	189	38.4	15.3	1.28	1.28
B-12-2	15.3	37.5	188	38.1	15.2	15.3	37.8	187	38.2	15.2	1.32	1.32
B-13-1	15.4	45.0	102	45.4	15.3	15.4	45.6	102	45.4	15.3	1.24	1.24
B-13-2	14.7	44.8	103	45.5	15.5	14.7	45.4	103	45.0	15.5	1.30	1.30
B-14-1	15.4	64.9	151	64.6	15.4	15.4	64.7	150	64.9	15.4	1.24	1.24
B-14-2	15.4	64.4	150	64.4	15.6	15.4	64.5	150	65.1	15.6	1.29	1.29
B-15-1	15.6	79.3	188	80.3	15.2	15.6	79.8	185	79.7	15.2	1.26	1.26
B-15-2	15.3	80.0	188	80.2	15.2	15.3	79.8	188	79.6	15.2	1.24	1.24
B-16-1	15.2	64.0	101	64.0	15.5	15.2	63.9	101	64.1	15.5	1.30	1.30
B-16-2	15.0	63.7	101	63.9	15.3	15.0	63.6	101	63.9	15.3	1.31	1.31
B-17-1	13.9	77.1	150	77.3	14.0	13.9	77.4	149	76.2	14.0	1.28	1.28
B-17-2	14.9	83.9	149	77.2	15.0	14.9	77.3	151	77.2	15.0	1.28	1.28
B-18-1	15.4	89.2	185	89.7	15.4	15.4	89.2	187	89.2	15.4	1.30	1.30
B-18-2	15.5	89.2	185	89.2	14.6	15.5	89.1	184	89.2	14.6	1.30	1.30
B-3-3	16.6	49.8	174	49.0	15.7	16.6	48.6	172	49.7	15.7	1.17	1.17
B-3-4	16.4	49.0	175	49.4	14.4	16.4	49.0	175	49.0	14.4	1.17	1.17
B-9-1	16.3	88.3	180	87.1	17.7	16.3	88.4	180	87.6	17.7	1.17	1.17
B-9-2	17.2	88.3	179	88.4	16.6	17.2	88.2	178	87.9	16.6	1.17	1.17
B-C1-1	16.1	37.9	250	37.2	17.1	16.1	37.2	250	37.6	17.1	1.24	1.24
B-C1-2	16.4	37.9	248	37.0	16.6	16.4	37.0	249	37.5	16.6	1.18	1.18
B-C2-1	16.7	38.2	315	37.4	16.7	16.7	37.6	316	37.4	16.7	1.18	1.18
B-C2-2	16.2	37.8	315	37.8	16.0	16.2	37.0	315	37.8	16.0	1.17	1.17

Table B.7b - LaBoube [LaB 78] Test Specimen Dimensions

Specimen	d_1 (mm)	B_1 (mm)	D_1 (mm)	B_2 (mm)	d_2 (mm)	d_3 (mm)	B_3 (mm)	D_2 (mm)	B_4 (mm)	d_4 (mm)	t (mm)	r_1 (mm)
MB-10-1	15.2	37.8	102	37.6	15.3	15.2	37.2	103	37.9	15.3	1.26	1.26
MB-10-2	14.9	37.5	107	38.0	15.6	14.9	37.8	109	38.0	15.6	1.29	1.29
MB-11-1	15.2	38.2	151	38.2	16.2	15.2	37.5	151	38.3	16.2	1.28	1.28
MB-11-2	15.4	37.7	151	38.1	15.5	15.4	38.4	151	38.2	15.5	1.26	1.26
MB-12-1	15.3	38.2	186	38.2	15.4	15.3	38.2	186	37.4	15.4	1.31	1.31
MB-12-2	15.4	37.9	186	38.3	15.5	15.4	38.3	185	38.4	15.5	1.30	1.30
MB-16-1	15.2	63.6	101	63.8	15.5	15.2	63.6	101	64.1	15.5	1.30	1.30
MB-16-2	15.5	64.0	100	64.0	15.6	15.5	64.1	100	63.9	15.6	1.30	1.30
MB-17-1	15.4	77.3	149	77.0	15.2	15.4	76.9	149	77.4	15.2	1.30	1.30
MB-17-2	15.4	77.3	149	77.2	15.5	15.4	78.0	149	77.3	15.5	1.30	1.30
MB-18-1	15.2	89.2	187	88.8	15.4	15.2	89.2	186	89.3	15.4	1.29	1.29
MB-18-2	15.3	89.5	187	88.8	15.4	15.3	89.5	187	89.4	15.4	1.31	1.31
MB-3-1	17.1	48.5	174	49.9	15.0	17.1	49.6	174	48.5	15.0	1.17	1.17
MB-3-2	15.7	48.7	175	50.2	16.0	15.7	49.2	174	49.7	16.0	1.17	1.17
MB-9-1	14.9	87.4	172	88.4	15.1	14.9	88.1	173	87.6	15.1	1.18	1.18
MB-9-2	15.9	88.3	172	88.3	16.9	15.9	88.5	172	88.3	16.9	1.17	1.17
MB-C1-1	16.4	37.5	248	37.8	16.1	16.4	37.4	248	38.2	16.1	1.22	1.22
MB-C1-2	16.4	37.6	250	37.3	15.8	16.4	38.6	249	38.1	15.8	1.24	1.24
MB-C2-1	16.8	37.0	314	37.1	16.3	16.8	36.8	314	37.0	16.3	1.18	1.18
MB-C2-2	16.6	37.5	315	37.8	15.9	16.6	37.2	314	37.4	15.9	1.25	1.25

Table B.8a - LaBoube [LaB 78] Test Specimen Dimension Ratios

Specimen	h (mm)	h/t	w (mm)	w/t	d (mm)	d/t	d _f /w	w/h
B-1-1a	120	94.4	46.2	36.4	12.8	10.1	0.332	0.386
B-1-1b	119	94.0	45.7	36.0	12.8	10.1	0.336	0.383
B-1-2a	121	96.2	46.1	36.7	12.9	10.3	0.334	0.381
B-1-2b	120	95.8	45.9	36.5	12.9	10.3	0.336	0.381
B-2-1a	152	120	45.5	35.8	12.9	10.1	0.339	0.298
B-2-1b	152	120	45.1	35.5	12.9	10.1	0.341	0.296
B-2-2a	153	122	45.1	35.8	12.7	10.1	0.337	0.294
B-2-2b	153	122	45.4	36.1	12.7	10.1	0.335	0.296
B-3-1a	181	144	45.0	35.6	13.0	10.3	0.345	0.248
B-3-1b	181	144	45.9	36.3	13.0	10.3	0.338	0.253
B-3-2a	181	145	46.3	37.2	13.1	10.5	0.336	0.256
B-3-2b	182	146	45.9	36.9	13.1	10.5	0.339	0.253
B-10-1a	97.4	75.4	32.5	25.2	11.6	9.00	0.437	0.334
B-10-1b	96.4	74.6	32.3	25.0	11.6	9.00	0.440	0.335
B-10-2a	97.2	78.9	32.7	26.5	12.6	10.3	0.463	0.336
B-10-2b	97.2	78.9	33.2	27.0	12.6	10.3	0.455	0.342
B-11-1a	146	115	32.5	25.6	12.9	10.1	0.475	0.222
B-11-1b	146	115	33.1	26.0	12.9	10.1	0.466	0.226
B-11-2a	146	114	32.9	25.8	12.8	10.1	0.467	0.226
B-11-2b	145	114	33.3	26.1	12.8	10.1	0.462	0.230
B-12-1a	182	143	32.7	25.7	12.9	10.1	0.472	0.180
B-12-1b	184	144	33.1	25.9	12.9	10.1	0.467	0.180
B-12-2a	183	138	32.2	24.4	12.7	9.60	0.476	0.176
B-12-2b	182	138	32.6	24.7	12.7	9.60	0.470	0.179
B-13-1a	97.0	78.0	40.0	32.1	12.9	10.4	0.386	0.412
B-13-1b	97.0	77.9	40.6	32.6	12.9	10.4	0.380	0.419
B-13-2a	97.7	75.4	39.6	30.5	12.1	9.37	0.372	0.405
B-13-2b	97.7	75.4	40.3	31.1	12.1	9.37	0.366	0.412
B-14-1a	146	117	59.9	48.2	12.9	10.4	0.257	0.412
B-14-1b	145	117	59.8	48.0	12.9	10.4	0.258	0.411
B-14-2a	145	113	59.3	45.9	12.8	9.91	0.259	0.408
B-14-2b	145	113	59.4	46.0	12.8	9.91	0.259	0.409
B-15-1a	183	145	74.3	59.1	13.1	10.4	0.210	0.406
B-15-1b	180	143	74.7	59.4	13.1	10.4	0.209	0.414
B-15-2a	183	147	75.0	60.3	12.9	10.3	0.204	0.410
B-15-2b	183	147	74.8	60.1	12.9	10.3	0.205	0.409
B-16-1a	95.5	73.7	58.8	45.4	12.6	9.71	0.258	0.615
B-16-1b	96.0	74.1	58.7	45.3	12.6	9.71	0.258	0.611
B-16-2a	95.3	72.8	58.5	44.7	12.4	9.48	0.257	0.614
B-16-2b	95.8	73.2	58.4	44.6	12.4	9.48	0.257	0.609
B-17-1a	145	113	72.0	56.1	11.3	8.83	0.193	0.497
B-17-1b	145	113	72.3	56.4	11.3	8.83	0.192	0.500

Note: Dimension ratios are given for both C-sections (a, b) in each test specimen.

Table B.8b - LaBoube [LaB 78] Test Specimen Dimension Ratios

Specimen	h (mm)	h/t	w (mm)	w/t	d (mm)	d/t	d _t /w	w/h
B-17-2a	144	112	78.7	61.4	12.3	9.62	0.189	0.548
B-17-2b	146	114	72.2	56.3	12.3	9.62	0.206	0.495
B-18-1a	180	139	84.0	64.9	12.8	9.88	0.183	0.468
B-18-1b	182	140	84.0	64.9	12.8	9.88	0.183	0.462
B-18-2a	180	139	84.0	64.7	12.9	9.92	0.184	0.466
B-18-2b	179	138	83.9	64.6	12.9	9.92	0.184	0.468
B-3-3a	170	145	45.2	38.7	14.2	12.2	0.367	0.266
B-3-3b	167	143	43.9	37.6	14.2	12.2	0.378	0.263
B-3-4a	170	146	44.4	38.0	14.0	12.0	0.369	0.261
B-3-4b	170	145	44.3	37.9	14.0	12.0	0.370	0.261
B-9-1a	175	150	83.6	71.5	14.0	12.0	0.195	0.477
B-9-1b	175	150	83.7	71.7	14.0	12.0	0.195	0.477
B-9-2a	175	149	83.7	71.6	14.8	12.7	0.205	0.479
B-9-2b	173	148	83.6	71.5	14.8	12.7	0.205	0.482
B-C1-1a	245	197	33.0	26.5	13.6	11.0	0.489	0.135
B-C1-1b	245	197	32.2	25.9	13.6	11.0	0.501	0.132
B-C1-2a	243	206	33.2	28.1	14.1	11.9	0.495	0.136
B-C1-2b	244	207	32.3	27.3	14.1	11.9	0.509	0.132
B-C2-1a	310	262	33.5	28.3	14.3	12.1	0.498	0.108
B-C2-1b	311	263	32.9	27.8	14.3	12.1	0.507	0.106
B-C2-2a	310	265	33.1	28.3	13.9	11.9	0.490	0.107
B-C2-2b	310	266	32.3	27.7	13.9	11.9	0.502	0.104
MB-10-1a	97.3	77.3	32.8	26.0	12.7	10.1	0.464	0.337
MB-10-1b	97.6	77.5	32.2	25.5	12.7	10.1	0.473	0.330
MB-10-2a	102	78.9	32.4	25.1	12.3	9.56	0.461	0.318
MB-10-2b	104	80.4	32.6	25.3	12.3	9.56	0.457	0.314
MB-11-1a	146	114	33.1	25.8	12.6	9.84	0.459	0.226
MB-11-1b	146	114	32.4	25.2	12.6	9.84	0.469	0.222
MB-11-2a	146	116	32.7	26.0	12.9	10.2	0.471	0.224
MB-11-2b	146	116	33.4	26.5	12.9	10.2	0.462	0.229
MB-12-1a	181	138	33.0	25.2	12.6	9.67	0.463	0.182
MB-12-1b	181	139	32.9	25.2	12.6	9.67	0.463	0.182
MB-12-2a	181	140	32.7	25.3	12.8	9.88	0.470	0.181
MB-12-2b	180	139	33.1	25.6	12.8	9.88	0.465	0.184
MB-16-1a	95.8	73.9	58.4	45.1	12.6	9.73	0.260	0.610
MB-16-1b	95.4	73.6	58.4	45.1	12.6	9.73	0.260	0.613
MB-16-2a	95.1	73.5	58.9	45.4	13.0	10.0	0.264	0.619
MB-16-2b	94.8	73.2	58.9	45.5	13.0	10.0	0.264	0.621
MB-17-1a	144	111	72.2	55.7	12.8	9.90	0.214	0.501
MB-17-1b	144	111	71.8	55.4	12.8	9.90	0.215	0.498
MB-17-2a	144	111	72.1	55.6	12.8	9.86	0.213	0.500
MB-17-2b	144	111	72.8	56.2	12.8	9.86	0.211	0.505

Note: Dimension ratios are given for both C-sections (a, b) in each test specimen.

Table B.8c - LaBoube [LaB 78] Test Specimen Dimension Ratios

Specimen	h (mm)	h/t	w (mm)	w/t	d (mm)	d/t	d _f /w	w/h
MB-18-1a	182	141	84.0	65.1	12.6	9.75	0.180	0.462
MB-18-1b	181	140	84.0	65.1	12.6	9.75	0.180	0.463
MB-18-2a	182	139	84.3	64.4	12.6	9.67	0.181	0.464
MB-18-2b	182	139	84.2	64.4	12.6	9.67	0.181	0.462
MB-3-1a	169	145	43.8	37.5	14.8	12.6	0.390	0.259
MB-3-1b	169	145	45.0	38.5	14.8	12.6	0.380	0.266
MB-3-2a	170	146	44.1	37.7	13.4	11.5	0.357	0.259
MB-3-2b	169	145	44.5	38.1	13.4	11.5	0.354	0.263
MB-9-1a	167	142	82.7	70.0	12.5	10.6	0.180	0.494
MB-9-1b	168	142	83.4	70.6	12.5	10.6	0.178	0.497
MB-9-2a	167	143	83.6	71.6	13.5	11.6	0.190	0.501
MB-9-2b	167	143	83.8	71.8	13.5	11.6	0.189	0.502
MB-C1-1a	243	200	32.6	26.8	13.9	11.5	0.502	0.134
MB-C1-1b	243	200	32.6	26.8	13.9	11.5	0.503	0.134
MB-C1-2a	245	197	32.6	26.3	13.9	11.2	0.503	0.133
MB-C1-2b	244	196	33.7	27.1	13.9	11.2	0.487	0.138
MB-C2-1a	310	262	32.3	27.3	14.5	12.2	0.521	0.104
MB-C2-1b	310	262	32.0	27.1	14.5	12.2	0.525	0.103
MB-C2-2a	310	249	32.5	26.1	14.1	11.3	0.509	0.105
MB-C2-2b	309	248	32.2	25.9	14.1	11.3	0.514	0.104

Note: Dimension ratios are given for both C-sections (a, b) in each test specimen.

Table B.9 - LaBoube [LaB 78] Test Specimen Material Properties

Series	t (mm)	F _y (MPa)	F _u (MPa)	Series	t (mm)	F _y (MPa)	F _u (MPa)
B-1-1	1.27	325	432	B-15-1	1.26	371	504
B-1-2	1.26	325	432	B-15-2	1.24	371	504
B-2-1	1.27	325	432	B-16-1	1.30	371	504
B-2-2	1.26	325	432	B-16-2	1.31	371	504
B-3-1	1.26	325	432	B-17-1	1.28	371	504
B-3-2	1.24	325	432	B-17-2	1.28	371	504
B-10-1	1.29	371	504	B-18-1	1.30	371	504
B-10-2	1.23	371	504	B-18-2	1.30	371	504
B-11-1	1.27	371	504	B-3-3	1.17	231	344
B-11-2	1.28	371	504	B-3-4	1.17	231	344
B-12-1	1.28	371	504	B-9-1	1.17	231	344
B-12-2	1.32	371	504	B-9-2	1.17	231	344
B-13-1	1.24	371	504	B-C1-1	1.24	302	384
B-13-2	1.30	371	504	B-C1-2	1.18	302	384
B-14-1	1.24	371	504	B-C2-1	1.18	302	384
B-14-2	1.29	371	504	B-C2-2	1.17	302	384

Table B.10 - LaBoube [LaB 78] Test Specimen Material Properties and Bottom Plate Dimensions

Series	t-bpl (mm)	w-bpl (mm)	t (mm)	F _y (MPa)	F _u (MPa)
MB-10-1	1.27	105	1.26	371	504
MB-10-2	1.27	105	1.29	371	504
MB-11-1	1.27	131	1.28	371	504
MB-11-2	1.27	131	1.26	371	504
MB-12-1	1.28	159	1.31	371	504
MB-12-2	1.30	162	1.30	371	504
MB-16-1	1.27	88.8	1.30	371	504
MB-16-2	1.27	88.6	1.30	371	504
MB-17-1	1.27	89.0	1.30	371	504
MB-17-2	1.27	89.0	1.30	371	504
MB-18-1	1.27	89.0	1.29	371	504
MB-18-2	1.27	89.0	1.31	371	504
MB-3-1	1.30	176	1.17	231	344
MB-3-2	1.30	176	1.17	231	344
MB-9-1	1.31	126	1.18	231	344
MB-9-2	1.31	126	1.17	231	344
MB-C1-1	1.24	155	1.22	302	384
MB-C1-2	1.24	155	1.24	302	384
MB-C2-1	1.24	204	1.18	302	384
MB-C2-2	1.24	204	1.25	302	384

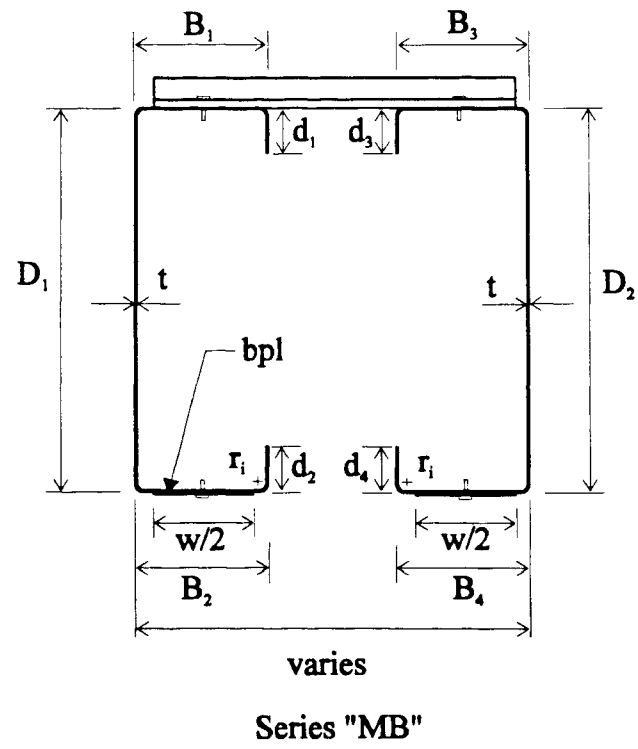
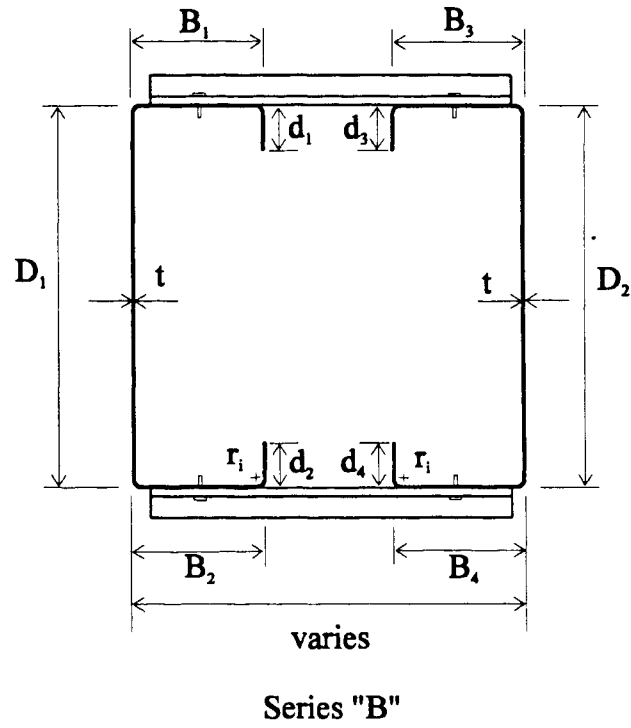


Figure B.4 - LaBoube [LaB 78] Test Specimen Cross Sections

Table B.11 - Moreyra [Mor 93] Test Specimen Information

Specimen	d_1 (mm)	B_1 (mm)	D_1 (mm)	B_2 (mm)	d_2 (mm)	t (mm)	r_i (mm)	F_y (MPa)
A-W	28.5	61.3	217	63.0	24.9	1.80	4.76	397
A-T	28.5	62.2	217	62.8	24.7	1.80	4.76	392
A-TB	28.7	62.5	219	63.4	24.9	1.80	4.76	438
B-W	24.9	62.8	217	62.2	28.4	1.80	4.76	396
B-T	24.9	63.0	217	62.1	28.5	1.80	4.76	405
B-TB	24.1	63.2	219	62.6	28.9	1.80	4.76	425
C-W	22.3	62.2	217	63.0	24.3	1.75	4.76	413
C-T	22.0	62.1	217	63.1	24.4	1.85	4.76	399
C-TB	22.3	62.8	219	63.5	25.0	1.80	4.76	432

Table B.12 - Moreyra [Mor 93] Test Specimen Dimension Ratios

Specimen	h (mm)	h/t	w (mm)	w/t	d (mm)	d/t	d_1/w	w/h
A-W	204	113	48.2	26.7	21.9	12.2	0.591	0.236
A-T	204	113	49.1	27.2	22.0	12.2	0.581	0.241
A-TB	206	114	49.4	27.4	22.1	12.3	0.581	0.240
B-W	204	113	49.7	27.5	18.4	10.2	0.502	0.244
B-T	204	113	49.8	27.6	18.4	10.2	0.501	0.244
B-TB	206	114	50.1	27.8	17.6	9.74	0.482	0.243
C-W	204	117	49.2	28.1	15.8	9.02	0.454	0.241
C-T	204	110	48.9	26.4	15.4	8.31	0.451	0.240
C-TB	206	114	49.7	27.5	15.7	8.73	0.449	0.241

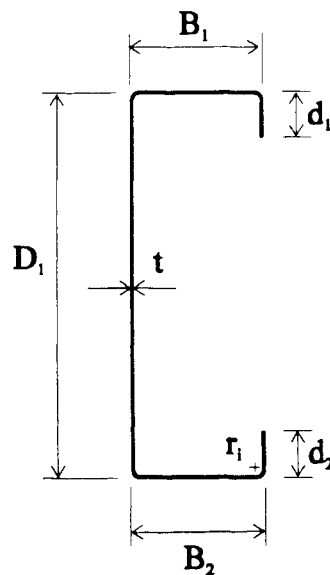
**Figure B.5 - Moreyra [Mor 93] Test Specimen Cross Section**

Table B.13 - Schardt & Schrade [Scha 82] Test Specimen Information

Specimen	d_1 (mm)	B_1 (mm)	D_1 (mm)	B_2 (mm)	d_2 (mm)	t (mm)	r_1 (mm)	F_y (MPa)	F_u (MPa)
1.1.b	15.1	69.8	180	70.2	15.0	0.997	0.997	361	398
1.2.a	15.1	64.6	182	64.7	15.0	0.993	0.993	325	374
1.2.b	15.2	64.7	181	64.6	14.8	0.990	0.990	372	405
1.3.a	15.1	60.3	181	60.5	15.3	1.00	1.00	360	379
1.3.b	15.1	59.7	181	59.9	15.2	0.993	0.993	338	384
1.4.a	14.9	49.5	182	49.4	14.9	0.987	0.987	371	400
1.4.b	15.0	49.4	182	49.4	15.2	0.987	0.987	339	385
1.5.a	15.3	45.3	182	45.5	15.2	1.00	1.00	369	401
1.5.b	15.3	45.4	183	45.4	14.8	1.01	1.01	322	382
2.1.a	14.7	64.6	181	64.1	14.8	0.990	1.49	329	391
2.1.b	14.9	64.2	181	64.3	14.7	0.990	1.49	374	409
2.2.a	14.9	49.4	181	49.3	14.8	0.990	1.49	322	383
2.2.b	15.0	49.7	180	49.9	14.9	0.990	1.49	363	406
3.1.a	10.4	69.4	181	69.2	10.1	0.990	0.990	227	342
3.1.b	10.6	71.0	180	70.7	10.7	1.01	1.01	224	341
3.2.a	10.0	60.5	181	60.4	10.4	1.01	1.01	337	388
3.2.b	10.3	60.5	180	60.0	10.4	1.00	1.00	360	411
3.3.a	10.2	50.7	181	50.7	10.3	1.01	1.01	334	385
3.3.b	10.3	50.7	180	50.6	10.7	1.01	1.01	357	405
4.1.a	10.5	70.8	181	71.1	10.3	1.02	1.53	259	339
4.1.b	11.3	70.9	180	71.6	10.0	1.02	1.53	257	339
4.2.a	10.8	61.6	180	61.6	10.8	1.03	1.54	257	341
4.2.b	10.2	60.7	181	61.4	10.2	1.02	1.53	262	339
4.3.a	10.7	50.6	180	50.6	8.0	1.01	1.52	271	340
4.3.b	10.2	50.7	180	50.8	10.6	1.01	1.52	266	344

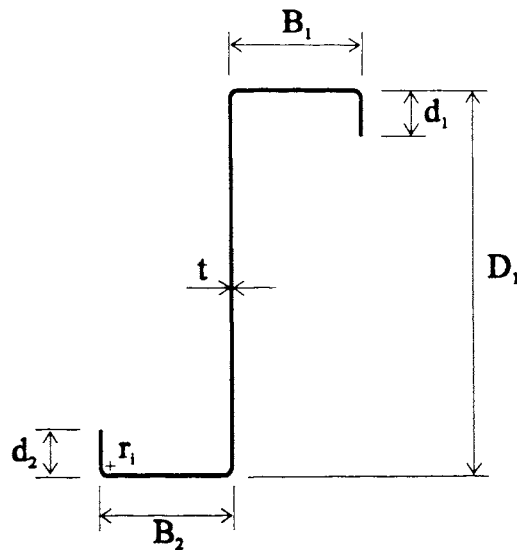
**Figure B.6 - Schardt & Schrade [Scha 82] Test Specimen Cross Section**

Table B.14 - Schardt & Schrade [Scha 82] Test Specimen Dimension Ratios

Specimen	h (mm)	h/t	w (mm)	w/t	d (mm)	d/t	d _r /w	w/h
1.1.b	176	177	65.8	66.1	13.2	13.2	0.230	0.374
1.2.a	178	179	60.7	61.1	13.2	13.2	0.250	0.341
1.2.b	177	179	60.7	61.3	13.3	13.4	0.251	0.343
1.3.a	177	177	56.3	56.1	13.1	13.1	0.268	0.318
1.3.b	177	178	55.8	56.1	13.1	13.2	0.270	0.315
1.4.a	178	180	45.5	46.1	12.9	13.1	0.327	0.256
1.4.b	178	180	45.5	46.1	13.1	13.2	0.331	0.256
1.5.a	178	177	41.3	41.2	13.3	13.3	0.371	0.233
1.5.b	179	178	41.4	41.1	13.3	13.2	0.371	0.231
2.1.a	176	177	59.6	60.2	12.2	12.4	0.247	0.339
2.1.b	176	178	59.3	59.9	12.5	12.6	0.252	0.337
2.2.a	176	177	44.5	44.9	12.5	12.6	0.336	0.253
2.2.b	175	177	44.8	45.2	12.6	12.7	0.336	0.256
3.1.a	177	178	65.4	66.1	8.41	8.50	0.159	0.371
3.1.b	176	174	67.0	66.6	8.56	8.50	0.158	0.382
3.2.a	177	176	56.5	56.1	8.02	7.97	0.178	0.319
3.2.b	176	175	56.5	56.3	8.26	8.23	0.182	0.321
3.3.a	176	175	46.6	46.2	8.21	8.13	0.219	0.264
3.3.b	175	174	46.6	46.2	8.28	8.20	0.221	0.266
4.1.a	175	173	65.7	64.6	7.98	7.85	0.160	0.375
4.1.b	175	172	65.8	64.5	8.72	8.55	0.171	0.376
4.2.a	174	170	56.4	55.0	8.26	8.05	0.192	0.324
4.2.b	176	173	55.7	54.7	7.70	7.57	0.184	0.317
4.3.a	175	173	45.6	45.1	8.13	8.05	0.234	0.261
4.3.b	175	172	45.6	45.0	7.63	7.52	0.223	0.261

Table B.15 - Schuster [Schu 92] Test Specimen Dimensions

Specimen	d_1 (mm)	B_1 (mm)	D_1 (mm)	B_2 (mm)	d_2 (mm)	d_3 (mm)	B_3 (mm)	D_2 (mm)	B_4 (mm)	d_4 (mm)	t (mm)	r_i (mm)
BS1	12.0	41.0	203	41.0	12.0	12.0	41.0	203	41.0	12.0	1.21	2.42
BS2	12.0	41.0	203	41.0	12.0	12.0	41.0	203	41.0	12.0	1.21	2.42
CS1	13.0	40.0	203	40.0	13.0	13.0	40.0	203	40.0	13.0	1.22	2.44
CS2	13.0	40.0	204	40.0	13.0	13.0	40.0	203	40.0	13.0	1.22	2.44
CS3	13.0	41.0	204	40.0	13.0	13.0	40.0	203	40.0	13.0	1.22	2.44

Table B.16 - Schuster [Schu 92] Test Specimen Dimension Ratios

Specimen	h (mm)	h/t	w (mm)	w/t	d (mm)	d/t	d_i/w	w/h
BS1-A	196	162	33.7	27.9	8.37	6.92	0.356	0.172
BS1-B	196	162	33.7	27.9	8.37	6.92	0.356	0.172
BS2-A	196	162	33.7	27.9	8.37	6.92	0.356	0.172
BS2-B	196	162	33.7	27.9	8.37	6.92	0.356	0.172
CS1-A	196	160	32.7	26.8	9.34	7.66	0.398	0.167
CS1-B	196	160	32.7	26.8	9.34	7.66	0.398	0.167
CS2-A	197	161	32.7	26.8	9.34	7.66	0.398	0.166
CS2-B	196	160	32.7	26.8	9.34	7.66	0.398	0.167
CS3-A	197	161	33.7	27.6	9.34	7.66	0.386	0.171
CS3-B	196	160	32.7	26.8	9.34	7.66	0.398	0.167

Note: Dimension ratios are given for both C-sections (A, B) in each test Specimen.

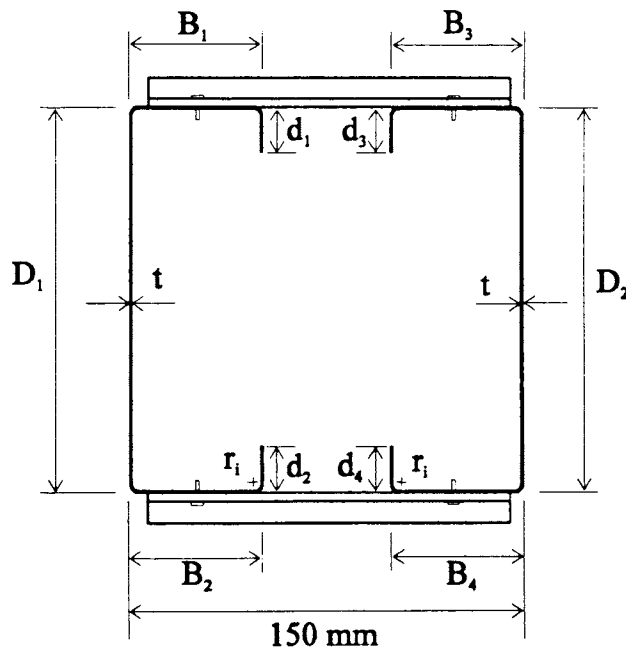
**Figure B.7 - Schuster [Schu 92] Test Specimen Cross Section**

Table B.17 - Schuster [Schu 92] Test Specimen Material Properties

Series	t (mm)	F _y (MPa)	F _u (MPa)	% Elong.
BS	1.21	271	360	31.3
CS	1.22	331	359	35.8

Note: Material properties are based on an average of three coupon tests per series.
Percent elongation is based on a 50mm gauge length.

Table B.18 - Shan [Shan 94] Test Specimen Dimensions

Specimen	d ₁ (mm)	B ₁ (mm)	D ₁ (mm)	B ₂ (mm)	d ₂ (mm)	d ₃ (mm)	B ₃ (mm)	D ₂ (mm)	B ₄ (mm)	d ₄ (mm)	t (mm)	r _i (mm)
3B,18,1&2(N)	13.2	42.2	93.0	41.1	11.9	11.9	40.9	93.5	42.2	13.2	1.12	2.38
3B,18,3&4(N)	12.4	42.2	92.5	41.9	12.7	12.4	41.7	92.5	41.4	12.2	1.12	2.38
3B,20,1&2(N)	11.9	41.4	91.4	41.4	11.7	11.9	41.1	91.4	41.4	11.7	0.89	2.38
3B,20,3&4(N)	12.2	41.4	91.4	41.4	11.7	11.7	41.4	91.4	41.4	11.9	0.89	2.38
3B,20,5&6(N)	11.9	41.4	91.2	41.1	11.9	11.9	41.1	91.4	41.1	11.7	0.89	2.38
2B,16,1&2(N)	11.4	41.1	63.0	40.9	13.0	11.4	41.4	63.0	40.9	13.0	1.45	2.38
2B,16,3&4(N)	13.0	40.9	63.0	41.4	11.9	11.7	41.4	63.0	40.9	13.0	1.45	2.38
2B,20,1&2(N)	10.4	41.4	62.0	41.4	12.4	10.2	41.7	62.0	41.1	12.7	0.84	2.38
2B,20,3&4(N)	9.90	41.4	62.5	40.9	13.2	10.2	41.4	62.2	40.9	13.0	0.84	2.38
8A,14,1&2(N)	11.9	35.1	205	35.1	10.4	11.9	35.1	205	35.1	10.7	1.85	2.38
8A,14,3&4(N)	12.2	35.1	205	35.1	9.9	10.2	35.1	205	35.1	12.4	1.85	2.38
8A,14,5&6(N)	11.9	34.8	205	35.1	10.2	11.7	35.1	205	35.1	10.7	1.85	2.38
8A,14,7&8(N)	12.7	35.3	204	35.6	10.7	10.9	35.6	204	35.3	13.0	1.68	2.38
8A,14,9&10(N)	11.2	35.6	204	35.3	12.2	12.2	35.3	204	35.3	11.2	1.68	2.38
8B,14,1&2(N)	16.0	41.4	204	41.4	16.5	16.8	41.7	204	41.4	16.3	1.73	2.38
8B,14,3&4(N)	16.0	41.4	204	41.4	16.5	16.5	41.4	204	41.4	16.0	1.73	2.38
8B,14,5&6(N)	15.7	41.1	204	41.4	16.5	16.5	41.4	204	41.4	15.7	1.63	2.38
8B,14,7&8(N)	17.0	41.4	204	41.1	15.0	15.0	41.4	204	41.4	17.0	1.63	2.38
8D,14,1&2(N)	15.2	63.5	202	63.5	12.4	13.0	63.5	202	63.5	15.0	1.63	2.38
8D,14,3&4(N)	15.0	63.2	202	63.5	12.7	12.7	63.5	202	63.5	15.2	1.63	2.38
8A,20,1&2(N)	10.2	35.1	201	34.8	11.7	11.4	35.1	201	35.1	10.4	0.79	2.38
8A,20,3&4(N)	11.7	34.8	202	35.1	9.90	10.7	35.1	201	34.5	11.2	0.79	2.38
8B,20,1&2(N)	15.7	41.4	202	41.7	15.7	15.7	41.9	203	41.7	15.5	0.79	2.38
8B,20,3&4(N)	15.7	41.4	202	41.4	15.7	15.7	41.7	202	41.4	15.7	0.79	2.38
8B,20,5&6(N)	15.5	41.4	202	41.4	15.5	15.5	41.4	202	41.4	15.5	0.79	2.38
8D,20,1&2(N)	16.3	63.2	202	62.2	14.7	15.2	62.2	202	63.5	16.5	1.09	2.38
8D,20,3&4(N)	16.5	63.2	202	62.5	14.7	14.7	62.2	202	63.2	16.5	1.09	2.38
12B,16,1&2(N)	13.0	41.4	304	41.4	13.7	14.0	41.4	303	41.4	12.2	1.57	2.38
12B,16,3&4(N)	11.7	41.7	304	41.4	14.2	14.0	41.4	304	41.4	12.4	1.57	2.38

Table B.19a - Shan [Shan 94] Test Specimen Dimension Ratios

Specimen	h (mm)	h/t	w (mm)	w/t	d (mm)	d/t	d _f /w	w/h
3B,18,1&2(N)_A	86.0	76.9	35.2	31.5	9.71	8.69	0.376	0.409
3B,18,1&2(N)_B	86.5	77.4	33.9	30.3	8.44	7.55	0.352	0.392
3B,18,3&4(N)_A	85.5	76.5	35.2	31.5	8.95	8.01	0.354	0.412
3B,18,3&4(N)_B	85.5	76.5	34.7	31.0	8.95	8.01	0.359	0.406
3B,20,1&2(N)_A	84.9	95.5	34.9	39.2	8.67	9.75	0.342	0.411
3B,20,1&2(N)_B	84.9	95.5	34.6	38.9	8.67	9.75	0.345	0.408
3B,20,3&4(N)_A	84.9	95.5	34.9	39.2	8.92	10.0	0.350	0.411
3B,20,3&4(N)_B	84.9	95.5	34.9	39.2	8.41	9.46	0.335	0.411
3B,20,5&6(N)_A	84.6	95.2	34.9	39.2	8.67	9.75	0.342	0.412
3B,20,5&6(N)_B	84.9	95.5	34.6	38.9	8.67	9.75	0.345	0.408
2B,16,1&2(N)_A	55.3	38.2	33.5	23.1	7.60	5.25	0.341	0.605
2B,16,1&2(N)_B	55.3	38.2	33.7	23.3	7.60	5.25	0.339	0.610
2B,16,3&4(N)_A	55.3	38.2	33.2	23.0	9.12	6.30	0.390	0.601
2B,16,3&4(N)_B	55.3	38.2	33.7	23.3	7.85	5.43	0.346	0.610
2B,20,1&2(N)_A	55.5	66.3	35.0	41.7	7.19	8.58	0.298	0.630
2B,20,1&2(N)_B	55.5	66.3	35.2	42.0	6.94	8.28	0.288	0.634
2B,20,3&4(N)_A	56.0	66.9	35.0	41.7	6.69	7.98	0.283	0.624
2B,20,3&4(N)_B	55.8	66.6	35.0	41.7	6.94	8.28	0.291	0.627
8A,14,1&2(N)_A	197	106	26.6	14.3	7.70	4.15	0.449	0.135
8A,14,1&2(N)_B	197	106	26.6	14.3	7.70	4.15	0.449	0.135
8A,14,3&4(N)_A	197	106	26.6	14.3	7.96	4.29	0.459	0.135
8A,14,3&4(N)_B	197	106	26.6	14.3	5.92	3.20	0.382	0.135
8A,14,5&6(N)_A	197	106	26.3	14.2	7.70	4.15	0.453	0.134
8A,14,5&6(N)_B	197	106	26.6	14.3	7.45	4.02	0.440	0.135
8A,14,7&8(N)_A	196	117	27.2	16.2	8.64	5.16	0.467	0.139
8A,14,7&8(N)_B	196	117	27.4	16.4	6.86	4.09	0.398	0.140
8A,14,9&10(N)_A	196	117	27.4	16.4	7.12	4.25	0.407	0.140
8A,14,9&10(N)_B	196	117	27.2	16.2	8.13	4.85	0.448	0.138
8B,14,1&2(N)_A	196	114	33.2	19.2	11.9	6.89	0.482	0.169
8B,14,1&2(N)_B	196	114	33.4	19.4	12.7	7.33	0.501	0.170
8B,14,3&4(N)_A	196	114	33.2	19.2	11.9	6.89	0.482	0.169
8B,14,3&4(N)_B	196	114	33.2	19.2	12.4	7.18	0.498	0.169
8B,14,5&6(N)_A	196	121	33.1	20.4	11.7	7.22	0.475	0.169
8B,14,5&6(N)_B	196	121	33.4	20.5	12.5	7.69	0.494	0.170
8B,14,7&8(N)_A	196	121	33.4	20.5	13.0	8.00	0.510	0.170
8B,14,7&8(N)_B	196	121	33.4	20.5	11.0	6.75	0.449	0.170
8D,14,1&2(N)_A	194	119	55.5	34.1	11.2	6.91	0.275	0.286
8D,14,1&2(N)_B	194	120	55.5	34.1	8.95	5.50	0.233	0.285
8D,14,3&4(N)_A	194	120	55.2	34.0	11.0	6.75	0.271	0.284
8D,14,3&4(N)_B	194	120	55.5	34.1	8.69	5.35	0.229	0.285

Note: Dimension ratios are given for both C-sections (A, B) in each test Specimen.

Table B.19b - Shan [Shan 94] Test Specimen Dimension Ratios

Specimen	h (mm)	h/t	w (mm)	w/t	d (mm)	d/t	d _i /w	w/h
8A,20,1&2(N)_A	195	248	28.7	36.5	6.99	8.88	0.354	0.147
8A,20,1&2(N)_B	195	248	28.7	36.5	8.26	10.5	0.398	0.147
8A,20,3&4(N)_A	195	248	28.5	36.1	8.52	10.8	0.411	0.146
8A,20,3&4(N)_B	195	248	28.7	36.5	7.50	9.52	0.372	0.147
8B,20,1&2(N)_A	196	248	35.1	44.5	12.6	16.0	0.449	0.179
8B,20,1&2(N)_B	196	249	35.6	45.2	12.6	16.0	0.443	0.181
8B,20,3&4(N)_A	196	248	35.1	44.5	12.6	16.0	0.449	0.179
8B,20,3&4(N)_B	196	249	35.3	44.9	12.6	16.0	0.446	0.180
8B,20,5&6(N)_A	196	248	35.1	44.5	12.3	15.7	0.442	0.179
8B,20,5&6(N)_B	196	248	35.1	44.5	12.3	15.7	0.442	0.179
8D,20,1&2(N)_A	195	178	56.3	51.5	12.8	11.7	0.289	0.289
8D,20,1&2(N)_B	195	179	55.3	50.6	11.8	10.8	0.276	0.284
8D,20,3&4(N)_A	195	179	56.3	51.5	13.0	11.9	0.293	0.289
8D,20,3&4(N)_B	195	179	55.3	50.6	11.3	10.3	0.266	0.284
12B,16,1&2(N)_A	296	188	33.5	21.3	9.00	5.71	0.387	0.113
12B,16,1&2(N)_B	295	188	33.5	21.3	10.0	6.36	0.417	0.113
12B,16,3&4(N)_A	296	188	33.7	21.4	7.73	4.91	0.346	0.114
12B,16,3&4(N)_B	296	188	33.5	21.3	10.0	6.36	0.417	0.113

Note: Dimension ratios are given for both C-sections (A, B) in each test Specimen.

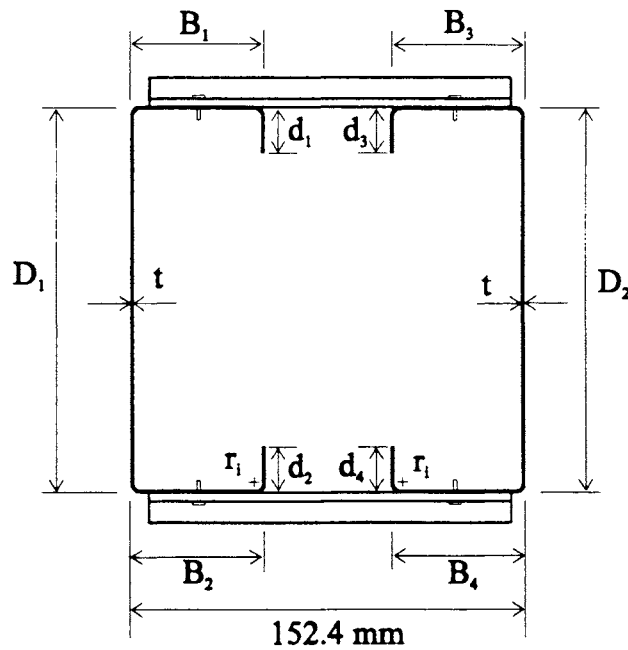
**Figure B.8 - Shan [Shan 94] Test Specimen Cross Section**

Table B.20 - Shan [Shan 94] Test Specimen Material Properties

Series	t (mm)	F _y (MPa)	F _u (MPa)	Series	t (mm)	F _y (MPa)	F _u (MPa)
3,18,1&2(N)	1.12	434	558	8B,14,3&4(N)	1.73	252	378
3,18,3&4(N)	1.12	434	558	8B,14,5&6(N)	1.63	368	559
3,20,1&2(N)	0.89	421	565	8B,14,7&8(N)	1.63	368	559
3,20,3&4(N)	0.89	421	565	8D,14,1&2(N)	1.63	347	529
3,20,5&6(N)	0.89	421	565	8D,14,3&4(N)	1.63	347	529
2,16,1&2(N)	1.45	400	538	8A,20,1&2(N)	0.79	274	496
2,16,3&4(N)	1.45	400	538	8A,20,3&4(N)	0.79	274	496
2,20,1&2(N)	0.84	448	517	8B,20,1&2(N)	0.79	296	545
2,20,3&4(N)	0.84	448	517	8B,20,3&4(N)	0.79	296	545
8A,14,1&2(N)	1.85	205	391	8B,20,5&6(N)	0.79	296	545
8A,14,3&4(N)	1.85	205	391	8D,20,1&2(N)	1.09	266	447
8A,14,5&6(N)	1.85	205	391	8D,20,3&4(N)	1.09	266	447
8A,14,7&8(N)	1.68	384	560	12B,16,1&2(N)	1.57	425	512
8A,14,9&10(N)	1.68	384	560	12B,16,3&4(N)	1.57	425	512
8B,14,1&2(N)	1.73	252	378				

Table B.21 - Willis & Wallace [Wil 90a] Test Specimen Information

Specimen	d ₁ (mm)	B ₁ (mm)	D ₁ (mm)	B ₂ (mm)	d ₂ (mm)	t (mm)	r _i (mm)	F _y (MPa)
1C2	27.0	58.8	203	58.8	27.0	1.55	3.10	372
1C3	24.6	58.8	203	58.8	27.8	1.55	3.10	372
1C4	21.4	58.8	203	58.8	27.8	1.55	3.10	372
1C5	22.2	63.5	203	63.5	23.8	1.60	3.20	414

Table B.22 - Willis & Wallace [Wil 90a] Test Specimen Dimension Ratios

Specimen	h (mm)	h/t	w (mm)	w/t	d (mm)	d/t	d _i /w	w/h
1C2	194	125	49.5	31.9	22.4	14.4	0.546	0.255
1C3	194	125	49.5	31.9	20.0	12.9	0.498	0.255
1C4	194	125	49.5	31.9	16.8	10.8	0.433	0.255
1C5	192	120	53.9	33.7	17.4	10.9	0.412	0.281

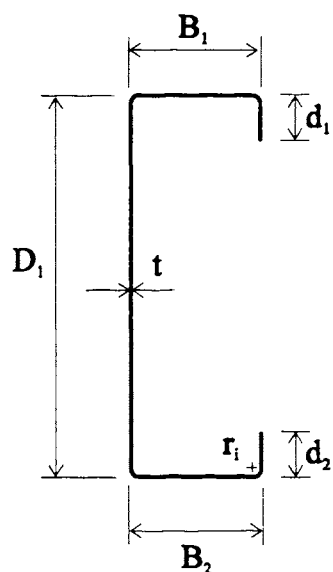


Figure B.9 - Willis & Wallace [Wil 90a] Test Specimen Cross Section

Table B.23 - Winter [Win 47] Test Specimen Information

Specimen	d_1 (mm)	B_1 (mm)	D_1 (mm)	B_2 (mm)	d_2 (mm)	t (mm)	r_i (mm)	bpl (mm)	F_y (MPa)
B1	20.4	76.7	203	76.7	23.7	1.64	1.71	-	257
B2	20.1	75.7	155	76.1	23.4	1.55	1.49	-	209
B3	21.8	102	203	102	24.8	1.69	2.08	-	257
B4	19.1	101	201	100	27.1	3.74	4.03	-	228
B5	14.3	50.2	101	49.9	16.6	1.52	1.58	-	208
B6	19.8	101	202	102	25.0	2.82	2.60	-	250
B7	18.9	64.9	101	64.6	22.9	1.53	1.59	-	208
B8	20.1	76.6	150	76.2	24.9	2.75	2.56	-	242
B9	20.0	75.9	202	76.5	24.3	2.77	2.50	-	250
B10	19.1	63.1	100	63.1	24.3	2.72	2.75	-	242
C1	18.3	83.8	203	101	29.1	1.56	1.62	25.3	261
C2	15.4	64.8	201	81.5	25.1	1.17	1.07	26.4	222
C3	24.7	128	204	152	28.3	1.57	1.58	24.7	261
C4	15.0	101	202	127	27.4	1.14	0.31	30.9	222
C5	15.7	57.2	202	77.5	27.7	1.52	1.52	28.7	261

Table B.24 - Winter [Win 47] Test Specimen Dimension Ratios

Specimen	h (mm)	h/t	w (mm)	w/t	d (mm)	d/t	d ₁ /w	w/h
B1	196	119	70.0	42.6	17.1	10.4	0.292	0.357
B2	149	96.2	69.6	45.0	17.0	11.0	0.288	0.468
B3	195	116	94.4	56.0	18.0	10.7	0.231	0.483
B4	185	49.6	85.6	22.9	11.3	3.03	0.223	0.462
B5	94.6	62.2	44.0	28.9	11.2	7.35	0.325	0.465
B6	191	67.8	90.1	32.0	14.4	5.12	0.220	0.472
B7	94.9	61.9	58.7	38.3	15.8	10.3	0.322	0.618
B8	140	50.8	66.0	24.0	14.8	5.39	0.305	0.472
B9	191	69.0	65.4	23.6	14.8	5.33	0.306	0.342
B10	89.1	32.8	52.2	19.2	13.6	5.00	0.365	0.585
C1	197	126	77.4	49.5	15.2	9.69	0.237	0.393
C2	197	168	60.3	51.6	13.2	11.3	0.256	0.307
C3	198	126	122	77.7	21.5	13.7	0.202	0.615
C4	200	176	98.3	86.6	13.5	11.9	0.152	0.493
C5	196	129	51.1	33.5	12.7	8.33	0.308	0.261

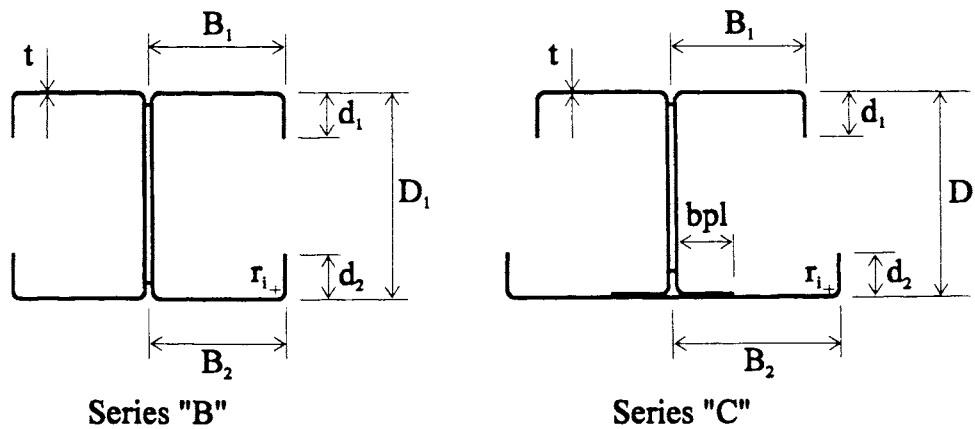
**Figure B.10 - Winter [Win 47] Test Specimen Cross Sections**

Table B.25a - k Values for Edge Stiffener Stress Gradient Methods

Specimen	$k_{1,2,3}$	k_4	k_5	Specimen	$k_{1,2,3}$	k_4	k_5
E-45.6B-1	0.430	0.489	0.566	2G,16,3&4(N)_A	0.430	0.561	0.649
E-45.6B-2	0.430	0.515	0.595	2G,16,3&4(N)_B	0.430	0.534	0.618
E-45.6B-3	0.430	0.623	0.722				
E-45.6B-4	0.430	0.726	0.842	B2	0.430	0.509	0.589
				B4	0.430	0.466	0.540
B-10-1a	0.430	0.517	0.599	B5	0.430	0.516	0.597
B-10-1b	0.430	0.518	0.600	B6	0.430	0.475	0.550
				B7	0.430	0.564	0.652
2G,16,1&2(N)_A	0.430	0.529	0.612	B8	0.430	0.504	0.584
2G,16,1&2(N)_B	0.430	0.529	0.612	B9	0.430	0.480	0.556
				B10	0.430	0.549	0.635

Note: 1) S136 uniform compressive stress at the top of the flat width (Current).
 2) S136 uniform compressive stress at the mid-point of the flat width.
 3) S136 uniform compressive stress at the third point of the flat width.
 4) Cohen/Eurocode stress gradient.
 5) ISO stress gradient.

Table B.25b - M_T/M_P Ratios - Edge Stiffener Stress Gradient Methods

Specimen	S136 ₁			S136 ₂		S136 ₃	
	M_T (kN·m)	M_P (kN·m)	M_T/M_P	M_P (kN·m)	M_T/M_P	M_P (kN·m)	M_T/M_P
E-45.6B-1	21.5	17.2	1.25	17.2	1.25	17.2	1.25
E-45.6B-2	21.5	18.3	1.17	18.3	1.17	18.3	1.17
E-45.6B-3	21.6	20.3	1.07	20.4	1.06	20.3	1.06
E-45.6B-4	21.2	19.3	1.10	19.5	1.09	19.5	1.09
B-10-1	6.26	5.89	1.06	5.89	1.06	5.89	1.06
2B,16,1&2(N)	3.82	3.50	1.09	3.50	1.09	3.50	1.09
2B,16,3&4(N)	3.90	3.61	1.08	3.61	1.08	3.61	1.08
B2	10.8	10.4	1.04	10.4	1.04	10.4	1.04
B4	49.4	44.4	1.11	44.4	1.11	44.4	1.11
B5	4.84	4.54	1.06	4.54	1.06	4.54	1.06
B6	38.3	34.7	1.10	34.7	1.10	34.7	1.10
B7	5.59	5.58	1.00	5.58	1.00	5.58	1.00
B8	22.7	21.1	1.08	21.1	1.08	21.1	1.08
B9	34.5	32.2	1.07	32.2	1.07	32.2	1.07
B10	12.1	10.6	1.14	10.6	1.14	10.6	1.14
Mean			1.10		1.09		1.09
Std. Dev.			0.059		0.059		0.059
Coeff. of Var.			0.058		0.058		0.058

Table B.25c - M_T/M_P Ratios - Edge Stiffener Stress Gradient Methods

Specimen	S136 ₄			S136 ₅	
	M_T (kN·m)	M_P (kN·m)	M_T/M_P	M_P (kN·m)	M_T/M_P
E-45.6B-1	21.5	17.2	1.25	17.2	1.25
E-45.6B-2	21.5	18.3	1.17	18.3	1.17
E-45.6B-3	21.6	20.5	1.05	20.6	1.05
E-45.6B-4	21.2	19.7	1.08	19.8	1.07
B-10-1	6.26	5.89	1.06	5.89	1.06
2B,16,1&2(N)	3.82	3.50	1.09	3.50	1.09
2B,16,3&4(N)	3.90	3.61	1.08	3.61	1.08
B2	10.8	10.4	1.04	10.4	1.04
B4	49.4	44.4	1.11	44.4	1.11
B5	4.84	4.54	1.06	4.54	1.06
B6	38.3	34.7	1.10	34.7	1.10
B7	5.59	5.58	1.00	5.58	1.00
B8	22.7	21.1	1.08	21.1	1.08
B9	34.5	32.2	1.07	32.2	1.07
B10	12.1	10.6	1.14	10.6	1.14
Mean			1.09		1.09
Std. Dev.			0.059		0.060
Coeff. of Var.			0.059		0.059

- Note: 1) S136 uniform compressive stress at the top of the flat width (Current).
 2) S136 uniform compressive stress at the mid-point of the flat width.
 3) S136 uniform compressive stress at the third point of the flat width.
 4) Cohen/Eurocode stress gradient.
 5) ISO stress gradient.

Table B.26 - Charnvarnichborikarn [Cha 92] M_T/M_P Ratios - Local Buckling Methods

Specimen	S136			AISI		Dinovitzer		Sooi	
	M_T (kN·m)	M_P (kN·m)	M_T/M_P	M_P (kN·m)	M_T/M_P	M_P (kN·m)	M_T/M_P	M_P (kN·m)	M_T/M_P
2.7-0.00-1a	5.88	5.18	1.14	5.58	1.05	5.18	1.14	5.50	1.07
2.7-0.00-2a	6.08	5.28	1.15	5.71	1.06	5.28	1.15	5.63	1.08
2.7-0.00-1b	6.19	6.49	0.95	7.10	0.87	6.49	0.95	6.75	0.92
2.7-0.00-2b	6.08	6.55	0.93	7.13	0.85	6.55	0.93	6.76	0.90
2.7-0.15-1	6.11	6.47	0.94	7.06	0.87	6.47	0.94	6.67	0.92
2.7-0.15-2	6.00	6.62	0.91	7.26	0.83	6.62	0.91	6.85	0.88
2.7-0.25-1	6.11	7.09	0.86	7.75	0.79	7.09	0.86	7.27	0.84
2.7-0.25-2	6.51	7.08	0.92	7.76	0.84	7.08	0.92	7.30	0.89
2.7-0.50-1	6.58	8.26	0.80	9.08	0.72	8.26	0.80	8.42	0.78
2.7-0.50-2	6.64	8.40	0.79	9.25	0.72	8.40	0.79	8.56	0.78
2.7-0.75-1	7.02	9.60	0.73	10.49	0.67	9.60	0.73	9.72	0.72
2.7-0.75-2	6.62	9.49	0.70	10.40	0.64	9.49	0.70	9.61	0.69
2.7-1.00-1	7.13	9.69	0.74	10.62	0.67	9.69	0.74	9.81	0.73
2.7-1.00-2	6.82	9.39	0.73	10.30	0.66	9.39	0.73	9.48	0.72
2.7-1.25-1	6.94	9.52	0.73	10.41	0.67	9.52	0.73	9.66	0.72
2.7-1.25-2	7.29	9.26	0.79	10.08	0.72	9.26	0.79	9.36	0.78
2.7-1.50-1	7.05	9.04	0.78	9.77	0.72	9.04	0.78	9.17	0.77
2.7-1.50-2	7.21	9.20	0.78	9.98	0.72	9.20	0.78	9.36	0.77
2.7-2.00-1	6.90	8.22	0.84	8.78	0.79	8.22	0.84	8.42	0.82
2.7-2.00-2	7.13	8.40	0.85	9.00	0.79	8.40	0.85	8.62	0.83

Table B.27a - Charnvarnichborikarn [Cha 92] M_T/M_P Ratios - Flange/Web Distortional Buckling Methods

Specimen	Lau & Hancock			Lau & Hancock		Lau & Hancock		Marsh	
	M_T (kN·m)	M_P (kN·m)	M_T/M_P	M_P (kN·m)	M_T/M_P	M_P (kN·m)	M_T/M_P	M_P (kN·m)	M_T/M_P
2.7-0.00-1a	5.88	-	-	-	-	-	-	-	-
2.7-0.00-2a	6.08	-	-	-	-	-	-	-	-
2.7-0.00-1b	6.19	3.99	1.55	4.82	1.28	3.50	1.77	3.08	2.01
2.7-0.00-2b	6.08	4.21	1.44	4.90	1.24	3.69	1.65	3.30	1.84
2.7-0.15-1	6.11	4.18	1.46	4.83	1.26	3.67	1.67	3.27	1.87
2.7-0.15-2	6.00	4.39	1.37	4.95	1.21	3.85	1.56	3.43	1.75
2.7-0.25-1	6.11	5.50	1.11	5.50	1.11	4.77	1.28	4.51	1.36
2.7-0.25-2	6.51	5.22	1.25	5.39	1.21	4.56	1.43	4.20	1.55
2.7-0.50-1	6.58	7.49	0.88	7.49	0.88	6.48	1.02	7.09	0.93
2.7-0.50-2	6.64	7.66	0.87	7.66	0.87	6.65	1.00	7.35	0.90
2.7-0.75-1	7.02	8.57	0.82	8.57	0.82	7.56	0.93	8.70	0.81
2.7-0.75-2	6.62	8.51	0.78	8.51	0.78	7.50	0.88	8.61	0.77
2.7-1.00-1	7.13	8.94	0.80	8.94	0.80	8.01	0.89	8.68	0.82
2.7-1.00-2	6.82	8.64	0.79	8.64	0.79	7.73	0.88	8.35	0.82
2.7-1.25-1	6.94	9.08	0.76	9.08	0.76	8.15	0.85	9.09	0.76
2.7-1.25-2	7.29	8.82	0.83	8.82	0.83	7.92	0.92	8.83	0.83
2.7-1.50-1	7.05	8.84	0.80	8.84	0.80	7.91	0.89	9.15	0.77
2.7-1.50-2	7.21	9.04	0.80	9.04	0.80	8.10	0.89	9.39	0.77
2.7-2.00-1	6.90	8.33	0.83	8.33	0.83	7.35	0.94	9.28	0.74
2.7-2.00-2	7.13	8.54	0.83	8.54	0.83	7.54	0.95	9.53	0.75

Table B.27b - Charnvarnichborikarn [Cha 92] M_T/M_P Ratios - Flange/Web Distortional Buckling Methods

Specimen	Moreyra 1			Moreyra 2	
	M_T (kN·m)	M_P (kN·m)	M_T/M_P	M_P (kN·m)	M_T/M_P
2.7-0.00-1a	5.88	-	-	-	-
2.7-0.00-2a	6.08	-	-	-	-
2.7-0.00-1b	6.19	6.01	1.03	6.24	0.99
2.7-0.00-2b	6.08	6.03	1.01	6.27	0.97
2.7-0.15-1	6.11	5.95	1.03	6.19	0.99
2.7-0.15-2	6.00	6.12	0.98	6.36	0.94
2.7-0.25-1	6.11	6.48	0.94	6.79	0.90
2.7-0.25-2	6.51	6.53	1.00	6.83	0.95
2.7-0.50-1	6.58	7.50	0.88	7.87	0.84
2.7-0.50-2	6.64	7.60	0.87	7.98	0.83
2.7-0.75-1	7.02	8.26	0.85	8.57	0.82
2.7-0.75-2	6.62	8.18	0.81	8.50	0.78
2.7-1.00-1	7.13	8.53	0.84	8.60	0.83
2.7-1.00-2	6.82	8.20	0.83	8.26	0.83
2.7-1.25-1	6.94	8.71	0.80	8.71	0.80
2.7-1.25-2	7.29	8.40	0.87	8.40	0.87
2.7-1.50-1	7.05	8.42	0.84	8.42	0.84
2.7-1.50-2	7.21	8.63	0.84	8.63	0.84
2.7-2.00-1	6.90	8.37	0.82	8.37	0.82
2.7-2.00-2	7.13	8.62	0.83	8.62	0.83

Table B.28 - Cohen [Coh 87] M_T/M_P Ratios - Local Buckling Methods

Specimen	S136			AISI		Dinovitzer		Sooi	
	M_T (kN·m)	M_P (kN·m)	M_T/M_P	M_P (kN·m)	M_T/M_P	M_P (kN·m)	M_T/M_P	M_P (kN·m)	M_T/M_P
It1-rmin-d90-1L1	27.8	22.4	1.24	23.0	1.21	22.4	1.24	23.8	1.17
It1-rmin-3/2d90-1L1	29.5	26.8	1.10	27.7	1.06	26.8	1.10	27.7	1.06
It1-rmin-3/2d90-2L1	35.6	26.8	1.33	27.7	1.28	26.8	1.33	27.7	1.28
It1-rmin-3/2d90-3L1	32.7	26.8	1.22	27.7	1.18	26.8	1.22	27.7	1.18
It2-rmin-d90-1L1	70.5	55.7	1.27	59.9	1.18	57.5	1.23	57.8	1.22
It2-rmin-d90-2L1	73.3	55.7	1.32	59.9	1.22	57.5	1.28	57.8	1.27
It2-rmin-3/2d90-1L1	78.6	66.3	1.19	68.1	1.16	66.3	1.19	67.8	1.16
It2-rmin-3/2d90-2L1	78.5	66.3	1.18	68.1	1.15	66.3	1.18	67.8	1.16
IIt1-rmin-d90-1L0	27.4	22.4	1.22	23.0	1.19	22.4	1.22	23.8	1.15
IIt1-rmin-d90-1L1	26.4	22.4	1.18	23.0	1.15	22.4	1.18	23.8	1.11
IIt1-rmin-d90-2L1	25.8	22.4	1.15	23.0	1.12	22.4	1.15	23.8	1.08
IIt1-rmin-3/2d90-1L1	29.5	26.8	1.10	27.7	1.06	26.8	1.10	27.7	1.06
IIt2-rmin-d90-1L1	66.2	55.7	1.19	59.9	1.10	57.5	1.15	57.8	1.14
IIt2-rmin-3/2d90-1L1	73.2	66.3	1.10	68.1	1.08	66.3	1.10	67.8	1.08

Table B.29a - Cohen [Coh 87] M_T/M_P Ratios - Flange/Web Distortional Buckling Methods

Specimen	Lau & Hancock 1			Lau & Hancock 2		Lau & Hancock 3		Marsh	
	M_T (kN·m)	M_P (kN·m)	M_T/M_P	M_P (kN·m)	M_T/M_P	M_P (kN·m)	M_T/M_P	M_P (kN·m)	M_T/M_P
It1-rmin-d90-1L1	27.8	20.4	1.36	20.4	1.36	17.6	1.58	18.7	1.48
It1-rmin-3/2d90-1L1	29.5	24.2	1.22	24.2	1.22	21.2	1.39	20.9	1.41
It1-rmin-3/2d90-2L1	35.6	24.2	1.47	24.2	1.47	21.2	1.68	20.9	1.71
It1-rmin-3/2d90-3L1	32.7	24.2	1.35	24.2	1.35	21.2	1.54	20.9	1.57
It2-rmin-d90-1L1	70.5	55.1	1.28	55.1	1.28	49.3	1.43	54.3	1.30
It2-rmin-d90-2L1	73.3	55.1	1.33	55.1	1.33	49.3	1.49	54.3	1.35
It2-rmin-3/2d90-1L1	78.6	59.2	1.33	59.2	1.33	53.8	1.46	60.2	1.31
It2-rmin-3/2d90-2L1	78.5	59.2	1.33	59.2	1.33	53.8	1.46	60.2	1.30
IIt1-rmin-d90-1L0	27.4	20.4	1.34	20.4	1.34	17.6	1.56	18.7	1.46
IIt1-rmin-d90-1L1	26.4	20.4	1.30	20.4	1.30	17.6	1.50	18.7	1.41
IIt1-rmin-d90-2L1	25.8	20.4	1.26	20.4	1.26	17.6	1.46	18.7	1.38
IIt1-rmin-3/2d90-1L1	29.5	24.2	1.22	24.2	1.22	21.2	1.39	20.9	1.41
IIt2-rmin-d90-1L1	66.2	55.1	1.20	55.1	1.20	49.3	1.34	54.3	1.22
IIt2-rmin-3/2d90-1L1	73.2	59.2	1.24	59.2	1.24	53.8	1.36	60.2	1.22

Table B.29b - Cohen [Coh 87] M_T/M_P Ratios - Flange/Web Distortional Buckling Methods

Specimen	Moreyra 1			Moreyra 2	
	M_T (kN·m)	M_P (kN·m)	M_T/M_P	M_P (kN·m)	M_T/M_P
It1-rmin-d90-1L1	27.8	20.9	1.33	22.1	1.26
It1-rmin-3/2d90-1L1	29.5	22.9	1.29	23.2	1.27
It1-rmin-3/2d90-2L1	35.6	22.9	1.55	23.2	1.53
It1-rmin-3/2d90-3L1	32.7	22.9	1.42	23.2	1.41
It2-rmin-d90-1L1	70.5	62.9	1.12	65.8	1.07
It2-rmin-d90-2L1	73.3	62.9	1.17	65.8	1.12
It2-rmin-3/2d90-1L1	78.6	67.9	1.16	70.7	1.11
It2-rmin-3/2d90-2L1	78.5	67.9	1.16	70.7	1.11
IIt1-rmin-d90-1L0	27.4	20.9	1.31	22.1	1.24
IIt1-rmin-d90-1L1	26.4	20.9	1.26	22.1	1.20
IIt1-rmin-d90-2L1	25.8	20.9	1.23	22.1	1.17
IIt1-rmin-3/2d90-1L1	29.5	22.9	1.29	23.2	1.27
IIt2-rmin-d90-1L1	66.2	62.9	1.05	65.8	1.01
IIt2-rmin-3/2d90-1L1	73.2	67.9	1.08	70.7	1.04

Table B.30 - Desmond [Des 78a] M_T/M_P Ratios - Local Buckling Methods

Specimen	S136			AISI		Dinovitzer		Sooi	
	M_T (kN·m)	M_P (kN·m)	M_T/M_P	M_P (kN·m)	M_T/M_P	M_P (kN·m)	M_T/M_P	M_P (kN·m)	M_T/M_P
E-45.6B-1	21.5	17.2	1.25	17.3	1.24	17.2	1.25	17.3	1.24
E-45.6B-2	21.5	18.3	1.17	18.4	1.17	18.3	1.17	18.4	1.17
E-45.6B-3	21.6	20.3	1.07	20.3	1.07	20.3	1.07	20.3	1.07
E-45.6B-4	21.2	19.3	1.10	19.3	1.10	19.3	1.10	19.3	1.10

Table B.31a - Desmond [Des 78a] M_T/M_P Ratios - Flange/Web Distortional Buckling Methods

Specimen	Lau & Hancock 1			Lau & Hancock 2		Lau & Hancock 3		Marsh	
	M_T (kN·m)	M_P (kN·m)	M_T/M_P	M_P (kN·m)	M_T/M_P	M_P (kN·m)	M_T/M_P	M_P (kN·m)	M_T/M_P
E-45.6B-1	21.5	15.8	1.36	15.8	1.36	13.5	1.59	14.0	1.54
E-45.6B-2	21.5	17.2	1.25	17.2	1.25	14.8	1.45	16.0	1.34
E-45.6B-3	21.6	19.0	1.14	19.0	1.14	16.8	1.28	17.6	1.23
E-45.6B-4	21.2	19.0	1.12	19.0	1.12	17.0	1.25	18.2	1.17

Table B.31b - Desmond [Des 78a] M_T/M_P Ratios - Flange/Web Distortional Buckling Methods

Specimen	Moreyra 1			Moreyra 2	
	M_T (kN·m)	M_P (kN·m)	M_T/M_P	M_P (kN·m)	M_T/M_P
E-45.6B-1	21.5	17.2	1.25	18.3	1.17
E-45.6B-2	21.5	18.0	1.19	18.8	1.14
E-45.6B-3	21.6	18.8	1.15	18.8	1.15
E-45.6B-4	21.2	18.4	1.15	18.4	1.15

Table B.32a - LaBoube [LaB 78] M_T/M_P Ratios - Local Buckling Methods

Specimen	S136			AISI		Dinovitzer		Sooi	
	M_T (kN·m)	M_P (kN·m)	M_T/M_P	M_P (kN·m)	M_T/M_P	M_P (kN·m)	M_T/M_P	M_P (kN·m)	M_T/M_P
B-1-1	8.25	7.09	1.16	7.31	1.13	7.09	1.16	7.26	1.14
B-1-2	8.33	7.09	1.18	7.32	1.14	7.09	1.18	7.26	1.15
B-2-1	10.8	9.23	1.17	10.0	1.08	9.23	1.17	9.44	1.14
B-2-2	10.7	9.12	1.17	9.94	1.07	9.12	1.17	9.31	1.14
B-3-1	12.9	11.1	1.17	12.3	1.05	11.1	1.17	10.9	1.19
B-3-2	13.3	11.0	1.22	12.1	1.10	11.0	1.22	10.7	1.25
B-10-1	6.26	5.89	1.06	5.89	1.06	5.89	1.06	5.89	1.06
B-10-2	6.15	5.62	1.09	5.64	1.09	5.62	1.09	5.65	1.09
B-11-1	10.2	9.33	1.09	10.0	1.01	9.33	1.09	9.48	1.07
B-11-2	9.73	9.34	1.04	10.1	0.97	9.34	1.04	9.51	1.02
B-12-1	12.7	12.0	1.06	13.4	0.95	12.0	1.06	11.4	1.12
B-12-2	12.4	12.4	1.00	14.1	0.88	12.4	1.00	12.0	1.03
B-13-1	6.50	5.86	1.11	5.90	1.10	5.86	1.11	5.91	1.10
B-13-2	6.92	6.06	1.14	6.09	1.14	6.06	1.14	6.09	1.14
B-14-1	11.4	9.68	1.17	10.6	1.07	9.68	1.17	9.91	1.15
B-14-2	11.4	10.1	1.12	11.2	1.02	10.1	1.12	10.4	1.09
B-15-1	13.9	12.6	1.10	13.2	1.05	12.6	1.10	12.3	1.13
B-15-2	14.7	12.4	1.19	13.0	1.13	12.4	1.19	12.1	1.22
B-16-1	7.46	6.45	1.16	6.52	1.14	6.45	1.16	6.52	1.14
B-16-2	7.12	6.48	1.10	6.54	1.09	6.48	1.10	6.54	1.09
B-17-1	10.8	9.67	1.12	10.5	1.04	9.67	1.12	10.0	1.08
B-17-2	11.1	9.97	1.11	10.8	1.03	9.97	1.11	10.3	1.07
B-18-1	14.4	13.0	1.11	13.6	1.06	13.0	1.11	13.0	1.11
B-18-2	13.9	13.0	1.07	13.6	1.02	13.0	1.07	13.0	1.07
B-3-3	7.78	7.41	1.05	7.98	0.98	7.41	1.05	7.54	1.03
B-3-4	7.80	7.48	1.04	8.06	0.97	7.48	1.04	7.60	1.03
B-9-1	8.01	8.47	0.95	9.16	0.87	8.47	0.95	8.65	0.93
B-9-2	8.50	8.66	0.98	9.40	0.90	8.66	0.98	8.85	0.96
B-C1-1	12.7	13.4	0.95	14.4	0.89	13.4	0.95	11.0	1.16
B-C1-2	12.9	12.4	1.04	13.2	0.98	12.4	1.04	9.86	1.31
B-C2-1	14.4	16.1	0.89	16.7	0.86	16.1	0.89	10.7	1.34
B-C2-2	15.5	15.7	0.99	16.2	0.95	15.7	0.99	10.5	1.48

Table B.32b - LaBoube [LaB 78] M_T/M_P Ratios - Local Buckling Methods

Specimen	S136			AISI		Dinovitzer		Sooi	
	M_T (kN·m)	M_P (kN·m)	M_T/M_P	M_P (kN·m)	M_T/M_P	M_P (kN·m)	M_T/M_P	M_P (kN·m)	M_T/M_P
MB-10-1	7.43	6.24	1.19	6.48	1.15	6.24	1.19	6.44	1.15
MB-10-2	7.24	6.81	1.06	7.11	1.02	6.81	1.06	7.05	1.03
MB-11-1	11.2	10.0	1.12	10.5	1.07	10.0	1.12	10.5	1.06
MB-11-2	11.9	9.73	1.22	10.2	1.17	9.73	1.22	10.2	1.16
MB-12-1	13.9	13.0	1.07	13.4	1.04	13.0	1.07	13.3	1.04
MB-12-2	13.8	12.8	1.08	13.2	1.05	12.8	1.08	13.2	1.05
MB-16-1	7.08	6.68	1.06	6.91	1.03	6.68	1.06	6.88	1.03
MB-16-2	7.58	6.70	1.13	6.92	1.10	6.70	1.13	6.90	1.10
MB-17-1	12.1	10.5	1.16	10.9	1.11	10.5	1.16	11.1	1.09
MB-17-2	11.2	10.4	1.07	10.9	1.03	10.4	1.07	11.1	1.01
MB-18-1	14.5	13.1	1.11	13.4	1.08	13.1	1.11	13.5	1.07
MB-18-2	13.2	13.4	0.98	13.8	0.96	13.4	0.98	13.9	0.95
MB-3-1	7.88	7.92	0.99	8.20	0.96	7.92	0.99	8.39	0.94
MB-3-2	7.88	7.90	1.00	8.17	0.96	7.90	1.00	8.38	0.94
MB-9-1	8.44	7.98	1.06	8.24	1.02	7.98	1.06	8.51	0.99
MB-9-2	8.57	8.11	1.06	8.36	1.02	8.11	1.06	8.61	1.00
MB-C1-1	13.8	13.5	1.02	13.8	1.00	13.5	1.02	12.6	1.09
MB-C1-2	14.3	14.1	1.01	14.4	0.99	14.1	1.01	13.2	1.08
MB-C2-1	16.1	16.6	0.97	16.8	0.96	16.6	0.97	14.2	1.14
MB-C2-2	16.2	18.1	0.90	18.3	0.89	18.1	0.90	15.5	1.04

Table B.33a - LaBoube [LaB 78] M_T/M_P Ratios - Flange/Web Distortional Buckling Methods

Specimen	Lau & Hancock 1			Lau & Hancock 2		Lau & Hancock 3		Marsh	
	M_T (kN·m)	M_P (kN·m)	M_T/M_P	M_P (kN·m)	M_T/M_P	M_P (kN·m)	M_T/M_P	M_P (kN·m)	M_T/M_P
B-1-1	8.25	6.51	1.27	6.51	1.27	5.83	1.41	6.46	1.28
B-1-2	8.33	6.49	1.28	6.49	1.28	5.82	1.43	6.45	1.29
B-2-1	10.8	8.49	1.27	8.49	1.27	7.63	1.42	8.31	1.30
B-2-2	10.7	8.39	1.27	8.39	1.27	7.53	1.41	8.23	1.30
B-3-1	12.9	9.92	1.30	9.92	1.30	8.97	1.44	9.99	1.30
B-3-2	13.3	9.73	1.37	9.73	1.37	8.78	1.52	9.80	1.36
B-10-1	6.26	5.05	1.24	5.05	1.24	4.63	1.35	5.10	1.23
B-10-2	6.15	4.82	1.27	4.82	1.27	4.41	1.39	4.90	1.25
B-11-1	10.2	8.10	1.25	8.10	1.25	7.42	1.37	8.19	1.24
B-11-2	9.73	8.11	1.20	8.11	1.20	7.42	1.31	8.19	1.19
B-12-1	12.7	9.91	1.29	9.91	1.29	9.17	1.39	10.6	1.20
B-12-2	12.4	10.5	1.19	10.5	1.19	9.69	1.28	11.1	1.12
B-13-1	6.50	5.27	1.23	5.27	1.23	4.76	1.37	5.29	1.23
B-13-2	6.92	5.54	1.25	5.54	1.25	5.01	1.38	5.53	1.25
B-14-1	11.4	8.84	1.29	8.84	1.29	7.63	1.49	8.47	1.34
B-14-2	11.4	9.35	1.22	9.35	1.22	8.09	1.41	8.98	1.27
B-15-1	13.9	10.3	1.35	10.3	1.35	8.98	1.55	9.22	1.51
B-15-2	14.7	9.94	1.48	10.0	1.47	8.72	1.69	8.87	1.66
B-16-1	7.46	6.06	1.23	6.06	1.23	5.28	1.41	5.79	1.29
B-16-2	7.12	6.10	1.17	6.10	1.17	5.32	1.34	5.83	1.22
B-17-1	10.8	8.27	1.31	8.27	1.31	7.09	1.53	7.07	1.53
B-17-2	11.1	8.32	1.33	8.32	1.33	7.14	1.55	7.20	1.54
B-18-1	14.4	9.89	1.46	10.7	1.34	8.71	1.66	8.48	1.70
B-18-2	13.9	9.94	1.40	10.7	1.29	8.75	1.59	8.49	1.63
B-3-3	7.78	6.63	1.17	6.63	1.17	6.10	1.28	6.59	1.18
B-3-4	7.80	6.67	1.17	6.67	1.17	6.14	1.27	6.61	1.18
B-9-1	8.01	7.69	1.04	7.69	1.04	6.61	1.21	7.06	1.13
B-9-2	8.50	7.84	1.08	7.84	1.08	6.75	1.26	6.39	1.33
B-C1-1	12.7	9.96	1.28	9.96	1.28	9.43	1.35	11.9	1.07
B-C1-2	12.9	8.95	1.44	8.95	1.44	8.45	1.52	10.9	1.18
B-C2-1	14.4	9.44	1.52	9.44	1.52	8.96	1.60	13.8	1.04
B-C2-2	15.5	9.08	1.70	9.08	1.70	8.62	1.79	13.3	1.16

Table B.33b - LaBoube [LaB 78] M_T/M_P Ratios - Flange/Web Distortional Buckling Methods

Specimen	Lau & Hancock			Lau & Hancock		Lau & Hancock		Marsh	
	M_T	M_P	M_T/M_P	M_P	M_T/M_P	M_P	M_T/M_P	M_P	M_T/M_P
	(kN·m)	(kN·m)		(kN·m)		(kN·m)		(kN·m)	
MB-10-1	7.43	5.53	1.34	5.53	1.34	5.08	1.46	5.49	1.35
MB-10-2	7.24	6.05	1.20	6.05	1.20	5.56	1.30	5.98	1.21
MB-11-1	11.2	9.00	1.24	9.00	1.24	8.26	1.35	8.94	1.25
MB-11-2	11.9	8.77	1.36	8.77	1.36	8.04	1.48	8.73	1.36
MB-12-1	13.9	11.4	1.21	11.4	1.21	10.5	1.32	11.4	1.22
MB-12-2	13.8	11.3	1.23	11.3	1.23	10.4	1.33	11.2	1.23
MB-16-1	7.08	6.42	1.10	6.42	1.10	5.60	1.27	6.14	1.15
MB-16-2	7.58	6.44	1.18	6.44	1.18	5.61	1.35	6.17	1.23
MB-17-1	12.1	9.51	1.27	9.51	1.27	8.16	1.48	8.57	1.41
MB-17-2	11.2	9.47	1.18	9.47	1.18	8.12	1.38	8.49	1.32
MB-18-1	14.5	10.1	1.44	11.1	1.31	8.91	1.63	8.70	1.67
MB-18-2	13.2	10.4	1.26	11.3	1.16	9.22	1.43	9.00	1.47
MB-3-1	7.88	7.41	1.06	7.41	1.06	6.84	1.15	7.28	1.08
MB-3-2	7.88	7.32	1.08	7.32	1.08	6.74	1.17	7.13	1.10
MB-9-1	8.44	7.55	1.12	7.55	1.12	6.49	1.30	6.81	1.24
MB-9-2	8.57	7.65	1.12	7.65	1.12	6.58	1.30	7.02	1.22
MB-C1-1	13.8	11.1	1.24	11.1	1.24	10.4	1.33	12.0	1.16
MB-C1-2	14.3	11.6	1.23	11.6	1.23	10.8	1.32	12.4	1.15
MB-C2-1	16.1	12.4	1.30	12.4	1.30	11.6	1.39	14.5	1.11
MB-C2-2	16.2	13.7	1.19	13.7	1.19	12.8	1.27	15.7	1.03

Table B.33c - LaBoube [LaB 78] M_T/M_P Ratios - Flange/Web Distortional Buckling Methods

Specimen	Moreyra 1			Moreyra 2	
	M_T (kN·m)	M_P (kN·m)	M_T/M_P	M_P (kN·m)	M_T/M_P
B-1-1	8.25	6.87	1.20	7.19	1.15
B-1-2	8.33	6.81	1.22	7.12	1.17
B-2-1	10.8	8.46	1.28	8.83	1.22
B-2-2	10.7	8.31	1.28	8.68	1.23
B-3-1	12.9	9.42	1.37	9.84	1.32
B-3-2	13.3	9.17	1.45	9.58	1.39
B-10-1	6.26	5.74	1.09	5.89	1.06
B-10-2	6.15	5.51	1.12	5.68	1.08
B-11-1	10.2	8.75	1.16	9.05	1.12
B-11-2	9.73	8.78	1.11	9.10	1.07
B-12-1	12.7	9.94	1.28	10.3	1.24
B-12-2	12.4	10.7	1.16	11.0	1.13
B-13-1	6.50	6.00	1.08	6.27	1.04
B-13-2	6.92	6.28	1.10	6.57	1.05
B-14-1	11.4	8.71	1.31	9.15	1.24
B-14-2	11.4	9.32	1.22	9.83	1.16
B-15-1	13.9	10.5	1.32	11.1	1.25
B-15-2	14.7	10.3	1.43	10.8	1.35
B-16-1	7.46	6.22	1.20	6.46	1.15
B-16-2	7.12	6.30	1.13	6.56	1.08
B-17-1	10.8	8.82	1.23	9.36	1.16
B-17-2	11.1	8.94	1.24	9.38	1.18
B-18-1	14.4	11.0	1.31	11.6	1.24
B-18-2	13.9	11.0	1.26	11.6	1.19
B-3-3	7.78	6.09	1.28	6.18	1.26
B-3-4	7.80	6.12	1.27	6.21	1.25
B-9-1	8.01	6.44	1.24	6.57	1.22
B-9-2	8.50	6.49	1.31	6.55	1.30
B-C1-1	12.7	9.27	1.38	9.30	1.37
B-C1-2	12.9	8.23	1.57	8.26	1.56
B-C2-1	14.4	8.41	1.71	8.42	1.71
B-C2-2	15.5	8.07	1.92	8.09	1.91

Table B.33d - LaBoube [LaB 78] M_T/M_P Ratios - Flange/Web Distortional Buckling Methods

Specimen	Moreyra 1			Moreyra 2	
	M_T (kN·m)	M_P (kN·m)	M_T/M_P	M_P (kN·m)	M_T/M_P
MB-10-1	7.43	6.29	1.18	6.44	1.15
MB-10-2	7.24	6.87	1.05	7.05	1.03
MB-11-1	11.2	9.77	1.14	10.1	1.11
MB-11-2	11.9	9.42	1.26	9.74	1.22
MB-12-1	13.9	11.7	1.19	12.0	1.15
MB-12-2	13.8	11.5	1.20	11.8	1.17
MB-16-1	7.08	6.60	1.07	6.85	1.03
MB-16-2	7.58	6.30	1.20	6.81	1.11
MB-17-1	12.1	9.65	1.25	10.1	1.20
MB-17-2	11.2	9.63	1.16	10.1	1.11
MB-18-1	14.5	11.4	1.28	12.0	1.21
MB-18-2	13.2	11.7	1.13	12.4	1.07
MB-3-1	7.88	6.83	1.15	6.91	1.14
MB-3-2	7.88	6.74	1.17	6.86	1.15
MB-9-1	8.44	6.50	1.30	6.74	1.25
MB-9-2	8.57	6.46	1.33	6.60	1.30
MB-C1-1	13.8	10.2	1.36	10.2	1.36
MB-C1-2	14.3	10.6	1.34	10.7	1.34
MB-C2-1	16.1	10.6	1.52	10.6	1.52
MB-C2-2	16.2	11.8	1.37	11.8	1.37

Table B.34 - Moreyra [Mor 93] M_T/M_P Ratios - Local Buckling Methods

Specimen	S136			AISI		Dinovitzer		Sooi	
	M_T (kN·m)	M_P (kN·m)	M_T/M_P	M_P (kN·m)	M_T/M_P	M_P (kN·m)	M_T/M_P	M_P (kN·m)	M_T/M_P
A-W	14.0	15.1	0.93	16.2	0.86	15.1	0.93	15.3	0.91
A-T	11.9	15.0	0.80	16.1	0.74	15.0	0.80	15.3	0.78
A-TB	14.4	16.5	0.87	18.0	0.80	16.5	0.87	16.6	0.87
B-W	13.2	15.1	0.87	16.3	0.81	15.2	0.87	15.4	0.86
B-T	11.7	15.3	0.77	16.5	0.71	15.3	0.77	15.5	0.76
B-TB	14.0	15.5	0.91	17.0	0.82	15.6	0.90	15.6	0.90
C-W	15.6	13.9	1.12	15.4	1.02	14.1	1.11	14.0	1.11
C-T	13.1	14.9	0.88	16.1	0.81	15.0	0.87	15.2	0.86
C-TB	15.0	14.9	1.00	16.6	0.90	15.2	0.99	15.1	0.99

Table B.35a - Moreyra [Mor 93] M_T/M_P Ratios - Flange/Web Distortional Buckling Methods

Specimen	Lau & Hancock 1			Lau & Hancock 2		Lau & Hancock 3		Marsh	
	M_T (kN·m)	M_P (kN·m)	M_T/M_P	M_P (kN·m)	M_T/M_P	M_P (kN·m)	M_T/M_P	M_P (kN·m)	M_T/M_P
A-W	14.0	13.2	1.06	13.2	1.06	12.0	1.17	13.7	1.02
A-T	11.9	13.2	0.91	13.2	0.91	11.9	1.00	13.5	0.88
A-TB	14.4	14.3	1.01	14.3	1.01	12.9	1.12	14.9	0.96
B-W	13.2	13.1	1.01	13.1	1.01	11.8	1.12	13.2	1.00
B-T	11.7	13.3	0.88	13.3	0.88	12.0	0.98	13.4	0.87
B-TB	14.0	13.8	1.01	13.8	1.01	12.4	1.13	13.9	1.01
C-W	15.6	12.6	1.24	12.6	1.24	11.3	1.38	12.6	1.24
C-T	13.1	13.3	0.98	13.3	0.98	12.0	1.09	13.2	0.99
C-TB	15.0	13.7	1.10	13.7	1.10	12.2	1.23	13.6	1.10

Table B.35b - Moreyra [Mor 93] M_T/M_P Ratios - Flange/Web Distortional Buckling Methods

Specimen	Moreyra 1			Moreyra 2	
	M_T (kN·m)	M_P (kN·m)	M_T/M_P	M_P (kN·m)	M_T/M_P
A-W	14.0	14.6	0.96	15.2	0.92
A-T	11.9	14.5	0.82	15.1	0.79
A-TB	14.4	15.8	0.91	16.4	0.88
B-W	13.2	14.4	0.92	14.9	0.89
B-T	11.7	14.6	0.80	15.2	0.77
B-TB	14.0	15.2	0.92	15.7	0.89
C-W	15.6	13.7	1.14	14.3	1.09
C-T	13.1	14.9	0.88	15.4	0.85
C-TB	15.0	15.1	1.00	15.6	0.96

Table B.36 - Schardt & Schrade [Scha 82] M_T/M_P Ratios - Local Buckling Methods

Specimen	S136			AISI		Dinovitzer		Sooi	
	M_T (kN·m)	M_P (kN·m)	M_T/M_P	M_P (kN·m)	M_T/M_P	M_P (kN·m)	M_T/M_P	M_P (kN·m)	M_T/M_P
1.1.b	4.22	4.24	0.99	4.39	0.96	4.24	0.99	3.83	1.10
1.2.a	3.75	4.03	0.93	4.21	0.89	4.03	0.93	3.66	1.02
1.2.b	4.06	4.32	0.94	4.47	0.91	4.32	0.94	3.82	1.06
1.3.a	3.86	4.29	0.90	4.47	0.86	4.29	0.90	3.82	1.01
1.3.b	4.03	4.07	0.99	4.25	0.95	4.07	0.99	3.65	1.10
1.4.a	4.28	4.18	1.02	4.38	0.98	4.18	1.02	3.58	1.19
1.4.b	3.97	3.93	1.01	4.14	0.96	3.93	1.01	3.45	1.15
1.5.a	3.97	4.17	0.95	4.39	0.90	4.17	0.95	3.59	1.10
1.5.b	3.94	3.85	1.02	4.11	0.96	3.85	1.02	3.43	1.15
2.1.a	4.22	3.93	1.07	4.10	1.03	3.93	1.07	3.59	1.18
2.1.b	4.25	4.27	0.99	4.42	0.96	4.27	0.99	3.80	1.12
2.2.a	3.81	3.83	0.99	4.07	0.94	3.83	0.99	3.44	1.11
2.2.b	4.03	4.13	0.98	4.33	0.93	4.13	0.98	3.61	1.12
3.1.a	3.44	2.66	1.29	2.84	1.21	2.66	1.29	2.62	1.31
3.1.b	3.50	2.71	1.29	2.90	1.21	2.71	1.29	2.70	1.30
3.2.a	3.72	3.40	1.09	3.55	1.05	3.40	1.09	3.11	1.20
3.2.b	3.83	3.53	1.08	3.67	1.04	3.53	1.08	3.18	1.20
3.3.a	3.53	3.38	1.05	3.56	0.99	3.38	1.05	3.05	1.16
3.3.b	3.89	3.51	1.11	3.68	1.06	3.51	1.11	3.13	1.24
4.1.a	3.83	3.03	1.27	3.20	1.20	3.03	1.27	2.96	1.29
4.1.b	3.83	3.10	1.24	3.28	1.17	3.10	1.24	3.04	1.26
4.2.a	3.92	3.04	1.29	3.26	1.20	3.04	1.29	2.97	1.32
4.2.b	3.64	2.99	1.22	3.19	1.14	2.99	1.22	2.90	1.26
4.3.a	3.58	3.00	1.19	3.25	1.10	3.00	1.19	2.84	1.26
4.3.b	3.58	2.93	1.22	3.16	1.13	2.93	1.22	2.80	1.28

Table B.37a - Schardt & Schrade [Scha 82] M_T/M_P Ratios - Flange/Web Distortional Buckling Methods

Specimen	Lau & Hancock 1			Lau & Hancock 2		Lau & Hancock 3		Marsh	
	M_T (kN·m)	M_P (kN·m)	M_T/M_P	M_P (kN·m)	M_T/M_P	M_P (kN·m)	M_T/M_P	M_P (kN·m)	M_T/M_P
1.1.b	4.22	3.20	1.32	3.25	1.30	2.84	1.48	3.10	1.36
1.2.a	3.75	3.24	1.16	3.24	1.16	2.85	1.32	3.04	1.24
1.2.b	4.06	3.29	1.23	3.29	1.23	2.91	1.39	3.00	1.35
1.3.a	3.86	3.41	1.13	3.41	1.13	3.01	1.28	3.26	1.18
1.3.b	4.03	3.28	1.23	3.28	1.23	2.89	1.39	3.17	1.27
1.4.a	4.28	3.25	1.32	3.25	1.32	2.93	1.46	3.41	1.25
1.4.b	3.97	3.15	1.26	3.15	1.26	2.85	1.39	3.31	1.20
1.5.a	3.97	3.29	1.21	3.29	1.21	3.00	1.32	3.58	1.11
1.5.b	3.94	3.15	1.25	3.15	1.25	2.88	1.37	3.39	1.16
2.1.a	4.22	3.17	1.33	3.17	1.33	2.78	1.52	2.91	1.45
2.1.b	4.25	3.26	1.30	3.26	1.30	2.88	1.47	2.95	1.44
2.2.a	3.81	3.10	1.23	3.10	1.23	2.80	1.36	3.21	1.19
2.2.b	4.03	3.26	1.24	3.26	1.24	2.93	1.38	3.38	1.19
3.1.a	3.44	2.30	1.49	2.30	1.49	1.99	1.72	2.00	1.72
3.1.b	3.50	2.36	1.48	2.36	1.48	2.04	1.71	2.05	1.71
3.2.a	3.72	2.60	1.43	2.69	1.38	2.32	1.61	2.35	1.58
3.2.b	3.83	2.62	1.46	2.78	1.38	2.34	1.63	2.37	1.61
3.3.a	3.53	2.84	1.24	2.84	1.24	2.51	1.40	2.61	1.35
3.3.b	3.89	2.89	1.35	2.89	1.35	2.56	1.52	2.62	1.49
4.1.a	3.83	2.45	1.56	2.45	1.56	2.15	1.78	2.10	1.83
4.1.b	3.83	2.61	1.47	2.61	1.47	2.27	1.69	2.27	1.69
4.2.a	3.92	2.70	1.45	2.70	1.45	2.35	1.67	2.55	1.54
4.2.b	3.64	2.61	1.39	2.61	1.39	2.27	1.60	2.42	1.50
4.3.a	3.58	2.67	1.34	2.67	1.34	2.37	1.51	2.54	1.41
4.3.b	3.58	2.62	1.37	2.62	1.37	2.32	1.54	2.47	1.45

Table B.37b - Schardt & Schrade [Scha 82] M_T/M_P Ratios - Flange/Web Distortional Buckling Methods

Specimen	Moreyra 1			Moreyra 2	
	M_T (kN·m)	M_P (kN·m)	M_T/M_P	M_P (kN·m)	M_T/M_P
1.1.b	4.22	3.10	1.36	3.16	1.34
1.2.a	3.75	2.90	1.29	2.97	1.26
1.2.b	4.06	3.08	1.32	3.16	1.28
1.3.a	3.86	3.09	1.25	3.20	1.21
1.3.b	4.03	2.92	1.38	3.02	1.34
1.4.a	4.28	2.93	1.46	3.07	1.39
1.4.b	3.97	2.80	1.42	2.93	1.35
1.5.a	3.97	2.99	1.33	3.14	1.27
1.5.b	3.94	2.82	1.40	2.95	1.33
2.1.a	4.22	2.89	1.46	2.98	1.41
2.1.b	4.25	3.12	1.36	3.21	1.32
2.2.a	3.81	2.77	1.38	2.90	1.31
2.2.b	4.03	2.96	1.36	3.10	1.30
3.1.a	3.44	2.06	1.67	2.18	1.58
3.1.b	3.50	2.12	1.65	2.24	1.56
3.2.a	3.72	2.67	1.39	2.82	1.32
3.2.b	3.83	2.76	1.39	2.91	1.31
3.3.a	3.53	2.64	1.34	2.78	1.27
3.3.b	3.89	2.73	1.42	2.88	1.35
4.1.a	3.83	2.40	1.59	2.54	1.51
4.1.b	3.83	2.45	1.56	2.59	1.48
4.2.a	3.92	2.44	1.61	2.57	1.53
4.2.b	3.64	2.40	1.52	2.52	1.44
4.3.a	3.58	2.39	1.50	2.50	1.43
4.3.b	3.58	2.35	1.52	2.47	1.45

Table B.38 - Schuster [Schu 92] M_T/M_P Ratios - Local Buckling Methods

Specimen	S136			AISI		Dinovitzer		Sooi	
	M_T (kN·m)	M_P (kN·m)	M_T/M_P	M_P (kN·m)	M_T/M_P	M_P (kN·m)	M_T/M_P	M_P (kN·m)	M_T/M_P
BS1	8.46	9.07	0.93	10.3	0.82	9.07	0.93	8.77	0.96
BS2	8.61	9.07	0.95	10.3	0.84	9.07	0.95	8.77	0.98
CS1	9.05	10.8	0.83	11.9	0.76	10.9	0.83	10.0	0.90
CS2	9.05	10.9	0.83	11.9	0.76	10.9	0.83	10.1	0.90
CS3	9.29	10.8	0.86	11.9	0.78	10.9	0.86	10.0	0.93

Table B.39a - Schuster [Schu 92] M_T/M_P Ratios - Flange/Web Distortional Buckling Methods

Specimen	Lau & Hancock 1			Lau & Hancock 2		Lau & Hancock 3		Marsh	
	M_T (kN·m)	M_P (kN·m)	M_T/M_P	M_P (kN·m)	M_T/M_P	M_P (kN·m)	M_T/M_P	M_P (kN·m)	M_T/M_P
BS1	8.46	7.84	1.08	7.84	1.08	7.26	1.17	8.02	1.05
BS2	8.61	7.84	1.10	7.84	1.10	7.26	1.19	8.02	1.07
CS1	9.05	8.95	1.01	8.95	1.01	8.27	1.09	9.42	0.96
CS2	9.05	8.96	1.01	8.96	1.01	8.28	1.09	9.44	0.96
CS3	9.29	8.99	1.03	8.99	1.03	8.30	1.12	9.43	0.98

Table B.39b - Schuster [Schu 92] M_T/M_P Ratios - Flange/Web Distortional Buckling Methods

Specimen	Moreyra 1			Moreyra 2	
	M_T (kN·m)	M_P (kN·m)	M_T/M_P	M_P (kN·m)	M_T/M_P
BS1	8.46	7.46	1.13	7.66	1.10
BS2	8.61	7.46	1.15	7.66	1.12
CS1	9.05	8.65	1.05	8.95	1.01
CS2	9.05	8.66	1.05	8.95	1.01
CS3	9.29	8.67	1.07	8.98	1.04

Table B.40 - Shan [Shan 94] M_T/M_P Ratios - Local Buckling Methods

Specimen	S136			AISI		Dinovitzer		Sooi	
	M_T (kN·m)	M_P (kN·m)	M_T/M_P	M_P (kN·m)	M_T/M_P	M_P (kN·m)	M_T/M_P	M_P (kN·m)	M_T/M_P
3B,18,1&2(N)	5.71	4.62	1.24	4.72	1.21	4.62	1.24	4.70	1.21
3B,18,3&4(N)	5.07	4.56	1.11	4.66	1.09	4.56	1.11	4.64	1.09
3B,20,1&2(N)	2.91	3.24	0.90	3.43	0.85	3.24	0.90	3.34	0.87
3B,20,3&4(N)	3.10	3.24	0.96	3.43	0.90	3.24	0.96	3.34	0.93
3B,20,5&6(N)	3.43	3.23	1.06	3.42	1.00	3.23	1.06	3.33	1.03
2B,16,1&2(N)	3.82	3.50	1.09	3.49	1.10	3.56	1.07	3.50	1.09
2B,16,3&4(N)	3.90	3.61	1.08	3.60	1.08	3.64	1.07	3.61	1.08
2B,20,1&2(N)	2.03	1.88	1.08	1.90	1.07	1.88	1.08	1.90	1.07
2B,20,3&4(N)	2.01	1.88	1.07	1.90	1.06	1.88	1.07	1.90	1.06
8A,14,1&2(N)	13.5	11.2	1.20	11.2	1.20	11.2	1.20	11.2	1.20
8A,14,3&4(N)	13.7	11.1	1.23	11.2	1.22	11.1	1.23	11.2	1.22
8A,14,5&6(N)	13.6	11.2	1.22	11.2	1.22	11.2	1.22	11.2	1.22
8A,14,7&8(N)	15.3	17.4	0.88	19.2	0.80	17.4	0.88	17.7	0.87
8A,14,9&10(N)	15.7	17.4	0.90	19.2	0.82	17.4	0.90	17.6	0.89
8B,14,1&2(N)	14.9	14.1	1.06	14.6	1.02	14.1	1.06	14.5	1.03
8B,14,3&4(N)	14.7	14.1	1.05	14.6	1.01	14.1	1.05	14.5	1.02
8B,14,5&6(N)	18.1	18.3	0.99	20.0	0.90	18.3	0.99	18.5	0.98
8B,14,7&8(N)	18.1	18.3	0.99	19.9	0.91	18.3	0.99	18.5	0.98
8D,14,1&2(N)	20.1	18.0	1.12	20.0	1.00	18.0	1.12	18.5	1.09
8D,14,3&4(N)	20.7	17.9	1.16	20.0	1.04	17.9	1.16	18.4	1.13
8A,20,1&2(N)	4.07	4.56	0.89	4.75	0.86	4.56	0.89	3.39	1.20
8A,20,3&4(N)	4.12	4.64	0.89	4.84	0.85	4.64	0.89	3.43	1.20
8B,20,1&2(N)	5.38	5.46	0.98	5.63	0.95	5.46	0.98	4.05	1.33
8B,20,3&4(N)	5.38	5.45	0.99	5.62	0.96	5.45	0.99	4.04	1.33
8B,20,5&6(N)	5.32	5.44	0.98	5.62	0.95	5.44	0.98	4.04	1.32
8D,20,1&2(N)	9.51	9.12	1.04	9.75	0.98	9.12	1.04	8.61	1.10
8D,20,3&4(N)	9.31	9.10	1.02	9.72	0.96	9.10	1.02	8.59	1.08
12B,16,1&2(N)	22.5	28.9	0.78	30.5	0.74	28.9	0.78	21.5	1.05
12B,16,3&4(N)	23.4	28.5	0.82	30.1	0.78	28.7	0.82	21.2	1.10

Table B.41a - Shan [Shan 94] M_T/M_P Ratios - Flange/Web Distortional Buckling Methods

Specimen	Lau & Hancock 1			Lau & Hancock 2		Lau & Hancock 3		Marsh	
	M_T (kN·m)	M_P (kN·m)	M_T/M_P	M_P (kN·m)	M_T/M_P	M_P (kN·m)	M_T/M_P	M_P (kN·m)	M_T/M_P
3B,18,1&2(N)	5.71	4.18	1.37	4.18	1.37	3.70	1.54	4.14	1.38
3B,18,3&4(N)	5.07	4.19	1.21	4.19	1.21	3.70	1.37	4.13	1.23
3B,20,1&2(N)	2.91	2.94	0.99	2.94	0.99	2.54	1.14	2.89	1.01
3B,20,3&4(N)	3.10	2.93	1.06	2.93	1.06	2.54	1.22	2.88	1.07
3B,20,5&6(N)	3.43	2.93	1.17	2.93	1.17	2.53	1.35	2.88	1.19
2B,16,1&2(N)	3.82	3.28	1.17	3.28	1.17	3.01	1.27	3.22	1.19
2B,16,3&4(N)	3.90	3.31	1.18	3.31	1.18	3.06	1.28	3.28	1.19
2B,20,1&2(N)	2.03	1.72	1.18	1.72	1.18	1.48	1.37	1.63	1.24
2B,20,3&4(N)	2.01	1.71	1.17	1.71	1.17	1.47	1.36	1.62	1.24
8A,14,1&2(N)	13.5	10.4	1.29	10.4	1.29	9.98	1.35	10.3	1.31
8A,14,3&4(N)	13.7	10.4	1.32	10.4	1.32	9.92	1.38	10.2	1.35
8A,14,5&6(N)	13.6	10.4	1.31	10.4	1.31	9.95	1.37	10.2	1.33
8A,14,7&8(N)	15.3	15.6	0.98	15.6	0.98	14.5	1.05	15.5	0.99
8A,14,9&10(N)	15.7	15.6	1.01	15.6	1.01	14.5	1.08	15.5	1.01
8B,14,1&2(N)	14.9	13.1	1.13	13.1	1.13	12.4	1.20	12.9	1.15
8B,14,3&4(N)	14.7	13.1	1.12	13.1	1.12	12.4	1.19	12.9	1.14
8B,14,5&6(N)	18.1	16.1	1.12	16.1	1.12	14.9	1.21	16.3	1.11
8B,14,7&8(N)	18.1	16.1	1.12	16.1	1.12	14.9	1.21	16.2	1.11
8D,14,1&2(N)	20.1	16.7	1.20	16.7	1.20	14.7	1.37	16.1	1.25
8D,14,3&4(N)	20.7	16.6	1.25	16.6	1.25	14.6	1.42	16.0	1.30
8A,20,1&2(N)	4.07	3.15	1.29	3.15	1.29	2.93	1.39	3.77	1.08
8A,20,3&4(N)	4.12	3.16	1.30	3.16	1.30	2.95	1.40	3.83	1.08
8B,20,1&2(N)	5.38	3.79	1.42	3.79	1.42	3.50	1.53	4.74	1.13
8B,20,3&4(N)	5.38	3.79	1.42	3.79	1.42	3.50	1.54	4.74	1.13
8B,20,5&6(N)	5.32	3.77	1.41	3.77	1.41	3.49	1.53	4.70	1.13
8D,20,1&2(N)	9.51	7.86	1.21	7.86	1.21	6.99	1.36	7.70	1.24
8D,20,3&4(N)	9.31	7.84	1.19	7.84	1.19	6.97	1.34	7.66	1.21
12B,16,1&2(N)	22.5	19.7	1.14	19.7	1.14	18.6	1.21	23.8	0.94
12B,16,3&4(N)	23.4	19.6	1.19	19.6	1.19	18.4	1.27	23.4	1.00

Table B.41b - Shan [Shan 94] M_T/M_P Ratios - Flange/Web Distortional Buckling Methods

Specimen	Moreyra 1			Moreyra 2	
	M_T (kN·m)	M_P (kN·m)	M_T/M_P	M_P (kN·m)	M_T/M_P
3B,18,1&2(N)	5.71	4.99	1.14	5.22	1.09
3B,18,3&4(N)	5.07	4.94	1.03	5.17	0.98
3B,20,1&2(N)	2.91	3.22	0.90	3.38	0.86
3B,20,3&4(N)	3.10	3.22	0.96	3.37	0.92
3B,20,5&6(N)	3.43	3.21	1.07	3.37	1.02
2B,16,1&2(N)	3.82	3.66	1.04	3.81	1.00
2B,16,3&4(N)	3.90	3.72	1.05	3.82	1.02
2B,20,1&2(N)	2.03	1.95	1.04	2.04	1.00
2B,20,3&4(N)	2.01	1.95	1.03	2.05	0.98
8A,14,1&2(N)	13.5	11.2	1.21	11.2	1.21
8A,14,3&4(N)	13.7	11.1	1.23	11.1	1.23
8A,14,5&6(N)	13.6	11.1	1.23	11.1	1.23
8A,14,7&8(N)	15.3	17.3	0.89	17.6	0.87
8A,14,9&10(N)	15.7	17.3	0.91	17.6	0.89
8B,14,1&2(N)	14.9	14.5	1.03	14.5	1.03
8B,14,3&4(N)	14.7	14.5	1.02	14.5	1.02
8B,14,5&6(N)	18.1	17.7	1.03	18.1	1.00
8B,14,7&8(N)	18.1	17.6	1.03	18.0	1.00
8D,14,1&2(N)	20.1	17.3	1.16	18.1	1.11
8D,14,3&4(N)	20.7	17.3	1.20	18.0	1.15
8A,20,1&2(N)	4.07	2.73	1.49	2.83	1.44
8A,20,3&4(N)	4.12	2.75	1.50	2.84	1.45
8B,20,1&2(N)	5.38	3.27	1.64	3.40	1.58
8B,20,3&4(N)	5.38	3.27	1.64	3.40	1.58
8B,20,5&6(N)	5.32	3.26	1.63	3.39	1.57
8D,20,1&2(N)	9.51	6.82	1.39	7.14	1.33
8D,20,3&4(N)	9.31	6.81	1.37	7.12	1.31
12B,16,1&2(N)	22.5	18.9	1.19	19.5	1.16
12B,16,3&4(N)	23.4	18.7	1.25	19.3	1.21

Table B.42 - Willis & Wallace [Wil 90a] M_T/M_P Ratios - Local Buckling Methods

Specimen	S136			AISI		Dinovitzer		Sooi	
	M_T (kN·m)	M_P (kN·m)	M_T/M_P	M_P (kN·m)	M_T/M_P	M_P (kN·m)	M_T/M_P	M_P (kN·m)	M_T/M_P
1C2	9.78	10.3	0.95	11.4	0.86	10.3	0.95	10.3	0.95
1C3	10.6	10.4	1.02	11.5	0.92	10.4	1.02	10.4	1.01
1C4	11.0	10.2	1.08	11.3	0.97	10.2	1.08	10.2	1.07
1C5	13.0	11.6	1.12	12.8	1.01	11.6	1.12	11.7	1.12

Table B.43a - Willis & Wallace [Wil 90a] M_T/M_P Ratios - Flange/Web Distortional Buckling Methods

Specimen	Lau & Hancock 1			Lau & Hancock 2		Lau & Hancock 3		Marsh	
	M_T (kN·m)	M_P (kN·m)	M_T/M_P	M_P (kN·m)	M_T/M_P	M_P (kN·m)	M_T/M_P	M_P (kN·m)	M_T/M_P
1C2	9.78	9.21	1.06	9.21	1.06	8.35	1.17	9.80	1.00
1C3	10.6	9.16	1.15	9.16	1.15	8.30	1.27	9.52	1.11
1C4	11.0	9.01	1.22	9.01	1.22	8.11	1.35	9.09	1.21
1C5	13.0	10.3	1.26	10.3	1.26	9.18	1.42	10.4	1.26

Table B.43b - Willis & Wallace [Wil 90a] M_T/M_P Ratios - Flange/Web Distortional Buckling Methods

Specimen	Moreyra 1			Moreyra 2	
	M_T (kN·m)	M_P (kN·m)	M_T/M_P	M_P (kN·m)	M_T/M_P
1C2	9.78	9.52	1.03	9.90	0.99
1C3	10.6	9.41	1.12	9.79	1.08
1C4	11.0	9.23	1.19	9.61	1.14
1C5	13.0	10.7	1.22	11.2	1.16

Table B.44 - Winter [Win 47] M_T/M_P Ratios - Local Buckling Methods

Specimen	S136			AISI		Dinovitzer		Sooi	
	M_T (kN·m)	M_P (kN·m)	M_T/M_P	M_P (kN·m)	M_T/M_P	M_P (kN·m)	M_T/M_P	M_P (kN·m)	M_T/M_P
B1	18.3	17.7	1.03	18.7	0.98	17.7	1.03	18.3	1.00
B2	10.8	10.4	1.04	10.4	1.04	10.4	1.04	10.4	1.04
B3	22.1	19.6	1.13	20.8	1.06	19.6	1.13	20.3	1.09
B4	49.4	44.4	1.11	44.3	1.11	44.4	1.11	44.4	1.11
B5	4.84	4.54	1.06	4.54	1.06	4.54	1.06	4.54	1.06
B6	38.3	34.7	1.10	34.7	1.11	35.8	1.07	34.7	1.10
B7	5.59	5.58	1.00	5.57	1.00	5.59	1.00	5.58	1.00
B8	22.7	21.1	1.08	21.1	1.08	21.1	1.08	21.1	1.08
B9	34.5	32.2	1.07	32.2	1.07	32.2	1.07	32.2	1.07
B10	12.1	10.6	1.14	10.6	1.14	10.6	1.14	10.6	1.14
C1	18.4	16.6	1.11	17.7	1.04	16.6	1.11	17.4	1.06
C2	11.1	9.08	1.22	9.51	1.17	9.08	1.22	9.28	1.20
C3	19.9	19.9	1.00	20.8	0.96	19.9	1.00	20.9	0.95
C4	10.2	8.72	1.17	8.91	1.15	8.72	1.17	9.13	1.12
C5	16.5	14.2	1.16	15.3	1.08	14.4	1.15	15.0	1.10

Table B.45a - Winter [Win 47] M_T/M_P Ratios - Flange/Web Distortional Buckling Methods

Specimen	Lau & Hancock 1			Lau & Hancock 2		Lau & Hancock 3		Marsh	
	M_T (kN·m)	M_P (kN·m)	M_T/M_P	M_P (kN·m)	M_T/M_P	M_P (kN·m)	M_T/M_P	M_P (kN·m)	M_T/M_P
B1	18.3	16.4	1.12	16.4	1.12	14.7	1.24	16.2	1.13
B2	10.8	9.33	1.15	9.33	1.15	8.51	1.26	9.21	1.17
B3	22.1	18.4	1.20	18.4	1.20	16.0	1.38	17.5	1.26
B4	49.4	41.2	1.20	41.2	1.20	38.5	1.28	40.1	1.23
B5	4.84	4.12	1.18	4.12	1.18	3.88	1.25	4.09	1.18
B6	38.3	33.2	1.15	33.2	1.15	30.3	1.27	32.1	1.19
B7	5.59	5.00	1.12	5.00	1.12	4.67	1.20	4.96	1.13
B8	22.7	19.1	1.19	19.1	1.19	18.0	1.26	18.9	1.20
B9	34.5	28.8	1.20	28.8	1.20	27.0	1.28	28.5	1.21
B10	12.1	9.90	1.22	9.90	1.22	9.51	1.27	9.85	1.23
C1	18.4	15.9	1.16	15.9	1.16	14.0	1.32	15.5	1.19
C2	11.1	8.35	1.33	8.35	1.33	7.48	1.48	8.03	1.38
C3	19.9	18.0	1.10	18.0	1.10	15.4	1.29	13.2	1.50
C4	10.2	7.28	1.41	7.42	1.38	6.39	1.60	6.21	1.65
C5	16.5	13.6	1.22	13.6	1.22	12.4	1.33	13.1	1.26

Table B.45b - Winter [Win 47] M_T/M_P Ratios - Flange/Web Distortional Buckling Methods

Specimen	Moreyra 1			Moreyra 2	
	M_T (kN·m)	M_P (kN·m)	M_T/M_P	M_P (kN·m)	M_T/M_P
B1	18.3	15.5	1.18	16.2	1.13
B2	10.8	8.87	1.21	9.13	1.18
B3	22.1	16.5	1.34	17.0	1.30
B4	49.4	45.4	1.09	46.1	1.07
B5	4.84	4.54	1.06	4.54	1.06
B6	38.3	36.6	1.05	38.3	1.00
B7	5.59	5.42	1.03	5.47	1.02
B8	22.7	21.1	1.08	21.1	1.08
B9	34.5	32.1	1.07	32.2	1.07
B10	12.1	10.6	1.14	10.6	1.14
C1	18.4	14.6	1.26	15.3	1.20
C2	11.1	7.06	1.57	7.38	1.50
C3	19.9	15.0	1.32	15.0	1.32
C4	10.2	6.56	1.56	6.75	1.52
C5	16.5	13.3	1.24	13.8	1.20

Table B.46 - Statistical Comparison of Dinovitzer [Din 92] and S136 [CSA 94] Test to Predicted Bending Moment Ratios For Case II Test Specimens

Test Specimen		Dinovitzer	S136
<u>Waterloo Data</u> (7 Tests)	Mean	1.04	1.06
	Std. Dev.	0.090	0.097
	Coeff. of Var.	0.106	0.111
<u>Existing Data</u> (20 Tests)	Mean	1.00	1.01
	Std. Dev.	0.147	0.158
	Coeff. of Var.	0.090	0.166
<u>Waterloo & Existing Data</u> (27 Tests)	Mean	1.01	1.02
	Std. Dev.	0.134	0.145
	Coeff. of Var.	0.138	0.147
<u>Existing Data w/o Dist. Bckl.</u> (9 Tests)	Mean	1.13	1.15
	Std. Dev.	0.087	0.100
	Coeff. of Var.	0.090	0.101
<u>Waterloo & Existing Data w/o Dist. Bckl.</u> (16 Tests)	Mean	1.09	1.11
	Std. Dev.	0.096	0.104
	Coeff. of Var.	0.095	0.101

Appendix 'C'

Example Calculations

Example Calculations Test Specimen

Test specimen C2-DW65-3-A was used in all of the example calculations.

The Dinovitzer [Din 92] exponent method calculations were also detailed using test specimen C2-DW20-3-A.

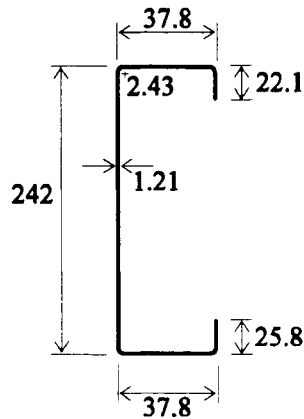


Figure C.1 - C2-DW65-3-A Test Specimen Dimensions (mm)

corner angle	90°
F_y	326 MPa
F_u	369 MPa

L	Flat width of centroidal line of element.
Y	Distance from centroid of element to extreme compressive fibre.
I'	Line moment of inertia of element about its own centroid.
E	Young's modulus (203000 MPa).
G	Shear modulus (78000 MPa).
μ	Poisson's ratio (0.3).
r	Centre line corner radius ($r = r_i + t/2 = 3.04$ mm).
r_o	Outside corner radius ($r_o = r_i + t = 3.64$ mm).

Gross Section Properties

Line Element Definitions

Compressive Lip

$$\begin{aligned} L_1 &= 22.1 - 3.64 &= 18.5 \text{ mm} \\ Y_1 &= 3.64 + 18.5 / 2 &= 12.9 \text{ mm} \\ I'_1 &= 18.5^3 / 12 &= 528 \text{ mm}^3 \end{aligned}$$

Compressive Lip/Flange Corner

$$\begin{aligned} L_2 &= 3.04 (\pi / 2) &= 4.78 \text{ mm} \\ Y_2 &= 3.64 - 3.04 (2 / \pi) &= 1.70 \text{ mm} \\ I'_2 &= 0.149 (3.04)^3 &= 4.19 \text{ mm}^3 \end{aligned}$$

Compressive Flange

$$\begin{aligned} L_3 &= 37.8 - 2(3.64) &&= 30.5 \text{ mm} \\ Y_3 &= 1.21 / 2 &&= 0.605 \text{ mm} \\ I'_3 &= 0.0 &&= 0.0 \text{ mm}^3 \end{aligned}$$

Compressive Flange/Web Corner

$$\begin{aligned} L_4 &= 3.04 (\pi / 2) &&= 4.78 \text{ mm} \\ Y_4 &= 3.64 - 3.04 (2 / \pi) &&= 1.70 \text{ mm} \\ I'_4 &= 0.149 (3.04)^3 &&= 4.19 \text{ mm}^3 \end{aligned}$$

Compressive and Tensile Web

$$\begin{aligned} L_5 &= 242 - 2(3.64) &&= 235 \text{ mm} \\ Y_5 &= 3.64 + 235 / 2 &&= 121 \text{ mm} \\ I'_5 &= 235^3 / 12 &&= 1081490 \text{ mm}^3 \end{aligned}$$

Tensile Flange/Web Corner

$$\begin{aligned} L_7 &= 3.04 (\pi / 2) &&= 4.78 \text{ mm} \\ Y_7 &= 242 - 3.64 + 3.04 (2 / \pi) &&= 240 \text{ mm} \\ I'_7 &= 0.149 (3.04)^3 &&= 4.19 \text{ mm}^3 \end{aligned}$$

Tensile Flange

$$\begin{aligned} L_8 &= 37.8 - 2(3.64) &&= 30.5 \text{ mm} \\ Y_8 &= 242 - 1.21 / 2 &&= 241 \text{ mm} \\ I'_8 &= 0.0 &&= 0.0 \text{ mm}^3 \end{aligned}$$

Tensile Lip/Flange Corner

$$\begin{aligned} L_9 &= 3.04 (\pi / 2) &&= 4.78 \text{ mm} \\ Y_9 &= 242 - 3.64 + 3.04 (2 / \pi) &&= 240 \text{ mm} \\ I'_9 &= 0.149 (3.04)^3 &&= 4.19 \text{ mm}^3 \end{aligned}$$

Tensile Lip

$$\begin{aligned} L_{10} &= 25.8 - 3.64 &&= 22.2 \text{ mm} \\ Y_{10} &= 242 - 3.64 - 22.2 / 2 &&= 227 \text{ mm} \\ I'_{10} &= 22.2^3 / 12 &&= 912 \text{ mm}^3 \end{aligned}$$

Element	L (mm)	Y (mm)	LY (mm ²)	LY ² (mm ³)	I' (mm ³)
1	18.5	12.9	239	3079	528
2	4.78	1.70	8.13	13.8	4.19
3	30.5	0.605	18.5	11.2	0.0
4	4.78	1.70	8.13	13.8	4.19
5	235	121	28435	3440635	1081490
7	4.78	240	1147	275328	4.19
8	30.5	241	7351	1771471	0.0
9	4.78	240	1147	275328	4.19
10	22.2	227	5039	1143944	912

$$\Sigma \text{Gross} \quad 356 \quad \quad \quad 43393 \quad 6909824 \quad 1082947$$

$$Y_{CG} = 43393 / 356 = \underline{122 \text{ mm}} \quad \text{Eq. 3.1}$$

$$I_{XG} = 1.21 (1082947 + 6909824 - 356 (122)^2) = \underline{3.26 \times 10^6 \text{ mm}^4} \quad \text{Eq. 3.2}$$

$$S_{XG} = 3.26 \times 10^6 / 122 = \underline{26.7 \times 10^3 \text{ mm}^3} \quad \text{Eq. 3.3}$$

Gross moment resistance.

$$M_{RG} = 26.7 \times 10^3 (326) = \underline{8.70 \text{ kN}\cdot\text{m}} \quad \text{Eq. 3.5}$$

S136-94 [CSA 94] Moment Resistance for Laterally Supported MembersEffective Width of Compressive Flange

$$w/t = 30.5 / 1.21 = 25.2 < 60 \therefore \text{OK.} \quad \text{Cl. 5.4}$$

$$W_{\text{lim1}} = 0.644 \sqrt{\frac{0.43 \cdot 203000}{326}} = 10.5 \quad \text{Cl. 5.6.2.3}$$

$$W_{\text{lim2}} = 0.644 \sqrt{\frac{4 \cdot 203000}{326}} = 32.1 \quad \text{Cl. 5.6.2.3}$$

$$W_{\text{lim1}} < w/t < W_{\text{lim2}} \therefore \text{Case II flange} \quad \text{Cl. 5.6.2.3}$$

$$d/t = 18.5 / 1.21 = 15.3 > 14 \therefore \text{NOT OK. (See Chapter 6 for revised limit)} \quad \text{Cl. 5.6.2.3}$$

$$d_f/w = 22.1 / 30.5 = 0.725 < 0.8 \therefore \text{OK.} \quad \text{Cl. 5.6.2.3}$$

$$I_s = 1.21 \cdot 18.5^3 \sin^2(90) / 12 = 638 \text{ mm}^4 \quad \text{Cl. 5.6.2.3}$$

$$I_a = 399 \cdot 1.21^4 (25.2/32.1 - 0.327)^3 = 82.2 \text{ mm}^4 \quad \text{Cl. 5.6.2.3}$$

$$I_r = 638 / 82.2 = 7.76 \quad \text{Cl. 5.6.2.3}$$

$$I_r > 1 \text{ and } 0.25 < d_f/w < 0.8 \therefore k = 5.25 - 5(0.725) = 1.63 \quad \text{Cl. 5.6.2.3 (Table 6)}$$

$$W_{\text{lim}} = 0.644 \sqrt{\frac{1.63 \cdot 203000}{326}} = 20.5 \quad \text{Cl. 5.6.2.1}$$

$$w/t > W_{\text{lim}} \therefore \text{flange must be reduced in width.} \quad \text{Cl. 5.6.2.1}$$

$$\frac{w_e}{t} = 0.95 \sqrt{\frac{1.63 \cdot 203000}{326}} \left[1 - \frac{0.208}{25.2} \sqrt{\frac{1.63 \cdot 203000}{326}} \right] = 22.3 \quad \text{Cl. 5.6.2.1}$$

$$w_e = 22.3 \cdot 1.21 = 27.0 \text{ mm}$$

$$\% \text{ effective} = 27.0 / 30.5 = 88.5\%$$

Effective Width of Compressive Lip

Use gross neutral axis ($Y_{\text{CG}} = 122 \text{ mm}$) for stress calculation.

$$f_3 = \frac{326}{122} (122 - 3.64) = 316 \text{ MPa} \quad \text{Cl. 5.6.2.3}$$

$$W_{\text{lim}} = 0.644 \sqrt{\frac{0.43 \cdot 203000}{316}} = 10.7 \quad \text{Cl. 5.6.2.1}$$

$$d/t > W_{\text{lim}} \therefore \text{lip must be reduced in width.} \quad \text{Cl. 5.6.2.1}$$

$$\frac{d_e}{t} = 0.95 \sqrt{\frac{0.43 \cdot 203000}{316}} \left[1 - \frac{0.208}{15.3} \sqrt{\frac{0.43 \cdot 203000}{316}} \right] = 12.2 \quad \text{Cl. 5.6.2.1}$$

$$d_e = 12.2 \cdot 1.21 = 14.8 \text{ mm}$$

$$I_r > 1 \therefore d_r = d_e = 14.8 \text{ mm} \quad \text{Cl. 5.6.2.3}$$

$$\% \text{ effective} = 14.8 / 18.5 = 80.0\%$$

Effective Width of Web

Use gross neutral axis ($Y_{CG} = 122 \text{ mm}$) for stress calculation.

$$h/t = 235 / 1.21 = 194 < 200 \therefore \text{OK.} \quad \text{Cl. 5.4}$$

$$f_1 = \frac{326}{122} (122 - 3.64) = 316 \text{ MPa} \quad \text{Cl. 5.6.2.8}$$

$$f_2 = \frac{-326}{122} (242 - 122 - 3.64) = -311 \text{ MPa} \quad \text{Cl. 5.6.2.8}$$

$$q = \left| \frac{-311}{316} \right| = 0.984 \quad \text{Cl. 5.6.2.8}$$

$$0 < q < 1 \therefore k = 4 + 2(1 + 0.984)^3 + 2(1 + 0.984) = 23.6 \quad \text{Cl. 5.6.2.8}$$

$$W_{lim} = 0.644 \sqrt{\frac{23.6 \cdot 203000}{316}} = 79.3 \quad \text{Cl. 5.6.2.1}$$

$$h/t > W_{lim} \therefore \text{web must be reduced in width.} \quad \text{Cl. 5.6.2.1}$$

$$\frac{h_e}{t} = 0.95 \sqrt{\frac{23.6 \cdot 203000}{316}} \left[1 - \frac{0.208}{194} \sqrt{\frac{23.6 \cdot 203000}{316}} \right] = 102 \quad \text{Cl. 5.6.2.1}$$

$$b_1 = 102 \cdot 1.21 / (3 + 0.984) = 31.0 \text{ mm} \quad \text{Cl. 5.6.2.8}$$

$$b_2 = 102 \cdot 1.21 / (1 + 0.984) - 31.0 = 31.2 \text{ mm} \quad \text{Cl. 5.6.2.8}$$

check $b_1 + b_2 < h_{comp}$

$$h_{comp} = 122 - 3.64 = 118 \text{ mm}$$

$$h_{tens} = 235 - 118 = 117 \text{ mm}$$

$$b_1 + b_2 = 31.0 + 31.2 = 62.2 < 118 \therefore \text{effective width OK.}$$

$$\% \text{ effective} = (62.2 + 235 - 118) / 235 = 76.3\%$$

Element	L (mm)	Y (mm)	LY (mm ²)	LY ² (mm ³)	I' (mm ³)
ΣGross	356		43393	6909824	1082947
Comp.	-18.5		-239	-3079	-528
Lip	+14.8	11.0	+163	+1791	+270
Comp.	-30.5		-18.5	-11.2	0.0
Flange	+27.0	0.605	+16.3	+9.88	0.0
Web	-235		-28435	-3440635	-1081490
b ₁	+31.0	19.1	+592	+11309	+2483
b ₂	+31.2	106	+3307	+350563	+2531
h _{tens}	+117	181	+21177	+3833037	+133468
ΣEffective	293		39956	7662809	139681

$$Y_{CGE} = 39956 / 293 = 136 \text{ mm}$$

Eq. 3.1

$Y_{CGE} \neq Y_{CG}$ previous \therefore Assume $Y_{CG} = 138 \text{ mm}$.

Recalculate Effective Widths

Effective Width of Compressive Flange

Effective flange width remains as previous.

Effective Width of Compressive Lip

Use effective neutral axis ($Y_{CGE} = 138 \text{ mm}$) for stress calculation.

$$f_3 = \frac{326}{138}(138 - 3.64) = 317 \text{ MPa} \quad \text{Cl. 5.6.2.3}$$

$$W_{lim} = 0.644 \sqrt{\frac{0.43 \cdot 203000}{317}} = 10.7 \quad \text{Cl. 5.6.2.1}$$

$d/t > W_{lim} \therefore$ lip must be reduced in width. Cl. 5.6.2.1

$$\frac{d_e}{t} = 0.95 \sqrt{\frac{0.43 \cdot 203000}{317}} \left[1 - \frac{0.208}{15.3} \sqrt{\frac{0.43 \cdot 203000}{317}} \right] = 12.2 \quad \text{Cl. 5.6.2.1}$$

$$d_e = 12.2 \cdot 1.21 = 14.8 \text{ mm}$$

$I_r > 1 \therefore d_r = d_e = 14.8 \text{ mm}$ Cl. 5.6.2.3

$$\% \text{ effective} = 14.8 / 18.5 = 80.0\%$$

Effective Width of Web

Use effective neutral axis ($Y_{CGE} = 138$ mm) for stress calculation.

$$f_1 = \frac{326}{138}(138 - 3.64) = 317 \text{ MPa} \quad \text{Cl. 5.6.2.8}$$

$$f_2 = \frac{-326}{138}(242 - 138 - 3.64) = -237 \text{ MPa} \quad \text{Cl. 5.6.2.8}$$

$$q = \left| \frac{-237}{317} \right| = 0.748 \quad \text{Cl. 5.6.2.8}$$

$$0 < q < 1 \therefore k = 4 + 2(1 + 0.748)^3 + 2(1 + 0.748) = 18.2 \quad \text{Cl. 5.6.2.8}$$

$$W_{lim} = 0.644 \sqrt{\frac{18.2 \cdot 203000}{317}} = 69.5 \quad \text{Cl. 5.6.2.1}$$

$h/t > W_{lim} \therefore$ web must be reduced in width. Cl. 5.6.2.1

$$\frac{h_e}{t} = 0.95 \sqrt{\frac{18.2 \cdot 203000}{317}} \left[1 - \frac{0.208}{194} \sqrt{\frac{18.2 \cdot 203000}{317}} \right] = 90.7 \quad \text{Cl. 5.6.2.1}$$

$$b_1 = 90.7 \cdot 1.21 / (3 + 0.748) = 29.3 \text{ mm} \quad \text{Cl. 5.6.2.8}$$

$$b_2 = 90.7 \cdot 1.21 / (1 + 0.748) - 29.3 = 33.5 \text{ mm} \quad \text{Cl. 5.6.2.8}$$

check $b_1 + b_2 < h_{comp}$

$$h_{comp} = 138 - 3.64 = 134 \text{ mm}$$

$$h_{tens} = 235 - 134 = 101 \text{ mm}$$

$$b_1 + b_2 = 29.3 + 33.5 = 62.8 < 134 \therefore \text{effective width OK.}$$

$$\% \text{ effective} = (62.8 + 235 - 134) / 235 = 69.7\%$$

Element	L (mm)	Y (mm)	LY (mm ²)	LY ² (mm ³)	I' (mm ³)
Σ Gross	356		43393	6909824	1082947
Comp.	-18.5		-239	-3079	-528
Lip	+14.8	11.0	+163	+1791	+270
Comp.	-30.5		-18.5	-11.2	0.0
Flange	+27.0	0.605	+16.3	+9.88	0.0
Web	-235		-28435	-3440635	-1081490
b ₁	+29.3	18.3	+536	+9812	+2096
b ₂	+33.5	121	+4054	+490474	+3133
h _{tens}	+101	189	+19089	+3607821	+85858
Σ Effective	278		38559	7576007	92286

$$Y_{CGE} = 38559 / 278 = \underline{139 \text{ mm}} \quad \text{Eq 3.1}$$

$Y_{CGE} \approx Y_{CG}$ previous \therefore End iterations.

$$I_{XE} = 1.21(92286 + 7576007 - 278(139)^2) = \underline{2.78 \times 10^6 \text{ mm}^4} \quad \text{Eq. 3.2}$$

$$S_{XE} = 2.78 \times 10^6 / 139 = \underline{20.0 \times 10^3 \text{ mm}^3} \quad \text{Eq. 3.3}$$

Effective moment resistance S136-94

$$M_{RE} = 20.0 \times 10^3 (326) = \underline{6.52 \text{ kN}\cdot\text{m}} \quad \text{Eq. 3.5}$$

Note: The above results may differ from those found in Appendix 'A' due to the use of 8 significant digits in the computer program (this applies to all example calculations).

Dinovitzer [Din 92] Exponent Method with S136-94 [CSA 94] Moment Resistance for Laterally Supported Members

Compressive Flange Plate Buckling Coefficient

$$I_r = 7.76$$

$$d_f/w = 0.725 < 0.8 \therefore \text{OK}$$

$$I_r > 1 \text{ and } 0.25 < d_f/w < 0.8$$

$$\therefore k = 5.25 - 5(0.725) = 1.63$$

Dinovitzer Flange Plate Buckling Coefficient

Same plate buckling coefficient as the current S136 method.

Dinovitzer's exponent method will only affect the plate buckling coefficient of Case II sections with $I_r < 1$.

Dinovitzer's exponent method calculations are detailed using section C2-DW20-3-A.

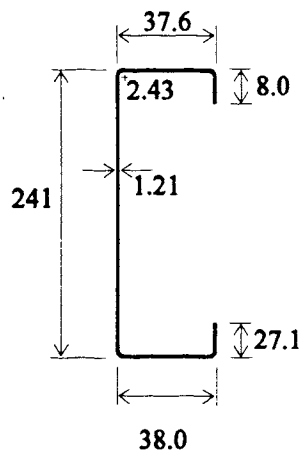


Figure C.2 - C2-DW20-3-A Test Specimen Dimensions (mm)

corner angle 90°

F_y 326 MPa

F_u 369 MPa

E Young's modulus (203000 MPa).

G Shear modulus (78000 MPa).

μ Poisson's ratio (0.3).

r Centre line corner radius ($r = r_i + t/2 = 3.04$ mm).

r_o Outside corner radius ($r_o = r_i + t = 3.64$ mm).

Current S136 Compressive Flange Plate Buckling Coefficient

$$w = 37.6 - 2(3.64) = 30.3 \text{ mm}$$

$$w/t = 30.3 / 1.21 = 25.0 < 60 \therefore \text{OK}$$

Cl. 5.4

$$W_{lim1} = 0.644 \sqrt{\frac{0.43 \cdot 203000}{326}} = 10.5$$

Cl. 5.6.2.3

$$W_{lim2} = 0.644 \sqrt{\frac{4 \cdot 203000}{326}} = 32.1$$

Cl. 5.6.2.3

$$W_{lim1} < w/t < W_{lim2} \therefore \text{Case II flange}$$

$$d = 8.0 - 3.64 = 4.36 \text{ mm}$$

$$d/t = 4.36 / 1.21 = 3.60 < 14 \therefore \text{OK}$$

Cl. 5.6.2.3

$$d_i/w = 8.0 / 30.3 = 0.264 < 0.8 \therefore \text{OK}$$

Cl. 5.6.2.3

$$I_s = 1.21 \cdot 4.36^3 \sin^2(90) / 12 = 8.36 \text{ mm}^4$$

Cl. 5.6.2.3

$$I_a = 399 \cdot 1.21^4 (25.0 / 32.1 - 0.327)^3 = 78.9 \text{ mm}^4$$

Cl. 5.6.2.3

$$I_r = 8.36 / 78.9 = 0.106$$

Cl. 5.6.2.3

$$I_r < 1 \text{ and } 0.25 < d_i/w < 0.8$$

$$\therefore k = (4.82 - 5(0.264)) 0.106^{1/2} + 0.43 = \underline{1.57}$$

SI36 Flange Plate Buckling CoefficientDinovitzer Compressive Flange Plate Buckling Coefficient

$$n = \frac{25}{43} - \frac{37 \cdot 25.0}{192} \sqrt{\frac{326}{203000}} = 0.388$$

$$0.333 \leq n \leq 0.5 \therefore \text{OK}$$

$$k = (4.82 - 5(0.264)) 0.106^{0.388} + 0.43 = \underline{1.90}$$

Dinovitzer Flange Plate Buckling Coefficient

Sooi [Soo 93] Web Approach with S136-94 [CSA 94] Moment Resistance for Laterally Supported Members

Effective Width of Compressive Flange

$$w/t = 30.5 / 1.21 = 25.2 < 60 \therefore \text{OK} \quad \text{Cl. 5.4}$$

$$W_{\text{lim}1} = 0.644 \sqrt{\frac{0.43 \cdot 203000}{326}} = 10.5 \quad \text{Cl. 5.6.2.3}$$

$$W_{\text{lim}2} = 0.644 \sqrt{\frac{4 \cdot 203000}{326}} = 32.1 \quad \text{Cl. 5.6.2.3}$$

$$W_{\text{lim}1} < w/t < W_{\text{lim}2} \therefore \text{Case II flange} \quad \text{Cl. 5.6.2.3}$$

$$d/t = 18.5 / 1.21 = 15.3 > 14 \therefore \text{NOT OK (See Chapter 6 for revised limit)} \quad \text{Cl. 5.6.2.3}$$

$$d_f/w = 22.1 / 30.5 = 0.725 < 0.8 \therefore \text{OK} \quad \text{Cl. 5.6.2.3}$$

$$I_s = 1.21 \cdot 18.5^3 \sin^2(90) / 12 = 638 \text{ mm}^4 \quad \text{Cl. 5.6.2.3}$$

$$I_a = 399 \cdot 1.21^4 (25.2/32.1 - 0.327)^3 = 82.2 \text{ mm}^4 \quad \text{Cl. 5.6.2.3}$$

$$I_r = 638 / 82.2 = 7.76 \quad \text{Cl. 5.6.2.3}$$

$$I_r > 1 \text{ and } 0.25 < d_f/w < 0.8 \therefore k = 5.25 - 5(0.725) = 1.63 \quad \text{Cl. 5.6.2.3 (Table 6)}$$

$$W_{\text{lim}} = 0.644 \sqrt{\frac{1.63 \cdot 203000}{326}} = 20.5 \quad \text{Cl. 5.6.2.1}$$

$$w/t > W_{\text{lim}} \therefore \text{flange must be reduced in width} \quad \text{Cl. 5.6.2.1}$$

$$\frac{w_e}{t} = 0.95 \sqrt{\frac{1.63 \cdot 203000}{326}} \left[1 - \frac{0.208}{25.2} \sqrt{\frac{1.63 \cdot 203000}{326}} \right] = 22.3 \quad \text{Cl. 5.6.2.1}$$

$$w_e = 22.3 \cdot 1.21 = 27.0 \text{ mm}$$

$$\% \text{ effective} = 27.0 / 30.5 = 88.5\%$$

Effective Width of Compressive Lip

Use effective neutral axis ($Y_{\text{CGE}} = 149 \text{ mm}$) for stress calculation.

$$f_3 = \frac{326}{149} (149 - 3.64) = 318 \text{ MPa} \quad \text{Cl. 5.6.2.3}$$

$$W_{\text{lim}} = 0.644 \sqrt{\frac{0.43 \cdot 203000}{318}} = 10.7 \quad \text{Cl. 5.6.2.1}$$

$d/t > W_{lim} \therefore$ lip must be reduced in width Cl. 5.6.2.1

$$\frac{d_e}{t} = 0.95 \sqrt{\frac{0.43 \cdot 203000}{318}} \left[1 - \frac{0.208}{15.3} \sqrt{\frac{0.43 \cdot 203000}{318}} \right] = 12.2 \quad \text{Cl. 5.6.2.1}$$

$$d_e = 12.2 \cdot 1.21 = 14.8 \text{ mm}$$

$I_r > 1 \therefore d_r = d_e = 14.8 \text{ mm}$ Cl. 5.6.2.3

$$\% \text{ effective} = 14.8 / 18.5 = 80.0\%$$

Effective Width of Web

Use effective neutral axis ($Y_{CGE} = 149 \text{ mm}$) for stress calculation.

$h/t = 235 / 1.21 = 194 < 200 \therefore$ OK Cl. 5.4

$$f_1 = \frac{326}{149} (149 - 3.64) = 318 \text{ MPa} \quad \text{Cl. 5.6.2.8}$$

$$f_2 = \frac{-326}{149} (242 - 149 - 3.64) = -196 \text{ MPa} \quad \text{Cl. 5.6.2.8}$$

$$q = \left| \frac{-196}{318} \right| = 0.616 \quad \text{Cl. 5.6.2.8}$$

$$0 < q < 1 \therefore k = 4 + 2(1 + 0.616)^3 + 2(1 + 0.616) = 15.7 \quad \text{Cl. 5.6.2.8}$$

$$W_{lim} = 0.644 \sqrt{\frac{15.7 \cdot 203000}{318}} = 64.5 \quad \text{Cl. 5.6.2.1}$$

$h/t > W_{lim} \therefore$ web must be reduced in width Cl. 5.6.2.1

$$\frac{h_e}{t} = 0.95 \sqrt{\frac{15.7 \cdot 203000}{318}} \left[1 - \frac{0.208}{194} \sqrt{\frac{15.7 \cdot 203000}{318}} \right] = 84.9 \quad \text{Cl. 5.6.2.1}$$

$$h_e = 84.9 \cdot 1.21 = 103 \text{ mm}$$

$$h_{tens} = 242 - 3.64 - 149 = 89.4 \text{ mm}$$

$$h_{comp} = 103 - 89.4 = 13.6 \text{ mm}$$

$$\% \text{ effective} = 103 / 235 = 43.8\%$$

Element	L (mm)	Y (mm)	LY (mm ²)	LY ² (mm ³)	I' (mm ³)
ΣGross	356		43393	6909824	1082947
Comp.	-18.5		-239	-3079	-528
Lip	+14.8	11.0	+163	+1791	+270
Comp.	-30.5		-18.5	-11.2	0.0
Flange	+27.0	0.605	+16.3	+9.88	0.0
Web	-235		-28435	-3440635	-1081490
h _{comp}	+13.6	10.4	+141	+1471	+210
h _{tens}	+89.4	194	+17344	+3364658	+59543
ΣEffective	217		32365	6834029	60952

$$Y_{CGE} = 32365 / 217 = 149 \text{ mm}$$

Eq. 3.1

$Y_{CGE} \approx Y_{CG}$ previous \therefore End iterations.

$$I_{XE} = 1.21(60952 + 6834029 - 217(149)^2) = 2.51 \times 10^6 \text{ mm}^4$$

Eq. 3.2

$$S_{XE} = 2.51 \times 10^6 / 149 = 16.8 \times 10^3 \text{ mm}^3$$

Eq. 3.3

Effective moment resistance Sooi web method.

$$M_{RE} = 16.8 \times 10^3 (326) = 5.48 \text{ kN}\cdot\text{m}$$

Eq. 3.5

AISI [AISI 89a] Moment Resistance for Laterally Supported Members

E Young's Modulus (29500 ksi = 203395 MPa)

Effective Width of Compressive Flange

$$w/t = 30.5 / 1.21 = 25.2 < 60 \therefore \text{OK} \quad \text{Sec. B1.1}$$

$$S = 128 \sqrt{\frac{203395}{326}} = 32.0 \quad \text{Eq. B4-1}$$

$$S/3 = 32.0 / 3 = 10.7 \quad \text{Sec. B4.2}$$

$$S/3 < w/t < S \therefore \text{Case II flange} \quad \text{Sec. B4.2}$$

$$d/t = 18.5 / 1.21 = 15.3 < 60 \therefore \text{OK} \quad \text{Sec. B1.1}$$

$$D/w = 22.1 / 30.5 = 0.725 < 0.8 \therefore \text{OK} \quad \text{Sec. B4.2}$$

$$I_s = 1.21 \cdot 18.5^3 \sin^2(90) / 12 = 638 \text{ mm}^4 \quad \text{Eq. B4-2}$$

$$I_a = 399 \cdot 1.21^4 (25.2 / 32.0 - 0.33)^3 = 81.9 \text{ mm}^4 \quad \text{Eq. B4.2-6}$$

$$I_s / I_a = 638 / 81.9 = 7.79 \text{ (use } I_s / I_a = 1) \quad \text{Sec. B4.2}$$

$$0.25 < D/w < 0.8$$

$$\therefore k = 4.82 - 5(0.725) 1^{1/2} + 0.43 \leq 5.25 - 5(0.725) \quad \text{Eq. B4.2-9}$$

$$k = 1.63$$

$$\lambda = \frac{1.052}{\sqrt{1.63}} (25.2) \sqrt{\frac{326}{203395}} = 0.831 \quad \text{Eq. B2.1-4}$$

$$\lambda > 0.673 \therefore \text{flange must be reduced in width} \quad \text{Eq. B2.1-2}$$

$$\rho = (1 - 0.22 / 0.831) / 0.831 = 0.885 \quad \text{Eq. B2.1-3}$$

$$w_e = 30.5 \cdot 0.885 = 27.0 \text{ mm} \quad \text{Eq. B2.1-2}$$

$$\% \text{ effective} = 27.0 / 30.5 = 88.5\%$$

Effective Width of Compressive Lip

Use effective neutral axis ($Y_{CGE} = 135 \text{ mm}$) for stress calculation.

$$d/t = 18.5 / 1.21 = 15.3 < 60 \therefore \text{OK} \quad \text{Sec. B1.1}$$

$$f_3 = \frac{326}{135} (135 - 3.64) = 317 \text{ MPa} \quad \text{Fig. B4-2}$$

$$\lambda = \frac{1.052}{\sqrt{0.43}} (15.3) \sqrt{\frac{317}{203395}} = 0.969 \quad \text{Eq. B2.1-4}$$

$$\lambda > 0.673 \therefore \text{lip must be reduced in width} \quad \text{Eq. B2.1-2}$$

$$\rho = (1 - 0.22 / 0.969) / 0.969 = 0.798 \quad \text{Eq. B2.1-3}$$

$$d'_s = 18.5 \cdot 0.798 = 14.8 \text{ mm} \quad \text{Eq. B2.1-2}$$

$$I_s / I_a > 1 \therefore d_s = d'_s = 14.8 \text{ mm} \quad \text{Eq. B4.2-11}$$

$$\% \text{ effective} = 14.8 / 18.5 = 79.8\%$$

Effective Width of Web

Use effective neutral axis ($Y_{CGE} = 135 \text{ mm}$) for stress calculation.

$$h/t = 235 / 1.21 = 194 < 200 \therefore \text{OK} \quad \text{Sec. B1.1}$$

$$f_1 = \frac{326}{135} (135 - 3.64) = 317 \text{ MPa} \quad \text{Fig. B2.3-1}$$

$$f_2 = \frac{-326}{135} (242 - 135 - 3.64) = -250 \text{ MPa} \quad \text{Fig. B2.3-1}$$

$$\psi = \frac{-250}{317} = -0.789 \quad \text{Sec. B2.3}$$

$$k = 4 + 2(1 + 0.789)^3 + 2(1 - 0.789) = 19.0 \quad \text{Eq. B2.3-4}$$

$$\lambda = \frac{1.052}{\sqrt{19.0}} (194) \sqrt{\frac{317}{203395}} = 1.85 \quad \text{Eq. B2.1-4}$$

$$\lambda > 0.673 \therefore \text{web must be reduced in width} \quad \text{Eq. B2.1-2}$$

$$\rho = (1 - 0.22 / 1.85) / 1.85 = 0.476 \quad \text{Eq. B2.1-3}$$

$$b_e = 235 \cdot 0.476 = 112 \text{ mm} \quad \text{Eq. B2.1-2}$$

$$b_1 = 112 / (3 + 0.789) = 29.6 \text{ mm} \quad \text{Eq. B2.3-1}$$

$$\psi < -0.236 \quad \text{Sec. B2.3}$$

$$\therefore b_2 = 112 / 2 = 56.0 \text{ mm} \quad \text{Eq. B2.3-4}$$

check $b_1 + b_2 < h_{\text{comp}}$

$$h_{\text{comp}} = 135 - 3.64 = 131 \text{ mm}$$

$$h_{\text{tens}} = 235 - 131 = 104 \text{ mm}$$

$$b_1 + b_2 = 29.6 + 56.0 = 85.6 < 131 \therefore \text{effective width OK}$$

$$\% \text{ effective} = (85.6 + 235 - 131) / 235 = 80.7\%$$

Element	L (mm)	Y (mm)	LY (mm ²)	LY ² (mm ³)	I' (mm ³)
Σ Gross	356		43393	6909824	1082947
Comp.	-18.5		-239	-3079	-528
Lip	+14.8	11.0	+163	+1791	+270
Comp.	-30.5		-18.5	-11.2	0.0
Flange	+27.0	0.605	+16.3	+9.88	0.0
Web	-235		-28435	-3440635	-1081490
b ₁	+29.6	18.4	+545	+10021	+2161
b ₂	+56.0	107	+5992	+641144	+14635
h _{tens}	+104	187	+19448	+3636776	+93739
Σ Effective	303		40865	7755841	111734

$$Y_{CGE} = 40865 / 303 = \underline{135 \text{ mm}} \quad \text{Eq. 3.1}$$

$Y_{CGE} \approx Y_{CG}$ previous \therefore End iterations.

$$I_{XE} = 1.21(111734 + 7755841 - 303(135)^2) = \underline{2.84 \times 10^6 \text{ mm}^4} \quad \text{Eq. 3.2}$$

$$S_{XE} = 2.84 \times 10^6 / 135 = \underline{21.0 \times 10^3 \text{ mm}^3} \quad \text{Eq. 3.3}$$

Effective moment resistance AISI.

$$M_{RE} = 21.0 \times 10^3 (326) = \underline{6.85 \text{ kN}\cdot\text{m}} \quad \text{Eq. 3.5}$$

**Lau & Hancock [Lau 87] [Lau 90] Flange/Web Distortional Buckling Method 1 with AISI [AISI 89a]
Moment Resistance for Laterally Supported Members**

Distortional Buckling Stress

Based on centre line dimensions.

L	Compressive lip centre line width (22.1 - 1.21 / 2 = 21.5 mm)
F	Compressive flange centre line width (37.8 - 1.21 = 36.6 mm)
W	Web centre line width (242 - 1.21 = 241 mm)

Lip / Flange component properties

$$A = 1.21 (21.5 + 36.6) = 70.3 \text{ mm}^2 \quad \text{Eq. 7.1}$$

$$\bar{y} = \frac{21.5^2/2}{36.6 + 21.5} = 3.98 \text{ mm} \quad \text{Eq. 7.2}$$

$$\bar{x} = \frac{36.6^2/2 + 21.5 \cdot 36.6}{36.6 + 21.5} = 25.1 \text{ mm} \quad \text{Eq. 7.3}$$

$$J = \frac{1.21^3}{3} (21.5 + 36.6) = 34.3 \text{ mm}^4 \quad \text{Eq. 7.4}$$

$$I_x = \frac{36.6 \cdot 1.21^3}{12} + \frac{1.21 \cdot 21.5^3}{12} + 36.6 \cdot 1.21 \cdot 3.98^2 + 21.5 \cdot 1.21 \cdot \left(\frac{21.5}{2} - 3.98\right)^2 = 2901 \text{ mm}^4 \quad \text{Eq. 7.5}$$

$$I_y = \frac{1.21 \cdot 36.6^3}{12} + \frac{21.5 \cdot 1.21^3}{12} + 36.6 \cdot 1.21 \cdot \left(25.1 - \frac{36.6}{2}\right)^2 + 21.5 \cdot 1.21 \cdot (36.6 - 25.1)^2 = 10435 \text{ mm}^4 \quad \text{Eq. 7.6}$$

$$I_{xy} = 36.6 \cdot 1.21 \left(\frac{36.6}{2} - 25.1\right) (-3.98) + 21.5 \cdot 1.21 \left(\frac{21.5}{2} - 3.98\right) (36.6 - 25.1) = 3224 \text{ mm}^4 \quad \text{Eq. 7.7}$$

$$\beta_1 = 25.1^2 + \frac{2901 + 10435}{70.3} = 820 \text{ mm}^2 \quad \text{Eq. 7.8}$$

$$\lambda = 4.80 \left(\frac{2901 \cdot 36.6^2 \cdot 241}{2 \cdot 1.21^3}\right)^{0.25} = 612 \text{ mm} \quad \text{Eq. 7.9}$$

$$k_{\phi} = \frac{2 \cdot 203000 \cdot 1.21^3}{5.46(241 + 0.06 \cdot 612)} = 474 \text{ N} \cdot \text{mm} / \text{mm} \quad \text{Eq. 7.10}$$

$$\eta = \left(\frac{\pi}{612}\right)^2 = 2.64 \times 10^{-5} \text{ mm}^2 \quad \text{Eq. 7.11}$$

$$\alpha_1 = \frac{2.64 \times 10^{-5}}{820} (2901 \cdot 36.6^2 + 0.039 \cdot 34.3 \cdot 612^2) + \frac{474}{820 \cdot 2.64 \times 10^{-5} \cdot 203000} = 0.249 \text{ mm}^2 \quad \text{Eq. 7.12}$$

$$\alpha_2 = 2.64 \times 10^{-5} \left(10435 + \frac{2}{820} 3.98 \cdot 36.6 \cdot 3224 \right) = 0.306 \text{ mm}^2 \quad \text{Eq. 7.13}$$

$$\alpha_3 = 2.64 \times 10^{-5} \left(0.249 \cdot 10435 - \frac{2.64 \times 10^{-5}}{820} 3224^2 \cdot 36.6^2 \right) = 0.0568 \text{ mm}^4 \quad \text{Eq. 7.14}$$

Distortional Buckling Stress

$$F_{DB} = \frac{203000}{2 \cdot 70.3} \left((0.249 + 0.306) \pm \sqrt{(0.249 + 0.306)^2 - 4 \cdot 0.0568} \right) = \underline{391 \text{ MPa}} \quad \text{Eq. 7.15}$$

Nominal Buckling Stress

$$F_y / 2 = 326 / 2 = 163 \text{ MPa}$$

$$F_{DB} > F_y / 2$$

$$\therefore F_N = 326 \left(1 - \frac{326}{4 \cdot 391} \right) = \underline{258 \text{ MPa}} \quad \text{Eq. 7.16}$$

Calculate Effective Properties at the Nominal Buckling Stress

Effective Width of Compressive Flange

$$w/t = 30.5 / 1.21 = 25.2 < 60 \therefore \text{OK} \quad \text{Sec. B1.1}$$

$$k = 4.0$$

$$\lambda = \frac{1.052}{\sqrt{4.0}} (25.2) \sqrt{\frac{258}{203000}} = 0.473 \quad \text{Eq. B2.1-4}$$

$$\lambda < 0.673 \therefore \text{flange is fully effective} \quad \text{Eq. B2.1-1}$$

$$w_e = 30.5 \text{ mm} \quad \text{Eq. B2.1-1}$$

$$\% \text{ effective} = 100.0\%$$

Effective Width of Compressive Lip

$$d/t = 18.5 / 1.21 = 15.3 < 60 \therefore \text{OK} \quad \text{Sec. B1.1}$$

$$\lambda = \frac{1.052}{\sqrt{0.43}} (15.3) \sqrt{\frac{258}{203000}} = 0.875 \quad \text{Eq. B2.1-4}$$

$$\lambda > 0.673 \therefore \text{lip must be reduced in width} \quad \text{Eq. B2.1-2}$$

$$\rho = (1 - 0.22 / 0.875) / 0.875 = 0.856 \quad \text{Eq. B2.1-3}$$

$$d'_e = 18.5 \cdot 0.856 = 15.8 \text{ mm} \quad \text{Eq. B2.1-2}$$

$$\% \text{ effective} = 15.8 / 18.5 = 85.6\%$$

Effective Width of Web

Use effective neutral axis ($Y_{CGE} = 142 \text{ mm}$) for stress calculation.

$$h/t = 235 / 1.21 = 194 < 200 \therefore \text{OK}$$

Sec. B1.1

$$f_1 = \frac{258}{142} (142 - 3.64) = 251 \text{ MPa}$$

Fig. B2.3-1

$$f_2 = \frac{-258}{142} (242 - 142 - 3.64) = -175 \text{ MPa}$$

Fig. B2.3-1

$$\psi = \frac{-175}{251} = -0.697$$

Sec. B2.3

$$k = 4 + 2(1 + 0.697)^3 + 2(1 + 0.697) = 17.2$$

Eq. B2.3-4

$$\lambda = \frac{1.052}{\sqrt{17.2}} (194) \sqrt{\frac{251}{203000}} = 1.73$$

Eq. B2.1-4

$\lambda > 0.673 \therefore$ web must be reduced in width

Eq. B2.1-2

$$\rho = (1 - 0.22 / 1.73) / 1.73 = 0.505$$

Eq. B2.1-3

$$b_e = 235 \cdot 0.505 = 119 \text{ mm}$$

Eq. B2.1-2

$$h_{\text{tens}} = 242 - 3.64 - 142 = 96.4 \text{ mm}$$

$$h_{\text{comp}} = 119 - 96.4 = 22.6 \text{ mm}$$

$$\% \text{ effective} = 119 / 235 = 50.6\%$$

Element	L (mm)	Y (mm)	LY (mm ²)	LY ² (mm ³)	I' (mm ³)
Σ Gross	356		43393	6909824	1082947
Comp.	-18.5		-239	-3079	-528
Lip	+15.8	11.5	+182	+2090	+329
Web	-235		-28435	-3440635	-1081490
h_{comp}	+22.6	14.9	+337	+5017	+962
h_{tens}	+96.4	190	+18316	+3480040	+74653
Σ Effective	237		33554	6953257	76873

$$Y_{CGE} = 33554 / 237 = 142 \text{ mm}$$

Eq. 3.1

$Y_{CGE} \approx Y_{CG}$ previous \therefore End iterations.

$$I_{XE} = 1.21(76873 + 6953257 - 237(142)^2) = \underline{2.72 \times 10^6 \text{ mm}^4} \quad \text{Eq. 3.2}$$

$$S_{XE} = 2.72 \times 10^6 / 142 = \underline{19.2 \times 10^3 \text{ mm}^3} \quad \text{Eq. 3.3}$$

Flange/web distortional buckling moment resistance Lau & Hancock 1

$$M_{RE} = 19.2 \times 10^3 (258) = \underline{4.95 \text{ kN}\cdot\text{m}} \quad \text{Eq. 7.23}$$

Lau and Hancock [Lau 87] [Lau 90] Flange/Web Distortional Buckling Method 2 with AISI [AISI 89a] Moment Resistance for Laterally Supported Members

Varies from method 1 only by the column strength expressions used.

$$F_{DB} > \frac{F_y}{2} \quad F_N = F_y \left(1 - \frac{F_y}{4 \cdot F_{DB}} \right) \quad \text{Eq. 7.18}$$

$$F_{DB} \leq \frac{F_y}{2} \quad F_N = F_y \left(0.055 \left(\sqrt{\frac{F_y}{F_{DB}}} - 3.6 \right)^2 + 0.237 \right) \quad \text{Eq. 7.19}$$

Distortional Buckling Stress

From Lau and Hancock method 1

$$F_{DB} = 391 \text{ MPa}$$

$$F_y / 2 = 326 / 2 = 163 \text{ MPa}$$

$$F_{DB} > F_y / 2$$

Nominal Buckling Stress

$$\therefore F_N = 326 \left(1 - \frac{326}{4 \cdot 391} \right) = 258 \text{ MPa} \quad \text{Eq. 7.18}$$

Effective properties are the same as calculated for Lau and Hancock 1

$$Y_{CGE} = 142 \text{ mm} \quad \text{Eq. 3.1}$$

$$I_{XE} = 2.72 \times 10^6 \text{ mm}^4 \quad \text{Eq. 3.2}$$

$$S_{XE} = 19.2 \times 10^3 \text{ mm}^3 \quad \text{Eq. 3.3}$$

Flange/web distortional buckling moment resistance Lau & Hancock 2

$$M_{RE} = 4.95 \text{ kN}\cdot\text{m} \quad \text{Eq. 7.23}$$

Lau and Hancock [Lau 87] [Lau 90] Flange/Web Distortional Buckling Method 3 with AISI [AISI 89a] Moment Resistance for Laterally Supported Members

Varies from method 1 only by the column strength expressions used.

$$\lambda_c = \sqrt{\frac{F_y}{F_{DB}}} \quad \text{Eq. 7.20}$$

$$\lambda_c \leq 1.5 \quad F_N = 0.658^{\lambda_c^2} F_y \quad \text{Eq. 7.21}$$

$$\lambda_c > 1.5 \quad F_N = \frac{0.877}{\lambda_c^2} F_y \quad \text{Eq. 7.22}$$

Distortional Buckling Stress

From Lau and Hancock method 1

$$F_{DB} = 391 \text{ MPa}$$

Nominal Buckling Stress

$$\lambda_c = \sqrt{\frac{326}{391}} = 0.913 \quad \text{Eq. 7.20}$$

$$\lambda_c < 1.5 \quad \therefore F_N = 0.658^{0.913^2} 326 = 230 \text{ MPa} \quad \text{Eq. 7.21}$$

Calculate Effective Properties at the Nominal Buckling Stress

Effective Width of Compressive Flange

$$w/t = 30.5 / 1.21 = 25.2 < 60 \quad \therefore \text{OK} \quad \text{Sec. B1.1}$$

$$k = 4.0$$

$$\lambda = \frac{1.052}{\sqrt{4.0}} (25.2) \sqrt{\frac{230}{203000}} = 0.446 \quad \text{Eq. B2.1-4}$$

$$\lambda < 0.673 \quad \therefore \text{flange is fully effective} \quad \text{Eq. B2.1-1}$$

$$w_e = 30.5 \text{ mm} \quad \text{Eq. B2.1-1}$$

$$\% \text{ effective} = 100.0\%$$

Effective Width of Compressive Lip

$$d/t = 18.5 / 1.21 = 15.3 < 60 \quad \therefore \text{OK} \quad \text{Sec. B1.1}$$

$$\lambda = \frac{1.052}{\sqrt{0.43}} (15.3) \sqrt{\frac{230}{203000}} = 0.826 \quad \text{Eq. B2.1-4}$$

$\lambda > 0.673 \therefore$ lip must be reduced in width Eq. B2.1-2

$$\rho = (1 - 0.22 / 0.826) / 0.826 = 0.888 \quad \text{Eq. B2.1-3}$$

$$d'_s = 18.5 \cdot 0.888 = 16.4 \text{ mm} \quad \text{Eq. B2.1-2}$$

$$\% \text{ effective} = 16.4 / 18.5 = 88.8\%$$

Effective Width of Web

Use effective neutral axis ($Y_{CGE} = 139 \text{ mm}$) for stress calculation.

$$h/t = 235 / 1.21 = 194 < 200 \therefore \text{OK} \quad \text{Sec. B1.1}$$

$$f_1 = \frac{230}{139} (139 - 3.64) = 224 \text{ MPa} \quad \text{Fig. B2.3-1}$$

$$f_2 = \frac{-230}{139} (242 - 139 - 3.64) = -164 \text{ MPa} \quad \text{Fig. B2.3-1}$$

$$\psi = \frac{-164}{224} = -0.732 \quad \text{Sec. B2.3}$$

$$k = 4 + 2(1 + 0.732)^3 + 2(1 - 0.732) = 17.9 \quad \text{Eq. B2.3-4}$$

$$\lambda = \frac{1.052}{\sqrt{17.9}} (194) \sqrt{\frac{224}{203000}} = 1.60 \quad \text{Eq. B2.1-4}$$

$\lambda > 0.673 \therefore$ web must be reduced in width Eq. B2.1-2

$$\rho = (1 - 0.22 / 1.60) / 1.60 = 0.539 \quad \text{Eq. B2.1-3}$$

$$b_e = 235 \cdot 0.539 = 127 \text{ mm} \quad \text{Eq. B2.1-2}$$

$$h_{\text{tens}} = 242 - 3.64 - 139 = 99.4 \text{ mm}$$

$$h_{\text{comp}} = 127 - 99.4 = 27.6 \text{ mm}$$

$$\% \text{ effective} = 127 / 235 = 54.0\%$$

Element	L (mm)	Y (mm)	LY (mm ²)	LY ² (mm ³)	I' (mm ³)
Σ Gross	356		43393	6909824	1082947
Comp.	-18.5		-239	-3079	-528
Lip	+16.4	11.8	+194	+2284	+368
Web	-235		-28435	-3440635	-1081490
h_{comp}	+27.6	17.4	+480	+8356	+1752
h_{tens}	+99.4	189	+18787	+3550667	+81842
Σ Effective	246		34180	7027417	84891

$$Y_{CGE} = 34180 / 246 = \underline{139 \text{ mm}} \quad \text{Eq. 3.1}$$

$Y_{CGE} \approx Y_{CG}$ previous \therefore End iterations.

$$I_{XE} = 1.21(84891 + 7027417 - 246(139)^2) = \underline{2.85 \times 10^6 \text{ mm}^4} \quad \text{Eq. 3.2}$$

$$S_{XE} = 2.85 \times 10^6 / 139 = \underline{20.5 \times 10^3 \text{ mm}^3} \quad \text{Eq. 3.3}$$

Flange/web distortional buckling moment resistance Lau & Hancock 3

$$M_{RE} = 20.5 \times 10^3 (230) = \underline{4.72 \text{ kN}\cdot\text{m}} \quad \text{Eq. 7.23}$$

Marsh [Mar 90] Flange/Web Distortional Buckling Method with AISI [AISI 89a] Moment Resistance for Laterally Supported Members

The line moment of inertia method of calculation cannot be used for the Marsh approach as element thicknesses are reduced for partially effective areas.

L_i	flat width of element
A_i	area of element
Y_i	distance from centroid of element to extreme compressive fibre
I_i	moment of inertia of element about its own centroid
X	distance from centroid of element to neutral axis of section

Gross Element Definitions

Compressive Lip

$$\begin{aligned} L_1 &= 22.1 - 3.64 &= 18.5 \text{ mm} \\ A_1 &= 18.5 \cdot 1.21 &= 22.4 \text{ mm}^2 \\ Y_1 &= 3.64 + 18.5 / 2 &= 12.9 \text{ mm} \\ I_1 &= 1.21 \cdot 18.5^3 / 12 &= 638 \text{ mm}^4 \end{aligned}$$

Compressive Flange

$$\begin{aligned} L_3 &= 37.8 - 2(3.64) &= 30.5 \text{ mm} \\ A_3 &= 30.5 \cdot 1.21 &= 36.9 \text{ mm}^2 \\ Y_3 &= 1.21 / 2 &= 0.605 \text{ mm} \\ I_3 &= 30.5 \cdot 1.21^3 / 12 &= 4.50 \text{ mm}^4 \end{aligned}$$

Compressive Web (assume n.a. at 122mm)

$$\begin{aligned} L_5 &= 122 - 3.64 &= 118 \text{ mm} \\ A_5 &= 118 \cdot 1.21 &= 143 \text{ mm}^2 \\ Y_5 &= 3.64 + 118 / 2 &= 62.6 \text{ mm} \\ I_5 &= 1.21 \cdot 118^3 / 12 &= 165672 \text{ mm}^4 \end{aligned}$$

Tensile Flange/Web Corner

$$\begin{aligned} L_7 &= 3.04 (\pi / 2) &= 4.77 \text{ mm} \\ A_7 &= 4.77 \cdot 1.21 &= 5.77 \text{ mm}^2 \\ Y_7 &= 242 - 3.64 + 3.04 (2 / \pi) &= 240 \text{ mm} \\ I_7 &= 1.21 \cdot 0.149 (3.04)^3 &= 5.07 \text{ mm}^4 \end{aligned}$$

Tensile Lip/Flange Corner

$$\begin{aligned} L_9 &= 3.04 (\pi / 2) &= 4.77 \text{ mm} \\ A_9 &= 4.77 \cdot 1.21 &= 5.77 \text{ mm}^2 \\ Y_9 &= 242 - 3.64 + 3.04 (2 / \pi) &= 240 \text{ mm} \\ I_9 &= 1.21 \cdot 0.149 (3.04)^3 &= 5.07 \text{ mm}^4 \end{aligned}$$

Compressive Lip/Flange Corner

$$\begin{aligned} L_2 &= 3.04 (\pi / 2) &= 4.77 \text{ mm} \\ A_2 &= 4.77 \cdot 1.21 &= 5.77 \text{ mm}^2 \\ Y_2 &= 3.64 - 3.04 (2 / \pi) &= 1.70 \text{ mm} \\ I_2 &= 1.21 \cdot 0.149 \cdot (3.04)^3 &= 5.07 \text{ mm}^4 \end{aligned}$$

Compressive Flange/Web Corner

$$\begin{aligned} L_4 &= 3.04 (\pi / 2) &= 4.77 \text{ mm} \\ A_4 &= 4.77 \cdot 1.21 &= 5.77 \text{ mm}^2 \\ Y_4 &= 3.64 - 3.04 (2 / \pi) &= 1.70 \text{ mm} \\ I_4 &= 1.21 \cdot 0.149 (3.04)^3 &= 5.07 \text{ mm}^4 \end{aligned}$$

Tensile Web

$$\begin{aligned} L_6 &= 242 - 122 - 3.64 &= 116 \text{ mm} \\ A_6 &= 116 \cdot 1.21 &= 140 \text{ mm}^2 \\ Y_6 &= 122 + 116 / 2 &= 180 \text{ mm} \\ I_6 &= 1.21 \cdot 116^3 / 12 &= 157390 \text{ mm}^4 \end{aligned}$$

Tensile Flange

$$\begin{aligned} L_8 &= 37.8 - 2(3.64) &= 30.5 \text{ mm} \\ A_8 &= 30.5 \cdot 1.21 &= 36.9 \text{ mm}^2 \\ Y_8 &= 242 - 1.21 / 2 &= 241 \text{ mm} \\ I_8 &= 30.5 \cdot 1.21^3 / 12 &= 4.50 \text{ mm}^4 \end{aligned}$$

Tensile Lip

$$\begin{aligned} L_{10} &= 25.8 - 3.64 &= 22.2 \text{ mm} \\ A_{10} &= 22.2 \cdot 1.21 &= 26.9 \text{ mm}^2 \\ Y_{10} &= 242 - 3.64 - 22.2 / 2 &= 227 \text{ mm} \\ I_{10} &= 1.21 \cdot 22.2^3 / 12 &= 1103 \text{ mm}^4 \end{aligned}$$

Based on centre line dimensions.

βb	Compressive lip centre line width ($22.1 - 1.21 / 2 = 21.5 \text{ mm}$)
b	Compressive flange centre line width ($37.8 - 1.21 = 36.6 \text{ mm}$)
αb	Web centre line width ($242 - 1.21 = 241 \text{ mm}$)

$$\alpha = 241 / 36.6 = 6.58$$

$$\beta = 21.5 / 36.6 = 0.587$$

$$J = (1 + 0.587) \cdot 36.6 \cdot \frac{121^3}{3} = 34.3 \text{ mm}^4 \quad \text{Eq. 7.24}$$

$$k = \frac{3 \cdot 203000 \cdot 121^3}{16(6.58 + 0.6)36.6} = 257 \text{ N} \cdot \text{mm} / \text{mm} \quad \text{Eq. 7.25}$$

$$C_w = \frac{1}{3} 36.6^3 \cdot 121^3 \left(0.587^3 \left(\frac{36.6}{121} \right)^2 + 0.1 \right) = 5360662 \text{ mm}^6 \quad \text{Eq. 7.26}$$

$$I_p = (1 + 0.587(0.587^2 + 3)) \cdot 36.6^3 \frac{121}{3} = 58597 \text{ mm}^4 \quad \text{Eq. 7.27}$$

$$\lambda = \pi \left(\frac{203000 \cdot 58597}{78000 \cdot 34.3 + 2(203000 \cdot 5360662 \cdot 257)^{1/2}} \right)^{1/2} = 57.0 \text{ mm} \quad \text{Eq. 7.28}$$

$$\bar{\lambda} = \frac{57.0}{\pi} \sqrt{\frac{326}{203000}} = 0.727 \quad \text{Eq. 7.29}$$

$$\bar{\lambda} < \sqrt{2} \quad \therefore F_c = 326 \left(1 - \frac{0.727^2}{4} \right) = 283 \text{ MPa} \quad \text{Eq. 7.30}$$

Effective Thickness of Compressive Lip

$$\lambda_L = (3 + 0.6 \cdot 0.587) 0.587 \frac{36.6}{121} = 59.5 \text{ mm} \quad \text{Eq. 7.47}$$

$$\bar{\lambda}_L = \frac{59.5}{\pi} \sqrt{\frac{326}{203000}} = 0.759 \quad \text{Eq. 7.49}$$

$$\bar{\lambda}_L > \bar{\lambda} \quad \text{and} \quad \bar{\lambda}_L < \sqrt{2}$$

$$\therefore \bar{F}_L = 1 - \frac{0.759^2}{4} = 0.856 \quad \text{Eq. 7.51}$$

$$t_L = 1.21 \cdot 0.856^{1/2} = 1.12 \text{ mm} \quad \text{Eq. 7.50}$$

$$A_1 = 18.5 \cdot 1.12 = 20.7 \text{ mm}^2$$

$$I_1 = 1.12 \cdot 18.5^3 / 12 = 591 \text{ mm}^4$$

$$\% \text{ effective} = 1.12 / 1.21 = 92.6\%$$

Effective Thickness of Compressive Flange

$$\lambda_F = \frac{1.6 \cdot 36.6}{1.21} = 48.4 \text{ mm} \quad \text{Eq. 7.39}$$

$$\bar{\lambda}_F = \frac{48.4}{\pi} \sqrt{\frac{326}{203000}} = 0.617 \quad \text{Eq. 7.43}$$

$\bar{\lambda}_L < \bar{\lambda} \therefore$ Flange is fully effective

$$t_F = 1.21 \text{ mm}$$

% effective = 100%

Effective Thickness of Web

Use effective neutral axis ($Y_{CGE} = 132 \text{ mm}$) for stress calculation.

$$f_1 = \frac{283}{132} (132 - 3.64) = 275 \text{ MPa}$$

$$f_2 = \frac{-283}{132} (242 - 132 - 3.64) = -228 \text{ MPa}$$

$$\frac{f_2}{f_1} = \left| \frac{-228}{275} \right| = 0.829$$

$$\frac{f_2}{f_1} < 1 \therefore = 1.1 + \frac{-228}{2 \cdot 275} = 0.685 \quad \text{Eq. 7.33}$$

$$\lambda_w = \frac{0.685 \cdot 6.58 \cdot 36.6}{1.21} = 136 \text{ mm} \quad \text{Eq. 7.32}$$

$$\bar{\lambda}_w = \frac{136}{\pi} \sqrt{\frac{326}{203000}} = 1.73 \quad \text{Eq. 7.35}$$

$$\bar{\lambda}_w > \bar{\lambda} \quad \text{and} \quad \bar{\lambda}_w > \sqrt{2}$$

$$\therefore \bar{F}_w = \frac{1}{1.73^2} = 0.334 \quad \text{Eq. 7.38}$$

$$t_w = 1.21 \cdot 0.334^{1/2} = 0.699 \text{ mm} \quad \text{Eq. 7.36}$$

$L_5 = 132 - 3.64$	$= 128 \text{ mm}$	$L_6 = 242 - 132 - 3.64$	$= 106 \text{ mm}$
$A_5 = 128 \cdot 0.699$	$= 89.5 \text{ mm}^2$	$A_6 = 106 \cdot 1.21$	$= 128 \text{ mm}^2$
$Y_5 = 3.64 + 128 / 2$	$= 67.6 \text{ mm}$	$Y_6 = 132 + 106 / 2$	$= 185 \text{ mm}$
$I_5 = 0.699 \cdot 128^3 / 12$	$= 122159 \text{ mm}^4$	$I_6 = 1.21 \cdot 106^3 / 12$	$= 120094 \text{ mm}^4$

% effective = $(89.5 + 128) / (143 + 140) = 76.8\%$

Element	A (mm ²)	Y (mm)	AY (mm ²)	I (mm ⁴)	X (mm)	AX ² (mm ⁴)
1	20.7	12.9	267	591	119	293133
2	5.77	1.70	9.81	5.07	130	97513
3	36.9	0.605	22.3	4.50	131	633241
4	5.77	1.70	9.81	5.07	130	97513
5	89.5	67.6	6050	122159	64.4	371189
6	128	185	23680	120094	53.0	359552
7	5.77	240	1385	5.07	108	67301
8	36.9	241	8893	4.50	109	438409
9	5.77	240	1385	5.07	108	67301
10	26.9	227	6106	1103	95	242773
Σ Effective	362		47808	243976		2667925

$$Y_{CGE} = 47808 / 362 = \underline{132 \text{ mm}}$$

$$Y_{CGE} \approx Y_{CG} \therefore \text{End iterations}$$

$$I_{XE} = 243976 + 2667925 = \underline{2.91 \times 10^6 \text{ mm}^4}$$

$$S_{XE} = 2.91 \times 10^6 / 132 = \underline{22.0 \times 10^3 \text{ mm}^3}$$

Flange/web distortional buckling moment resistance Marsh.

$$M_{RE} = 22.0 \times 10^3 \cdot 283 = \underline{6.23 \text{ kN}\cdot\text{m}}$$

Eq. 7.53

Moreyra [Mor 93] Flange/Web Distortional Buckling Method 1 with AISI [AISI 89a] Moment Resistance for Laterally Supported Members

Nominal Buckling Stress

$$F_N = \frac{326}{\left(\frac{235}{1.21}\right)^{2/3} \left(0.186 + 0.114 \frac{30.5}{235}\right)^2} = 241 \text{ MPa} \quad \text{Eq. 7.54}$$

$$F_N < F_y \therefore \text{OK}$$

Effective Width of Compressive Lip

$$d/t = 18.5 / 1.21 = 15.3 < 60 \therefore \text{OK} \quad \text{Sec. B1.1}$$

$$\lambda = \frac{1.052}{\sqrt{0.43}} (15.3) \sqrt{\frac{241}{203000}} = 0.846 \quad \text{Eq. 7.55}$$

$$\lambda > 0.673 \therefore \text{lip must be reduced in width} \quad \text{Eq. B2.1-2}$$

$$\rho = (1 - 0.22 / 0.846) / 0.846 = 0.875 \quad \text{Eq. 7.58}$$

$$d'_s = 18.5 \cdot 0.875 = 16.2 \text{ mm} \quad \text{Eq. 7.56}$$

$$\% \text{ effective} = 16.2 / 18.5 = 87.5\%$$

Effective Width of Compressive Flange

$$w / t = 30.5 / 1.21 = 25.2 < 60 \therefore \text{OK} \quad \text{Sec. B1.1}$$

Lip / Flange component properties

$$u = \frac{\pi}{2} \left(2.43 + \frac{1.21}{2} \right) = 4.77 \text{ mm} \quad \text{Eq. 7.64}$$

$$c = \frac{2}{\pi} \left(2.43 + \frac{1.21}{2} \right) = 1.93 \text{ mm} \quad \text{Eq. 7.65}$$

$$I_{x_o} = 1.21 \left(4.77(3.04 - 1.93)^2 + 18.5 \left(3.04 + \frac{18.5}{2} \right)^2 + \frac{18.5^3}{12} \right) = 4027 \text{ mm}^4 \quad \text{Eq. 7.66}$$

$$I_{y_o} = 1.21 \left(\frac{30.5^3}{3} + 4.77(30.5 + 1.93)^2 + 18.5(30.5 + 3.04)^2 \right) = 42695 \text{ mm}^4 \quad \text{Eq. 7.67}$$

$$J = \frac{1.21^3}{3} (30.5 + 4.77 + 18.5) = 31.8 \text{ mm}^4 \quad \text{Eq. 7.69}$$

$$x = \frac{\left(4.77(3.04 - 1.93) + 18.5\left(\frac{18.5}{2} + 3.04\right)\right)}{(30.5 + 4.77 + 18.5)} = 4.33 \text{ mm} \quad \text{Eq. 7.70}$$

$$I_{yc} = 121 \left(30.5 \cdot 4.33^2 + 4.77(4.33 - 3.04 + 1.93)^2 + 18.5 \left(\frac{18.5}{2} + 3.04 - 4.33 \right)^2 + \frac{18.5^3}{12} \right) = 2809 \text{ mm}^4 \quad \text{Eq. 7.71}$$

$$D_w = \frac{203000 \cdot 1.21^3}{12(1 - 0.3^2)} = 32933 \text{ N} \cdot \text{mm} \quad \text{Eq. 7.72}$$

$$K_\phi = \frac{2 \cdot 32933}{235} \left(\frac{1}{\left(1 + \frac{2 \cdot 30.5}{3 \cdot 235}\right)} \right) = 258 \text{ N} \cdot \text{mm} / \text{mm} \quad \text{Eq. 7.62}$$

$$C_w = 30.5^2 \left(2809 - 30.5 \cdot \frac{1.21^3}{12} \right) = 2608884 \text{ mm}^6 \quad \text{Eq. 7.61}$$

$$I_p = 4027 + 42695 = 46722 \text{ mm}^4 \quad \text{Eq. 7.68}$$

$$\lambda_e = \pi \left(\frac{46722}{\frac{78000 \cdot 31.8}{203000} + 2 \left(\frac{258 \cdot 2608884}{203000} \right)^{1/2}} \right)^{1/2} = 60.2 \text{ mm} \quad \text{Eq. 7.60}$$

$$\lambda = \frac{60.2}{\pi} \left(\frac{241}{203000} \right)^{1/2} = 0.660 \quad \text{Eq. 7.59}$$

$\lambda < 0.673 \therefore$ flange is fully effective Eq. B2.1-1

$w_e = 30.5 \text{ mm}$ Eq. B2.1-1

% effective = 100.0%

Effective Width of Web

Use effective neutral axis ($Y_{CGE} = 140 \text{ mm}$) for stress calculation.

$h/t = 235 / 1.21 = 194 < 200 \therefore$ OK Sec. B1.1

$$f_1 = \frac{241}{140} (140 - 3.64) = 235 \text{ MPa} \quad \text{Fig. B2.3-1}$$

$$f_2 = \frac{-241}{140} (242 - 140 - 3.64) = -169 \text{ MPa} \quad \text{Fig. B2.3-1}$$

$$\psi = \frac{-169}{235} = -0.719 \quad \text{Eq. 7.77}$$

$$k = 4 + 2(1 + 0.719)^3 + 2(1 + 0.719) = 17.6 \quad \text{Eq. 7.75}$$

$$\lambda = \frac{1.052}{\sqrt{17.6}} (194) \sqrt{\frac{235}{203000}} = 1.66 \quad \text{Eq. 7.74}$$

$\lambda > 0.673 \therefore$ web must be reduced in width Eq. B2.1-2

$$\rho = (1 - 0.22 / 1.66) / 1.66 = 0.523 \quad \text{Eq. B2.1-3}$$

$$b_e = 235 \cdot 0.523 = 123 \text{ mm} \quad \text{Eq. 7.78}$$

$$h_{\text{tens}} = 242 - 3.64 - 140 = 98.4 \text{ mm}$$

$$h_{\text{comp}} = 123 - 98.4 = 24.6 \text{ mm} \quad \text{Eq. 7.79}$$

$$\% \text{ effective} = 123 / 235 = 52.3\%$$

Element	L (mm)	Y (mm)	LY (mm ²)	LY ² (mm ³)	I' (mm ³)
Σ Gross	356		43393	6909824	1082947
Comp.	-18.5		-239	-3079	-528
Lip	+16.2	11.7	+190	+2218	+354
Web	-235		-28435	-3440635	-1081490
h_{comp}	+24.6	15.9	+391	+6219	+1241
h_{tens}	+98.4	189	+18598	+3514946	+79397
Σ Effective	242		33898	6989493	81921

$$Y_{\text{CGE}} = 33898 / 242 = \underline{140 \text{ mm}} \quad \text{Eq. 3.1}$$

$Y_{\text{CGE}} \approx Y_{\text{CG}}$ previous \therefore End iterations.

$$I_{\text{XE}} = 1.21(81921 + 6989493 - 242(140)^2) = \underline{2.82 \times 10^6 \text{ mm}^4} \quad \text{Eq. 3.2}$$

$$S_{\text{XE}} = 2.82 \times 10^6 / 140 = \underline{20.1 \times 10^3 \text{ mm}^3} \quad \text{Eq. 3.3}$$

Flange/web distortional buckling moment resistance Moreyra I.

$$M_n = 20.1 \times 10^3 (241) = \underline{4.84 \text{ kN}\cdot\text{m}} \quad \text{Eq. 7.80}$$

Moreyra [Mor 93] Flange/Web Distortional Buckling Method 2 with AISI [AISI 89a] Moment Resistance for Laterally Supported Members

Varies from method 1 only by the definition of the flange/web rotational restraint ($2 K_\phi$).

Compressive Flange Effective Width

Lip / Flange component properties

$$K_\phi = \frac{4 \cdot 32933}{235} \left(\frac{1}{\left(1 + \frac{2 \cdot 305}{3 \cdot 235}\right)} \right) = 516 \text{ N} \cdot \text{mm} / \text{mm} \quad \text{Eq. 7.63}$$

$$\lambda_e = \pi \left(\frac{46722}{\frac{78000 \cdot 318}{203000} + 2 \left(\frac{516 \cdot 2608884}{203000} \right)^{1/2}} \right)^{1/2} = 513 \text{ mm} \quad \text{Eq. 7.60}$$

$$\lambda = \frac{513}{\pi} \left(\frac{241}{203000} \right)^{1/2} = 0.563 \quad \text{Eq. 7.59}$$

$\lambda < 0.673 \therefore$ flange is fully effective Eq. B2.1-1

$w_e = 30.5 \text{ mm}$ Eq. B2.1-1

% effective = 100.0%

Effective properties are the same as calculated for Moreyra 1

$$Y_{CGE} = 140 \text{ mm} \quad \text{Eq. 3.1}$$

$$I_{XE} = 2.82 \times 10^6 \text{ mm}^4 \quad \text{Eq. 3.2}$$

$$S_{XE} = 20.1 \times 10^3 \text{ mm}^3 \quad \text{Eq. 3.3}$$

Flange/web distortional buckling moment resistance Moreyra 2.

$$M_n = 4.84 \text{ kN} \cdot \text{m} \quad \text{Eq. 7.80}$$

Appendix 'D'

Additional Lau & Hancock Flange/Web Distortional Buckling Models

Additional Lau & Hancock Flange/Web Distortional Buckling Models [Lau 87] [Lau 90]

Two additional Lau & Hancock [Lau 87] [Lau 90] models were included in the comparison of flange/web distortional buckling methods. The models are presented in this Appendix because the main body of this work had been printed prior to completion of their analysis. The models detailed below are modifications of the flange/web distortional buckling equations for uniform compression members presented by Lau & Hancock [Lau 87] [Lau 90]. Model 5 follows the procedure set by Hancock for inclusion in the AISI Specification [AISI 89a].

The flange/web distortional buckling moment resistance is calculated following the typical Lau & Hancock [Lau 87] [Lau 90] procedure detailed in Chapter 7. Models 4 and 5 differ from the previous three models in the formulation of the strength expressions used to determine the nominal buckling stress, as shown below. The α_1 equation (Eq. 7.98) used to determine the distortional buckling stress for model 5 has been modified by Hancock on the basis of the Sharp approach [Sha 66].

Nominal buckling stress, F_N .

Models 4 and 5

Based on the column strength expressions developed by Hancock et al. [Han 94a] for post-buckling and sections formed from high yield strength steel, the nominal buckling stress is computed as follows.

$$\text{If } F_{DB} > 3.18 F_y \quad \text{then} \quad F_N = F_y. \quad (7.96)$$

$$\text{If } F_{DB} \leq 3.18 F_y \quad \text{then} \quad F_N = F_y \left(\frac{F_{DB}}{F_y} \right)^{0.6} \left(1 - 0.25 \left(\frac{F_{DB}}{F_y} \right)^{0.6} \right). \quad (7.97)$$

Distortional buckling stress, F_{DB} .

Model 5

$$\alpha_1 = \left(\eta I_x F^2 + \frac{J G}{E} + \frac{k_\phi}{\eta E} \right) / \beta_1 \quad (7.98)$$

Table D.1 - Test Data - Test / Predicted Bending Moment Ratios

Test Specimen	S136	AISI	L&H 1	L&H 2	L&H 3	L&H 4	L&H 5	Mar	Mor 1	Mor 2
	M_T/M_P									
<u>Excluding Charn...</u>										
<u>Data (21 Tests)</u>										
Mean	0.900	0.823	1.10	1.10	1.19	1.08	1.08	1.02	1.09	1.06
Std. Dev.	0.070	0.059	0.095	0.095	0.100	0.102	0.102	0.069	0.168	0.164
Coeff. of Var.	0.082	0.075	0.091	0.091	0.089	0.100	0.100	0.071	0.163	0.162
<u>Including Charn...</u>										
<u>Data (37 Tests)</u>										
Mean	0.859	0.786	1.03	1.02	1.13	0.997	0.997	1.02	0.998	0.974
Std. Dev.	0.086	0.076	0.183	0.164	0.197	0.152	0.152	0.254	0.172	0.165
Coeff. of Var.	0.103	0.100	0.183	0.166	0.180	0.157	0.157	0.258	0.177	0.175

Note: L&H, Mar and Mor refer to the Lau & Hancock [Lau 87] [Lau 90], Marsh [Mar 90] and Moreyra [Mor 93] flange/web distortional buckling methods, respectively.

Table D.2 - Comparison of Flange/Web Distortional Buckling Methods with Waterloo Test Data

Test Specimen	S136	AISI	L&H 1	L&H 2	L&H 3	L&H 4	L&H 5	Mar	Mor 1	Mor 2
	M_T	M_T/M_P								
	(kN·m)									
C1-DW30-2-A,B	24.3	0.91	0.83	1.14	1.14	1.18	1.10	1.10	1.02	1.11
C1-DW40-2-A,B	24.9	0.93	0.84	1.14	1.14	1.19	1.11	1.11	1.02	1.11
C1-DW60-2-A,B	25.6	0.90	0.81	1.12	1.12	1.16	1.08	1.08	0.96	1.10
C1-DW80-2-A,B	26.1	0.89	0.80	1.11	1.11	1.15	1.07	1.07	0.93	1.09
Mean		0.909	0.817	1.13	1.13	1.17	1.09	1.09	0.982	1.10
Std. Dev.		0.017	0.016	0.015	0.015	0.017	0.017	0.017	0.043	0.012
Coeff. of Var.		0.032	0.035	0.024	0.024	0.025	0.027	0.027	0.075	0.019

Table D.3 - Comparison of Flange/Web Distortional Buckling Methods with Available Test Data

Test Specimen	S136	AISI	L&H 1	L&H 2	L&H 3	L&H 4	L&H 5	Mar	Mor 1	Mor 2	
	M_T	M_T/M_p									
(kN·m)											
Moreyra [Mor 93]											
A-W	14.0	0.93	0.86	1.06	1.06	1.17	1.04	1.04	1.02	0.96	0.92
A-TB	14.4	0.87	0.80	1.01	1.01	1.12	1.00	1.00	0.96	0.91	0.88
B-W	13.2	0.87	0.81	1.01	1.01	1.12	0.99	0.99	1.00	0.92	0.89
B-TB	14.0	0.91	0.82	1.01	1.01	1.13	1.01	1.01	1.01	0.92	0.89
C-W	15.6	1.12	1.02	1.24	1.24	1.38	1.23	1.23	1.24	1.14	1.09
C-TB	15.0	1.00	0.90	1.10	1.10	1.23	1.09	1.09	1.10	1.00	0.96
Schuster [Schu 92]											
BS1	8.46	0.93	0.82	1.08	1.08	1.17	1.05	1.05	1.05	1.13	1.10
BS2	8.61	0.95	0.84	1.10	1.10	1.19	1.07	1.07	1.07	1.15	1.12
CS1	9.05	0.83	0.76	1.01	1.01	1.09	1.00	1.00	0.96	1.05	1.01
CS2	9.05	0.83	0.76	1.01	1.01	1.09	1.00	1.00	0.96	1.05	1.01
CS3	9.29	0.86	0.78	1.03	1.03	1.12	1.02	1.02	0.98	1.07	1.04
Shan [Shan 94]											
8A,14,7&8(N)	15.3	0.88	0.80	0.98	0.98	1.05	0.94	0.94	0.99	0.89	0.87
8A,14,9&10(N)	15.7	0.90	0.82	1.01	1.01	1.08	0.96	0.96	1.01	0.91	0.89
8A,20,1&2(N)	4.07	0.89	0.86	1.29	1.29	1.39	1.29	1.29	1.08	1.49	1.44
8A,20,3&4(N)	4.12	0.89	0.85	1.30	1.30	1.40	1.30	1.30	1.08	1.50	1.45
12B,16,1&2(N)	22.5	0.78	0.74	1.14	1.14	1.21	1.14	1.14	0.94	1.19	1.16
12B,16,3&4(N)	23.4	0.82	0.78	1.19	1.19	1.27	1.19	1.19	1.00	1.25	1.21
Mean		0.899	0.825	1.09	1.09	1.19	1.08	1.08	1.03	1.09	1.06
Std. Dev.		0.078	0.065	0.105	0.105	0.111	0.114	0.114	0.072	0.188	0.182
Coeff. of Var.		0.093	0.085	0.103	0.103	0.100	0.113	0.113	0.075	0.185	0.184

Note: L&H, Mar and Mor refer to the Lau & Hancock [Lau 87] [Lau 90], Marsh [Mar 90] and Moreyra [Mor 93] flange/web distortional buckling methods, respectively.

Table D.4 - Comparison of Flange/Web Distortional Buckling Methods with Charnvarnichborikarn Test Data [Cha 92]

Test Specimen	S136	AISI	L&H 1	L&H 2	L&H 3	L&H 4	L&H 5	Mar	Mor 1	Mor 2	
	M_T (kN·m)	M_T/M_P									
2.7-0.15-1	6.11	0.944	0.865	1.46	1.26	1.67	1.18	1.18	1.87	1.03	0.987
2.7-0.15-2	6.00	0.906	0.826	1.37	1.21	1.56	1.13	1.13	1.75	0.980	0.942
2.7-0.25-1	6.11	0.861	0.788	1.11	1.11	1.28	1.02	1.02	1.35	0.942	0.900
2.7-0.25-2	6.51	0.919	0.839	1.25	1.21	1.43	1.11	1.11	1.55	0.997	0.953
2.7-0.50-1	6.58	0.797	0.724	0.878	0.878	1.01	0.88	0.88	0.927	0.877	0.835
2.7-0.50-2	6.64	0.790	0.718	0.867	0.867	0.998	0.87	0.87	0.903	0.873	0.832
2.7-0.75-1	7.02	0.731	0.669	0.819	0.819	0.928	0.82	0.82	0.807	0.850	0.819
2.7-0.75-2	6.62	0.697	0.637	0.778	0.778	0.882	0.78	0.78	0.768	0.809	0.778
2.7-1.00-1	7.13	0.735	0.671	0.797	0.797	0.890	0.79	0.79	0.821	0.836	0.829
2.7-1.00-2	6.82	0.726	0.662	0.789	0.789	0.882	0.79	0.79	0.817	0.832	0.826
2.7-1.25-1	6.94	0.729	0.667	0.764	0.764	0.851	0.76	0.76	0.763	0.797	0.797
2.7-1.25-2	7.29	0.787	0.723	0.826	0.826	0.921	0.82	0.82	0.825	0.867	0.867
2.7-1.50-1	7.05	0.780	0.721	0.797	0.797	0.891	0.80	0.80	0.770	0.837	0.837
2.7-1.50-2	7.21	0.783	0.722	0.797	0.797	0.889	0.79	0.79	0.767	0.835	0.835
2.7-2.00-1	6.90	0.839	0.785	0.828	0.828	0.939	0.83	0.83	0.743	0.824	0.824
2.7-2.00-2	7.13	0.849	0.792	0.834	0.834	0.945	0.84	0.84	0.748	0.827	0.827
Mean	0.805	0.738	0.935	0.910	1.06	0.888	0.888	1.01	0.876	0.855	
Std. Dev.	0.075	0.070	0.228	0.176	0.266	0.139	0.139	0.386	0.071	0.059	
Coeff. of Var.	0.100	0.102	0.262	0.208	0.270	0.168	0.168	0.410	0.087	0.074	

Note: L&H, Mar and Mor refer to the Lau & Hancock [Lau 87] [Lau 90], Marsh [Mar 90] and Moreyra [Mor 93] flange/web distortional buckling methods, respectively.

